COMBINATION OF ANIONIC, RING-OPENING METATHESIS, LIVING RADICAL POLYMERIZATION FOR NOVEL NANOSTRUCTURED POLYMER SYNTHESIS

by

CHONG CHENG

A dissertation submitted to the Graduate Faculty in Chemistry in partial fulfillment of the requirements for the degree of Doctor of Philosophy, The City University of New York

2003

This manuscript has been read and accepted for the Graduate Faculty in Chemistry in satisfaction of the dissertation requirement for the degree of Doctor of Philosophy.

01/29/03
Date

Chair of Examining Committee

1/29/2003
Date

Executive Officer

Professor David C. Locke

Professor Steven Schwarz
Supervisory Committee

THE CITY UNIVERSITY OF NEW YORK

ABSTRACT

COMBINATION OF ANIONIC, RING-OPENING METATHESIS, LIVING RADICAL POLYMERIZATION FOR NOVEL NANOSTRUCTURED POLYMER SYNTHESIS

by

Chong Cheng

Adviser: Professor Nan-Loh Yang

Three types of living polymerization techniques – living anionic polymerization (LAP), ring-opening metathesis polymerization (ROMP), and living radical polymerization (LRP) – were investigated. Through strategic coordinations of these three techniques, a series of **first** syntheses of novel macroinitiators, macromonomers, and copolymers were accomplished as described below:

Nanostructured densely grafted copolymers were synthesized by combining LAP with ROMP based on 1,1-diphenylethylene (DPE) chemistry. DPE-norbornene bifunctional agent (DPE-NB) was synthesized, and selective polymerization of its norbornene functionality by ROMP yielded polyfunctional DPE-agent with quantitative DPE units. Polycarbanionic macroinitiators with quantitative initiator sites, including linear macroinitiators and a series of polystyrene-grafted macroinitiators, were synthesized by the reaction of polyfunctional DPE-agent with *sec*-butyllithium and poly(styryl)lithium. LAP using the linear polycarbanionic macroinitiators provided the only method till now for the synthesis of densely grafted copolymers with well-

controlled long grafts (DP_n up to 1000, block structures obtainable). LAP using the polystyrene-grafted polycarbanionic macroinitiators led to unique double-brush copolymers with graft junctions simultaneously carrying heterografts. Alternatively, double-brush copolymers were also prepared by macromonomer method. Norbornene-functionalized anionic monofunctional macroinitiator was synthesized by end-capping poly(styryl)lithium with DPE-NB. Novel diblock macromonomers with well-controlled short heterochains having block junctions connected to norbornene unit were synthesized by LAP using the macroinitiator. As the first homopolymerization of diblock macromonomers with non-terminal polymerizable group, ROMP of the diblock macromonomers gave poly(macromonomer)s with high conversion and controlled backbone DP_n. Additionally, homopolymer-based macromonomers with a terminal norbornenyl functionality were also synthesized through LAP, and ROMP of them was also investigated.

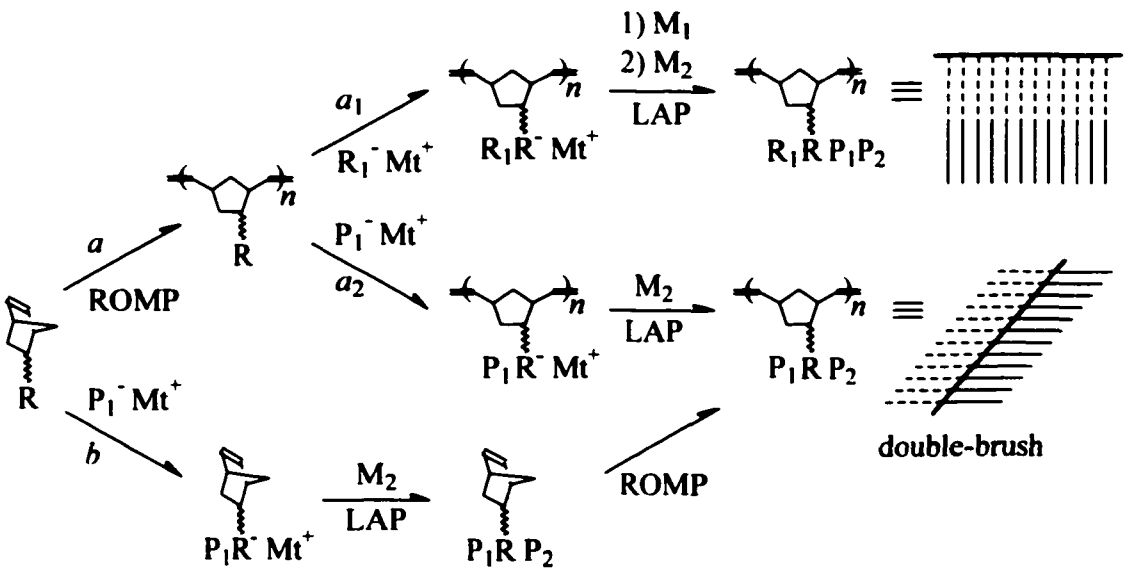

(R: $-Ph-\overset{\perp}{\underset{\perp}{Ph}}$; n can up to hundreds; LAP: living anionic polymerization)

Nanostructured grafted copolymers were also synthesized by combining LAP with LRP. Well-defined polyfunctional macroinitiators for stable free radical polymerization (SFRP) were synthesized by LAP with alkoxyamine-functionalized methacrylate. A series of well-defined grafted copolymers containing components with divergent polarities were synthesized based on SFRP using the macroinitiators.

With a wide variety of novel self-assembled nanostructures expected and a broad range of components with divergent properties obtainable, double-brush copolymers may have broad potential applications in areas including nanoparticle and nanocomposite preparation, surface and interface modification, drug and gene delivery, etc. Other types of nanostructured grafted copolymers are also expected to have various potential applications.

PREFACE

Polymerization generally is considered as a technique to produce polymer. However, how to develop the technique is a science, and at the same time, how to creatively apply the technique to achieve novel and unique macromolecular architectures is in a sense an art.

The objective of this dissertation is to deliver a polymerization solution where polymerization is not only a technique but also a science and even an art. On the other hand, whether this objective is realized or not needs the judgment not only from the author, I myself, but also from the readers, including you.

Life is as short as meteor, but if it also shines like meteor, then it might be meaningful. As there is light, so there is shadow. As I think, so I may hesitate.

Maybe it is this dissertation that is just the light of mine during these years with frequent hesitation.

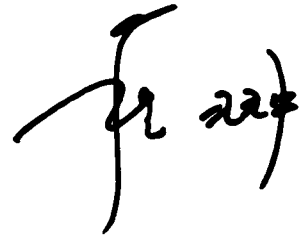

Chong Cheng

Staten Island, New York

January 2003

ACKNOWLEDGEMENTS

With this well-accomplished dissertation on hand, I would like to express my sincere gratitude for all who have helped me in my dissertation work. I thank Dr. Nan-Loh Yang for this unusual dissertation research opportunity that offered me so sufficient research freedom, and his generous support and kind helps that are crucial for any dissertation progress. I thank Ms. Sujin Jeong for experimental assistance, Dr. Hsin Wang for NMR support, Garcia Center for AFM and TEM characterization (Dr. Miriam Rafailovich, Dr. Henry White, Mr. Young-Soo Seo, Mr. Kyunghwan Yoon), UI-UC Mass Spectroscopy Lab for MALDI measurement (Dr. Yunping Huang). I thank Dr. David C. Locke and Dr. Steven Schwarz for their helpful suggestions for improvements and corrections on dissertation. Acknowledgement is made to Ph.D. program of Chemistry for doctoral study, College of Staten Island (CSI) and its chemistry department for hosting dissertation research, and NSF financial support via Garcia Center.

At the same time, I also wish to express my sincere appreciation to the people who are not involved in my dissertation work but are helpful for my professional growth. I thank Dr. Hongmin Zhang for preliminary professional education which provided solid foundation for my dissertation research. I thank Dr. George Odian for his excellent polymer lecture course, as well as various meaningful academic interactions. I thank Dr. Howard Haubenstock for his nice helps in a number of occasions. I thank Dr. Craig Hawker, Dr. Karen L. Wooley, and Dr. Jin-Shan Wang for their sincere suggestions for research development. I thank Dr. Krzysztof Matyjaszewski and Dr. Tadeusz Pakula for discussions on brush polymers. Acknowledgement is made to all references which comprise the basis of my dissertation research, as well as all the people in chemistry department of CSI and Ph.D. program of Chemistry for their geniality and numerous helps.

Finally, I wish to thank my family in China. It is the endless family love that is the strongest spiritual support for me in my life, including my dissertation period. Therefore I would like to own all my glory, either in career or in other aspects of life, to my family.

This dissertation is dedicated to:

my family,

all who helped,

all who appreciate its value.

CONTENTS OF TEXT

LIST OF TABLES

LIST OF FIGURES

Chapter 1

INTRODUCTION

A major aspect of modern polymer synthetic chemistry is the preparation of polymers with well-controlled structures based on living polymerization techniques [*1*]. Each technique has its virtues, as well as drawbacks. Therefore, strategic coordination of different techniques by using each of them to build up specific elements of the macromolecular architectures provides a versatile and elegant methodology for the synthesis of polymers with well-controlled complex architectures. With interesting complex macromolecular architectures, densely grafted copolymers have attracted widespread attention in the last decade. Different from conventional polymers, densely grafted copolymers can exhibit controlled nanosized morphologies, leading to broad potential applications for preparing polymer-based nanomaterials.

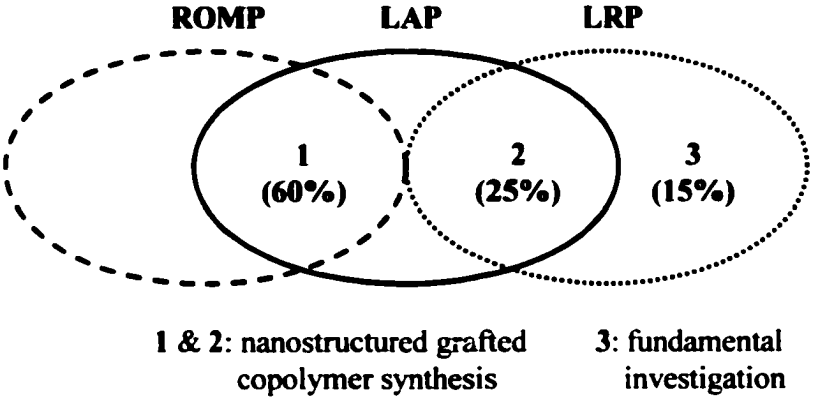

Figure 1-1. Overview of dissertation research

Figure 1-1 depicts research work described in this dissertation. The core parts (**1** & **2**) of this dissertation are nanostructured (densely) grafted copolymer synthesis by combining living anionic polymerization (LAP) with either ring-opening metathesis polymerization (ROMP) or living radical polymerization (LRP). The work based on combination of LAP and ROMP is described in Chapters 2-4. The work based on combination of LAP and LRP is described in Chapter 5. At the same time, this dissertation also includes some fundamental investigations related to LRP, and this part (**3**) of work is described in Chapters 6 and 7.

In the following sections, the essential background of this dissertation is presented. Living polymerization techniques are introduced with emphases on LAP, ROMP, and LRP. Combination of different living polymerization techniques is introduced as the key synthetic strategy for well-defined macromolecular architectures. Methodologies of the synthesis of grafted copolymers, especially densely grafted copolymers as the major targeted structures, are presented. Synthetic strategies for polymeric nanostructures with stabilized self-assembly are also presented.

1-1 Living Polymerization Techniques

Living polymerization was defined, by IUPAC in 1996, as a chain polymerization from which chain transfer and chain termination are absent [*2*]. However, with the fast development of polymer chemistry in the last decade, especially the progress made in mediated radical polymerization techniques, such a definition of living polymerization is facing challenges, and some amendments to this definition are required [*3, 4*]. In order

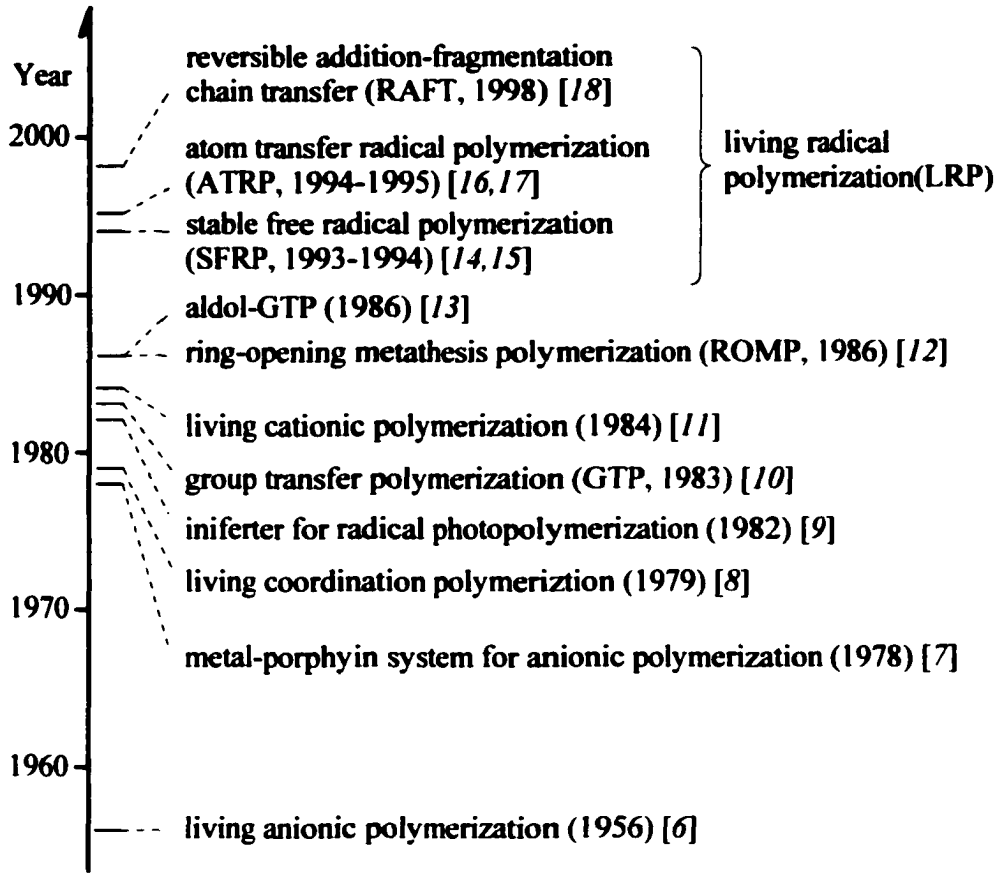

Figure 1-2. "Spectrum" of development for living polymerization techniques. (Based on nature of polymerization, ring-opening polymerization can be considered as radical, anionic, cationic, or coordination polymerization)

to cover all polymerization techniques used to synthesize well-defined polymers and simplify terminology, the definition of living polymerization is relaxed in this dissertation as a chain polymerization from which irreversible chain transfer and chain termination are negligible. Living polymerization provides the maximum degree of control for the synthesis of polymers with predictable, well-defined structures [5]. Therefore living polymerization has become a major research area in polymer synthetic chemistry since

Szwarc first reported living anionic polymerization in 1956, followed by the development of a number of other living polymerization techniques (**Figure 1-2**) [*6-18*].

1-1a **Living Anionic Polymerization (LAP).** For more than 40 years LAP has been the premier technique for the synthesis of model polymers with controlled structures and low polydispersities [*19, 20*]. Among all living polymerization techniques developed, LAP was considered as the most reliable and versatile method for the synthesis of a wide variety of well-defined polymers with the most accurate structural control. Its major advantage is the essential absence of termination and chain transfer reactions for many systems. However, because it typically requires very stringent reaction conditions and has poor tolerance for many functional groups, its commercial applications are limited and have not yet fully capitalized on its virtues in polymerization characteristics. Typical monomers of LAP include vinyl monomers such as styrenes, dienes, vinylpyridines, alkyl methacrylates, *tert*-butyl acrylate, and cyclic monomers such as lactones, epoxides, and cyclosiloxanes. Alkyllithiums are the most useful initiators for vinyl monomers; but the use of other organometallic reagents, instead of alkyllithiums, as initiators can be crucial for cyclic monomers. Typical solvents used in LAP include hydrocarbons and ethers.

Numerous polymers with complex architectures have been synthesized by LAP via a variety of synthetic strategies [*21*]. Among these synthetic strategies, applications of 1,1-diphenylethylene (DPE) chemistry and chlorosilane chemistry in LAP, capable of yielding a broad range of polymers with well-defined novel structures, have attracted increasing attention.

LAP is one of the key polymerization techniques used in Chapters 2-5. In many cases, especially in Chapters 2 and 3, LAP technique is applied in conjunction with DPE chemistry. The background of DPE chemistry is given in the introduction section of Chapter 2.

1-1b **Ring-Opening Metathesis Polymerization (ROMP).** ROMP is a polymerization technique based on olefin metathesis, which is metal-catalyzed redistribution of carbon-carbon double bonds. ROMP was first reported in 1960 [*22*] and has been developed as a living polymerization technique only since the 1980s [*12*] with the further development in olefin metathesis catalysts. Molybdenum-based and ruthenium-based alkylidenes, usually referred to as Schrock catalysts and Grubbs catalysts, were generally used as ROMP catalysts [*23-25*]. Only strained cycloalkenes can be used as monomers; highly strained norbornenes are the most used monomers. ROMP, especially when ruthenium-based initiators are used, has exceptionally high functional group tolerance. For the synthesis of a broad range of functionalized polymers directly from functional monomers, ROMP has attracted widespread attention as a unique synthetic method with potential commercial application. At the same time, ROMP of macromonomers can yield poly(macromonomer)s with relatively high conversion in a controlled manner, and has already been considered as a key method for poly(macromonomer) synthesis. Acyclic diene metathesis polymerization (ADMET) shares the same polymerization principles with ROMP, but uses dienes instead of cycloalkenes, as monomers. There are fewer reports available on ADMET as compared with ROMP.

ROMP is one of the essential polymerization techniques used in Chapters 2-4. In Chapter 2, it is used to selectively polymerize norbornenyl functionality of a DPE-norbornene bifunctional agent. In Chapters 3 and 4, it is used to polymerize norbornenyl-functionalized macromonomers.

1-1c **Living Radical Polymerization (LRP).** Development of LRP has been considered as a major advance in polymer synthetic chemistry in the last decade [*26, 27*]. Although some preliminary investigations were performed as early as the 1980s [*28, 29*], typical LRP systems have not been fully developed until three major types of LRP techniques, i.e. stable free radical polymerization (SFRP) [*30*], atom transfer radical polymerization (ATRP) [*31, 32*], and reversible addition-fragmentation transfer polymerization (RAFT) [18], were established. LRP systems differ from conventional radical polymerization systems in that there are mediation species for radical chain carriers to exert the so-called "persistent radical effect" [*33*] in LRP systems. Typical mediation species of radical chain carrier are: nitroxides (stable organic radicals, for reversible termination in SFRP), paramagnetic metal salts (metal-based stable radicals, for reversible termination in ATRP), and dithioesters (reversible chain transfer agents, for RAFT). For SFRP and ATRP, both the method using a bimolecular process (a conventional radical initiator plus mediating species) and the method using a unimolecular initiator (typically alkoxyamine for SFRP, and alkyl halide for ATRP) can yield polymers with low polydispersities. However, the latter method can, in general, lead to better control over polymerization and are much more suitable for the synthesis of polymers with complex architectures. For RAFT, a conventional radical initiator needs to

be used. Different from SFRP and ATRP based on irreversible termination, RAFT is based on irreversible chain transfer. Therefore, there are significant difficulties to synthesize well-defined polymers with complex architectures just through RAFT, and to date only linear polymers, including block copolymers, have been reported from preparation by RAFT. Currently, SFRP has a narrow range of applicable monomers. Both ATRP and RAFT have a relatively broad range of applicable monomers, but acidic monomers are not suitable for ATRP. LRP of ethylene has not been reported yet.

Because LRP can yield a broad range of well-defined polymers with different structural features under non-stringent reaction conditions [*34*], significant commercial applications of LRP are expected in the long term. However, for the time being, each major LRP technique needs to overcome a number of major disadvantages to become commercially viable. The application of SFRP requires the broadening of applicable monomer range to cover important monomers such as methacrylates. ATRP has attracted major attention, but because the metal-based catalyst used is toxic and electrically conducting, the resulting products generally cannot be directly used in some important application areas, such as biology, pharmacy, and electronics. Economical methods of removing metal-based species from ATRP products need to be developed. Additionally, when immobilized catalysts are used for ATRP, metal-based species can be removed readily from products. However, the polymerization systems have to suffer from very significant losses in catalyst efficiency and structural control capacity of polymer products due to their heterogeneous nature [*35*]. It is possible that whether ATRP can have important commercial application will heavily depend on the development of metal-free catalysts which work in polymerization systems following ATRP mechanism [*36*].

However, such metal-free catalysts have not been reported. For RAFT, its products have a dithioester end-group, which has associated odor and color, and currently it can only be used for the synthesis of linear polymers. Finally, no matter what type of LRP technique is used, the occurrence of irreversible biradical termination can become very considerable for the following cases: high monomer conversion, multifunctional or polyfunctional initiations, high (local) concentration of initiator, and high targeted molecular weight of polymer (MW > 100 000). Thus, LRP is a relatively limited living polymerization technique in terms of polymerization characteristics.

SFRP is one of the key polymerization techniques used in Chapter 5. Investigation of SFRP of methacrylates is described in Chapter 7. Efforts have been made to explore the possibility of developing new SFRP systems based on stable carbon-centered radical mediation, and the work is described in Chapter 6.

1-2 Combination of Living Polymerization Techniques for Polymer Synthesis

Along with the development of living polymerization techniques, the combination of living polymerization techniques has attracted increasing attention and has been considered as an important method for the synthesis of well-defined copolymers [*37*]. Due to the disadvantages of each individual living polymerization technique, in many cases it is very difficult or impossible to synthesize polymers with the desired architectures and components by using only one type of living polymerization technique, and synthetic strategies based on combination of different types of living polymerization

techniques require careful consideration. For instance, *iso*-butene can only be polymerized by cationic polymerization, while methyl methacrylate cannot be polymerized by cationic polymerization but can be polymerized by a number of techniques including anionic polymerization and radical polymerization. Therefore copolymers of poly(methyl methacrylate) and poly(*iso*-butene) can only be synthesized through combined polymerization techniques [*38*].

With each selected type of living polymerization technique to be used to build a particular part of an entire macromolecular architecture, combination of living polymerization techniques is especially suitable for the synthesis of novel polymers with complex architectures. As the major approach in our work, combination of living polymerization techniques is described in Chapters 2-5 for the synthesis of a series of grafted polymers with well-defined novel architectures.

1-3 Controlled Synthesis of Grafted Copolymers

Grafted copolymers can be considered as macromolecules with one or more junctions connecting a main chain backbone with side chains having constitutional or configurational features different from those of backbone. Controlled synthesis of grafted copolymers, especially novel nanostructured densely grafted copolymers, is the major subject in this dissertation. At the same time, the objective of the synthetic work is not only to develop new synthetic strategies and to achieve new and unique grafted architectures but also to control the morphologies and nanostructures of the final polymers.

***1-3a* Overview of Synthetic Methods.** Typically, "grafting from", "grafting onto", and "grafting through" methods can be used for controlled synthesis of grafted copolymers (**Scheme 1-1**) [*20, 34*].

Scheme 1-1

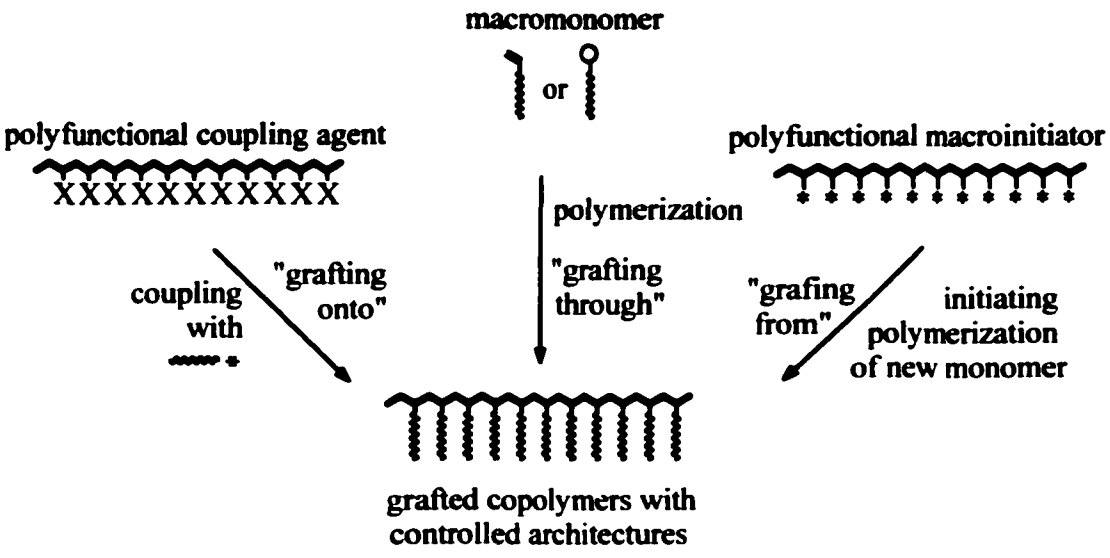

For the "grafting from" method, grafted copolymers are synthesized by polymerization using a macroinitiator with non-terminal initiator sites [*39*]. A (linear) polyfunctional macroinitiator is required to synthesize grafted copolymers with multiple grafts through this strategy. Well-controlled long grafts can be expected if compared with propagation, initiation is relatively fast. The major concern for controlled synthesis of grafted copolymers is then the synthesis of a well-defined polyfunctional macroinitiator, which governs the structures of backbone, graft density, and graft distribution of the grafted copolymers yielded. The purity of products is mainly dependent on whether a small molecule initiator is absent or not.

For the "grafting onto" method, grafted copolymers are synthesized by coupling reaction between polymer species with active ends and a polymeric coupling agent [*40*]. Nearly uniform grafts can be obtained, because polymer species with active ends usually are prepared by living polymerization. Backbone can also be well-controlled when a polymeric coupling agent is prepared based on living or controlled polymerization. However, this method has two major drawbacks. First, an excess of active polymer species generally is required to force the coupling reaction to completion, and therefore purification is needed to separate grafted copolymers from the crude products that also contain linear polymer species. Second, long grafts usually cannot be obtained because the reactivity of active polymer species for graft preparation decreases with chain length due to steric hindrance.

For the "grafting through" method, well-defined grafted copolymers are obtained by polymerization of macromonomers [*41*]. The structures of grafts can be accurately controlled via macromonomer prepared through living polymerization. High graft density and low graft density can be targeted respectively by homopolymerization of macromonomer and copolymerization of macromonomer with conventional monomer. However, because reactivity of macromonomers decreases with increasing molecular weight due to steric effects, long grafts also cannot be obtained. At the same time, the backbone control for grafted copolymers yielded is not good in most cases due to incomplete macromonomer conversion. For these systems, purification is also required to obtain grafted copolymers with high purity.

A general comparison of the three synthetic methods in their structural control capacity is summarized in **Table 1-1**, based on typical systems for each case. "Grafting

from" is used in Chapters 2 and 5. At the same time, for the synthesis of double-brush copolymers described in Chapter 2, a combination of "grafting from" and "grafting onto" methods was applied, and to the best of our knowledge, this is the first time that such a combined strategy for grafted copolymer synthesis was used. To use "grafting from" method, well-defined polyfunctional SFRP macroinitiators and polycarbanionic macroinitiators with controlled structures were synthesized. The background of well-defined polyfunctional macroinitiators is introduced below. "Grafting through", i.e. polymerization of macromonomers, is used in Chapters 3 and 4 to synthesize poly(macromonomer)s from norbornenyl-functionalized macromonomers. A general background of the synthesis and polymerization of macromonomers is given in the introduction section of Chapter 3. Specific background of synthesis and polymerization of norbornenyl-functionalized macromonomers is given in the introduction section of Chapter 4.

Table 1-1. Comparison of Synthetic Methods of Grafted Copolymers in Structural Control Capacity

method	backbone control	graft control	graft density
"grafting from"	good	fair, can be long	good, can be high
"grafting onto"	good	good (short)	unfavorable for high
"grafting through"	depends	good (short)	good, can be high

1-3b **Well-Defined Polyfunctional Macroinitiators.** It has been a long-term interest of polymer chemists to develop well-defined polyfunctional macroinitiators for

living polymerization, because these macroinitiators can be used to further synthesize a variety of well-defined grafted copolymers. However, due to synthetic difficulties, successful syntheses of well-defined polyfunctional macroinitiators have not been achieved until recently [*42-47*]. The typical synthetic strategy is shown in **Scheme 1-2.** Functionalized monomer with functional group *A* is prepared and is polymerized by living polymerization (type *a*) to yield well-defined polymer with quantitative functional group *A*. If group *A* can directly serve as an initiator site for living polymerization (type *b*), then the functionalized polymer can be referred to as a well-defined polyfunctional macroinitiator. If group *A* can be quantitatively converted into group *B* which can serve as an initiator site for living polymerization (type *b*), then the functionalized polymer with quantitative group *B* can be referred to as a well-defined polyfunctional macroinitiator. In the former case, type *b* generally is different from type *a*; in the latter case, type *b* can be either the same as or different from type *a*.

Scheme 1-2

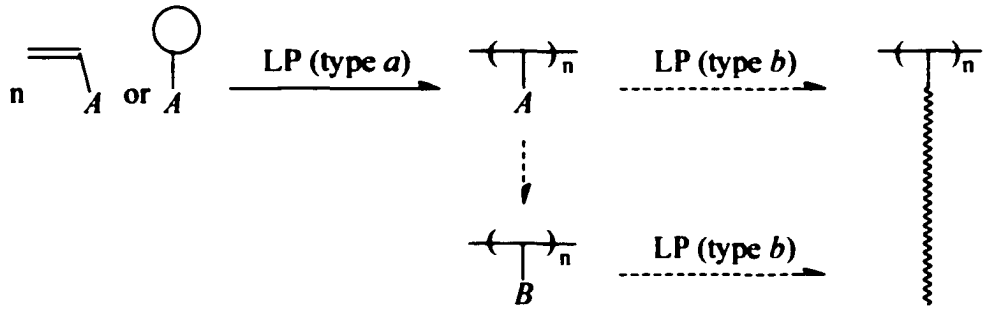

LP: living polymerization.

For anionic polymerization, no well-defined polycarbanionic macroinitiators have been reported. It is this dissertation that describes the first polycarbanionic macroinitiators with well-controlled number-average initiator site (Chapter 2). Polymerization using polycarbanionic macroinitiators provides the only method for the synthesis of densely grafted copolymers with relatively long grafts. The grafted polycarbanionic macroinitiators with initiator sites on graft junctions have novel complex architectures different from all types of polyfunctional macroinitiators reported, and they can further lead to unique double-brush copolymers.

For LRP, a number of well-defined ATRP polyfunctional macroinitiators have been reported, and from these macroinitiators, a variety of grafted copolymers with complex architectures have also been synthesized [*42-45*]. A number of SFRP polyfunctional macroinitiators have also been prepared and used for grafted copolymer synthesis before our work [*42, 48-50*]. Only one type of them, with statistically distributed alkoxyamine functionality, has well-defined structures [*42*]. On the other hand, in our synthetic efforts, an ensemble of well-defined SFRP polyfunctional macroinitiators with different structural features have been prepared by living anionic polymerization with an alkoxyamine-functionalized monomer, and from these macroinitiators, a variety of well-defined grafted copolymers with complex architectures have been further prepared (Chapter 5). Unlike polycarbanionic macroinitiators, LRP polyfunctional macroinitiators suffer from irreversible biradical terminations, especially irreversible biradical coupling. To control the structures of the grafted copolymers synthesized, special care should be taken and the preferred monomer conversion decreases as initiator site number and density increase.

Well-defined cationic polyfunctional macroinitiators have also been reported, and from these macroinitiators, a variety of grafted copolymers with complex structures have also been obtained [*46, 47*]. Although cationic polyfunctional macroinitiators were not prepared in our work, the polyfunctional DPE-agent reported in this dissertation potentially can also be converted into cationic polyfunctional macroinitiators [*51, 52*].

For other types of living polymerization techniques, no polyfunctional macroinitiators have been reported, and no efforts have been made to develop them in this work. desire

1-4 Synthetic Strategies for Polymeric Nanostructures with Stabilized Self-Assembly

Novel macromolecular architectures are of important significance, especially in theoretical aspect. At the same time, controlled polymeric morphologies are also desired by polymer chemists in their efforts to establish new applications of polymer materials [*53*]. Therefore, our synthetic designs for novel polymers with complex macromolecular architectures targeted new types of polymeric nanostructures with controlled self-assembled morphologies.

It is well known that block copolymers can form a wide variety of polymeric nanostructures based on self-assembly [*54*]. However, one of the major limitations of such nanostructures is their weak stability under changing environmental conditions. Therefore, as illustrated in **Scheme 1-3**, a number of strategies have been developed to obtain polymeric nanostructures with stabilized assemblies.

Typically, polymeric self-assemblies can be stabilized by linking the chain-ends of block copolymers with chemical bonds. Polymerization of diblock macromonomers with terminal polymerizable group [*55-57*], linking block polymeric species with polyfunctional coupling agents [*58*] or via bifunctional monomers [*59*], and block copolymerization using multifunctional initiators [*60*] or polyfunctional macroinitiators [*45, 61*] all can be considered as synthetic work following this strategy. The formed polymers typically can be referred to as star-block copolymers, graft-block copolymers, or unimolecular micelles can be used to further prepare a variety of polymer-based nanomaterials [*62, 63*].

Scheme 1-3

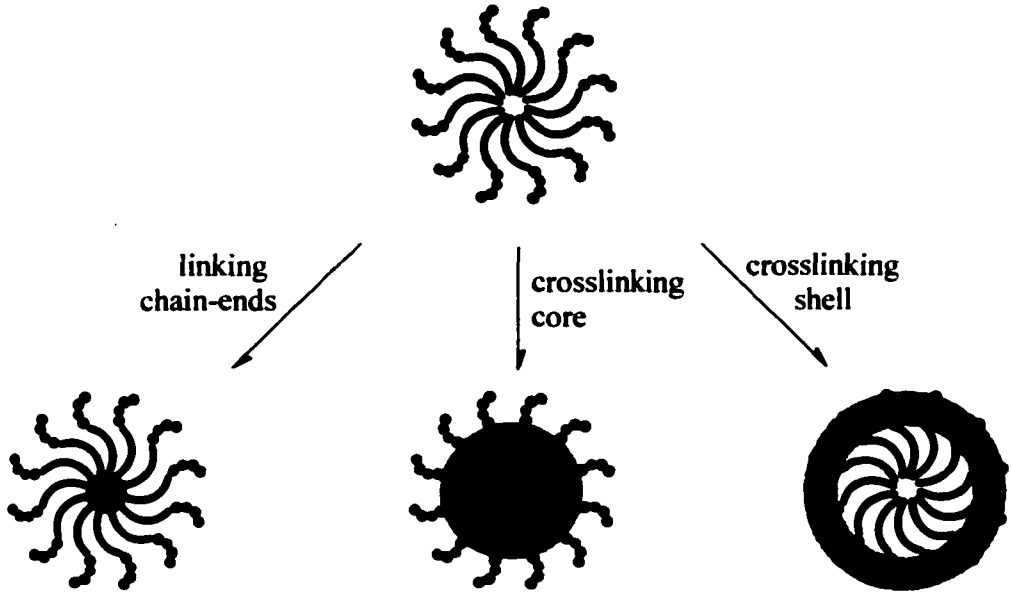

Recently, crosslinking chemistry has also been introduced to stabilize self-assemblies of block copolymers. Based on selective crosslinking either core part or shell part of core-shell self-assemblied nanostructures formed by block copolymers, a number

of stabilized novel polymeric nanostructures, including shell-crosslinked nanoparticles [*64*], nanocage [*65*], core-crosslinked nanofiber [*66*], nanotube [*67*], have been synthesized.

Some of our work on novel nanostructured polymer synthesis followed the first strategy, i.e. linking chain-ends of block copolymers, by block copolymerization using linear polycarbanionic macroinitiators (Chapter 2) or well-defined SFRP polyfunctional macroinitiators (Chapter 5).

Scheme 1-4

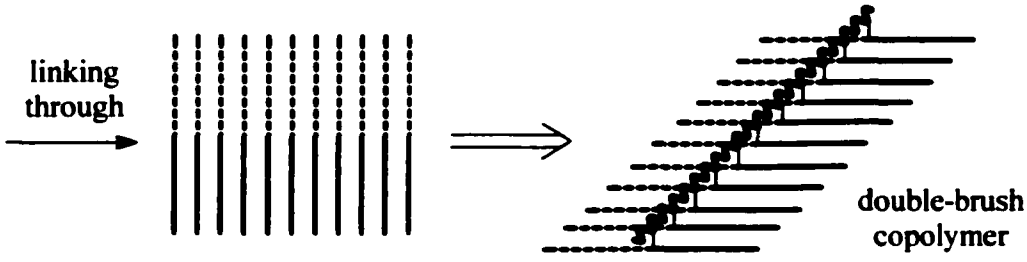

Some of our work on novel nanostructured polmer synthesis followed an original strategy of linking block junctions of block copolymers (**Scheme 1-4**), by either polymerization using grafted polyfunctional macroinitiators with initiator site on graft junctions (Chapter 2) or polymerization of diblock macromonomers with block junctions carrying polymerizable group (Chapter 3). The double-brush copolymers thus obtained have not only new and unique macromolecular architectures, but also possess novel self-assembled polymeric morphologies. Double-brush copolymers are expected to have borad potential applications in areas including nanoparticle and nanocomposite preparation, surface and interface modification, drug and gene delivery, etc.

Chapter 2

Synthesis of Grafted Copolymers, Including Double-Brush Copolymers, Based on Polycarbanionic Macroinitiators with Controlled Structures

Abstract: Linear polyfunctional DPE-agent was synthesized by ring-opening metathesis polymerization of norbornene functionality of DPE-norbornene bifunctional monomer with DPE functionality intact. Quantitative monoaddition of *sec*-butyllithium on DPE functionalities of polyfunctional DPE-agent yielded linear polycarbanionic macroinitiatiors with controlled structures. Densely grafted copolymers with relatively long grafts having block structures were synthesized by anionic polymerization using linear polycarbanionic macroinitiators. Based on monoaddition of poly(styryl)lithium on DPE functionalities of polyfunctional DPE-agent, polystyrene-grafted polycarbanionic macroinitiators with different structural features were synthesized. Representing novel and unique macromolecular architectures, a variety of double-brush copolymers, with graft junctions simultaneously connecting heterografts to backbone, were synthesized by anionic polymerization using polystyrene-grafted polycarbanionic macroinitiators. Amphiphilic double-brush copolymers were further obtained via subsequent modification reactions. Novel nanostructures of double-brush copolymers were expected by theoretical analysis, and were supported by preliminary characterization results.

2-1 Introduction

Scheme 2-1

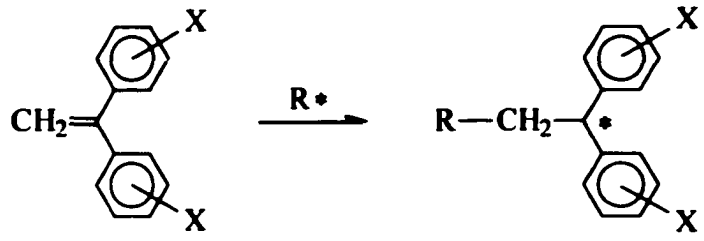

DPE-functionalized anion (as initiator), cation (as initiator), and radical (as mediating radical)

DPE-agent

X: can be H, simple functionalities, or polymer chains;
R: can be small molecular or polymeric structures;
•: can be anion, cation, or radical.

Synthesis of well-defined polymers is a major goal of polymer synthetic chemistry. Among many synthetic strategies developed for the synthesis of well-defined polymers, application of 1,1-diphenylethylene (DPE) chemistry in polymerization has attracted increasing attention [*1-27*]. The essence of DPE chemistry is that DPE and its derivatives generally are non-homopolymerizable due to steric hindrance, and at the same time, DPE-functionalized anion, cation, and radical have balanced stability due to resonance effects, therefore can be readily generated to serve as anionic initiator, cationic initiator, and mediating radical or to be further converted into various functionalities (**Scheme 2-1**). Thus, DPE has been used in radical polymerization recently to develop a synthetic method for block copolymers with industrial application potential [*2-4*]. DPE and its derivatives have also been used in cationic polymerization for the syntheses of block copolymer [*5, 6*], A_2B_2 heteroarm star copolymer [*7*], and macromonomer [*8*]. However, the most impressive successes of the application of DPE chemistry in

polymerization were achieved in anionic polymerization [*1, 9-27*]. Besides numerous block copolymers, functionalized polymers and macromonomers reported, bifunctional [*9, 10*], trifunctional [*11*] initiators and a wide variety of complex polymers have been synthesized by using DPE and its derivatives in anionic polymerization. These complex polymers include exact grafted copolymer with two branches [*12*], ABC hetero-3-arm star copolymers [*13-17*], A_2B_2 heteroarm star copolymers [*18, 19*], and many other heteroarm star copolymers (AB_3, AB_4, A_2B_4, A_2B_{12}, ABC_2, ABC_4, AB_2C_2, $A_2B_2C_2$) [*20-26*]. For all applications of DPE chemistry in polymerization, the structures of DPE-agents used are of critical importance. Many types of monofunctional DPE-agents, several types of bifunctional DPE-agents [*9, 10*], and one type of trifunctional DPE-agent [*11*] have been synthesized and applied. Moreover, DPE functionality has also been introduced on a silica surface for polymer brush synthesis [*27*]; polymer beads carrying DPE functionality have also been reported [*28*]. However, although it is obvious that a soluble polyfunctional DPE-agent is of importance to achieve new types of complex macromolecular architectures, it has not been reported yet. Significant efforts have been made in this dissertation research to develop polyfunctional DPE-agent. This chapter describes the first synthesis of a polyfunctional DPE-agent and its application to the syntheses of polyanionic macroinitiators and novel grafted copolymers, including graft-block copolymers and double-brush copolymers.

The polyfunctional DPE-agent was synthesized by selective polymerization of norbornenyl functionality of DPE-norbornene bifunctional agent by ring-opening metathesis polymerization (ROMP) with high selectivity towards strained carbon-carbon double bonds. Such successful synthesis illustrates that unlike typical chain

polymerization techniques, i.e. anionic, cationic, and radical polymerizations, ROMP can potentially serve as a universal technique for the synthesis of polymers with polyfunctional (substituted) vinyl functionality [*29*].

Linear and grafted polycarbanionic macroinitiators were synthesized by the reaction of polyfunctional DPE-agent with small molecule and polymeric organolithiums respectively. The polycarbanionic macroinitiators for living anionic polymerization with quantitative anionic initiator site per structure unit is a first synthesis since Szwarc first reported living anionic polymerization using carbanionic initiator in 1956 [*30*]. Efforts had been made before by others to develop polycarbanionic initiators through other strategies, but no polycarbanionic initiators with controlled structures could be obtained [*31*].

Linear polycarbanionic macroinitiator can be used to prepare densely grafted copolymers. Because of the excellent structural control ability of living anionic polymerization, this strategy actually provides the only way to date to give densely grafted copolymers with well-controlled long grafts (DP_n up to 1000). Other strategies [*32*], such as "grafting onto", "grafting through", or using other types of polyfunctional macroinitiators, were not successful for such syntheses. By manipulating block structures into grafts through sequential addition of different monomers, the graft-block copolymers synthesized from linear polycarbanionic macroinitiators can have core-shell spherical star-like morphology for short backbones relative to grafts and core-shell rod-like morphology for long backbones relative to grafts, and in principle, they can be used as template for the preparation of a variety of nanomaterials, such as nanoparticles, nanowires, and nanocomposites [*33, 34*].

On the other hand, grafted polycarbanionic macroinitiators with anionic sites on graft junctions are unique, and an analogous macroinitiator has not been reported before. Anionic polymerization using such grafted polycarbanionic macroinitiators directly yielded double-brush copolymers, which have graft junctions simultaneously carrying two heterografts. Chapter 3 also describes double-brush copolymer synthesis, but by ROMP of diblock macromonomer with nonterminal norborneneyl group. Other synthetic strategies, such as copolymerization of different types of macromonomers [*35*] or using polyfunctional coupling agent to link different types of polymers for side-chains [*36*], cannot lead to well-defined grafted polymer with double-brush architectures.

These double-brush copolymers not only represent a unique model type of macromolecular architectures, but also are expected to have a variety of novel nanostructures due to self-assembly of their two types of grafts. The nanostructures of double-brush copolymers may not be as stable as these of crosslinked nanoparticles, but would be much more stable than these of linear copolymers. At the same time, double-brush copolymers would be as easy to apply as linear copolymers. Thus, with well-organized polymeric components with contrasting properties (polar vs. nonpolar, hydrophobic vs. hydrophilic, non-ionic vs. cationic or anionic, insulator vs. ionic-conductor, non-biodegradable vs. biodegradable, high surface energy vs. low surface energy, and plastic vs. rubber) in unusual nanophase-separated regions, double-brush copolymers are expected to have broad potential applications in areas including nanoparticle and nanocomposite preparation, surface and interface modification, drug and gene delivery, etc.

In the next sections of this chapter, the synthesis of a polyfunctional DPE-agent and its applications in anionic polymerization for the preparation of polycarbanionic macroinitiators and densely grafted copolymers, especially double-brush copolymers, will be illustrated in detail; the preliminary characterization of the nanostructures of double-brush copolymers will also be described briefly. Further investigations on nanostructures of double-brush copolymers and applications of double-brush copolymers and graft-block copolymers will be carried out, but cannot be included in this dissertation.

2-2 General Synthetic Design

The synthetic strategy of grafted copolymers via polycarbanionic macroinititors with controlled structures is illustrated by **Scheme 2-2**. ROMP of DPE-functionalized norbornene (NB) monomer was carried out with DPE functionality intact. Linear polyfunctional DPE-agent formed was used to react with small-molecular alkyllithium to give linear polycarbanionic macroinitiators. Grafted copolymers, with long grafts and block structures of grafts, were synthesized by anionic graft polymerization using the linear polycarbanionic macroinitiators. Linear polyfunctional DPE-agent formed was used to react with polymeric alkyllithiums to give grafted polycarbanionic macroinitiators. With new and unique macromolecular architectures, double-brush copolymers were synthesized by anionic graft polymerization using the grafted polycarbanionic macroinitiators.

Scheme 2-2

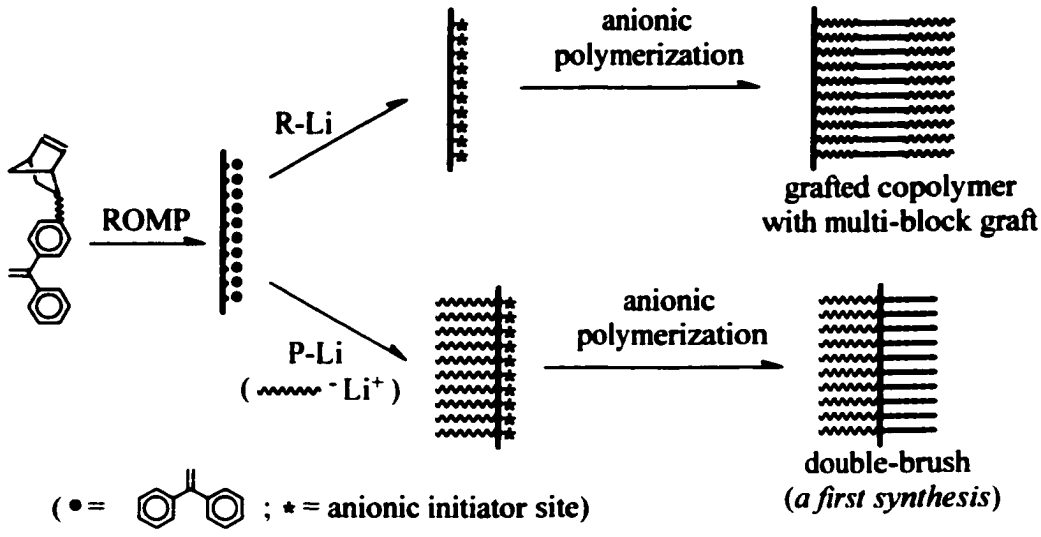

2-3 Synthesis of Polyfunctional 1,1-Diphenylethylene-Agent

Polyfunctional DPE-agent used in this study need have many DPE functionalities, optimally with quantitative number and regular distribution, connected to a linear main-chain (rather than a core) which is inert under typical anionic polymerization conditions. One can expect that polymerization of DPE-functionalized monomer with DPE functionalities intact yields the polyfunctional DPE-agent required. However, DPE functionality has reactivity under typical radical, anionic, and cationic polymerization conditions; typical condensation and most types of ring-opening polymerization, on the other hand, involve the formation of linkages that are vulnerable to carbanions. Thus, we finally focused on ROMP of DPE-functionalized norbornene monomer for the synthesis of polyfunctional DPE-agent (**Scheme 2-3**).

Scheme 2-3

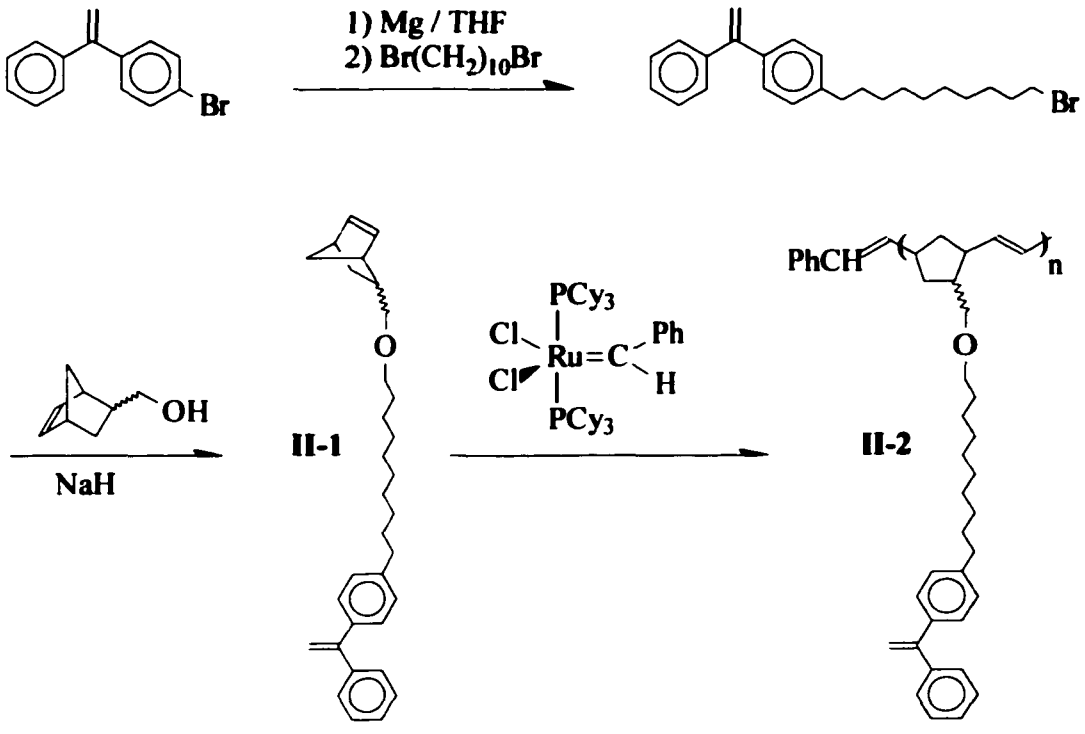

DPE-functionalized norbornene monomer **II-1** was synthesized first. Monomer **II-1** has both a norbornene functionality and a DPE functionality connected by a $-CH_2O(CH_2)_{10}-$ spacer alleviating steric effects between the two functionalities. Because *exo/endo* mixed 5-norbornene-2-methanol was used as a reactant, **II-1** initially yielded also contains both *exo* and *endo* isomers. TLC analysis showed that the *exo* and *endo* isomers have a small difference of about 0.05 in retention factor using 1:1 pentane-dichloromethane as eluent. With separation by flash column chromatography, small amounts of *exo*-**II-1** and *endo*-**II-1** were obtained besides a majority of *exo/endo* mixed **II-1**, that is, *exo/endo*-**II-1** (*exo/endo* = 43/57). The *exo*-**II-1** and *endo*-**II-1** were distinguished by GOSEY experiment, and their ^1H NMR spectra were shown in **Figure**

2-1. Highly strained norbornene functionality typically has high reactivity towards ROMP. DPE olefin moiety is not strained, and suffers steric hindrance due to the two phenyl groups substituted on the same side of double bond, therefore the DPE olefin moiety theoretically should have no or very low reactivity towards olefin metathesis. Thus, it is expected that polyfunctional DPE agent can be prepared by ROMP of the norbornene functionality of **II-1** with its DPE functionality intact. ROMP behavior of **II-1** was investigated and our expectation was verified.

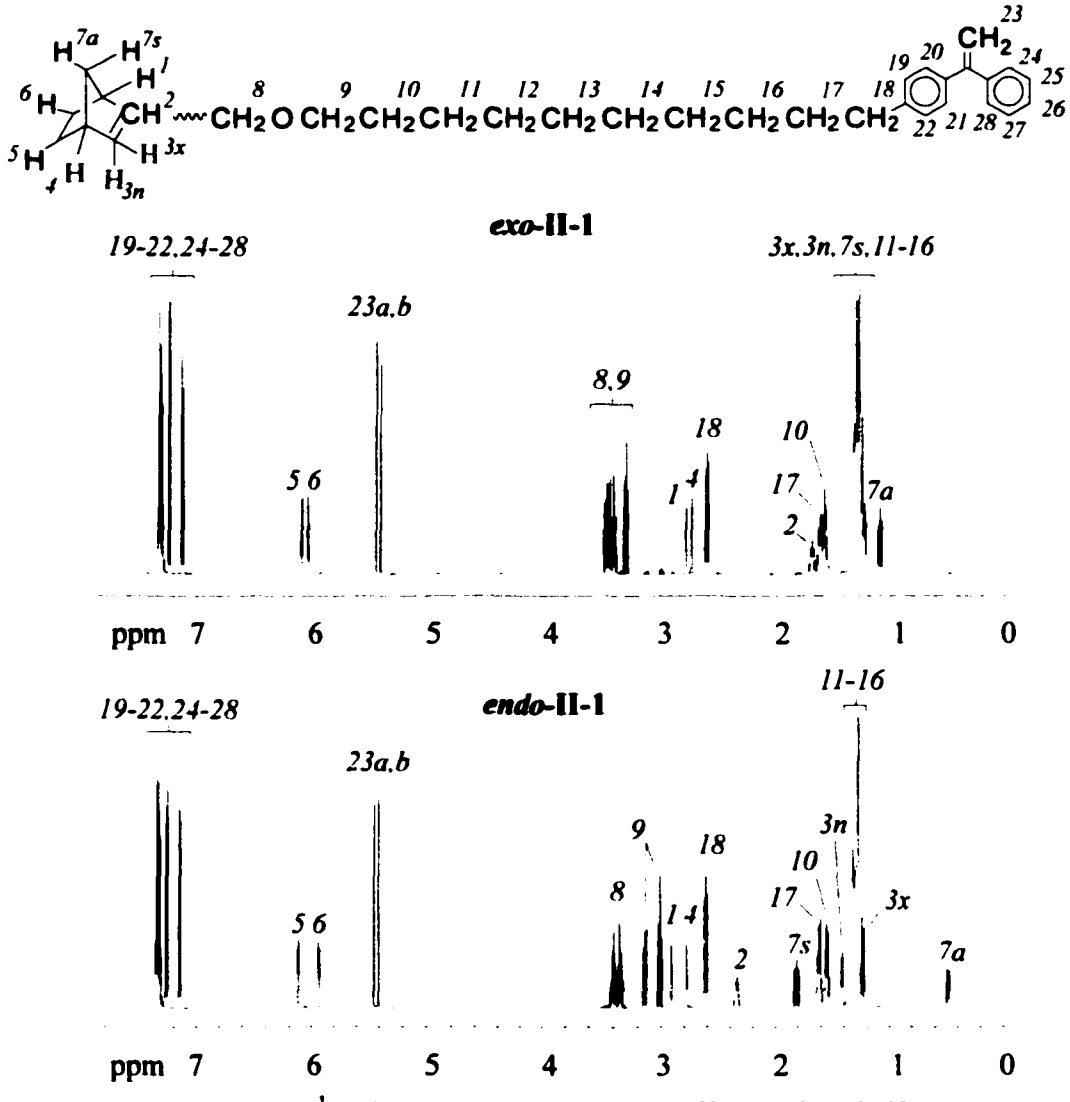

Figure 2-1. ^{1}H NMR spectra of **II-1** (*exo*-**II-1**, and *endo*-**II-1**)

Table 2-1. Synthesis of Polyfunctional DPE-Agent II-2 [a]

no	$[II\text{-}1]_0/[I]_0$	DP_{NMR}	PDI_{GPC} [b]	Initiation efficiency
II-2a	15	22	1.46	0.68
II-2b	200	220	1.79	0.91

[a] In THF; room temperature; 3 h. [b] Calibrated with linear polystyrenes.

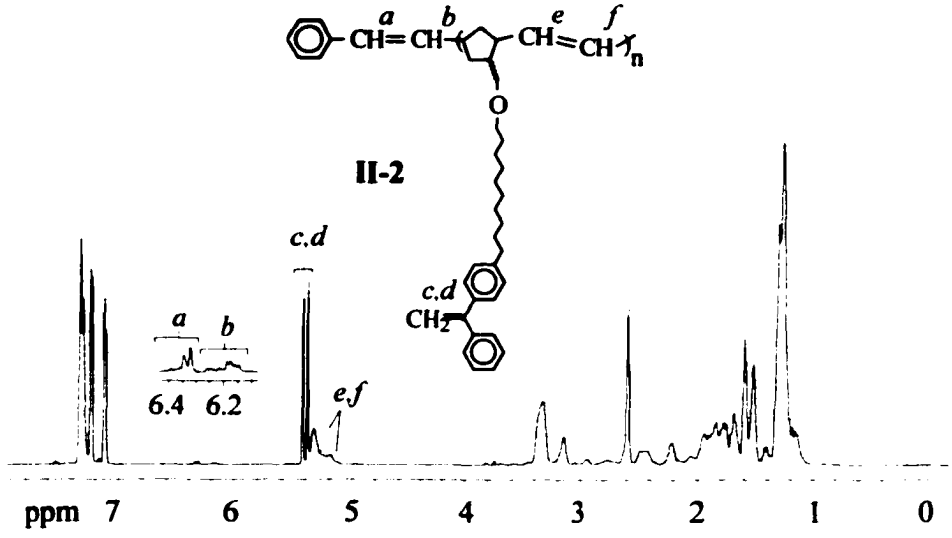

Figure 2-2. ^1H NMR spectrum of polyfunctional DPE agent **II-2**.

Two ROMP experiments of *exo/endo*-**II-1** were carried out in THF at room temperature (**Table 2-1**). Grubbs catalyst $RuCl_2(CHC_6H_5)[P(C_6H_{11})_3]_2$ was used as initiator because of its high functional group tolerance [*38*]. NMR analysis of the polymerization product, i.e. **II-2**, indicated that ROMP of **II-1** was a completely selective process with only norbornene functionality polymerized. As shown in **Figure 2-2**, the ^1H NMR spectrum of corresponding polymer **II-2** shows no resonance of norbornenyl alkene protons at 6.12, 6.05, and 5.94 ppm but has broad resonances of polynorbornene

alkene protons concentrated at 5.33 ppm, indicating that the norbornene functionality of **II-1** was completely converted into the high trans polynorbornene main-chain of **II-2**. On the other hand, the essentially quantitative ^{1}H NMR resonance intensities of DPE alkene protons of **II-2** at 5.44 and 5.40 ppm indicate that DPE functionality of **II-1** was not involved in the ROMP process. Because of the living characteristics of ROMP process, the α-chain-end of **II-2** should have C_6H_5CH=CH– moiety from the initiator. ^{1}H-^{13}C GHMBC and GHMQC 2D NMR characterization of **II-2** verified such α-chain-end structure and identified the ^{1}H NMR resonances of corresponding alkene protons at 6.43-6.09 ppm. Therefore, the number-average degree of polymerization (DP_n) of **II-2** can be determined by ^{1}H NMR by comparing the resonance intensities of the α-chain-end alkene protons with the resonance intensities of all DPE and polynorbornene alkene protons in monomer units at 5.00-5.50 ppm. The DP_n values thus obtained, 22 for **II-2a** and 220 for **II-2b**, were higher than the molar feed ratio of monomer to initiator, suggesting incomplete initiator consumption that was verified by ^{1}H NMR. Along with major ^{1}H NMR resonances for the propagating chain-end Ru=CH– proton of **II-2** around 18.96 ppm, minor ^{1}H NMR resonances of the Ru=CH– proton at 19.98 ppm for catalyst were observed in the polymerization solutions before they were terminated with ethyl vinyl ether, suggesting a slow initiation relative to propagation in ROMP of **II-1**. Monomodal molecular weight distribution of **II-2** was observed by GPC analysis, but the *PDI* values of 1.46 and 1.79 relative to linear polystyrene obtained for **II-2a** and **II-2b** respectively were not low because polymer chains of **II-2** could not begin to propagate at the same period of time due to slow initiation. Any effort to solidify **II-2** from solution finally resulted in insoluble product. However, **II-2** is relatively stable in solution, and no change

on composition or molecular weight could be detected by ^{1}H NMR and GPC analyses after storing the THF solution of **II-2** in room temperature for months.

Further investigation of ROMP of **II-1** was carried out using different catalysts, different solvents, and different types of isomers of **II-1**. When molybdenum-based Schrock initiator $Mo(C_{10}H_{12})(C_{12}H_{12}N)[OC(CH_3)(CF_3)_2]_2$ was empolyed as initiator [*14*], benzaldehyde was used for termination. The ROMP process is also selective for norbornene functionalities of **II-1**, but **II-2** yielded has high cis polynorbornene main-chain as indicated by the broad-line ^{1}H NMR resonances of polynorbornene alkene protons concentrated at 5.20 ppm, and the polydispersities of the **II-2** obtained by GPC were still around 1.50 due to slow initiation relative to propagation. The major drawback for the ROMP of **II-1** initiated by Schrock catalyst is that the initiation efficiency was relatively low (~20%) as indicated by ^{1}H NMR analysis based on resonance intensities of alkene protons of $C_6H_5CH{=}CH-$ moiety on ω-chain-end of **II-2** formed, presumably because part of initiator was consumed by impurities in the polymerization systems due to the high reactivity of the initiator. Different solvents were used for both Grubbs catalyst-initiated (THF, chloroform, methylene chloride) and Schrock catalyst-initiated (toluene, THF) ROMP systems, and no obvious effects of solvents on polymerization results were found. Important improvements in structural control of **II-2** were observed when *endo*-**II-1** was used as monomer (**Figure 2-3**).

ROMP of *exo*-**II-1**, *endo*-**II-1**, and *exo/endo*-**II-1** initiated by Grubbs catalyst with different molar feed ratio of monomer to initiator were carried out and polymerization results were compared. For each trial, complete monomer conversion was reached; DP_n of polymer **II-2** yielded was determined by ^{1}H NMR based on the α-chain-end alkene

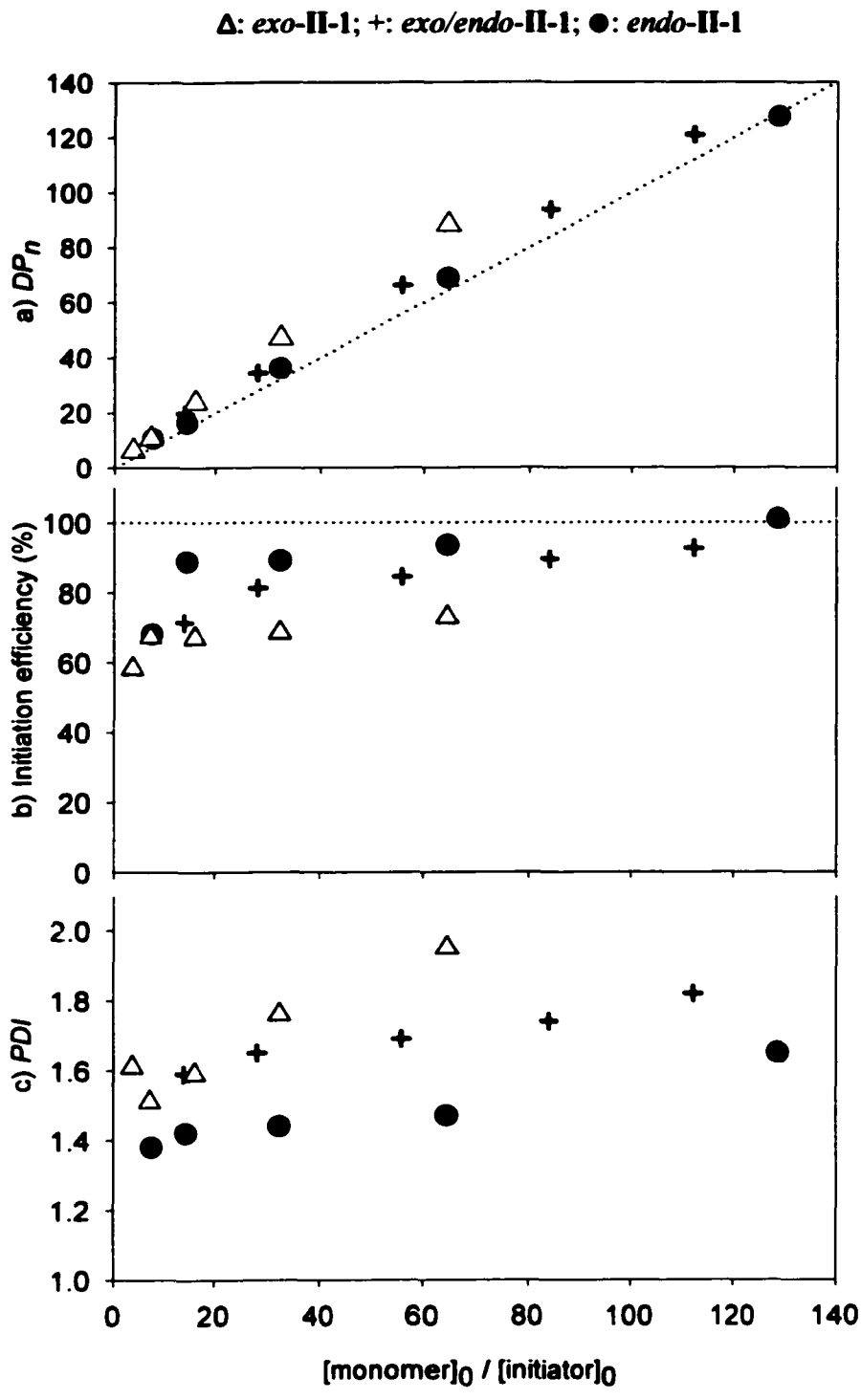

Figure 2-3. Dependence of a) DP_n, b) initiation efficiency, and c) *PDI* on molar feed ratio of monomer to Grubbs catalyst for ROMP of **II-1** in THF

protons at 6.43-6.09 ppm; initiation efficiency (I_e: $I_e=\{[\textbf{II-1}]_0/[\textbf{I}]_0\}/DP_n$) was calculated; polydispersity was determined by GPC relative to linear polystyrenes. As shown in **Figure 2-3**, the series using *endo*-**II-1** not only have excellent agreement between DP_n values of **II-2** and the molar feed ratio of monomer to initiator ($[\textbf{II-1}]_0/[\textbf{I}]_0$), but also have high initiation efficiency and exhibit lower polydispersities than the other two series using *exo*-**II-1** and *exo/endo*-**II-1**. At the same time, the series using *exo*-**II-1** showed contrary polymerization results, with somewhat poor agreement between DP_n values of **II-2** yielded and $[\textbf{II-1}]_0/[\textbf{I}]_0$, but lower initiation efficiency and higher *PDI* values than others. Such contrast indicates that the polymerization of *endo*-**II-1**, whose norbornene olefin suffers higher steric hindrance due to *endo*-substitution, has the highest rate ratio of initiation to propagation k_i/k_p, and the polymerization of *exo*-**II-1** has the lowest k_i/k_p. Thus, it can be further expected that polyfunctional DPE-agent with predetermined DP_n and low polydispersity can be synthesized by ROMP of DPE-norbornene bifunctional monomer with further increased steric hindrance towards its norbornene olefin moiety. Because only a small amount of *endo*-**II-1** was separated, polyfunctional DPE-agents prepared from *exo/endo*-**II-1**, i.e. **II-2a** and **II-2b**, were used for further reactions.

2-4 Synthesis of Grafted Copolymers Based on Linear Polycarbanionic Macroinitiators

2-4a **Synthesis of Linear Polycarbanionic Macroinitiators.** To synthesize linear polycarbanionic macroinitiators, small molecule alkyllithium is needed to react with polyfunctional DPE-agent. Thus, *sec*-butyllithium (*s*-BuLi) was chosen to react with

polyfunctional DPE-agent **II-2** because it has higher reactivity than most other commercially available small molecule alkyllithiums (**Scheme 2-4**) [*31*]. THF was used as solvent to avoid the formation of insoluble product due to carbanion association.

Scheme 2-4

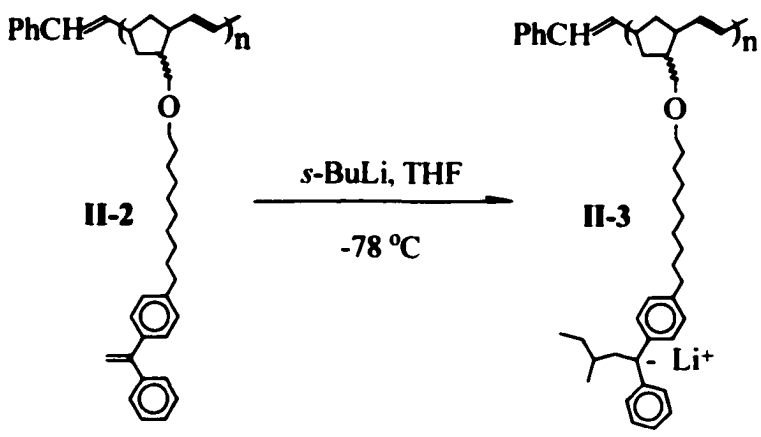

Table 2-2. Synthesis of Linear Polycarbanionic Macroinitiator II-3

entry	DPE-agent	conv(%) [a]	N_{DPE-Li} [b]
II-3a	**II-2a**	100	22
II-3b	**II-2b**	100	220

[a] Conversion of DPE functionalities on **II-2**, by ^{1}H NMR from its methanol-terminated adduct. [b] Number-average DPE-functionalized alkyllithium species on **II-3**.

The reaction was induced by adding excess *s*-BuLi ($[s\text{-BuLi}]_0/[DPE]_0 = 2.0$) into the THF solution of **II-2** at -78 °C. Fast formation of DPE-functionalized alkyllithium species was indicated by the immediate appearance of its characteristic red color. As a result, linear polyanionic macroinitiator **II-3** with quantitatively one DPE-functionalized

alkyllithium site per repeating unit was yielded (**Table 2-2**). Because of high reactivity of **II-3**, direct analysis of **II-3** is not feasible. Therefore the structures of **II-3** were probed through the methanol-terminated adduct of **II-3**. GPC analysis showed that compared with GPC peak of corresponding **II-2**, the GPC peak of the adduct moved a little to the high-molecular-weight side but had no change in shape and *PDI* value, indicating no occurrence of intermolecular crosslinking due to the non-homopolymerizability of DPE functionality. ^{1}H NMR analysis of the adduct (**Figure 2-4**) indicated that no matter whether **II-2a** or **II-2b** was used as reactant, the monoaddition of *s*-BuLi on DPE functionality was quantitative. The characteristic ^{1}H NMR resonance of DPE alkene protons at 5.44 and 5.40 ppm completely disappeared, suggesting the complete consumption of DPE functionalities. At the same time, new ^{1}H NMR resonances centered at 0.51, 0.62, 0.95, 1.76, 2.36 ppm were observed as the results of monoaddition. The resonances centered at 0.51 and 0.62 ppm corresponding to the methyl protons of *s*-BuLi fragment have the same integration area without considerable overlap with all other ^{1}H NMR resonances. Integration area of either of them relative to the area of the resonances for the alkene protons of polynorbornene main-chain at 5.50-5.00 ppm gave a value of 2.98:2.00 that is in a close agreement with the expected proton number ratio of 3:2, further confirming the quantitative addition of a stoichiometric amount of *s*-BuLi to DPE functionalities on **II-2** and also indicating that the ether linkage on $-CH_2O(CH_2)_{10}-$ spacer has a good stability towards DPE-functionalized alkyllithium species. On the other hand, the α-chain-end alkene unsaturation of **II-2** exhibited very low reactivity towards addition with *s*-BuLi. Nearly quantitative resonances for the alkene protons at 6.43-6.09 ppm were observed on the ^{1}H NMR spectrum of the methanol-terminated adduct of **II-3**.

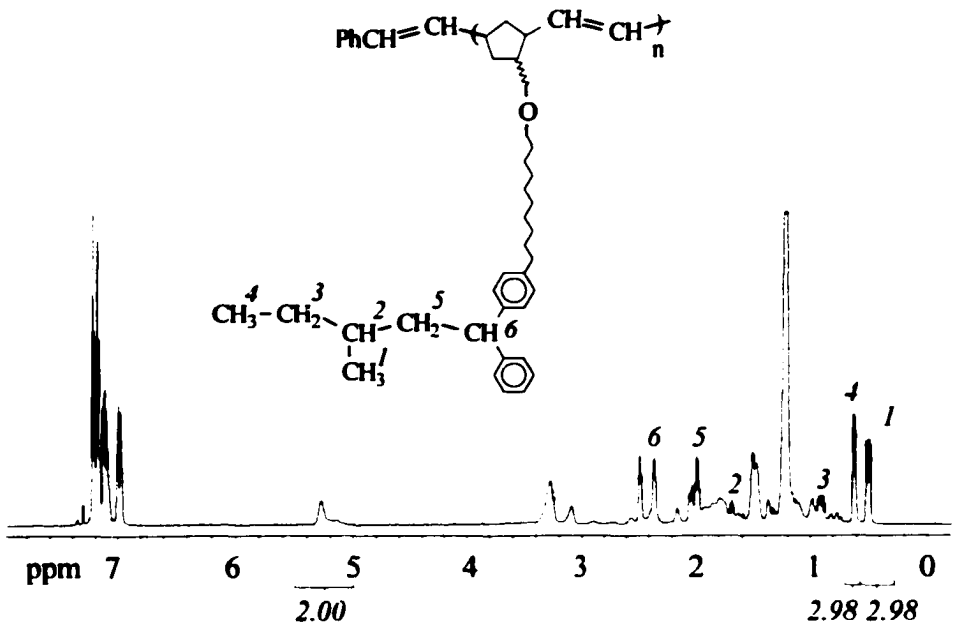

Figure 2-4. ^{1}H NMR spectrum of methanol-terminated adduct of **II-3**

***2-4b* Synthesis of Graft-Block Copolymers by Anionic Graft Polymerization Using Linear Polycarbanionic Macroinitiators.** With quantitatively one DPE-functionalized alkyllithium anionic initiator site per repeating unit, linear polycarbanionic macroinitiators can be used to synthesize densely grafted copolymers via living anionic graft polymerization. Different from living radical polymerization systems that suffer irreversible biradical coupling reactions and are not suitable for well-controlled synthesis of long grafts [*40*], living anionic polymerization systems have no considerable occurrence of chain termination or transfer reactions, and therefore can be used to synthesize long grafts with accurate structural control. Typical monomers that can be initiated by DPE-functionalized alkyllithium include styrenes, dienes, methacrylates, *tert*-butyl acrylate (*t*-BA), and 2-vinylpyridine (2-VP) [*1*, *41*]. However, anionic polymerization of styrenes and dienes initiated by DPE-functionalized alkyllithium has a

slow initiation relative to propagation, resulting in broad length distribution of the polymer chain formed. Therefore, methyl methacrylate (MMA), the most common one of methacrylates, and *t*-BA were used as monomers for anionic graft polymerization using linear polycarbanionic macroinitiators **II-3**.

Scheme 2-5

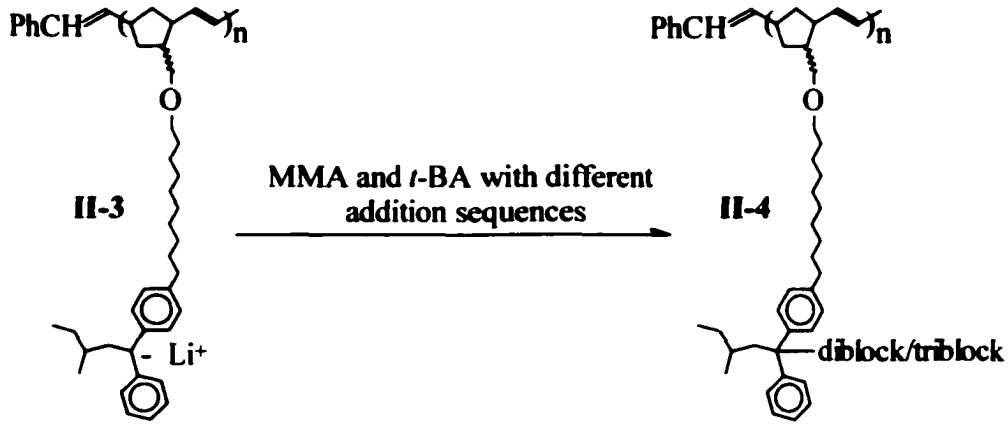

Table 2-3. Synthesis of Graft-Block Copolymer II-4

entry	initiator	N_G[a]	monomer addition[b]	graft formed[c]	M_n[d]	PDI[e]
II-4a	**II-3a**	22	100M; 100B	$-(M)_{94}(B)_{98}$	520K	1.16
II-4b	**II-3a**	22	100M; 100B; 100M	$-(M)_{94}(B)_{98}(M)_{100}$	740K	1.16
II-4c	**II-3a**	22	100B; 900M	$-(B)_{96}(M)_{810}$	2.5M	1.16
II-4d	**II-3b**	220	80B; 80M	$-(B)_{78}(M)_{75}$	4.2M	1.46

[a] Average graft number . [b] By the sequence of addition; number means the molar feed ratio of monomer to DPE-functionalized initiator site; M: MMA, B: *t*-BA. [c] DP_n for each block was estimated by ^{1}H NMR. [d] M_n calculated from graft number and graft size.

[e] By GPC calibrated with linear polystyrenes.

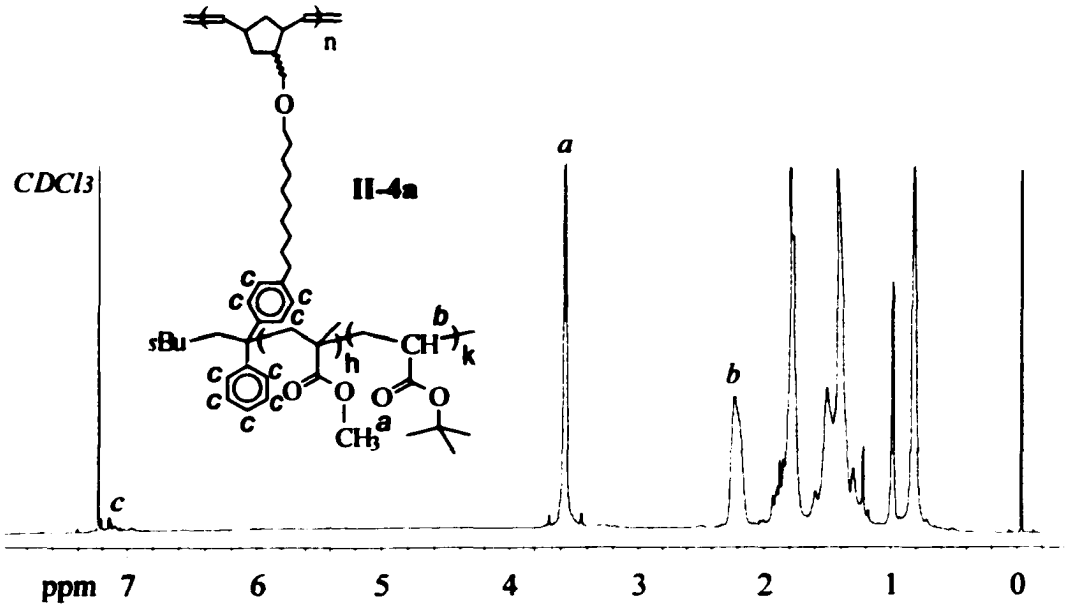

Figure 2-5. ^{1}H NMR spectrum of **II-4a**

Anionic graft polymerization initiated by linear polycarbanionic macroinitiator **II-3** was carried out in THF using ten equivalents of lithium chloride, as additive, relative to DPE-functionalized alkyllithium sites. Because DPE-functionalized alkyllithium has good stability but *s*-BuLi has very poor stability in THF, fresh **II-3** solutions, which contain *s*-BuLi because an excess of *s*-BuLi was used in the preprartion of **II-3**, allowed to stand at -78 °C for 1-2 h to selectively remove most *s*-BuLi remaining without considerable influence on the concentration of DPE-functionalized alkyllithium sites before they were employed for anionic graft polymerization. Targeting a variety of block structures of grafts, both MMA and *t*-BMA were used as monomers for all trials following different addition sequence; sufficient intervals (~1 h) were arranged between monomer additions to allow complete monomer conversion for the formation of each block on the grafts (**Scheme 2-5**). The polymerization temperature for preparing

poly(MMA) blocks on grafts was -78 °C; and the polymerization temperature for preparing poly(*t*-BA) blocks on grafts was -40 °C, because the polymerization solutions were too viscous to be stirred effectively under even lower temperatures. As a result, densely grafted copolymers with grafts having block structures **II-4** were obtained (**Table 2-3**).

It has been established that DPE-functionalized alkyllithium can nearly quantitatively initiate anionic polymerization of MMA and *t*-BA in THF in the presence of lithium chloride at low temperature [*1*], therefore the number-average of grafts of **II-4** can be assumed to be equal to the number-average DPE-functionalized alkyllithium sites on macroinitiator **II-3**. ^{1}H NMR analysis of **II-4** showed the resonances of both MMA and *t*-BA monomer units (**Figure 2-5**). For **II-4a**, **II-4c**, and **II-4d** with diblock grafts, the DP_n values for poly(MMA) and poly(*t*-BA) blocks were determined based on resonance intensities of ester methyl protons of MMA units centered at 3.57 ppm (***a***) and resonance intensities of the methine proton of *t*-BA units centered at 2.23 ppm (***b***) relative to resonance intensities of aromatic protons of the DPE junction at 7.6-6.7 ppm (***c***) after subtraction of resonance intensities from solvent $CDCl_3$ centered at 7.24 ppm. **II-4b** with poly(MMA)-*b*-poly(*t*-BA)-*b*-poly(MMA) triblock grafts was prepared from the same trial for the preparation of **II-4a**, and therefore the DP_n of the third block, that is the second poly(MMA) block, of the graft of **II-4b**, was determined by ^{1}H NMR based on increased resonance intensities of ester methyl protons of MMA units of **II-4b** relative to **II-4a**. With excellent agreement, the experimental DP_n values for polymer blocks on grafts of **II-4** were generally lower than the molar feed ratio of monomer to DPE-functionalized alkyllithium site by a few percent due to the consumption of monomers by very small

amounts of *s*-BuLi present in **II-3** solution. GPC analysis of crude products of the trials showed that linear polymers with GPC peak areas relative to several percent of GPC peak areas of **II-4** were produced as side products. These small amounts of linear polymers with block structures were eluted after the major products of **II-4**. Based on GPC relative to linear polystyrenes, these linear polymers have longer chains than grafts on **II-4**, because of the higher local concentration ratio of monomer to anionic center for separated anionic centers forming linear polymers as compared with anionic centers growing from macroinitiators. The polydispersities of grafts on **II-4** cannot be determined directly. However, fast initiation, which led grafts to be formed on the same time scale for each trial, was indicated by complete disappearance of the red characteristic color of DPE-functionalized anions with only about 2 equivalents of monomer relative to DPE-functionalized initiator site added into **II-3** solutions. Furthermore, the polydispersities of grafts on **II-4** can be probed through the polydispersities of the linear polymers formed as side product. For all trials, the linear polymers with block structures have relatively low polydispersities with monomodal GPC peaks, suggesting the living nature of anionic polymerization and ready crossover between MMA and *t*-BA monomers. Fast initiation, coupled with ready crossover reaction, should lead to relatively low polydispersities of grafts on **II-4**. A typical GPC curve of crude products for the synthesis of **II-4** was shown in **Figure 2-6**.

Because of densely grafted architectures of **II-4** samples, M_n and *PDI* values obtained by GPC relative to linear polystyrenes are significantly underestimated. The M_n values of **II-4** calculated from graft size and graft number can be considered as a more accurate estimation of real M_n values. The relatively low *PDI* values of **II-4** samples

(1.16, 1.46) by GPC reflect their relatively narrow hydrodynamic volume distribution. Considering the living nature of the anionic graft polymerization, the *PDI* values of polyfunctional DPE-agents used (1.46, 1.79) can be considered as a better estimation of the polydispersities of **II-4** samples.

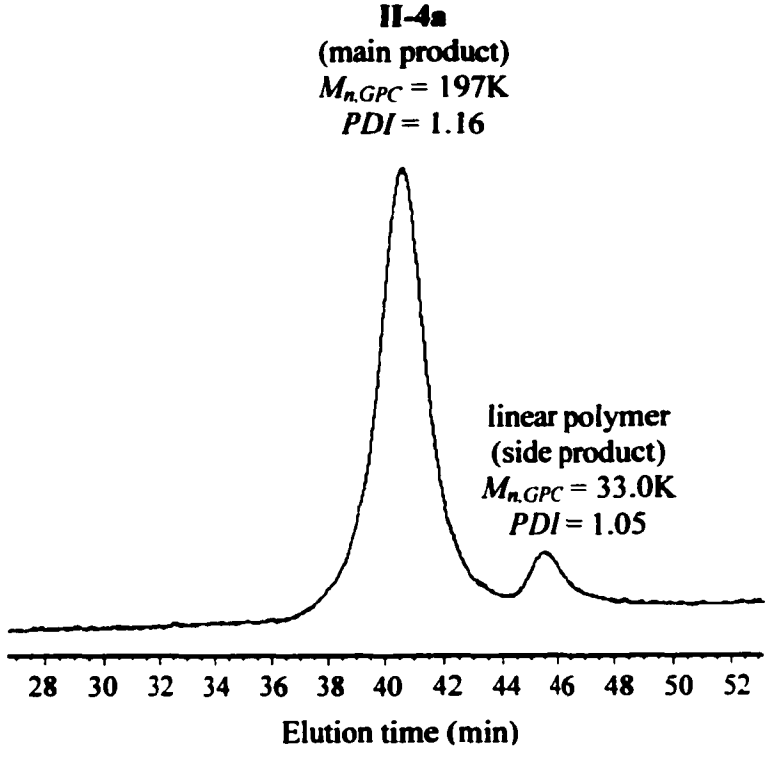

Figure 2-6. GPC curve for the crude product for the synthesis of **II-4a**.

(M_n and *PDI* are relative to linear polystyrenes)

II-4a, **II-4b**, and **II-4c** have relatively long grafts as compared with the backbone; considering that there are five carbons on each repeating unit on backbone, **II-4d** has much longer backbone than grafts. Therefore, **II-4a**, **II-4b**, and **II-4c** actually are star-like copolymers, and on the other hand, **II-4d** would be cylinder-brush copolymers.

2-4c **Synthesis of Amphiphilic Graft-Block Copolymers.** There are poly(MMA) and poly(*t*-BA) blocks on the grafts of block-graft copolymers **II-4a**, **II-4b**, **II-4c**, and **II-4d**. Compared with methyl ester groups in poly(MMA) blocks, the *tert*-butyl ester groups in poly(*t*-BA) blocks can be converted into carboxylic acid functionalities readily. Therefore, by selective conversion of *tert*-butyl ester groups in poly(*t*-BA) blocks with methyl ester groups in poly(MMA) blocks intact, amphiphilic graft-block copolymers with grafts having both hydrophobic poly(MMA) block and hydrophilic poly(acrylic acid) block can be prepared from **II-4a**, **II-4b**, **II-4c**, and **II-4d** respectively. Block-graft copolymers **II-4c** and **II-4d** have diblock poly(*t*-BA)-*b*-poly(MMA) grafts with one end of poly(*t*-BA) block connecting with the backbone, and therefore amphiphilic graft-block copolymers synthesized from them have a hydrophilic poly(acrylic acid)-based inner part and a hydrophobic poly(MMA)-based outer part, and can further serve as unimolecular inverse-micelle for the preparation of nanomaterials [*33, 34*]. Encouraged by such potential applications, synthesis of amphiphilic graft-block

Scheme 2-6

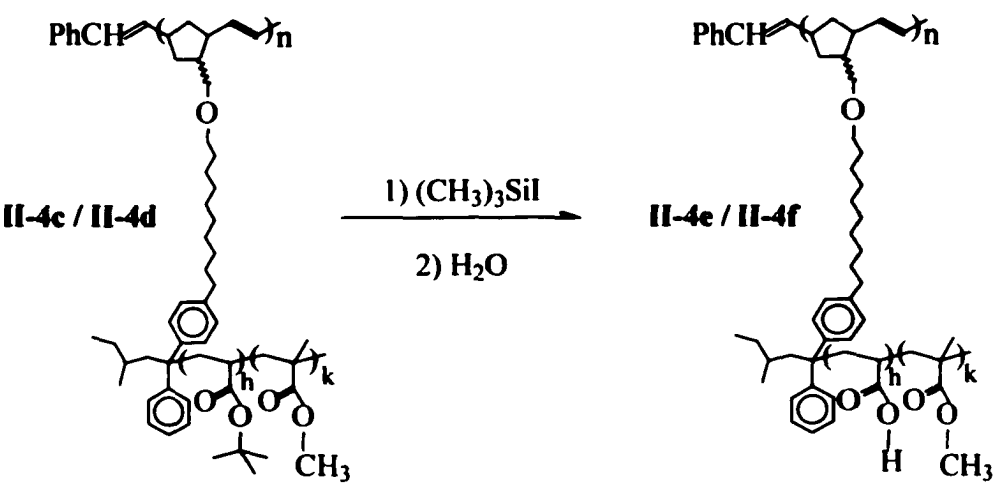

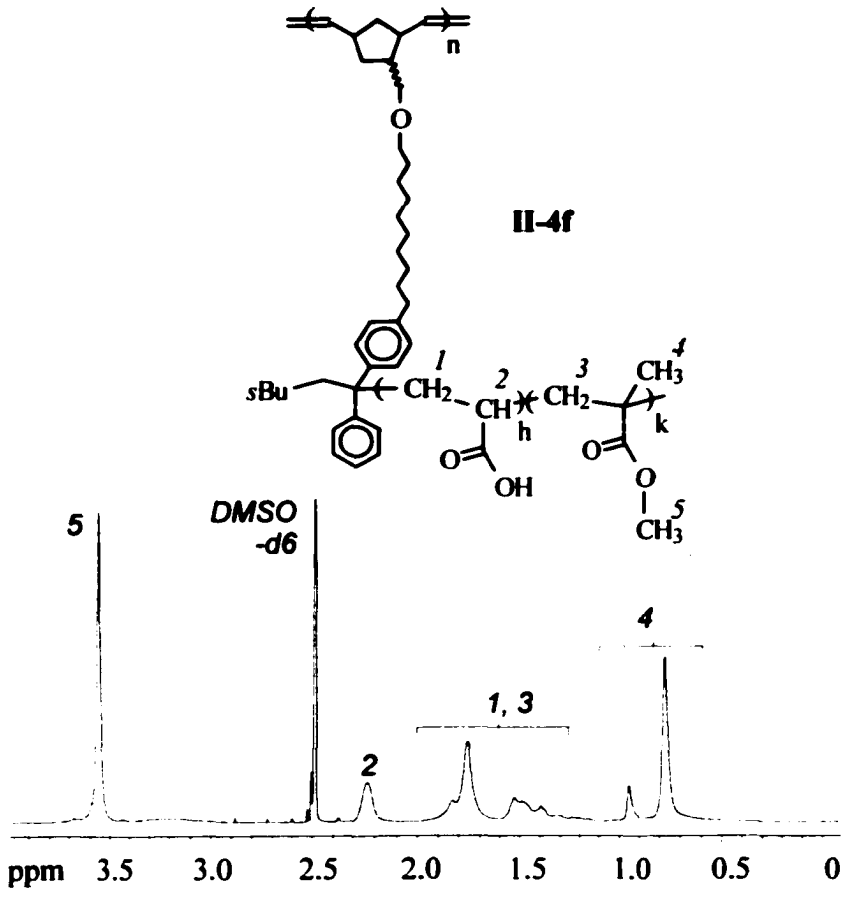

Figure 2-7. ^{1}H NMR spectrum of **II-4f**

copolymers from **II-4c** and **II-4d** was investigated.

Reactions of excess amounts of iodotrimethylsilane [*42*] with **II-4c** and **II-4d** at room temperature for 2 h followed by hydrolysis in water yielded corresponding amphiphilic block-graft copolymers **II-4e** and **II-4f** (**Scheme 2-6**). ^{1}H NMR analysis of **II-4e** and **II-4f** verified that initial *t*-BA units in **II-4c** and **II-4d** were completely converted into acrylic acid units based on the disappearance of resonances of ester *tert*-butyl protons centered at 1.41 ppm (**Figure 2-7**). At the same time, consistent molar fractions of MMA units in **II-4e** and **II-4f** determined by ^{1}H NMR were consistent with

the molar fractions of MMA units in their parent copolymers **II-4c** and **II-4d**, indicating that MMA units with methyl ester groups were essentially stable under the reaction conditions used. Thus, the well-defined poly(acrylic acid)-*b*-poly(MMA) diblock grafts on **II-4e** and **II-4f** were established.

2-5 Synthesis of Double-Brush Copolymers Based on Polystyrene-Grafted Polycarbanionic Macroinitiators

2-5a **Synthesis of Polystyrene-Grafted Polycarbanionic Macroinitiators.** Besides a small molecule alkyllithiumy, poly(styryl)lithium (PSLi) can also be used to react with polyfunctional DPE agent **II-2** with excellent efficiency. Therefore, a variety of polystyrene-grafted polycarbanionic macroinitiators with anionic initiator site on the graft junction were synthesized based on the living linking reactions between PSLi and **II-2** (**Scheme 2-7**). To avoid insoluble products resulting from association of carbanions and to maintain good stability of carbanions, reactions were carried out in THF or THF/benzene (3/1) at -78 °C. For low polydispersiteis of polystyrene grafts, PSLi species used were prepared by anionic polymerization initiated by *s*-BuLi in benzene at room temperature or in THF at -78 °C. The structures of polyanionic macroinitiators essentially depend on three factors, including the size of polyfunctional DPE-agent **II-2**, the size of PSLi, and the extent of reaction for DPE functionalities on **II-2** with PSLi. Both **II-2a** and **II-2b**, as well as a variety of PSLi species, were used in the synthesis of polyanionic macroinitiators. The extent of reaction for DPE functionalities on **II-2** with PSLi, which directly decides the number of polystyrene grafts on macroiniators, was either determined

by ^{1}H NMR analysis of the separated methanol-terminated adducts of polyanionic macroinitiators, or estimated by GPC analysis of terminated reaction mixtures for the synthesis of polyanionic macroinitiators. Initially, the number of DPE-functionalized anionic initiator sites is equal to the number of polystyrene grafts on the macroiniators. However, initiator site number of macroinitiator can be controlled to be lower than the number of polystyrene chains grafted, by partial termination of anioinic initiator sites.

Scheme 2-7

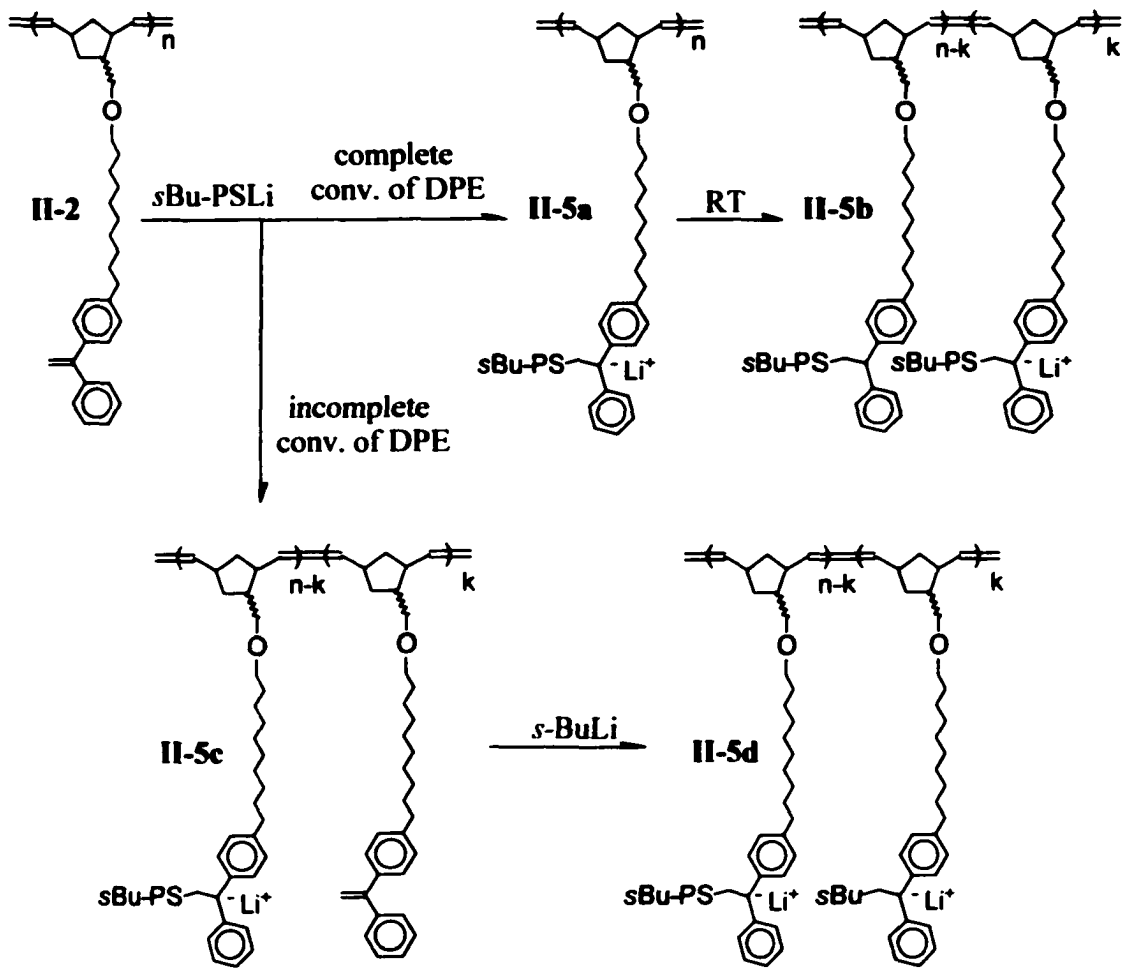

Table 2-4. Synthesis of Polystyrene-Grafted Polycarbanionic Macroinitiator II-5

	DPE-agent		PSLi[d]		$[PSLi]_0$	time	macroinitiator			
entry	no	DP_n	DP_n	PDI	$[DPE]_0$	(h)	GD_{PS}(%)[e]	N_{PS}[f]	ID (%)[g]	N_I[h]
II-5a1	**II-2a**	22	3.0	-	1.5	1	100	22	100	22
II-5a2[a]	**II-2b**	22	3.0	-	1.5	1	100	22	100	22
II-5a3	**II-2b**	220	9.6	1.20	3.0	1	100	220	100	22
II-5a4	**II-2b**	220	81	1.10	1.5	1	100	22	100	22
II-5a5	**II-2b**	220	81	1.10	1.5	1	100	220	100	220
II-5b[b]	**II-2b**	220	9.6	1.20	3.0	1	100	220	70	154
II-5c1	**II-2b**	220	81	1.10	0.5	12	41	90	41	90
II-5c2	**II-2b**	220	227	1.05	1.2	2.5	65	143	65	143
II-5d[c]	**II-2b**	220	81	1.10	0.5	12	41	90	100	220

[a] Deuterated PSLi used. [b] From **II-5a3** by standing at room temperature for 36h. [c] From **II-5c1** by further employing *s*-BuLi for DPE functionalities remaining. [d] Detected through methanol-terminated adduct. [e] Graft density relative to initial DPE functionality, equal to reaction extent of DPE functionality with PSLi. [f] Average number of polystyrene chains grafted = GD_{PS}(%) × $DP_{n,\text{II-2}}$. [g] Initiator site density relative to initial DPE functionality. [h] Average number of initiator sites = *ID* (%) × $DP_{n,\text{II-2}}$.

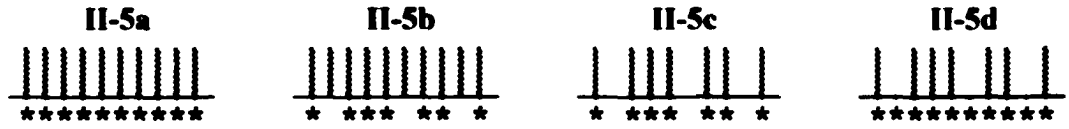

*: DPE-functionalized anionic initiator site

———— : polynorbornene backbone; —— : polystyrene graft or short chain

Figure 2-8. Schematic representations of **II-5**.

Furthermore, in the case that the reaction of DPE functionalities on **II-2** with PSLi was incomplete, initiator site number can also be controlled to be equal to the number of the repeating units of the polynorbornene main-chain by further treating DPE functionalities remaining with *s*-BuLi. Four types of polystyrene-grafted polycarbanionic macroinitiators were obtained. The synthetic results are summarized in **Table 2-4**, and their schematic representations are shown in **Figure 2-8**.

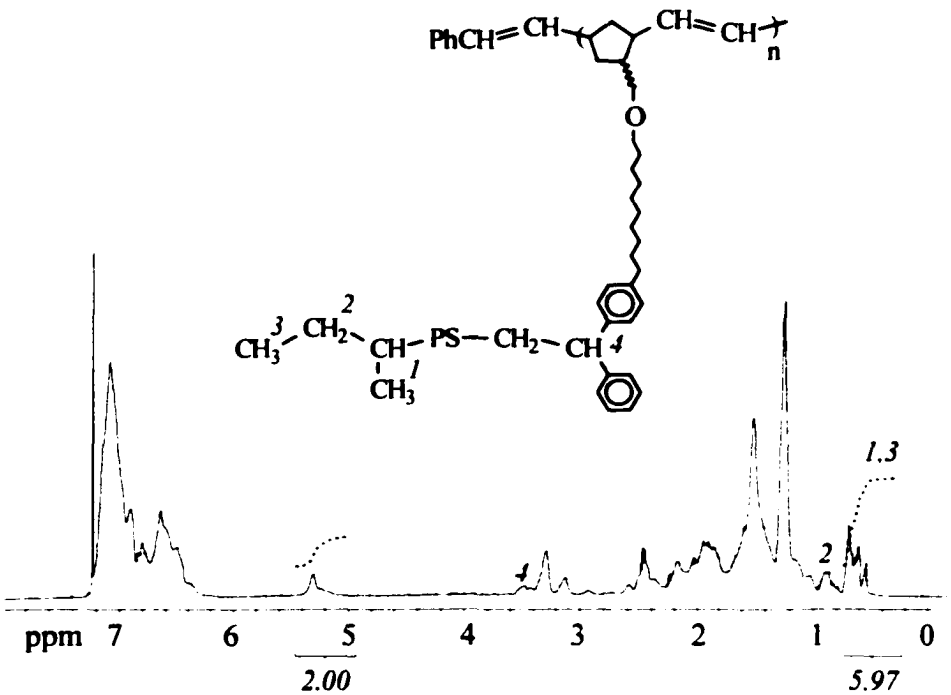

Figure 2-9. ^{1}H NMR spectrum of methanol-terminated adduct of **II-5a3**.

Macroinitiator **II-5a** series have one polystyrene short chain or graft and one DPE-functionalized anionic initiator site relative to each repeating unit of the polynorbornene backbone. They were synthesized by employing excesses of PSLi (with DP_n of 3.0, 9.6 and 81) to react with **II-2**. ^{1}H NMR analysis of the methanol-terminated

adducts of **II-5a** indicates the quantitative reaction of DPE functionalities with stoichiometric amounts of PSLi. Complete consumption of DPE functionalities was reflected by the disappearance of resonances of DPE alkene protons at 5.40 and 5.44 ppm. For methanol-terminated adducts of **II-5a4** and **II-5a5**, resonances for the alkene protons of polynorbornene main-chain concentrated at 5.33 ppm were very broad and could not be determined quantitatively due to the main-chain being densely grafted with relative long polystyrene chains. However, in the ^{1}H NMR spectra of methanol-terminated adducts of **II-5a1**, **II-5a2** and **II-5a3** (**Figure 2-9**), integration area ratios of the resonances for the methyl protons of the *sec*-butyl group (0.78-0.40 ppm) to the resonances for the alkene protons of the polynorbornene main-chain (5.33 ppm) accurately agree with the corresponding proton number ratio of 3:1 expected for stoichiometric monoaddition. The agreement of stoichiometric monoaddition of PSLi with complete consumption of DPE functionalities further indicated no considerable side reaction related to DPE functionalities, and therefore the extent of reaction for DPE functionalities with PSLi could be detected through characteristic resonances of DPE alkene protons at 5.40 and 5.44 ppm. Among the **II-5a** series, **II-5a1** and **II-5a2** have very short polystyrene chains (DP_n = 3.0), and are model macromolecules of polystyrene-grafted polycarbanionic macroiniators. The difference between them is that **II-6a2** has deuterated styrene units.

Macroinitiator **II-5b** was prepared by standing **II-5a3** solution at room temperature for 36 h. Because of limited stability DPE-functionalized anionic initiator sites in THF at room temperature, part of them initially on **II-5a3** lost reactivity by abstracting a proton from THF. Therefore **II-5b** has less average number of initiator sites

than **II-5a3**. To obtain initiator site density (which is defined as the ratio of the average number of initiator sites to number-average DPE functionalities of polyfunctional DPE-agent used) of **II-5b**, an adduct of **II-5b** was prepared through end-capping the DPE-functionalized anionic initiator sites on **II-5b** using an excess of ethylene oxide followed by protonation. Because the end-capping reaction can be considered as quantitative with only one equivalent ethylene oxide added on each anionic initiator site [*43*], number of ethylene oxide units in the adduct was equal to the number of anionic initiator site in **II-5b**. Therefore, by quantitative ^{1}H NMR analysis of the adduct (**Figure 2-10**), resonance intensities of CH_2O protons (***a***) of ethylene oxide unit centered at 2.92 ppm relative to resonance intensities of the alkene protons of polynorbornene main-chain concentrated at 5.33 ppm give the initiator site density of 70% for macroinitiator **II-5b**.

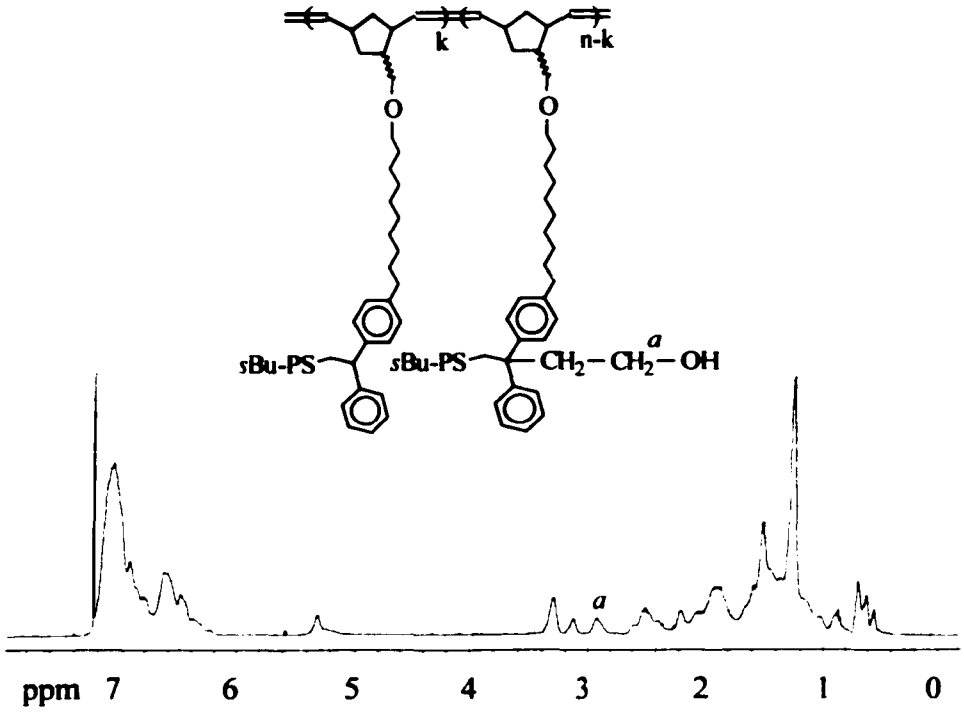

Figure 2-10. ^{1}H NMR spectrum of ethylene oxide-end-capped adduct of **II-5b**

Compared with **II-5a** series, macroinitiators **II-5c1** and **II-5c2** have low densities of polystyrene graft and DPE-functionalized anionic initiator site. They were prepared by living linking reaction of PSLi and polyfunctional DPE-agent **II-2b** with incomplete extent of reaction for DPE functionality. For the synthesis of **II-5c1**, a deficient amount of PSLi (DP_n = 81) relative to DPE functionality ($[PSLi]_0/[DPE]_0$ = 0.5) was employed to react with **II-2b** for 12h. The extent of reaction for DPE functionalities of 41% was finally reached for macroinitiator **II-5c1**, according to ^{1}H NMR resonance intensity of DPE alkene protons remaining in methanol-terminated adduct of **II-5c1**. It is obvious that a minor amount of PSLi added lost reactivity before the occurrence of addition reaction due to the limited stability of PSLi in polar solvent. Macroinitiator **II-5c2** was obtained by reacting with an excess of PSLi (DP_n = 227) with **II-2b** for 2.5 h. With relatively long chain, the PSLi species exhibits decreased reactivity towards DPE functionality, and therefore only incomplete addition of PSLi was finally obtained. The extent of reaction for DPE functionalities could not be determined by ^{1}H NMR analysis of the methanol-terminated adduct of **II-5c2**, because very low abundance of DPE alkene protons in the adduct. By GPC analysis of the methanol-terminated reaction mixture for the synthesis of **II-5c2**, the reaction extent of DPE functionalities on **II-2b** with PSLi was estimated as 65% based on the initial molar feed ratio of PSLi to **II-2b** and the ratio of GPC peak area of methanol-terminated adduct of **II-5c2** to the sum of GPC peak areas of methanol-terminated adduct of **II-5c2** and methanol-terminated adduct of unreacted PSLi. For both **II-5c1** and **II-5c2**, the densities of their polystyrene graft and DPE-functionalized anionic initiator site were equal to the extent of reaction for DPE functionalities.

Macroinitiator **II-5d** was prepared from **II-5c1**. Because there are DPE functionalities remaining in **II-5c1**, treatment of **II-5c1** with excess of *sec*-butyllithium gave macroinitiator **II-5d** within 1h. Complete reaction of DPE functionalities remaining in **II-5c1** with *s*-BuLi was verified by complete disappearance of ^{1}H NMR resonances of DPE alkene protons at 5.40 and 5.44 ppm for the methanol-terminated adduct of **II-5d**. Macroinitiator **II-5d** has the same density of polystyrene graft as **II-5c1**, but has one DPE-functionalized anionic initiator site relative to each repeating unit of polynorbornene backbone.

2-5b **Synthesis and Structure Study of Model Macromolecules of Double-Brush Copolymers.** Representing novel and unique macromolecular architectures, double-brush copolymers with graft junctions simultaneously connecting two heterografts to the backbone, can be synthesized by anionic graft polymerization using polystyrene-grafted macroinitiators **II-5**. It has been well established that anionic polymerization of a range of monomers, including methacrylates, *t*-BA, and 2-VP, initiated by DPE-functionalized alkyllithiums, yields nearly monodisperse polymers with predetermined DP_n. However, anionic polymerization of initiated by DPE-functionalized polyanionic macroinitiators has not been reported defore. To a great extent, the success of synthesis of double-brush copolymers with controlled architectures depends on the initiating efficiency of DPE-functionalized initiator sites of the macroinitiators used, which decides grafting efficiency and graft density of the second type of graft. Direct investigation of initiation using polystyrene-grafted macroinitiators is not feasible because the structures formed by initiation only represent very small parts of the final products and therefore

cannot be accurately determined by quantitative NMR analysis, therefore the initiation process needs to be probed through model macromolecules of double-brush copolymers synthesized from model polystyrene-grafted polyanionic macroinitiators **II-5a1** and **II-5a2**. Meanwhile, as the key structural characteristic of double-brush copolymers, the existence of DPE-based trifunctional junctions, which connect two different types of monomer units with backbone polymer, also needs to be probed through model macromolecules of double-brush copolymers.

Choosing MMA as monomer, model macromolecules of double-brush copolymers **II-6a1** and **II-6a2** were synthesized by titration of THF solutions of **II-5a1** and **II-5a2** with MMA at -78 °C in the presence of lithium chloride followed by labeling the initiated sites yielded with allyl groups (**Scheme 2-8**). The additions of MMA were stopped as soon as complete consumption of DPE-functionalized anionic initiator sites on macroinitiators, indicated by disappearance of their characteristic red color, was reached. Due to the high reactivity of MMA-functionalized anionic species with iodides [*44*], quantitative labeling the initiated sites by empolying excesses of allyl iodide can be

Scheme 2-8

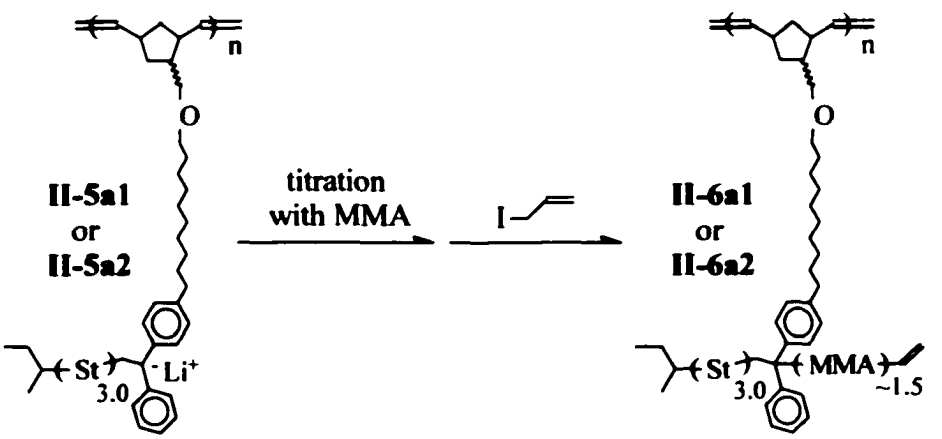

assumed. Quantitative ^{1}H NMR analysis of model polymers **II-6a1** and **II-6a2** (**Figure 2-11**) proved that the initiation with **II-5a1** and **II-5a2** was a very efficient and fast process.

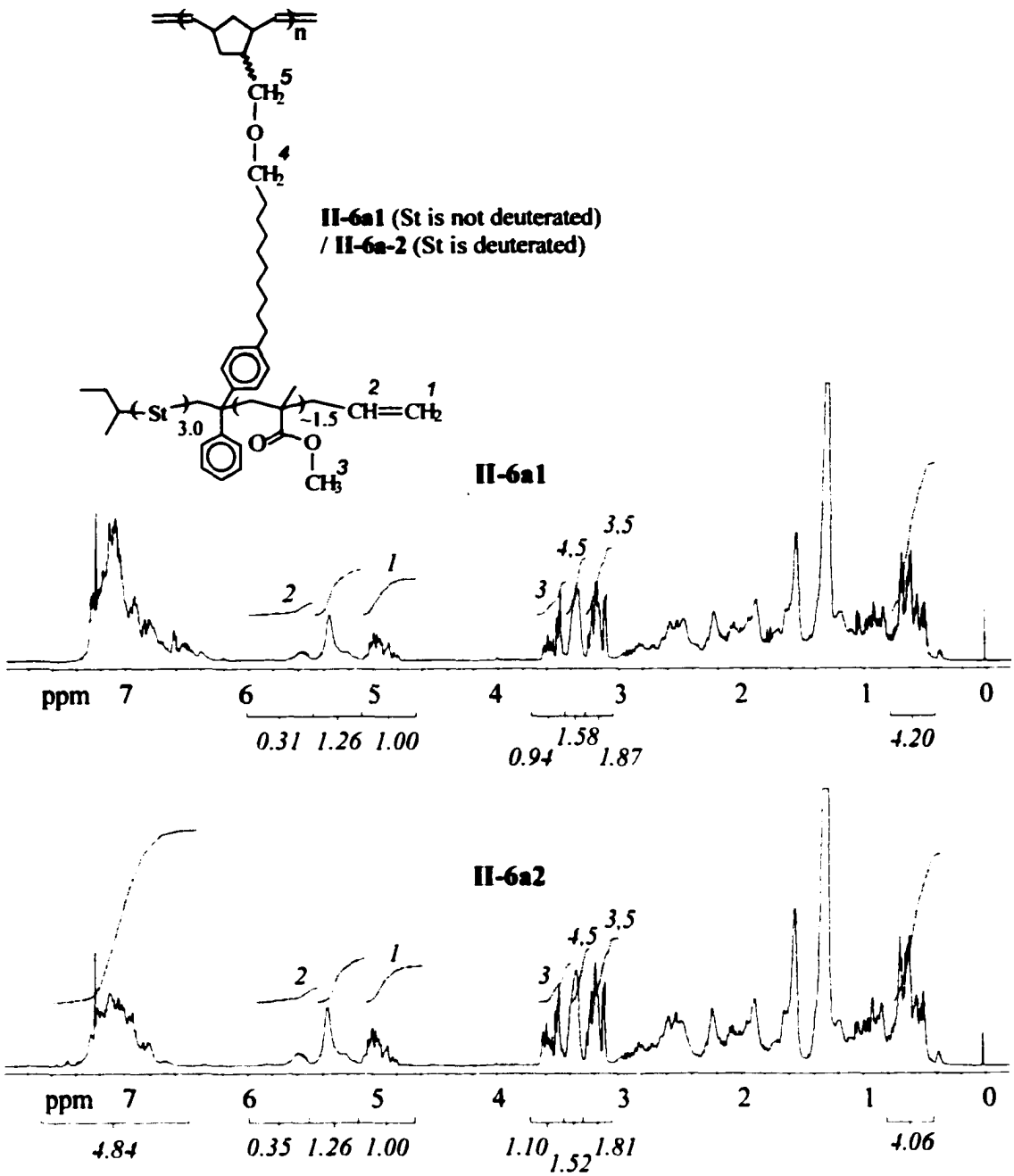

Figure 2-11. ^{1}H NMR spectra of **II-6a1** and **II-6a2**

Nearly quantitative initiation (efficiency: 95-99%) of initiator sites on polyanionic macroinitiators was verified. Initiation efficiency was determined by comparison between resonance intensities of allyl protons labeled and intensities of characteristic resonance of protons from the polynorbornene main-chain or the spacer. Part of the resonances of allyl methine protons were covered by resonances of alkene protons on polynorbornene main-chain; resonances for the methyl protons of the *s*-BuLi fragment at 0.78-0.40 ppm have very considerable overlap with resonances of α-methyl protons of MMA monomer unit centered around 0.85 ppm. Therefore the areas of the above resonances obtained by integration were not sufficiently accurate. On the other hand, the overlap of resonances of allyl methylene protons (5.11-4.60 ppm) and resonances of alkene protons on the polynorbornene main-chain is negligible; the resonances of three alkoxy methene protons on the spacer (3.45-3.29 ppm; centered at 3.35 ppm) have only slight overlap with adjacent resonances. The corresponding integration area ratios of the resonances at 5.11-4.60 ppm to the resonances at 3.45-3.29 ppm were 1:1.58 and 1:1.52 for **II-6a1** and **II-6a2** respectively. Compared with theoretical proton number ratio of 1:1.50 expected for quantitative initiation, these experimental ratios suggest initiation efficiencies of 95% and 99% of initiator sites on **II-5a1** and **II-5a2**. With deuterated styrene monomer units, model polymer **II-6a2** also has ^{1}H NMR resonances of diphenyl aromatic protons of at 7.64-6.46 ppm that can be used for quantitative determination. The theoretical proton number ratio of allyl methylene protons to diphenyl aromatic protons is 1:4.50 (2:9) under quantitative initiation. The integration of resonances of allyl methylene protons at 5.11-4.60 ppm relative to the area of resonances 7.64-6.46 ppm gave a ratio of 1:4.84; with subtracting the area of resonances of solvent of $CDCl_3$ at 7.24 ppm, the ratio was

refined as 1:4.70; Finally considering the isotope enrichment of 98% for deuterated styrene monomer unit, the experimental ratio was finally modified to 1:(4.55-4.70), corresponding to an initiation efficiency of 96-99% of initiator sites on **II-5a2**.

Moreover, compared with propagation, the initiation using polyanionic macroinitiators is very fast. The number average MMA monomer unit relative to initiator sites of **II-5a1** and **II-5a2** was determined based on the resonances of MMA methoxyl protons of **II-6a1** and **II-6a2**. The ^{1}H NMR resonances of methoxyl protons (concentrated on 3.69-3.45 ppm and 3.29-3.06 ppm) have only slight overlap with the resonances of three alkoxy methene protons (3.45-3.29 ppm; concentrated on 3.35 ppm), but completely overlap with the resonances of the rest one of alkoxy methene protons (i.e., NBCH*H*O-) at 3.29-3.06 ppm. The integration areas at 3.69-3.45 ppm (A_1), 3.45-3.29 ppm (A_2) and 3.29-3.06 ppm (A_3) were obtained, and the contribution of ^{1}H NMR resonance intensities of methoxyl protons can be represented by $A_1 + A_3 - A_2/3$. Comparing it with A_2 (or the integration area of resonance intensities of aromatic protons, only for **II-6a2**) finally gave the average numbers of MMA monomer unit of 1.45 and 1.58 relative to initial initiator sites of **II-5a1** and **II-5a2** respectively, indicating a very fast initiation relative to propagation by using these polyanionic macroinitiators.

DPE-based trifunctional junctions that simultaneously carry styrene and MMA units and connect to backbone through spacer were verified by ^{1}H-^{13}C GHMBC and GHMQC 2D NMR analysis of **II-6a1** and **II-6a2**. With deuterated styrene monomer unit, **II-6a2** has simplified NMR resonances and correlations compared with **II-6a1**. Based on ^{1}H-^{13}C GHMBC and GHMQC 2D NMR spectra of **II-6a2**, the positions of ^{13}C NMR resonances of carbons and ^{1}H NMR resonances of protons on the trifunctional junction

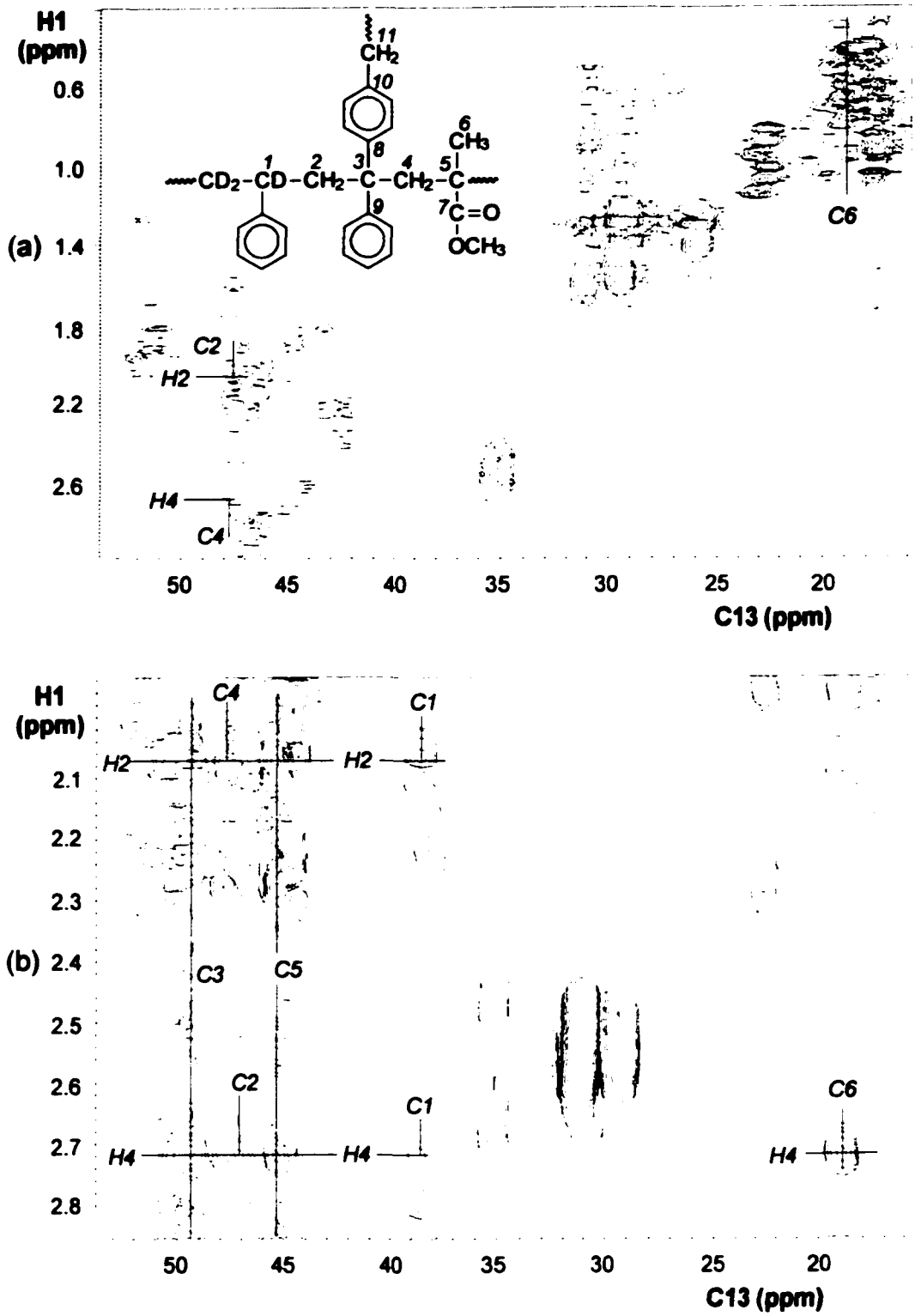

Figure 2-12. ^{1}H-^{13}C 2D-NMR a) GHMBC and b) GHMQC spectra related to trifunctional junctions in **II-6a2**

were identified, and the structure of trifunctional junction was verified through ^{1}H-^{13}C multi-bond correlations (**Figure 2-12**). The ^{1}H NMR resonance of methene protons (H2) of the DPE junction at 2.07 ppm have correlations with ^{13}C NMR resonances of methine carbon (C1) of the deuterated styrene unit at 38.5 ppm, quaternary carbon (C3) of the DPE junction at 49.4 ppm, methane carbon (C4) of MMA unit at 47.8 ppm, quaternary aliphatic carbon (C5) of MMA unit at 45.4 ppm, and two quaternary aromatic carbons (C9, C10) of the DPE unit at 143.7 and 146.4 ppm. The ^{1}H NMR resonance of methene protons (H4) of MMA unit at 2.72 ppm have correlations with ^{13}C NMR resonances of not only C1, C3, C4, C5, C9, C10, but also the methene carbon of the DPE junction (C2) at 47.4 ppm, α-methyl carbon (C6) of the MMA unit at 18.9 ppm, and ester carbon (C7) of the MMA unit at 177 ppm. The key correlations of the -St-DPE-MMA- connections were shown in **Figure 2-12b**. Moreover, the connection of polynorbornene main-chain and DPE unit through $-CH_2O(CH_2)_{10}-$ spacer was established by ^{1}H-^{13}C multi-bond correlations. The ^{1}H NMR resonace of methene protons (H11) at the end of the spacer at 2.60 ppm have correlations with ^{13}C NMR resonances of the quaternary aromatic carbon (C10) of the DPE unit at 140 ppm, and other aromatic carbons of the DPE units at 127 ppm, as well as adjacent carbons on the spacer at 31.1 and 29.3 ppm. On the other hand, ^{1}H NMR resonances of aromatic protons of the DPE unit at 6.76-7.13 ppm have correlations with ^{13}C NMR resonances of the methene carbon (C11) at the end of the spacer at 35.1 ppm. Similarly, all of the above correlations were also identified on ^{1}H-^{13}C 2D-NMR GHMQC spectrum of **II-6a1** which is even more complicated because of its undeuterated styrene units. Thus, it is unambiguous based on NMR evidence that DPE units in model polymers serve as trifunctional junctions connecting the St unit, MMA

unit, and $-CH_2O(CH_2)_{10}-$ spacer through its methene carbon, quaternary aliphatic carbon, and quaternary aromatic carbon respectively.

***2-5c* Synthesis of Double-Brush Copolymers by Anionic Graft Polymerization Using Polystyrene-Grafted Polycarbanionic Macroinitiators.** Extended from model macromolecules, a series of double-brush copolymers were synthesized by anionic graft polymerization in THF at -78 °C, using polystyrene-grafted polycarbanionic macroinitiators **II-5** series in the presence of lithium chloride (**Scheme 2-9**). MMA was chosen as the monomer in most cases; *t*-BA and 2-(dimethylamino)ethyl methacrylate (DMAEMA) were also used as monomers for graft polymerization initiated by **II-5b**. For all trials of polymerization, monomer was slowly added, and when only 2-5 equivalents of monomer relative to initial DPE-functionalized anionic initiator species were introduced into the polymerization solutions, complete initiator consumption was indicated by the disappearance of characteristic red color of anionic initiating species, suggesting relatively fast initiation. Polymerization time was 1 h for each trial. Methanol was used for termination. Complete monomer conversion was deduced based on the weights of crude products recovered from polymerization solutions by precipitation in methanol. Besides targeted double-brush copolymers as the major component, the crude products also contained linear polystyrene in all trials and linear diblock copolymer in some trials, formed by decomposition of PSLi used for macroinitiator preparation and PSLi-initiated anionic polymerization respectively. Separation of double-brush copolymers from the crude products was preformed readily by liquid chromatography eluted with ligroine-dichloromethane, and double-brush copolymers were eluted first

Scheme 2-9

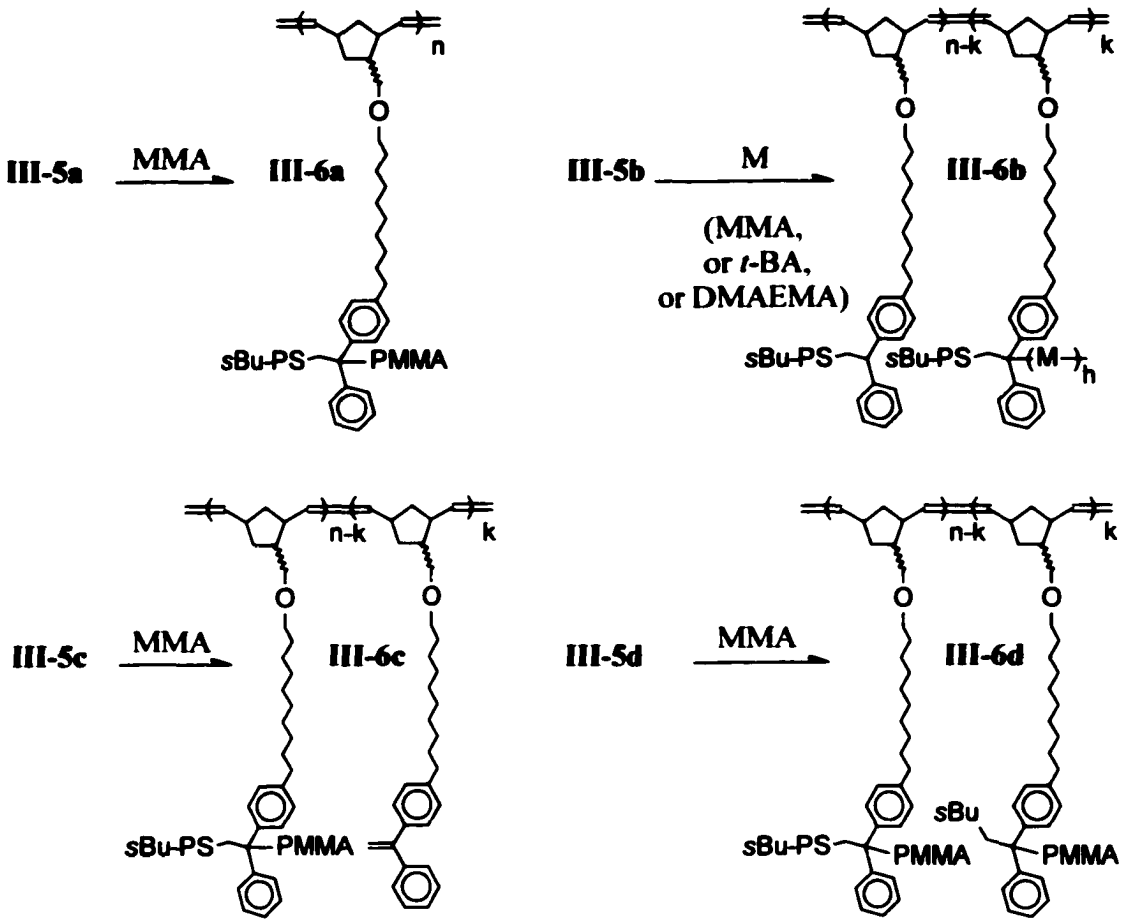

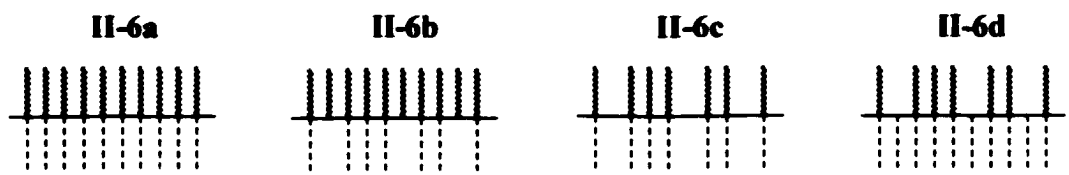

———— : polynorbornene backbone; —— : polystyrene graft or short chain:

----- : another type of polymer (PMMA in most cases) graft or short chain.

Figure 2-13. Schematic representations of double-brush copolymers **II-6.**

Table 2-5. Synthesis of Double-Brush Copolymers II-6

			double-brush copolymer									
		$[M]_0$[a]	$PNB_{backbone}$[b]		1st graft (PS)[c]			W_{St}[d]	2nd graft			
entry	initiator	$[Li]_0$	DP_n	PDI	N_G	DP_n	PDI	W_M	N_G[e]	DP_n[f]	M_n[g]	PDI[h]
II-6a3	**II-5a4**	120	22	1.46	22	81	1.10	0.83	22	101	420 K	1.11
II-6a4	**II-5a4**	240	22	1.46	22	81	1.10	0.40	22	213	660 K	1.15
II-6a5	**II-5a5**	120	220	1.79	220	81	1.10	0.73	220	115	4.5 M	1.51
II-6a6	**II-5a5**	240	220	1.79	220	81	1.10	0.36	220	233	7.1 M	1.42
II-6b1	**II-5b**	9.6	220	1.79	220	9.6	1.20	1.37	10.4	154	490 K	1.54
II-6b2	**II-5b**	9.6	220	1.79	220	9.6	1.20	1.03	9.7	154	540 K	1.64
II-6b3	**II-5b**	9.6	220	1.79	220	9.6	1.20	1.51	6.0	154	480 K	1.61
II-6c1	**II-5c1**	100	220	1.79	90	81	1.10	0.85	90	99	1.7 M	1.46
II-6c2	**II-5c2**	300	220	1.79	143	227	1.05	0.94	143	250	7.1 M	1.50
II-6d1	**II-5d**	40	220	1.79	90	81	1.10	0.84	220	41	1.7 M	1.42
II-6d2	**II-5d**	80	220	1.79	90	81	1.10	0.45	220	76	2.5 M	1.48

[a] Molar feed ratio of monomer to DPE-functionalized alkyllithium initiator site on macroinitiator. [b] Detected from corresponding polyfunctional DPE agent. [c] Determined in macroinitiator synthesis. [d] Weight ratio of styrene unit to the monomer unit of the other type of graft in copolymer; determined by ^1H NMR. [e] Average number of the second type of graft, estimated form average number of initiator sites on macroinitiator with assumption of complete initiation. [f] $DP_n = (104DP_{n,\text{PS graft}} \times N_{G,\text{PS graft}})/(MW_M \times N_{G,\text{2nd graft}} \times W_{St}/W_M)$. [g] M_n calculated from structural parameters of copolymers. [h] By GPC calibrated with linear polystyrene.

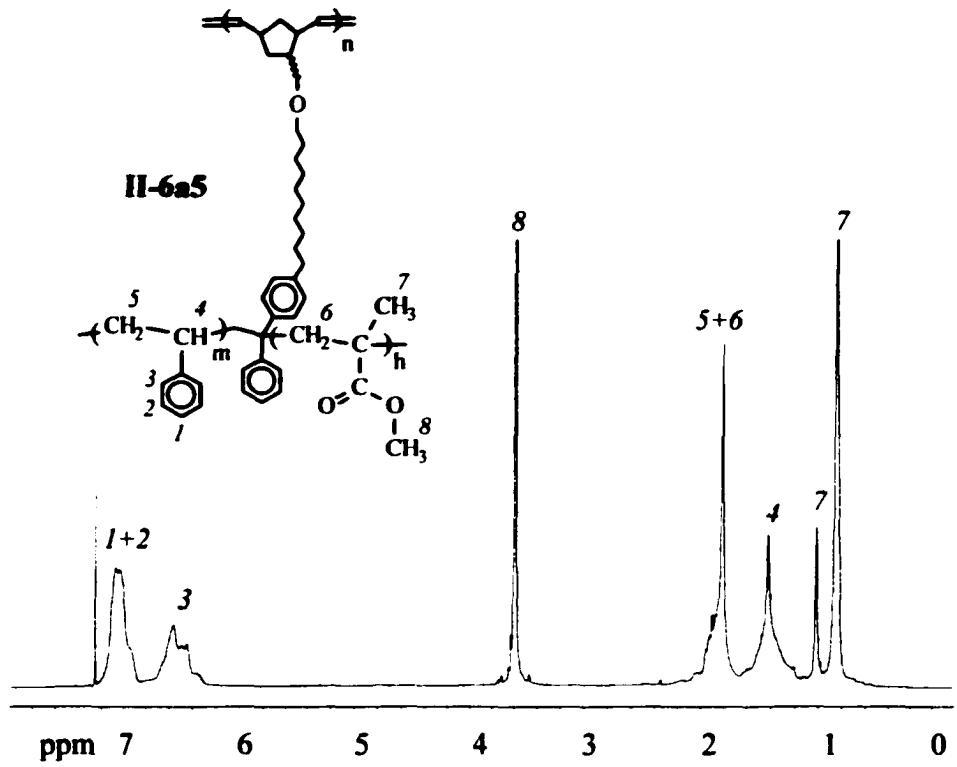

Figure 2-14. ^{1}H NMR spectrum of **II-6a5**

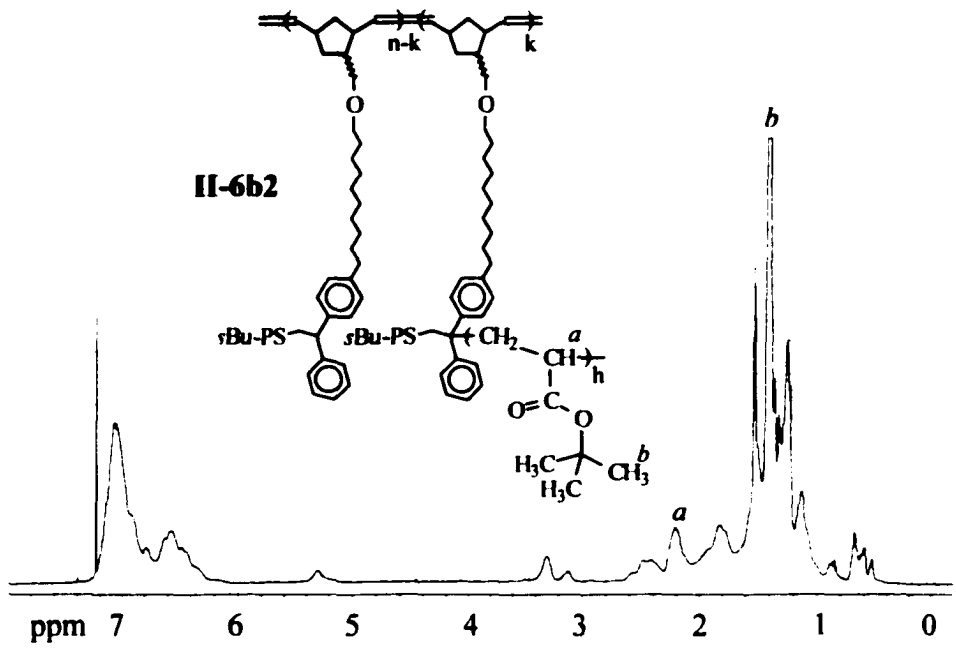

Figure 2-15. ^{1}H NMR spectrum of **II-6b2**

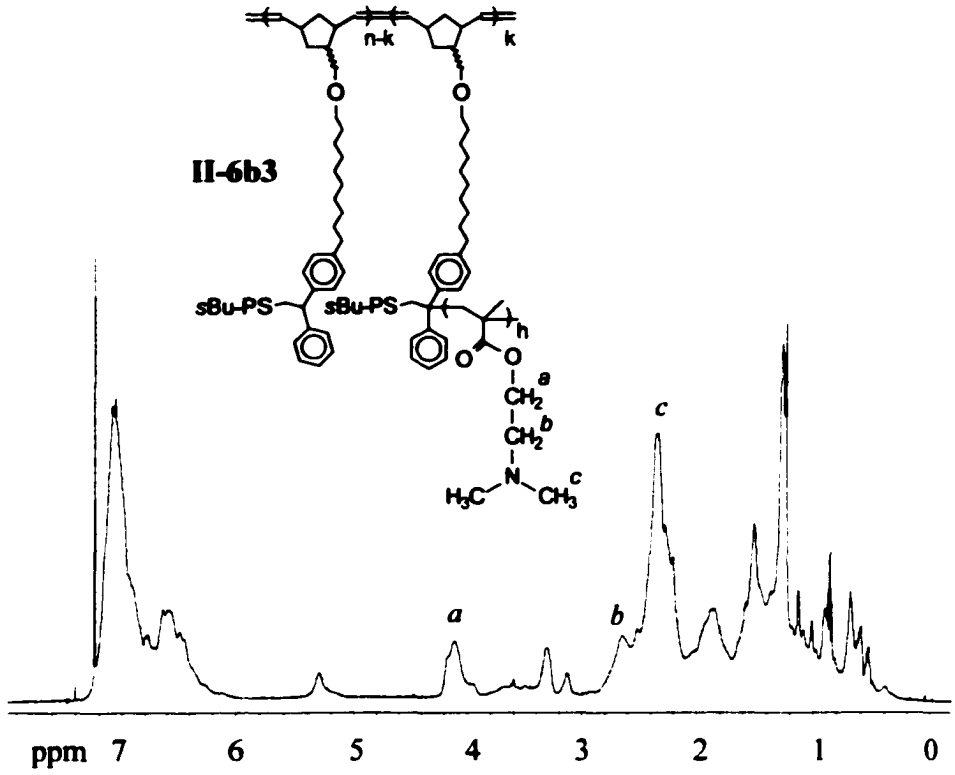

Figure 2-16. ^{1}H NMR spectrum of **II-6b3**

with retention factors (R_f) close to 1 [*45*].

Because four types of polystyrene-grafted polycarbanionic macroinitiators were used for anionic graft polymerization, four types of double-brush copolymers with different topological features were obtained. Double-brush copolymers **II-6a3**, **II-6a4**, **II-6a5**, and **II-6a6**, synthesized using macroinitiators **II-5a4** and **II-5a5** respectively, have both polystyrene grafts and poly(MMA) grafts with high graft density. Double-brush copolymers **II-6b1**, **II-6b2**, and **II-6b3**, synthesized using macroinitiators **II-5b**, have polystyrene grafts with high graft density and another type of grafts (poly(MMA) for **II-6b1**; poly(*t*-BA) for **II-6b2**; poly(DMAEMA) for **II-6b3**) with low graft density. Double-brush copolymers **III-6c1** and **III-6c2**, synthesized using macroinitiators **II-5c1** and

II-5c2 respectively, have both polystyrene grafts and poly(MMA) grafts with low graft density. Double-brush copolymers **II-6d1** and **II-6d2**, synthesized using macroinitiators **II-5d**, have polystyrene grafts with low graft density but poly(MMA) grafts with high graft density. Schematic representations of these double-brush copolymers were shown in **Figure 2-13**, and synthetic results of double-brush copolymers were shown in **Table 2-5**. The existence of a new type of major monomer units besides styrene units in double-brush copolymers was verified by ^{1}H NMR analysis (**Figure 2-14**, **Figure 2-15**, and **Figure 2-16**). The structural characteristics of polynorbornene backbone, the structural characteristic and graft density of polystyrene grafts were controlled in the synthesis of polyfunctional DPE-agent and the preparation of polystyrene-grafted polyanionic macroinitiators respectively. Only the structural characteristic and graft number of the second type of graft were dependent on anionic graft polymerization using polystyrene-grafted polyanionic macroinitiators. Because no linear counterpart was available for the second type of graft, their structural parameters were estimated. With the assumption of quantitative initiation of DPE-functionalized anionic initiator sites on macroinitiators, the average number of the second type of graft was equal to average number of initiator site on macroinintiator **II-5** used. The DP_n values of the second type of graft were calculated based on the weight ratio of styrene units to the monomer units for the second type of graft in double-brush copolymers determined by ^{1}H NMR and the estimated graft number. Based on the very high initiation efficiency of model polystyrene-grafted polyanionic macroinitiators, although the graft number and DP_n of the second type of graft were overestimated and underestimated respectively, the error in each case might be within 10%. In some trials, DP_n values of the second type of graft thus obtained were

considerably lower than the molar feed ratio of monomer to DPE-functionalized anionic species, as the result of considerable amounts of PSLi remaining (introduced in macroinitiator preparation) consumed some of monomer added. Additionally, although *PDI* of the second type of graft could not be determined, when they are not too short (that is, not for the second type of graft on **II-6b** series), low *PDI* values can be expected due to the fast initiation and living characteristics of anionic graft polymerization. The M_n values of entire double-brush copolymers, ranging from 4.2×10^5 to 7.1×10^6, were determined based on DP_n values of polynorbornene backbone and polystyrene graft, graft density of polystyrene graft, and weight ratio of monomer units on the two types of grafts. The *PDI* values of double-brush copolymers obtained by GPC analysis relative to linear polystyrene were obviously underestimated, and the *PDI* of corresponding polyfunctional DPE agent can be applied as better estimation of the *PDI* of these double-brush copolymers.

2-5d **Synthesis of Amphiphilic Double-Brush Copolymers.** Besides polystyrene short grafts, double-brush copolymers **II-6b2** and **II-6b3** have also poly(*t*-BA) and poly(DMAEMA) short grafts respectively. Because *t*-BA monomer unit can be converted into acrylic acid monomer unit by hydrolysis, and the amine functionality on DMAEMA monomer unit can be quaternized with the formation of a quaternary ammonium group [*46*], amphiphilic double-brush copolymers can be synthesized from **II-6b2** and **II-6b3**.

Amphiphilic double-brush copolymer **II-6b4** with both hydrophobic polystyrene short grafts and hydrophilic poly(acrylic acid) short grafts was synthesized by hydrolysis

of *t*-BA monomer unit of **II-6b2** using *p*-toluenesulfonic acid as catalyst in toluene at 100 °C for 5 h (**Scheme 2-10**). The structural characteristics of **II-6b4** are the same as these of **II-6b2** showed in **Table 2-5** except different monomer unit for the second type of graft. ^{1}H NMR analysis of **II-6b4** in acetone-d_6 verified complete hydrolysis based on disappearance of resonances of *tert*-butyl proton of *t*-BA monomer unit at 1.42 ppm.

Scheme 2-10

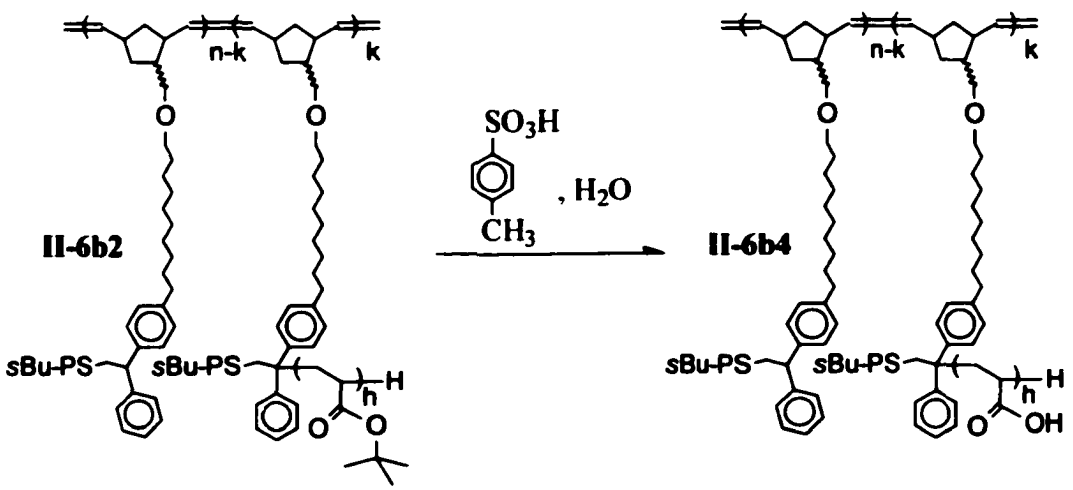

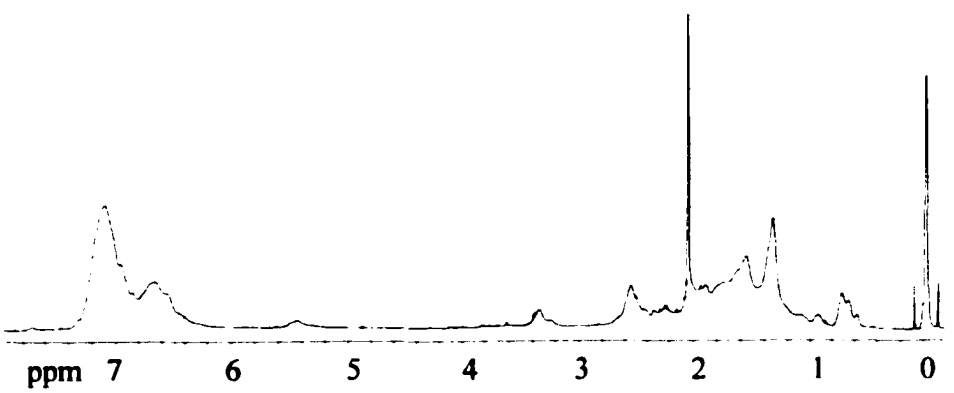

Figure 2-17. ^{1}H NMR spectrum of **II-6b4**

Scheme 2-11

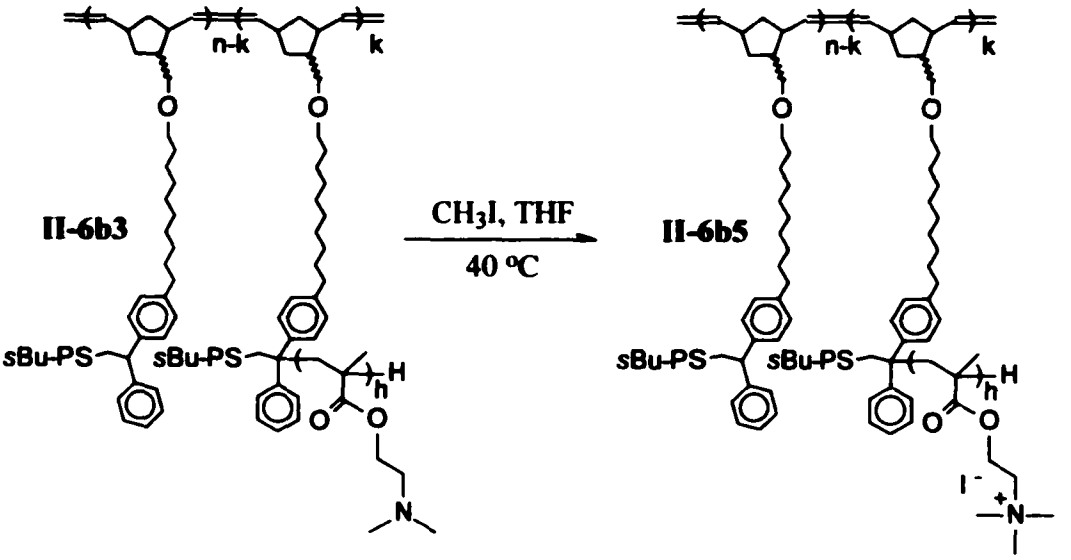

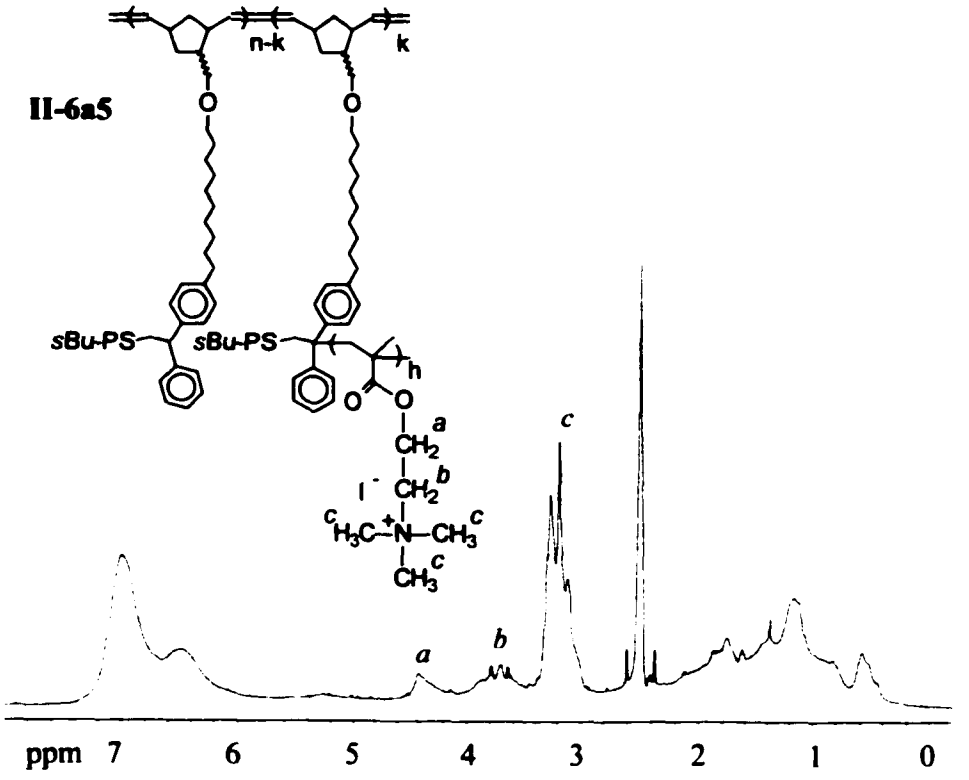

Figure 2-18. ^{1}H NMR spectrum of **II-6b5**

Amphiphilic double-brush copolymer **II-6b5** with both hydrophobic polystyrene short grafts and cationic quaternarized poly(DMAEMA) short grafts was synthesized by treating **II-6b3** with excess iodomethane in THF at 40 °C for 24 h (Scheme **2-11**). The structural characteristics of **II-6b5** are the same as these of **II-6b3** showed in **Table 2-5** except with a different monomer unit for the second type of graft. As yellow solid, **II-6b5** can be dissolved in THF, DMF, and DMSO. ^{1}H NMR analysis of **II-6b5** in DMSO-d_6 verified quantitative quaternization based on disappearance of the characteristic resonances of DMAEMA monomer unit centered at 4.12, 2.66, and 2.35 ppm with the presence of resonances of the quaternized DMAEMA monomer unit centered at 4.42, 3.72, and 3.20 ppm (**Figure 2-18**).

2-5e **Investigations on Anionic Ring-Opening Polymerization Using Polystyrene-Grafted Alkoxide-Based Polyfunctional Macroinitiators.** Because 1,1-diphenylalkyllithium sites on **II-5** can be readily converted into metal alkoxides, densely grafted copolymers with polystyrene side-chains and metal alkoxide side groups can be prepared from **II-5**. Metal alkoxides typically are useful initiators for anionic ring-opening polymerization of a broad range of monomers including ethylene oxide, ε-caprolactone (ε-CL), and cyclic siloxanes [*31*]. Therefore, these copolymers can be considered as polystyrene-grafted metal alkoxide-functionalized polyfunctional macroinitiators for anionic ring-opening polymerization. If they have sufficient initiation capacity, then new types of double-brush copolymers can be further synthesized. With this expectation, we investigated their initiation capacity through polymerization experiments.

Scheme 2-12

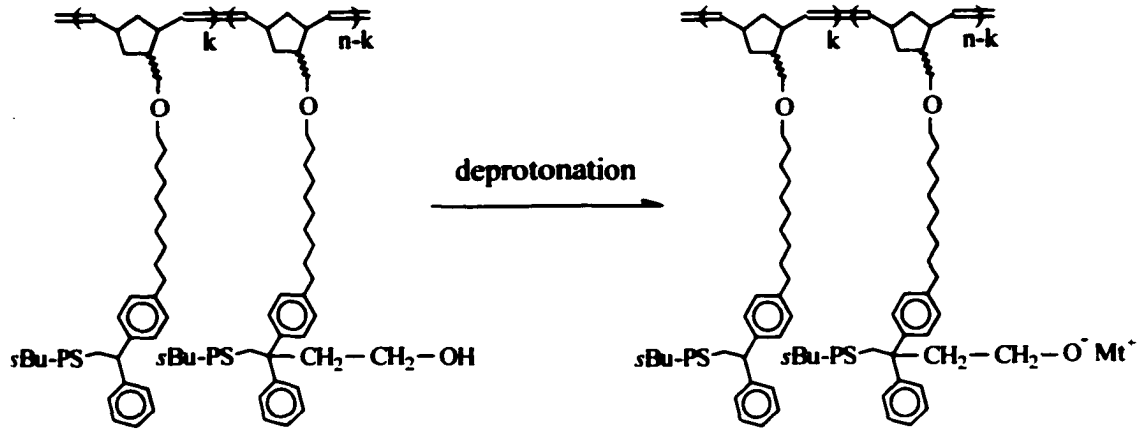

ethylene oxide-end-capped adduct of **II-5b**

Mt^+: Li^+, K^+, $(AlEt_2)^+$
(DPHLi,, DPE-K adduct, and $AlEt_3$ used for deprotonation)

Three types of metal alkoxide-functionalized polyfunctional macroinitiators were synthesized in situ by deprotonation of ethylene oxide-end-capped adduct of **II-5b** (**Scheme 2-12**). In the first two trials that DPHLi and DPE-potassium adduct were used for quantitative deprotonation by titration at -78 °C in THF, the formed macroinitiators were used respectively to initiate polymerization of hexamethylcyclotrisiloxane (D_3) for 15 min (followed by termination using chlorotrimethylsilane) and polymerization of ethylene oxide over 80 h at room temperature. In the third trial, triethylaluminum was used for deprotonation, and the formed macroinitiator was used to initiate polymerization of (ε-CL) for 30 h at room temperature [*45*].

However, the analytical results of polymers yielded suggest that these macroinitiators cannot lead to well-controlled products via anionic ring-opening polymerization. The polymers produced, which were recovered by precipitating

polymerization solution in methanol, have two types of monomer units (one is styrene, and the other is either ethylene oxide, or D_3, or ε-CL), as well as a polynorbornene-based backbone, according to ^{1}H NMR analysis. But out of our expectation, these polymers also showed longer elution times than the ethylene oxide-end-capped adduct of **II-5b**, indicating that their M_n values are lower than M_n of **II-5b**. Because the polydispersities of the polystyrene-grafted metal alkoxide-functionalized polyfunctional macroinitiators in situ prepared were expected to be quite broad according to the *PDI* of correspondent polyfunctional DPE-agent **II-2a** of 1.79, such results suggest that most monomers consumed were polymerized through the macroinitiator species with relatively low molecular weights. Because steric hindrance around the initiator site increases with the molecular weight of polyfunctional macroinitiator, it can be further inferred that the initiation process for anionic ring-opening polymerization is relatively sensitive to steric environment, and initiation capacity would drop greatly with increased steric hindrance.

Based on experimental results, it can be concluded that double-brush copolymers with controlled structures cannot be prepared using polystyrene-grafted metal alkoxide-functionalized polyfunctional macroinitiators. However, of note, the targeted double-brush copolymers with well-controlled poly(ethylene oxide) or poly(dimethyl siloxane) side-chains can be synthesized using macromonomer strategy, and the details are described in Chapter 3.

2.6 Expected Nanostructures and Preliminary Surface Morphology Characterization Results of Double-Brush Copolymers

2-6a **Expected Nanostructures.** With new and unique macromolecular architectures, double-brush copolymers are expected to have novel nanostructures and interesting properties. It is of both theoretical and practical importance to examine the nanostructures of double-brush copolymers, because such efforts, on one hand, would be helpful for us to form deeper understanding on polymeric nanostructures and its relationship with macromolecular architectures, and on the other hand, can hopefully lead to the development of new types of polymer-based nanomaterials.

In principle, novel nanostructures of double-brush copolymers are expected to result from the self-assembly of their two types of heterografts. Because the self-assembly behavior can be affected by the size of the backbone, size and property of heterografts, grafting density, number ratio of two types of heterografts, environment, as well as processing procedure, a series of nanostructures can be targeted by adjusting the above factors. As shown in **Table 2-6**, when backbone and heterografts have comparable sizes, double-brush copolymers may take a ***Janus*** type of nanostructure in solution and on surface (**a**); when the backbone is much longer than the heterografts, and at the same time, one type of heterograft has a much stronger attraction toward the environment or is significantly longer than the other, double-brush copolymers may take a ***nano-hotdog*** type of nanostructure in solution and on surface (**b**); when the backbone is much longer than densely grafted heterografts, and at the same time, both types of heterografts have comparable size and show not too different interaction with solvent, double-brush

copolymers may take an ***ornamented nano-hotdog*** type of nanostructure in solution (c), which may collapse to ***rod-like*** nanostructure with phase separation on the surface by dynamic control (c_1) or may form well-defined ***bilayer*** nanostructure on the surface by

Table 2-6. Expected Novel Nanostructures of Double-Brush Copolymers

nanostructure *in solution*	nanostructure profile *in solution*	nanostructure *on surface*
a 	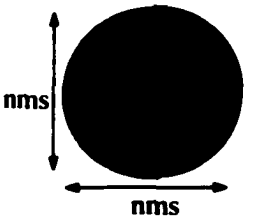	
b 	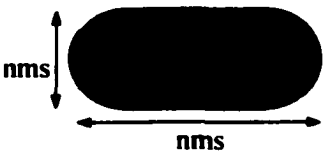	
c 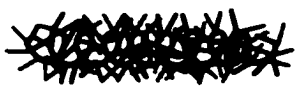	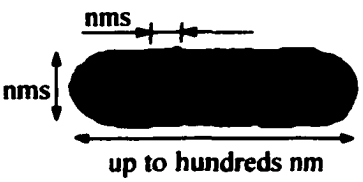	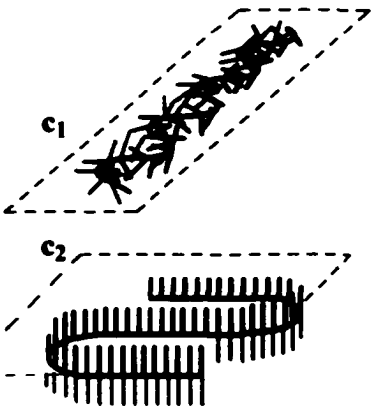
d 	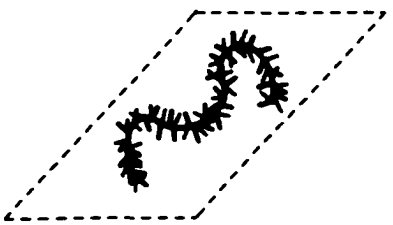	

thermodynamic control with one type of heterograft strongly attracted with surface (c_2); when the second type of heterograft is composed of polyelectrolyte, double-brush copolymers may take ***stretched-brush*** nanostructure in solution and on surface (**d**).

No prediction is made here for bulk morpohologies of double-brush copolymers because of their complexity. Bulk morphologies of A_8B_8 heteroarm star copolymers [*47*] might be a good reference for double-brush copolymers with a relatively short backbone compared with grafts. To the best of our knowledge, there is no suitable reference for double-brush copolymers with backbone longer than grafts. However, it is the latter case that attracts our major attention in synthesis and subsequent nanostructure investigation.

2-6b **Preliminary Surface Morphology Characterization Results.** Due to the limited availability of morphology characterization instruments for us, only preliminary surface morphology characterization has been done.

AFM characterization was carried out for spin-cast samples on silica surface. Collapsed rod-like morphologies (**Figure 2-19**) were obtained for the sample prepared by spin-casting diluted solution (0.1-0.2 mg/ml) of double-brush copolymer **II-6a6**, which has a polystyrene graft with DP_n of 81 and a poly(MMA) graft with DP_n of 233 simultaneously connected to each norbornene monomer unit in a relatively long polynorbornene backbone with DP_n of 220 (average about 1100 carbon atoms on backbone main-chain). The average dimensions of **II-6a6** molecules were up to 300-400 nm long, around 80 nm wide, and within few nm high. Spin-cast samples from other double-brush copolymers with long backbone, except **II-6b** series, exhibited similar surface morphologies but with varied width. The dimension in width, ranging from about

30 nm to about 100 nm, depends on graft size. For **II-6b** series, only images with poor resolution were obtained, due to their very short grafts (DP_n around 10 or less).

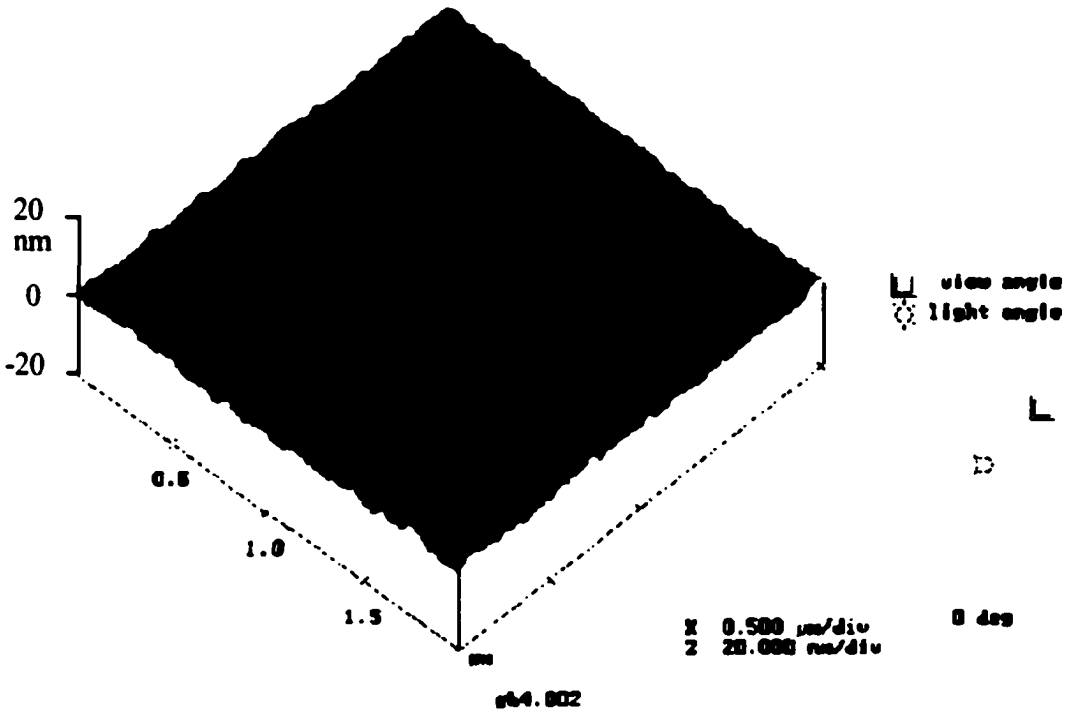

Figure 2-19. AFM 3-D image of double-brush copolymer **II-6a6**

Collapsed *ornamented nano-hotdog* type of nanostructures (**Table 2-6, c1**) were expected for these spin-cast double-brush copolymer macromolecules on surface. However, their phase separation of double-brush copolymers could not be detected by AFM, because of the limited sensitivity and resolution of AFM compared with the dimension of the copolymer samples, and the contacting mode available to us. Spin-cast samples from further diluted solutions (0.02-0.04 mg/ml) of double-brush copolymers, except **II-6b** series, exhibited better AFM images with each macromolecule well separated without significant overlap. But non-identical AFM images were obtained by

scanning the same region of the same sample twice, and this result suggests, using the contacting mode, the AFM tip can disturb the double-brush copolymer molecules on surface, and therefore their dimensions thus obtained cannot be accurate. The tapping mode should be better than the contacting mode for AFM measurement of brush polymers [*48*], but the AFM instrument available for us can only be operated using contacting mode.

Thus, TEM was then used to examine the self-assembly of the Langmuir-Blodgett (L-B) films of the copolymer samples. All L-B films were prepared under the same conditions. RuO_4 was used to selectively stain polystyrene, and polystyrene domains appeared black in TEM images. Because L-B technique typically results in a thermodynamically equilibrated monomolecular layer, with two types of grafts, the double-brush copolymer samples obtained (long backbone) are expected to have *bilayer* nanostructure (**Table 2-6**, $\mathbf{c_2}$) with polystyrene components on the top and poly(MMA) components on the bottom. These L-B films are relatively flat, with roughness under 1 nm by AFM.

With the same DP_n of polystyrene grafts, the TEM images of **II-6a6**, **II-6c1**, and **II-6d1** were compared (**Figure 2-20**). For all samples, single macromolecules cannot be recognized. Compared with the dark polystyrene domain, poly(MMA) domain is in the white region and may also be under the polystyrene domain. Distinct nano-sized 2-D network of polystyrene domain of L-B film of double-brush copolymer **II-6a6** was detected by TEM, and the dimension of polystyrene domain (~3 nm) corresponds to the aggregation of only a number of polystyrene grafts of individual macromolecule. An explanation was proposed, as shown in **Figure 2-21**. By L-B technique, phase separation

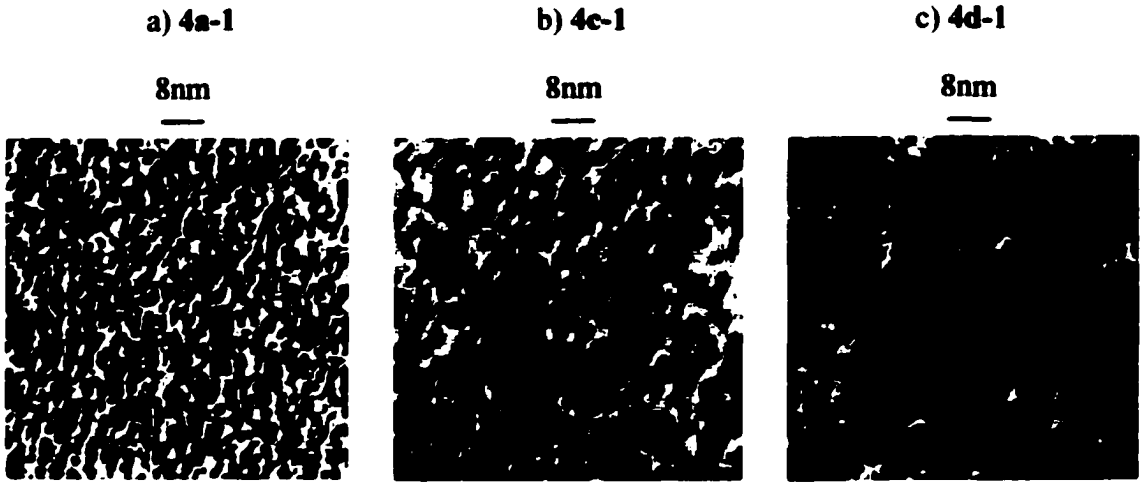

Figure 2-20. TEM images of L-B films of double-brush copolymers a) **II-6a6**, b) **II-6c1**, and c) **II-6d1**.

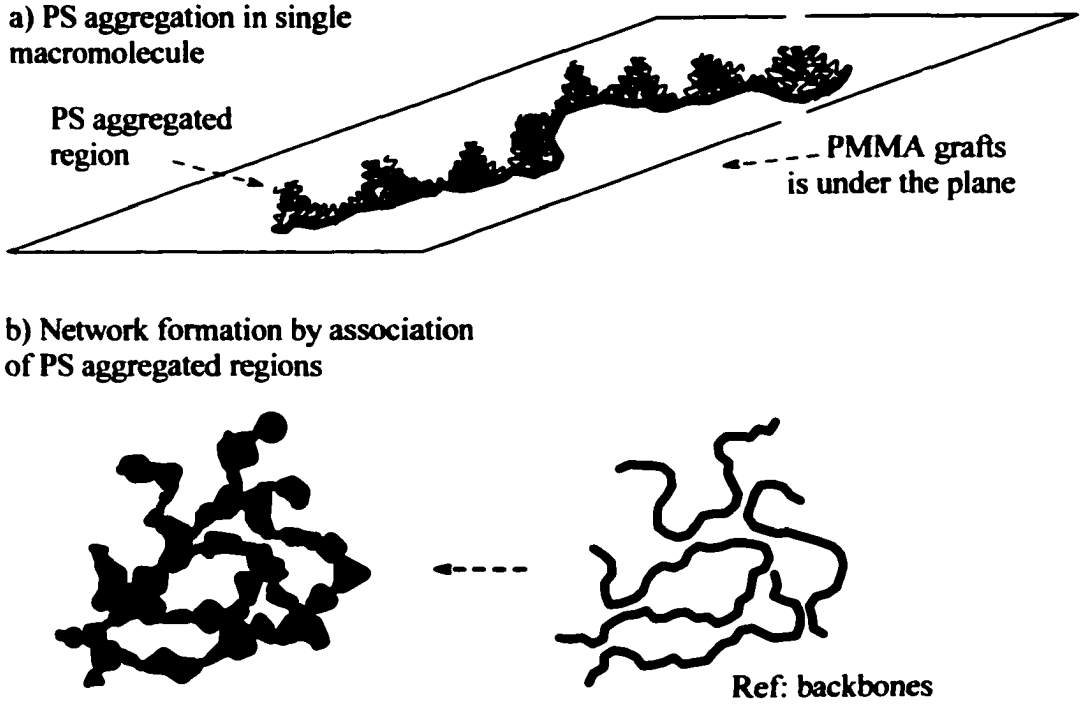

Figure 2-21. Proposed explanation of self-assembly in L-B films of double-brush copolymers.

of polystyrene blocks and poly(MMA) grafts occurred within individual macromolecule of **II-6a6**. Since the rigid backbone (with an average of 1100 carbon atoms) of **II-6a6** is much longer than its polystyrene grafts, the polystyrene grafts within an individual macromolecule aggregated along the backbone at a number of regions to give a ribbon-like polystyrene domain with varied width dimension. With densely grafted poly(MMA) grafts much longer than the polystyrene grafts, association of polystyrene aggregated regions was greatly restricted and occurred only occasionally to form "knot" of network. L-B film from copolymer **II-6c1** presented a similar nano-sized 2-D network of polystyrene domain but had an increased size of polystyrene domain with a dim edge, presumably as a collective result of topologically sparse placement of polystyrene grafts in **II-6c1**, and increased association of polystyrene aggregation regions due to decreased graft density and poly(MMA) graft length. Furthermore, the poly(MMA) grafts are significantly shorter than the polystyrene grafts in **II-6d1** and therefore are not effective in preventing the association of polystyrene aggregation regions in **II-6d1**. Thus, L-B film of **II-6d1** was nearly covered by polystyrene domain as detected by TEM. However, in the case of **II-6d1**, long polystyrene grafts are expected to be serve as effective spacers to restrict the aggregation of poly(MMA) grafts, and thus, there might be nano-sized 2-D network of poly(MMA) domain on the bottom layer of L-B film, although it cannot be detected by TEM. Further investigation of L-B films of double-brush copolymers is required to prove the above explanation and expectations.

2-7 Experimental

Materials. Grubbs catalyst $RuCl_2(CHC_6H_5)[P(C_6H_{11})_3]_2$ (Strem), Schrock catalyst $Mo(C_{10}H_{12})(C_{12}H_{12}N)[OC(CH_3)(CF_3)_2]_2$ (Strem), 5-norbornene-2-methanol (98%, *exo/endo*, Aldrich), *sec*-butyllithium (*s*-BuLi; 1.3 *M* in cyclohexane, Aldrich), lithium chloride (99.99%, Aldrich), iodotrimethylsilane (Me_3SiI; 97%, Aldrich), *p*-toluenesulfonic acid monohydrate (98.5%, Aldrich), and iodomethane (99%, Acros) were used as received. Nitrogen (>99.999%, Welco) was used as inert atmosphere for all reactions without further purification. Styrene (99.5%, Acros) and styrene-d_8 (98%, Polymer Source) were distilled over CaH_2 and then distilled over sodium. Methyl methacrylate (MMA; 99%, Aldrich) and *tert*-butyl acrylate (*t*-BA; 99%, TCI) were diluted with toluene, distilled over CaH_2 and then distilled from triethylaluminum. 2-(Dimethylamino)ethyl methacrylate (DMAEMA; 98%, Aldrich) was distilled over CaH_2. Benzene (99.9%, Acros) and toluene (99%, J.T.Baker) were distilled over CaH_2 and then distilled from 1,1-diphenylhexyllithium. Tetrahydrofuran (THF; 99.9%, Acros) was refluxed overnight over CaH_2 and then distilled from sodium naphthalene. Dichloromethane (99.9%, Acros), chloroform-*d* ($CDCl_3$; 99.8%, Acros), ethyl vinyl ether (99%, Aldrich) were distilled over CaH_2. Benzaldehyde (99.5%, Aldrich) and allyl iodide (98%, Acros) were distilled. 1-(4-Bromophenyl)-1-phenylethylene was synthesized using the literature procedure [*13*]. Poly(styryl)lithium (PSLi) was prepared by anionic polymerization of styrene using *s*-BuLi as initiator in benzene at room temperature or in THF at -78 °C.

1-[4-(3-Bromodecyl)phenyl]-1-phenylethylene. Grignard reagent was prepared from 1-(4-bromophenyl)-1-phenylethylene (26 g, 100 mmol) and magnesium (3.21g, 132 mmol) in THF at 45 °C for 3 h and then reacted with the THF solution of 1,10-dibromodecane (100 g, 333 mmol) in the presence of a catalytic amount of Li_2CuCl_4 at room temperature overnight. Then the reaction mixture was evaporated to dryness, diluted by dichloromethane, washed with water, and dried over $MgSO_4$. Removal of solvent under reduced pressure followed by flash column chromatography (9:1 cyclohexane-dichloromethane) yielded 1-[4-(3-bromodecyl)phenyl]-1-phenylethylene (16.4 g, 41 mmol, 41%) as a pale yellow liquid. ^{1}H NMR (600 MHz, $CDCl_3$, δ): 7.37-7.12 (m, 9H, Ar-H), 5.44 (d, 1H, =CH*H*), 5.40 (d, 1H, =C*H*H), 3.40 (t, 2H, CH_2), 2.61 (t, 2H, CH_2), 1.85 (p, 2H, CH_2), 1.62 (p, 2H, CH_2), 1.47-1.24 (m, 12H, 6 × CH_2).

DPE-Functionalized Norbornene Monomer II-1. 5-Norbornene-2-methanol (5.0 g, 40 mmol) was mixed with sodium hydride (1.3 g, 54 mmol) in THF at room temperature for 10 min. Then 1-[4-(3-bromodecyl)phenyl]-1-phenylethylene (9.2 g, 23 mmol) was added, and reaction mixture was kept at 50 °C for 24 h. The reaction mixture was evaporated to dryness, diluted by dichloromethane, washed with water, and dried over $MgSO_4$. Removal of solvent under reduced pressure followed by flash column chromatography (9:1 cyclohexane-dichloromethane) yielded to give **II-1** (7.3 g, 17 mmol, 72%) as a pale yellow liquid. **II-1** was purified by crystallization and repeated recrystallization from pentane at -20 °C. Further separation by flash column chromatography (pentane-dichloromethane gradient) afforded *exo*-enriched **II-1** (*exo*-**II-1**, *exo* > 95%; 0.14 g, 0.32 mmol), *endo*-enriched **II-1** (*endo*-**II-1**, *endo* > 98%; 0.51 g,

1.2 mmol), and *exo/endo*-mixed **II-1** (*exo/endo*-**II-1**, *exo/endo* = 43/57; 6.6 g, 15 mmol). ^{1}H NMR data were in **Figure 2-1**.

Polyfunctional DPE-Agent II-2. Ring-opening metathesis polymerization of **II-1** was carried out in a pre-flamed glass bottle with magnetic stirring in room temperature. All chemicals were transferred with dry syringes. Grubbs catalyst (solvent: chloroform-*d*, methylene chloride or THF) or Schrock catalyst (solvent: toluene or THF) was used as initiator. In the synthesis of **II-2a** and **II-2b**, polymerization was induced by adding THF solution of **II-1** into a THF solution of Grubbs initiator, and 3 h later polymerization was terminated with ethyl vinyl ether. The solution of poly(**II-1**), i.e. **II-2**, was then stored at room temperature. ^{1}H NMR (600 MHz, $CDCl_3$, δ): 7.40-7.06 (m, 9H, Ar-H), 6.43-6.09 (m, α-chain-end –CH=CH–), 5.42 (s, 1H, =CH*H*), 5.38 (s, 1H, =C*H*H), 5.33 (b, 2H of *cis* –CH=CH–), 5.20 (b, 2H of *trans* –CH=CH–), 3.33 (b, 3H of $NBCH_2OCH$*H*), 3.14 (b, 1H of $NBCH_2OC$*H*H), 3.08-2.54 (m, 3H, 1H of NB and 1 × CH_2), 2.45 (b, 1H of NB), 2.30-0.99 (m brs, 21 H, 5H of NB and 8 × CH_2).

Linear Polycarbanionic Macroinitiator II-3. Reaction between excess of *s*-BuLi and **II-2** was carried out at -78 °C in a pre-flamed glass bottle with magnetic stirring. All chemicals were transferred with dry syringes. *s*-BuLi was slowly added into THF solution of **II-2**. Red THF solution of **II-3** was yielded within 1 h and then was stored at -78 °C.

Graft-Block Copolymers II-4. Copolymers **II-4a**, **II-4b**, **II-4c**, and **II-4d** were synthesized by anionic graft polymerization using **II-3** as initiator. Polymerization was carried out in a pre-flamed glass bottle with magnetic stirring. All chemicals were transferred with dry syringes. After THF, a THF solution of lithium chloride, and a THF

solution of **II-3** were added, the flask was cooled to -78 °C in a methanol-dry ice bath. Then MMA and *t*-BA were added following different sequences, and the intervals between monomer additions were 1 h. After termination with methanol, the polymerization solution was precipitated into cold methanol or methanol-water (80/20). Crude copolymers recovered were purified by LC to remove any linear polymers. ^{1}H NMR (600 MHz, $CDCl_3$, δ): 7.37-6.73 (m, 9H of Ar-H of **II-2**), 3.56 (s, 3H of OCH_3 of MMA), 2.22 (s, 1H of CH of *t*-BA), 1.98-1.12 (m, 2H of CH_2 of MMA, 2H of CH_2 of *t*-BA, and 9H of *t*-C_4H_9 of *t*-BA), 1.06-0.63 (m, 3H of CH_3 of MMA).

Amphiphilic copolymers **II-4e** and **II-4f** were synthesized from **II-4c** and **II-4d** respectively by selective hydrolysis. Reactions were carried out in a pre-flamed glass bottle with magnetic stirring. **II-4c** and **II-4d** were dissolved in benzene, and then excesses of iodotrimethylsilane relative to *t*-BA units in copolymers were added. The reactions underwent at room temperature for 2 h before solvent was removed under reduced pressure. Reaction mixtures were dissolve in THF and then were precipitated in 0.1 *N* HCl aqueous solution containing $Na_2S_2O_3$ (discoloring agent). The copolymers recovered were purified by repeated precipitation from THF into pentane. ^{1}H NMR (600 MHz, DMSO-d_6, δ): 7.37-6.73 (m, 9H of Ar-H of **II-2**), 3.56 (s, 3H of OCH_3 of MMA), 2.23 (s, 1H of CH of AA), 1.98-1.12 (m, 2H of CH_2 of MMA, 2H of CH_2 of AA), 1.06-0.63 (m, 3H of CH_3 of MMA).

Polystyrene-Grafted Polycarbanionic Macroinitiator II-5. All reactions were carried out in a pre-flamed glass bottle with magnetic stirring. All chemicals were transferred with dry syringes. PSLi solution was slowly added into THF solution of **II-2** at -78 °C, and **II-5a** and **II-5c** were yielded within hours. **II-5b** was obtained by standing

II-5a3 solution at room temperature for 36 h. **II-5d** was obtained by further reacting **II-5c1** with an excess of *s*-BuLi at -78 °C for 1 h. All **II-5** solutions were red and were stored at -78 °C.

Double-Brush Grafted Copolymers II-6. Anionic graft polymerization initiated by **III-5** was carried out in a pre-flamed glass bottle with magnetic stirring. All chemicals were transferred with dry syringes. After THF, a THF solution of lithium chloride, and a THF solution of **II-5** were added, the flask was cooled to -78 °C in a methanol-dry ice bath.

For the synthesis of model macromolecules **II-6a1** and **II-6a2**, MMA was added dropwise into the flask, and the addition was stopped as soon as the red color of reaction mixture disappeared, and then an excess of allyl iodide was added. The flask was moved out from the methanol-dry ice bath and was kept at room temperature overnight. Then the polymerization solution was precipitated into methanol to yield **II-6a1** and **II-6a2**. Their NMR data were shown in **Figure 2-10** and **Figure 2-11**.

For the synthesis of other copolymers except **II-6b4** and **II-6b5**, polymerization was induced by addition of monomer, and then was terminated with methanol 1 h later. The polymerization solution was precipitated in methanol. Crude copolymers recovered were purified by LC to give **II-6** as white solid. Their ^{1}H NMR data were shown in **Figure 2-13**, **Figure 2-14**, and **Figure 2-15**.

For the synthesis of amphiphilic copolymer **II-6b4**, 0.29 g of **II-6b2**, 0.028 g *p*-toluenesulfonic acid and 0.28 g water were added into 6 ml toluene. The reaction mixture was heated at 100 °C for 5 h. Then the reaction mixture was evaporated to dryness,

dissolved by THF, and precipitated in pentane to finally give **II-6b4** as pale yellow solid. ^{1}H NMR data were shown in **Figure 2-16**.

For the synthesis of amphiphilic copolymer **II-6b5**, 0.17 g of **II-6b3** was dissolved in 12 ml THF, and 0.1 ml iodomethane was then added. After 24 h, the reaction mixture was precipitated in pentane to give **II-6b5** as yellow solid. ^{1}H NMR data were shown in **Figure 2-17**.

Characterization. NMR spectra were acquired at room temperature on a Varian 600 MHz spectrometer at room temperature. For each spectrum, 64 to 128 transients were collected with pulse angle of 39° and delay time of 3 s. For **II-2** samples which were synthesized not in $CDCl_3$, the solvents were replaced with $CDCl_3$ by repeated distillation under reduced pressure and addition of $CDCl_3$ for NMR measurement.

GPC measurements were performed at 40 °C on a Waters-150C instrument equipped with three Ultrastyragel columns (10^4, 10^5, 10^6 Å) and two Styragel columns (HR1, HR3) using a RI detector, linear polystyrene calibration, and THF as eluent at 1.0 mL/min.

AFM images were recorded with a Nanoscope III instrument operating in the contact mode, using tip with radius of about 20 nm. The samples were prepared by spin-casting diluted polymer solution on silica wafer.

TEM images were obtained using a JEOL 200 CX electron microscope. The samples were prepared by the Langmuir-Blodgett (L-B) technique. Each polymer sample was dissolved in chloroform at 1 mg/mL before spreading on the water. Each solution was spread using a micro-syringe at ambient temperature. A computer controlled KSV3000 double barrier L-B trough was used. Measurement of surface pressure-area (π-

A) diagram was followed by the transfer of monolayers, i.e. L-B films, onto hydrophilic silicon wafers at 15 dyne/cm. The barrier and film transferring speed were 5 mm/min and 2 mm/min respectively. Distilled and deionized water was used as the subphase.

2-8 Conclusions

Polyfunctional DPE-agents were prepared by selective polymerization of norbornene functionality of DPE-norbornene bifunctional monomer via ROMP, with DPE functionality intact. Polyfunctional DPE-agents react with *sec*-BuLi and poly(styryl)lithium quickly and quantitatively to give linear and polystyrene-grafted polyanionic macroinitiators respectively. These macroinitiators are the first reported polycarbanionic macroinitiators with controlled initiator sites.

Anionic polymerization using linear polycarbanionic macroinitiators provides the only method for the synthesis of densely grafted copolymers with unusually long grafts. Block structures of grafts can be obtained through sequential monomer addition.

With new and unique macromolecular architectures, double-brush copolymers were synthesized by anionic polymerization using polystyrene-grafted polyanionic macroinitiators. These double-brush copolymers are expected to possess a wide variety of novel nanostructures based on the self-assembly of their two types of heterografts, and such expectation was supported by the preliminary characterization results. Further investigation on their nanostructures is undergoing.

Chapter 3

Synthesis and Ring-Opening Metathesis Polymerization of Diblock Macromonomers with Block Junction Carrying Norbornenyl Functionality

Abstract: Five types of well-defined diblock macromonomers with block junction carrying a norbornenyl group were synthesized by anionic polymerization via DPE-norbornene bifunctional agent. For these diblock macromonomers, one block was poly(styrene-d_8), and the other block was poly(MMA), poly(*t*-BA), poly(2-vinylpyridine), poly(ethylene oxide), or poly(dimethylsiloxane). Both blocks had, in most cases, low DP_n around 10. Ring-opening metathesis polymerization (ROMP) of these diblock macromonomers using Grubbs initiator yielded corresponding poly(macromonomer)s with high conversion. In-situ ^{1}H NMR analysis showed that the formed poly(macromonomer)s have well-controlled DP_n, reflecting the living characteristic of the ROMP process. GPC analysis verified narrow monomodal molecular weight distribution of poly(macromonomer)s. Different polymerization kinetics for macromonomers were observed and were considered to be related to self-assemblies of macromonomers and poly(macromonomer)s. In terms of macromolecular architectures, these poly(macromonomer)s with heterografts are also double-brush copolymers, and are expected to possess novel nanophase-segregated morphologies.

3-1 Introduction

Synthesis and polymerization of macromonomers is an important research area of polymer synthetic chemistry [*1-3*]. In recent years, macromonomers typically were synthesized based on living polymerization techniques using functionalized initiator [*4-8*], chain-transfer agent [*9*], or functionalized terminating/end-capping agent [*10-13*]. Macromonomers thus produced can have well-controlled structures, including well-defined polymerizable functional group(s) and number-average molecular weight (M_n), as well as low polydispersities. Ocassionally, nonliving polymerization techniques, such as conventional radical polymerization [*14-16*], were also used in macromonomer synthesis. but macromonomers thus synthesized cannot have well-controlled M_n and low polydispersities.

Macromonomers can be classified based on their polymerizable functional group(s) and the polymerization technique(s) that can be used to polymerize them. Macromonomers to be polymerized by step polymerization have more than one functional group, such as acid, alcohol, or amine group [*17-19*]. Macromonomers with (substituted) vinyl functionality can be polymerized by chain polymerization. Radical polymerization [*20-30*] and coordination polymerization [*31-33*] have been generally used to polymerize these macromonomers; ionic polymerization, such as anionic polymerization [*34, 35*], occasionally have also been used but with considerable limitations, partly because ionic polymerization generally requires stringent reaction conditions. Macromonomers to be polymerized by ring-opening polymerization contain

polymerizable cyclic functionalities, such as lactone [*36*], pyrrole [*6*], oxazoline [*37*], or norbornene [*4, 38-46*].

Macromonomers can also be classified in terms of the polymers on which they are based. Many homopolymer-based macromonomers have been reported. At the same time, macromonomers having block structures have attracted increasing attention [*15, 28-30, 35, 41, 44*].

Along with polymerization using a macroinitiator with non-terminal initiator site(s) ("grafting-from") and coupling reactive polymer chains with a polymeric coupling agent ("grafting-onto"), polymerization of macromonomers is a versatile method for the synthesis of grafted copolymers. A wide variety of grafted copolymers have been synthesized by copolymerization of macromonomer with conventional monomer to give grafts with desired spacing along the backbone. However, poly(macromonomer)s synthesized by polymerization of macromonomer(s) without conventional monomer feed [*4, 27-30, 34, 34, 37-46*] have attracted increasing attention. Poly(macromonomer)s have extremely densely grafted macromolecular architectures with graft regularly bonded to each backbone monomer unit. As a result, poly(macromonomer)s can have special properties based on their unique molecular morphologies, ranging from star-shaped spheres when backbone and side-chains have comparable length to rod-like cylinders when backbone is sufficiently longer than side-chains [*47-57*]. Poly(macromonomer)s obtained from block macromonomers with terminal polymerizable functionality can further have core-shell spherical or cylindrical self-assemblied morphologies, and have been used as templates in special applications, such as preparation of nanoparticles or nanowires [*58*], and encapsulation of functional polymer materials [*59*]. However,

because macromonomers have much higher molecular weights than conventional monomers, the polymerizable group in macromonomer is only a small part of the molecule and therefore its reactivity is significantly decreased by steric hindrance. At the same time, in homopolymerization of macromonomers, the reactivity of propagating chain formed is also significantly decreased by collective steric effect from its side chains. Thus, in order to reach complete or nearly complete conversion in polymerization, the size of macromonomers has to be confined to molecular weight within a few thousands for typical homopolymerization of macromonomers with carbon-carbon double bond as polymerizable functionality, resulting in poly(macromonomer)s with one side chain for every two bonds in backbone. Poly(macromonomer)s with relatively long backbones have been synthesized successfully by radical polymerization [*27-30*]. Interestingly, radical polymerization of hydrophilic poly(ethylene oxide) macromonomers showed much higher polymerization rate in water than in benzene, presumably as a combined result of locally concentrated propagating radicals and monomers in their micellar organization [*20*]. Compared with poly(macromonomer)s synthesized from macromonomers with vinyl unsaturations, poly(macromonomer)s synthesized from macromonomers with polymerizable cyclic functionalities lead to increased spacing of grafts along the backbone. Occasionally these macromonomers with molecular weights above 5000, can still be polymerized with high yield, when initial molar feed ratio of macromonomer to initiator is not high [*37, 39, 40, 42, 44-46*].

Polymerization of macromonomers by living polymerization technique is of increasing significance, because it can yield grafted copolymers with controlled structural parameters, such as DP_n of backbone and graft number. Ring-opening metathesis

polymerization (ROMP) of norbornene-based macromonomers represents a key advancement from generally sluggish polymerization process for many other types of macromonomers. ROMP of macromonomers with terminal norbornenyl functionality can reach nearly complete conversion within hours, and at the same time, the M_n of macromonomers can be up to 10 000 [*39, 42, 44-46*]. A variety of poly(macromonomer)s with novel macromolecular architectures have been synthesized by ROMP [*41, 44*]. Molybdenum-based initiators, which have high reactivity, were used in most published reports of ROMP of norbornene-based macromonomers [*38-42, 44-46*]. At the same time, ruthenium-based initiators, which have lower reactivity but much better functional group tolerance than molybdenum-based initiators, were also used for ROMP of norbornene-based macromonomers [*43*].

Up to now, macromonomers with non-terminal polymerizable groups have been developed only to a limited extent, possibly due to their synthetic difficulties and relatively low reactivity. To the best of our knowledge, reported works on polymerization of homopolymer-based macromonomers with non-terminal polymerizable groups are very limited [*21, 22, 38*], and only one of them involves homopolymerization [*38*]. On the other hand, synthesis and polymerization of block macromonomers with non-terminal polymerizable groups is of special significance in polymer chemistry, because the corresponding poly(macromonomer)s have unique macromolecular architectures, and are expected to have novel self-assemblied morphologies and new applications. This chapter presents our research on synthesis and ROMP of diblock macromonomers with block junction carrying norbornenyl group. Well-defined macromonomers were prepared by living anionic polymerization based on 1,1-diphenylethylene (DPE) chemistry using

DPE-norbornene bifunctional agent. The background of DPE chemistry, especially its application in anionic polymerization, has been presented in the introduction section of Chapter 2. Ruthenium-based Grubbs initiator was used for ROMP of the macromonomers, yielding poly(macromonomer)s with well-controlled DP_n and high yield. Self-assembly-assistance for macromonomer polymerization suggested by ROMP of some of the macromonomers indicates a strategy to improve the generally slow polymerization rate of macromonomers. The poly(macromonomer)s produced have two types of polymer side-chains densely carried by the backbone, and therefore they are also double-brush copolymers. Different from the double-brush copolymers with relatively long heterografts obtained by anionic polymerization using grafted polycarbanionic macroinitiator described in Chapter 2, these double-brush copolymers obtained from ROMP of diblock macromonomers with non-terminal norbornenyl functionality have well-defined but relatively short heterografts. Thus, with two synthetic strategies developed suitable for the syntheses of double-brush copolymers with long and short side-chains respectively, this dissertation has provided solid synthetic foundation for further studies on double-brush macromolecular architectures.

3-2 General Research Design

The synthetic strategy of double-brush copolymer via ROMP of diblock macromonomers with block junction carrying norbornenyl functionality is illustrated by **Scheme 3-1**. DPE-norbornene bifunctional agent reacts with living polymer anion ($P_1^-Li^+$; prepared by anionic polymerization of M_1) through its DPE functionality, and the

macroinitiator formed is used directly or is converted into another type of macroinitiator to initiate anionic polymerization of M_2. The norbornenyl group is not involved in the anionic process [*4*, *41*, *44*], and the products yielded are macromonomers with norbornenyl group connected to the DPE junction of the diblock chain. ROMP of the macromonomers directly yields double-brush copolymers as poly(macromonomer)s.

Scheme 3-1

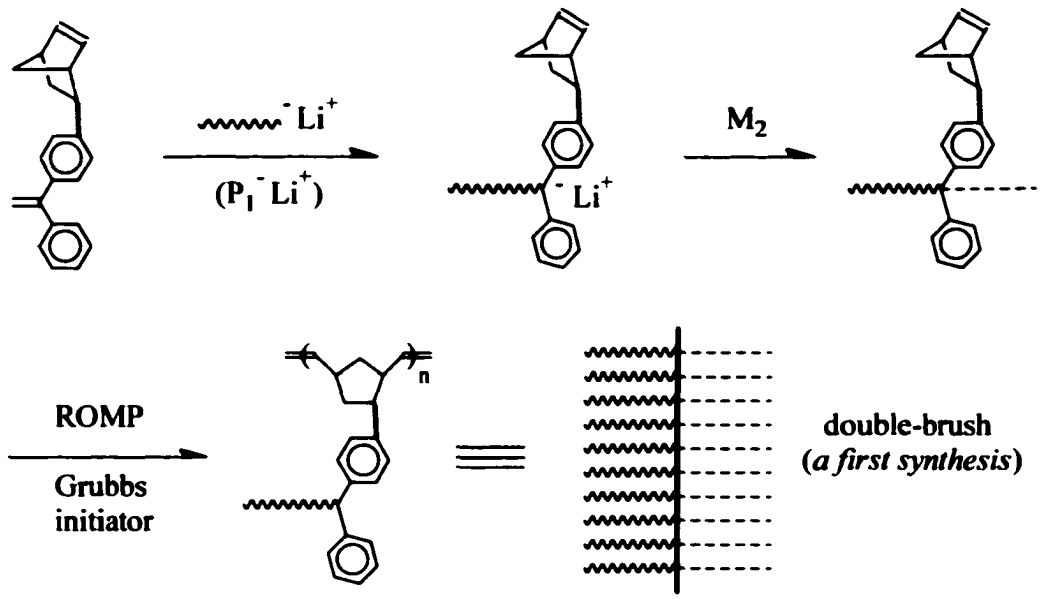

: P_1 [P(St-d_8)]; ------: P_2 [PMMA, P(*t*-BA), P(2-VP), PEO, or PDMS]

Deuterated poly(styryl)lithium, instead of non-deuterated poly(styryl)lithium, was used as $P_1^-Li^+$ to avoid interference from non-deuterated aromatic protons on ^1H NMR determination of α-backbone-end protons of the poly(macromonomer)s final products. Thus, poly(styrene-d_8) serves as the first block for the diblock macromonomer, as well as one type of hetergraft for double-brush architectures of poly(macromonomer)s. A variety of monomers, including methyl methacrylate (MMA), *tert*-butyl acrylate (*t*-BA), 2-

vinylpyridine (2-VP), ethylene oxide (EO), and hexamethylcyclotrisiloxane (D_3) were used as the second monomer for anionic polymerization. Thus, the second block for diblock macromonomer, as well as the other type of heterograft for double-brush architectures of poly(macromonomer)s can be either poly(MMA), or poly(*t*-BA), or poly(2-VP), or poly(ethylene oxide), or poly(dimethylsiloxane). To maintain reasonable reactivity of norbornenyl group for ROMP through alleviating steric hindrance, a spacer was designed to connect the norbornenyl group to the block junction, and each block of diblock macromonomers has relatively limited size. Because a variety of functionality, such as ester functionality and pyridine functionality, can exist in the diblock macromonomers, a Grubbs initiator [*60*] that has very good functional group tolerance was used for ROMP of macromonomers.

3-3 Synthesis of Diblock Macromonomers with Block Junction Carrying Norbornenyl Functionality

3-3a **Synthesis of Norbornene-Functionalized Poly(styrene-d_8)-Based 1,1-Diphenylalkyllithium.** To synthesize diblock macromonomers with a block junction carrying the norbornenyl functionality, norbornene-functionalized poly(styrene-d_8)-based 1,1-diphenylalkyllithium **III-1** was prepared at first. As shown in **Scheme 3-2**, poly(styryl-d_8)lithium with a DP_n of 10 was prepared by *sec*-butyllithium-initiated anionic polymerization of deuterated styrene in benzene at room temperature, with the initial molar feed ratio of monomer to initiator of 10. A DPE-functionalized norbornene

agent, i.e. **II-1** (*exo/endo* = 43/57), was used to react with an excess of deutrated poly(styryl)lithium in THF at -78 °C to yield the anionic macroinitiator **III-1**.

Scheme 3-2

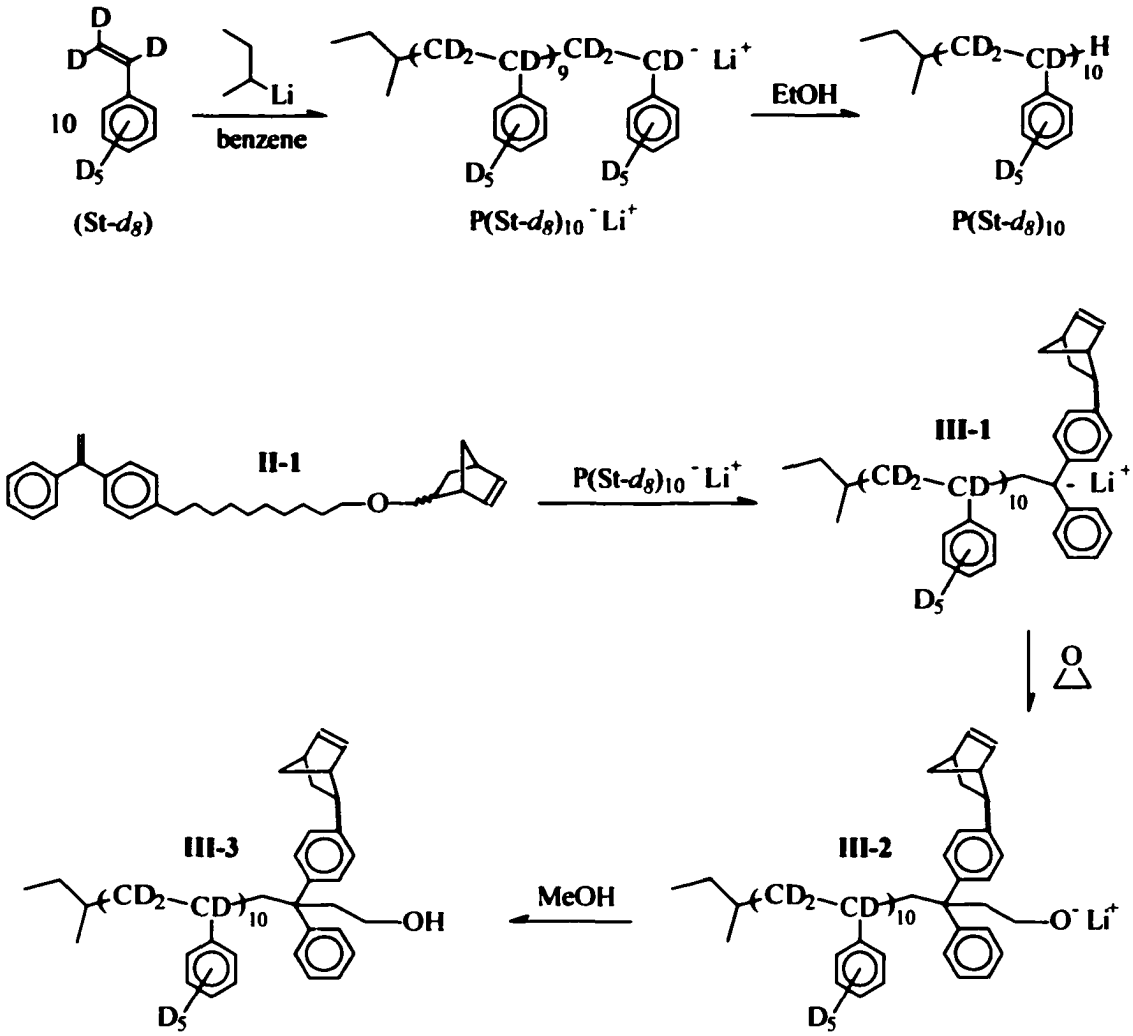

(| : the -$CH_2O(CH_2)_{10}$- spacer connecting norbornenyl group and DPE moiety.)

Well-controlled structure of poly(styryl-d_8)lithium used for the synthesis of **III-2** was verified using its methanol-terminated adduct, i.e. poly(styrene-d_8), because of the

high reactivity of poly(styryl-d_8)lithium. GPC analysis of the poly(styrene-d_8) was carried out using calibration with non-deuterated linear polystyrenes, showing the poly(styrene-d_8) with a peak molecular weight of 1030 (*DP* of 9.4) [*61*], and a polydispersity of 1.20. However, the results from GPC on our samples can only be considered as estimated data [*62*]. Therefore, MALDI analysis of the poly(styrene-d_8) was also performed (**Figure 3-1**). Using a dithranol matrix, MALDI spectrum obtained illustrated unambiguously that the poly(styrene-d_8) has the maximum intensity of molecular weight at 1177.40, corresponding to a *DP* of 10. At the same time, based on the relatively narrow molecular weight distribution of the poly(styrene-d_8) on its MALDI spectrum, its polydispersity was estimated to be below 1.2. ^{1}H NMR is, of course, not applicable for the poly(styrene-d_8) to determine DP_n.

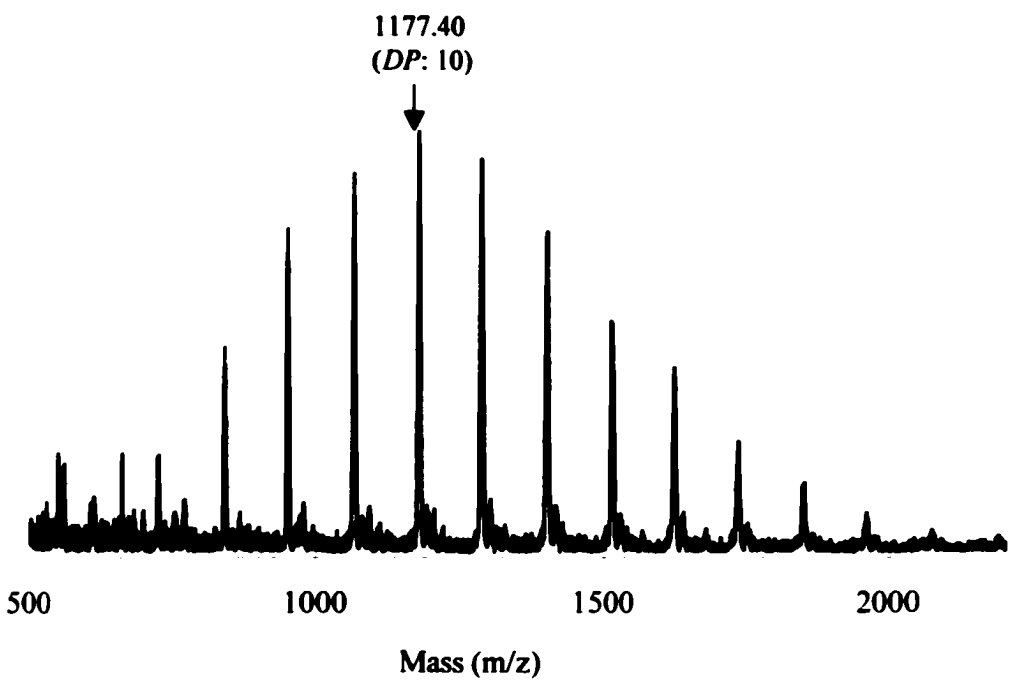

Figure 3-1. MALDI spectrum of poly(styrene-d_8).

Because of the relatively high reactivity of **III-1**, the structure of **III-1** was investigated through **III-3**, which was formed by end-capping **III-1** with ethylene oxide followed by protonation of the resulting **III-2** with acidified methanol. As a result, the well-controlled molecular structures of **III-1** were verified.

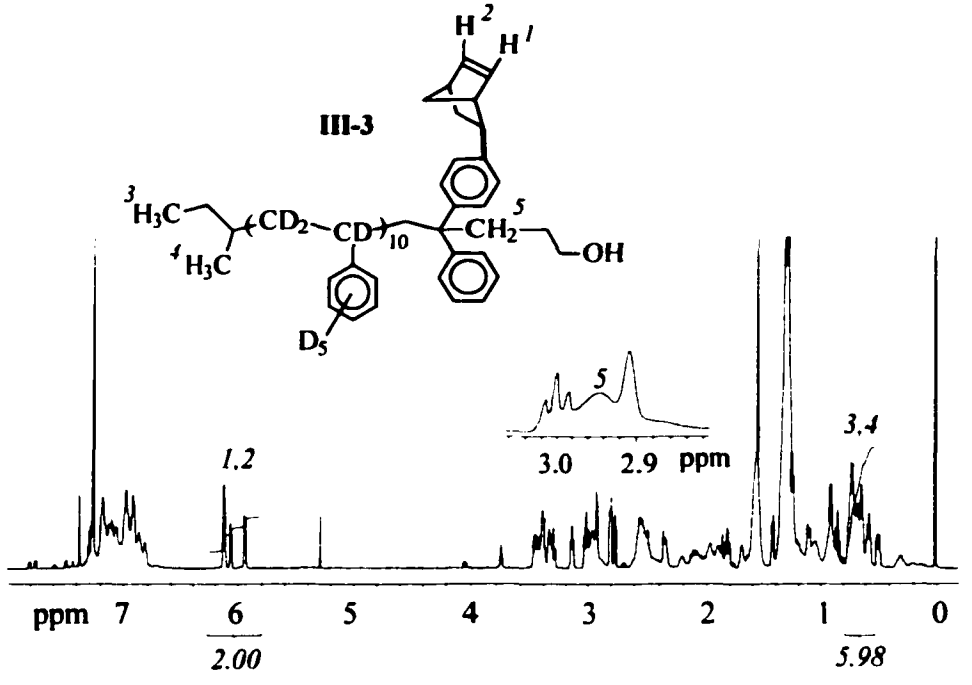

Figure 3-2. ^{1}H NMR spectrum of **III-3** (ethylene oxide-end-capped adduct of **III-1**).

The formation of **III-1** by quantitative monoaddition of poly(styryl-d_8)lithium to DPE functionality of **II-1** was confirmed by ^{1}H NMR analysis of **III-3**. As shown in **Figure 3-2**, resonances of the two alkene protons of norbornenyl group were at 6.15-5.89 ppm; resonances of the six methyl protons of *s*-BuLi fragment were concentrated at 0.77-0.50 ppm. The integration area ratio of these characteristic resonances gave a value of 2.00:5.98, in close agreement with the expected proton number ratio of 2:6, indicating that each molecule of poly(styrene-d_8)-based macroinitiator **III-1** carried a norbornenyl

group. At the same time, although the resonances of methylene protons from ethylene oxide unit centered at 2.94 ppm overlap with resonances of other protons and could not be analyzed quantitatively, its presence on ^{1}H NMR spectrum of **III-3** suggested anionic reactive site on **III-1**.

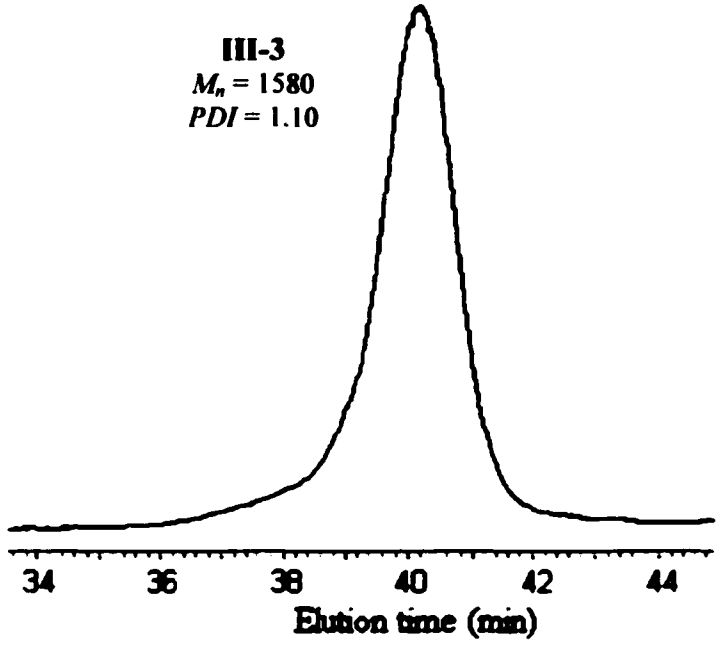

Figure 3-3. GPC curve of **III-3** (ethylene oxide-end-capped adduct of **III-1**).

Narrow molecular weight distribution of **III-1** was also illustrated by the very low polydispersity of 1.10 for its ethylene oxide-end-capped adduct **III-3** detected by GPC analysis (**Figure 3-3**). Because of higher molecular weight of **III-3** relative to poly(styrene-d_8), GPC analysis of **III-3** is much more reliable than GPC analysis of the poly(styrene-d_8) [*63*]. The M_n of 1580 of **III-3** obtained suggested a DP_n of 10 for **III-3**, as well as **III-1**.

3-3b **Synthesis of Diblock Macromonomers with Norbornenyl Group Carried by Block Junctions of Poly(St-d_8)-*b*-poly(MMA), Poly(St-d_8)-*b*-poly(*t*-BA), and Poly(St-d_8)-*b*-poly(2-VP).** Because 1,1-diphenylalkyllithiums are among the most useful initiators for anionic polymerization of methylacrylates, *tert*-butyl acrylate (*t*-BA), and 2-vinylpyridine (2-VP) [*64, 65*], anionic polymerization of MMA, *t*-BA, and 2-VP initiated by norbornene-functionalized poly(styrene-d_8)-based 1,1-diphenylalkyllithium **III-1** can directly yield the corresponding diblock macromonomers **III-4**, **III-5**, and **III-6** with the norbornenyl group connected to diblock junctions (**Scheme 3-3**).

Scheme 3-3

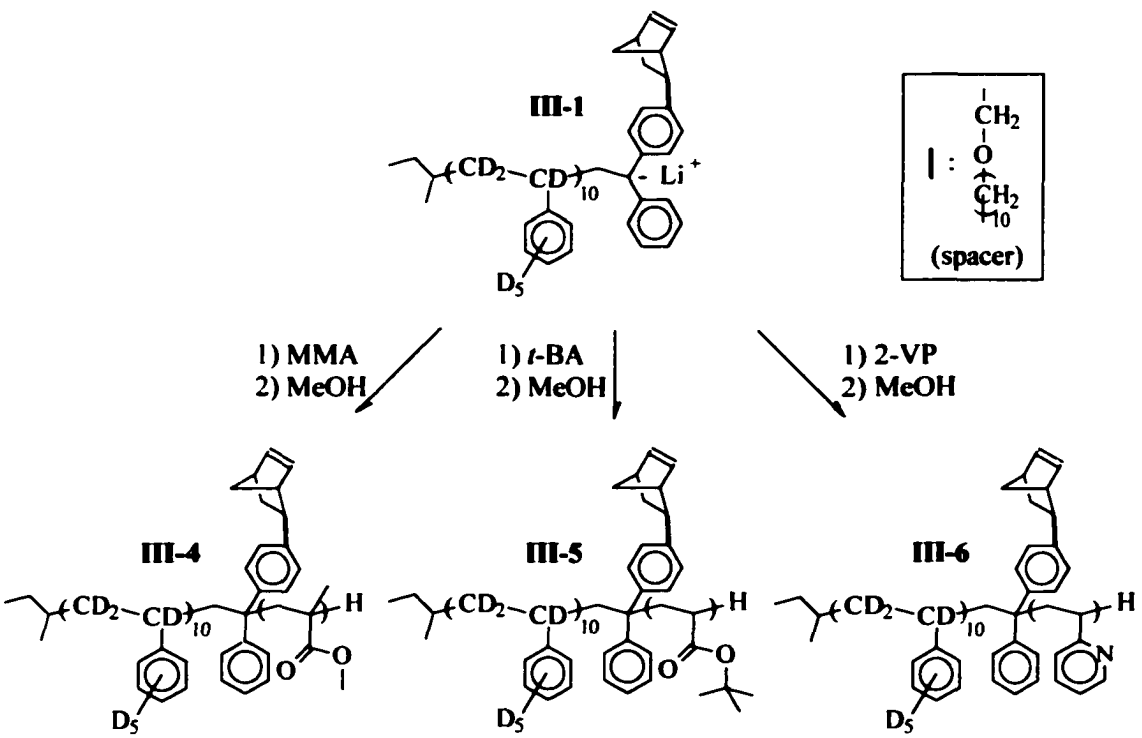

Anionic polymerization initiated by **III-1** wascarried out in THF at -78 °C under nitrogen, in the presence of 10 equivalents of lithium chloride relative to **III-1**. The molar

feed ratio of monomer to **III-1** was 10 for each of the three trials. Because resulting relatively short polymer chains were targeted, employing lithium chloride as additive was very important for the synthesis. Lithium chloride can effectively decrease the ratio of propagation rate constant to initiation rate constant to ensure the polymer chains to have well-averaged opportunity of growth [*66*]. For all trials, monomers were added dropwise into the reaction solutions. When 1.5 equivalents of MMA and *t*-BA were added respectively, the characteristic red color of **III-1** disappeared in the corresponding reaction solutions, indicating fast initiation relative to propagation. Because poly(2-vinylpyridine) anion also has red color, how fast the initiation was relative to propagation could not be judged based on experimental observation for the trial using 2-vinylpyridine as monomer. For all trials, polymerization times were 1 h for complete monomer conversion.

Diblock macromonomers **III-4**, **III-5**, and **III-6** were characterized by ^{1}H NMR, GPC and MALDI analyses. Well-controlled formation of the second blocks and low polydispersities of macromonomers were verified. ^{1}H NMR spectra of **III-4**, **III-5**, and **III-6** are shown in **Figure 3-4**. For all three macromonomers, their norbornenyl functional groups can be readily verified through the characteristic ^{1}H NMR resonances of the alkene protons at 6.15-5.89 ppm; at the same time, the formation of the second blocks can be verified by a number of ^{1}H NMR resonances of the protons from the new repeating units. For macromonomer **III-4** which has a norbornenyl group carried by the DPE block junction of poly(styrene-d_8)-*b*-poly(MMA) diblock copolymer, resonances of methylene protons (concentrated at 1.80 ppm) and α-methyl protons (concentrated at 0.83 ppm) of its MMA monomer units have severe overlap with adjacent resonances; on

the other hand, resonances of ester methyl protons (concentrated at 3.58 ppm) of its MMA monomer units have much less severe overlap with the resonances from $-CH_2OCH_2-$ protons on the spacer of the DPE-NB bifunctional agent. Therefore, based on the resonance intensities of norbornenyl alkene protons and resonance intensities of the ester methyl protons with the subtraction of the contribution of the resonances from $-CH_2OCH_2-$ structure, the DP_n of the poly(MMA) block of **III-4** was estimated to be 11 (M_n of 2700). For macromonomer **III-5** which has a norbornenyl group carried by the DPE block junction of poly(styrene-d_8)-*b*-poly(*t*-BA) diblock copolymer, all resonances from protons of *t*-BA monomer units overlap with resonances of protons from other parts of macromonomer. Therefore the resonance intensities for protons of *t*-BA monomer units can only be estimated, and the comparison of them with the resonance intensities of norbornenyl alkene protons finally led to an estimated DP_n of 10 for the poly(*t*-BA) block of **III-5**, corresponding to a M_n of 2900. For macromonomer **III-6** which has a norbornenyl group carried by the DPE block junction of poly(styrene-d_8)-*b*-poly(2-VP) diblock copolymer, the resonances of its norbornenyl alkene protons at 6.15-5.89 ppm were overlapped by resonances of three pyridine protons of 2-VP monomer units and could not be quantitatively analyzed. Therefore the DP_n of **III-6** of 10.4, corresponding to a M_n of 2700, was determined based on the comparison between the intensities of resonances of the pyridine proton just adjacent to amine functionality of 2-VP monomer units at 8.65-7.89 ppm and the intensities of resonances of the six methyl protons of *s*-BuLi fragment at 0.77-0.50 ppm.

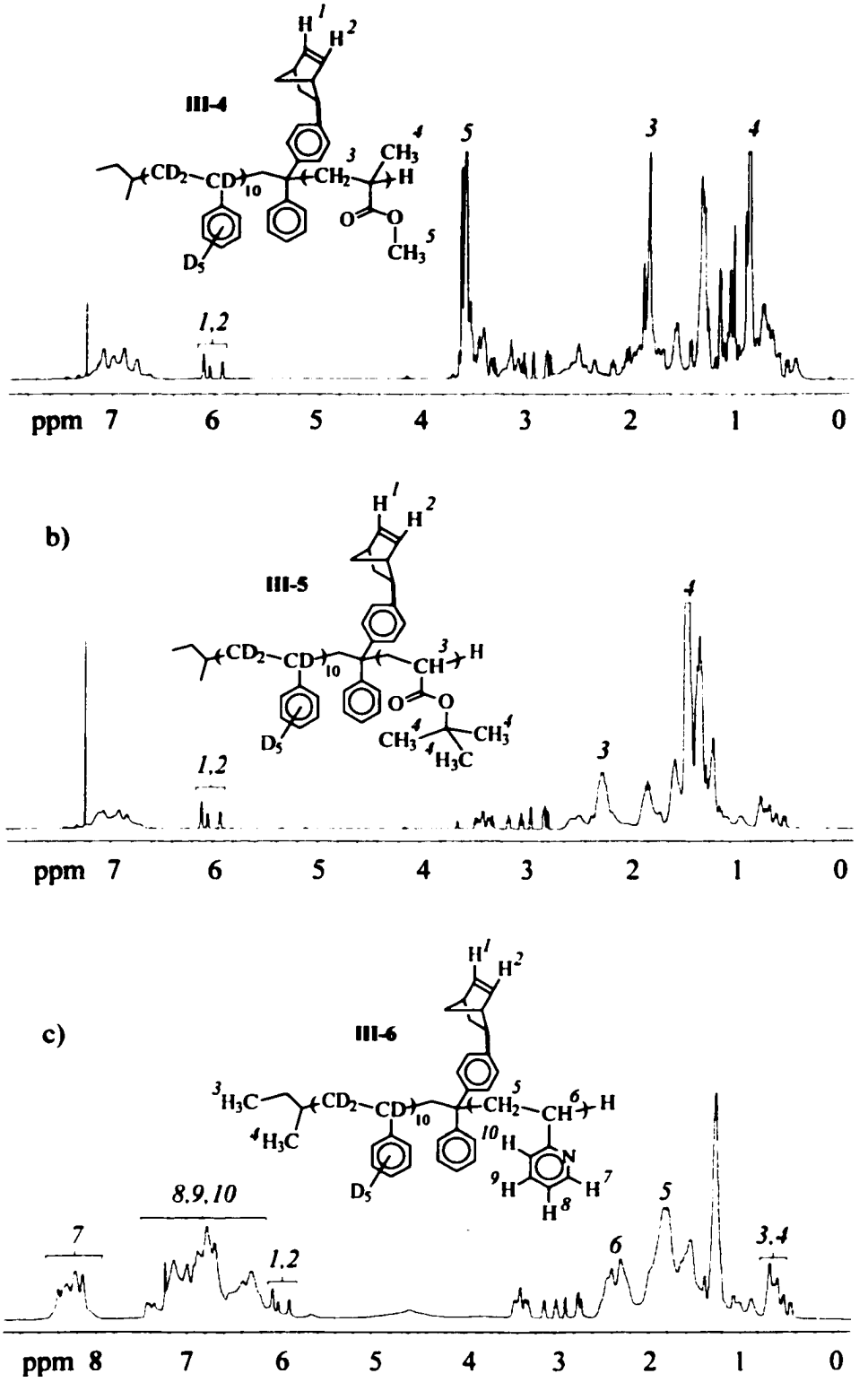

Figure 3-4. ^{1}H NMR spectra of a) **III-4**, b) **III-5**, and c) **III-6**.

Low polydispersities of macromonomers **III-4**, **III-5**, and **III-6** were verified by GPC analysis. As shown in **Figure 3-5**, all of the macromonomers exhibited a very narrow and monomodal GPC peak. GPC analysis of them also gave M_n values. However, because the structural differences between them and the polystyrene standards used for calibration, these M_n values obtained can only be considered as estimations.

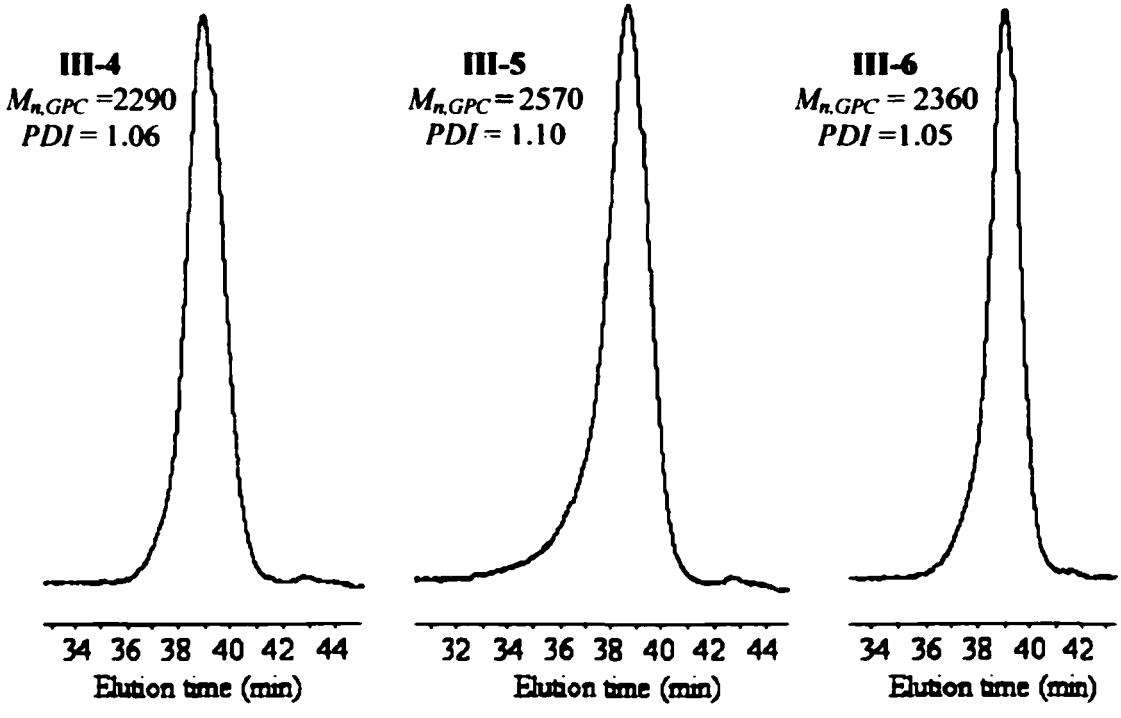

Figure 3-5. GPC curves of diblock macromonomers **III-4**, **III-5**, and **III-6**.

MALDI analysis was also carried out for the macromonomers. MALDI spectra of **III-4** and **III-5**, obtained from dithranol matrix, showed that both macromonomers have monomodal molecular weight distribution with signals at the molecular weight ranging from 1500 to 4300 with maximum signals at 2200-2600 and 2700-3000 respectively. With either dithranol matrix or 2,5-dihydroxybenzoic acid matrix used, MALDI spectra

of **III-6** obtained showed relatively good resolution (**Figure 3-6**), presumably because of ready cationization of **III-6** due to its basic pyridine functionality. Macromonomer **III-6** has also monomodal molecular weight distribution, with MALDI signals at the molecular weight ranging from 1750 to 4300 and a maximum signal at molecular weight around 2770.

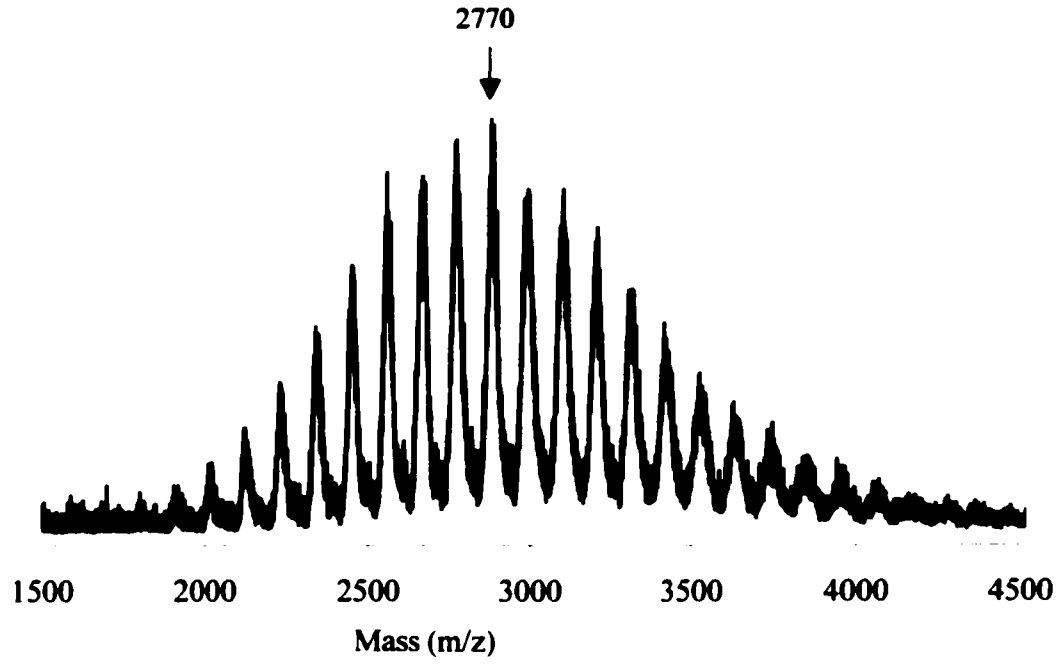

Figure 3-6. MALDI spectrum of macromonomer **III-6**.

***3-3c* Synthesis of Diblock Macromonomer with Norbornenyl Group Carried by Block Junction of Poly(St-d_8)-*b*-Poly(ethylene oxide).** Organopotassiums, other than organolithiums, are the most generally useful initiators for anionic ring-opening polymerization of ethylene oxide [*67*]. Therefore, to prepare macromonomer **III-7** with norbornenyl group connected by block junction of poly(styrene-d_8)-*b*-poly(ethylene oxide) diblock copolymer, norbornene-functionalized poly(styrene-d_8)-based alcohol

III-3, i.e. the ethylene oxide-end-capped adduct of **III-1**, was deprotonated with DPE-potassium adduct. The norbornene-functionalized poly(styrene-d_8)-based alkoxypotassium was used as the initiator for anionic ring-opening polymerization of ethylene oxide to yield the diblock macromonomer **III-7** (**Scheme 3-4**).

Scheme 3-4

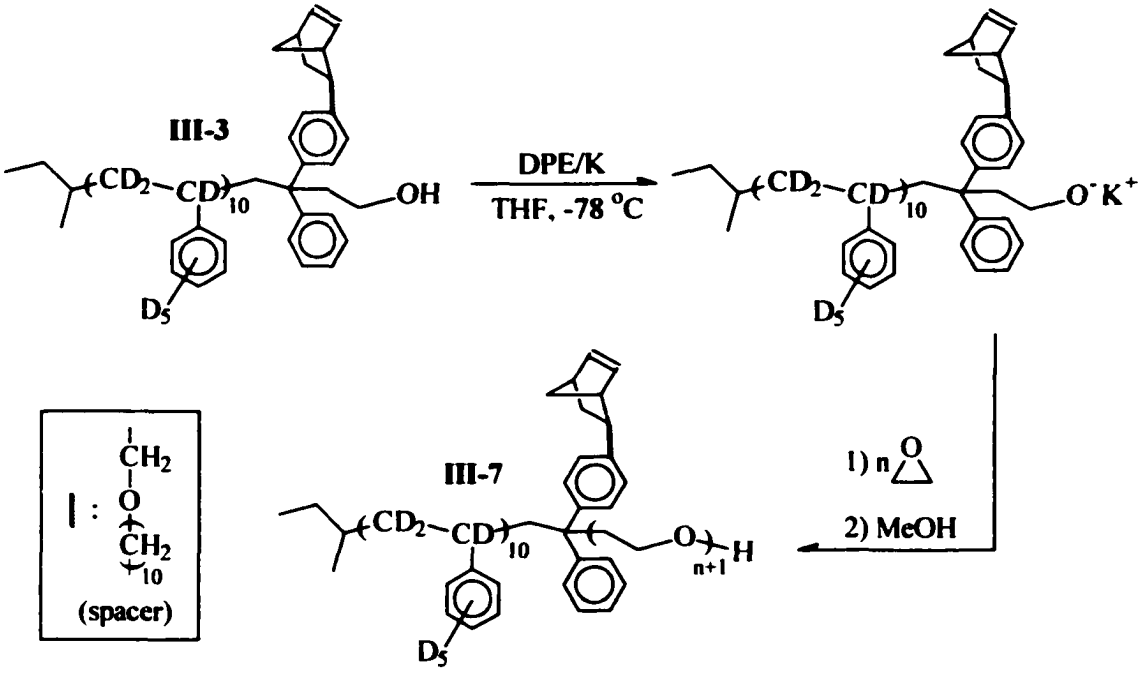

Deprotonation of **III-3** with DPE-potassium adduct was carried out in THF at -78 °C. DPE-potassium adduct solution was added dropwise into the **III-3** solution. Because DPE-potassium adduct has characteristic red color and deprotonation is a very fast process, the addition was stopped as soon as slight red color appeared in the reaction solution stably, indicating the end-point of deprotonation. Then 25 equivalents of ethylene oxide relative to **III-3** were added. After gradually increasing the temperature of

reaction solution, the polymerization solution was kept at 40 °C over one day to complete monomer conversion before termination with acidified methanol.

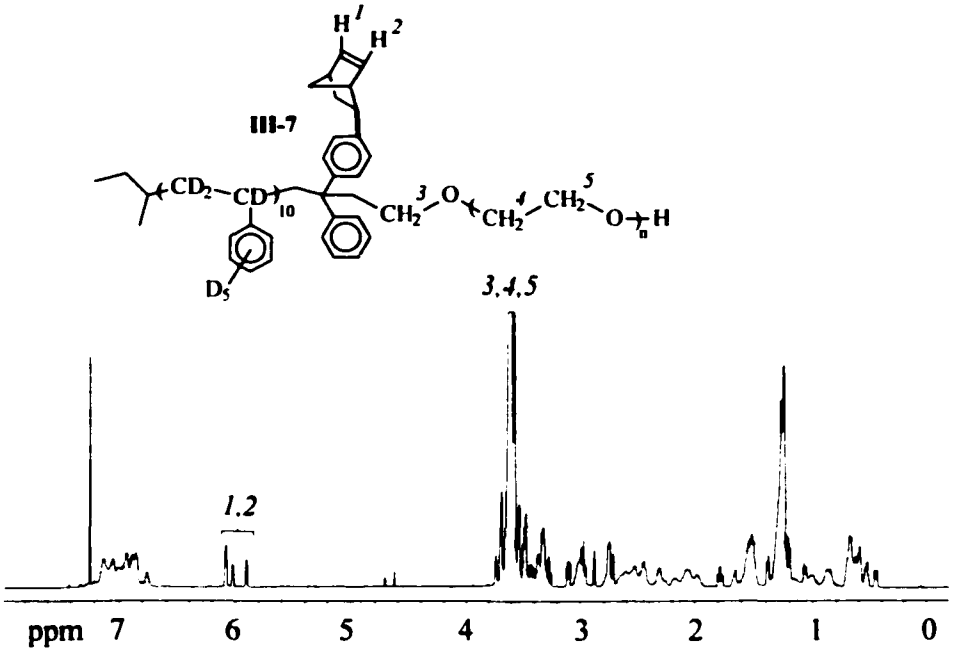

Figure 3-7. ^{1}H NMR spectrum of diblock macromonomer **III-7**.

Well-controlled formation of poly(ethylene oxide) block of **III-7** was verified by ^{1}H NMR, GPC, and MALDI analyses. As shown in **Figure 3-5**, ^{1}H NMR resonances of methylene protons of ethylene oxide monomer units centered at 3.62 ppm illustrated the presence of poly(ethylene oxide) block in **III-7**. Based on their intensities and the intensities of resonances of norbornenyl alkene protons at 6.14-5.89 ppm, the DP_n of the poly(ethylene oxide) block was determined as 28, corresponding to a M_n of 2850. The DP_n value obtained by ^{1}H NMR is in a close agreement with the theoretical value of 26 (one ethylene oxide monomer unit existed in the initiator used before polymeriztion). GPC analysis of **III-7** showed that it has very low polydispersity of 1.06 with

monomodal curve (**Figure 3-8**). MALDI analysis of **III-7**, using dithranol matrix, verified the monomodal molecular weight distribution of **III-7**, and showed the and signals with maximum intensities were in the molecular weight range of 2850-2900, in a good agreement with M_n deduced by ^{1}H NMR.

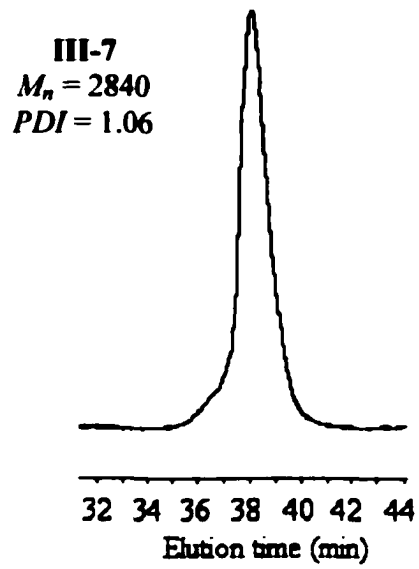

Figure 3-8. GPC curve of diblock macromonomer **III-7**.

***3-3d* Synthesis of Diblock Macromonomer with Norbornenyl Group Carried by Block Junction of Poly(St-d_8)-*b*-poly(dimethylsiloxane).** Both alkyllithiums and alkoxylithiums are very useful initiators for anionic ring-opening polymerization of hexamethylcyclotrisiloxane (D_3) [*68*]. However, D_3 is a cyclic monomer with relatively big size, and at the same time, there is significant steric hindrance around the alkyllithium initiator site of the norbornene-functionalized poly(styrene-d_8)-based 1,1-diphenylalkyllithium **III-1**. Therefore, instead of **III-1**, norbornene-functionalized poly(styrene-d_8)-based alkoxylithium **III-2**, which has decreased steric hindrance around

its alkoxylithium anionic initiator site, was used as the initiator for anionic ring-opening polymerization of D_3 (**Scheme 3-5**). **III-2** can be directly prepared by employing excess of ethylene oxide to react with **III-1** as shown in **Scheme 3-2**, but the remaining ethylene oxide might potentially interfere with anionic ring-opening polymerization of D_3. Therefore, **III-2** that was prepared by deprotonation of **III-3** with

Scheme 3-5

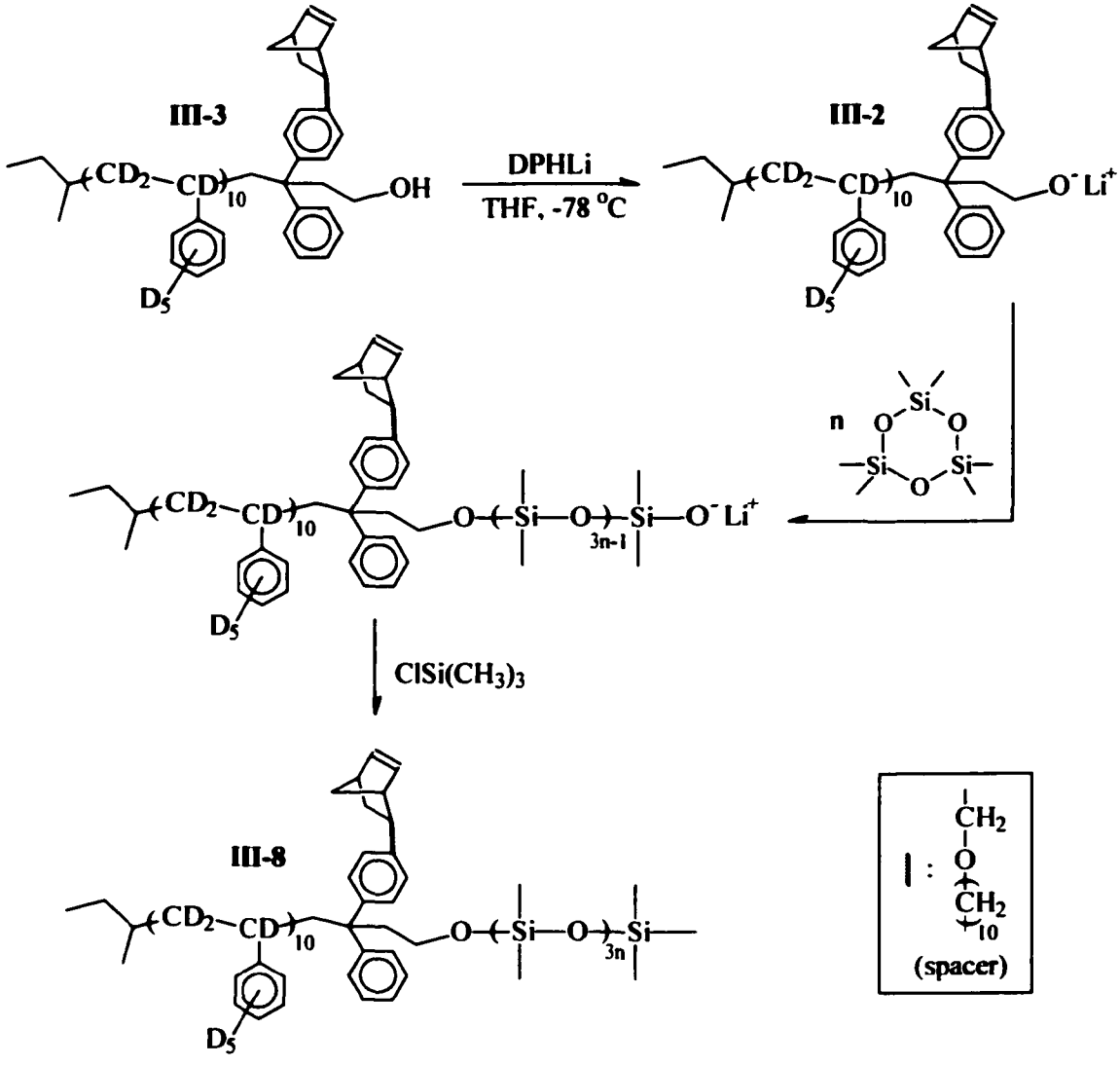

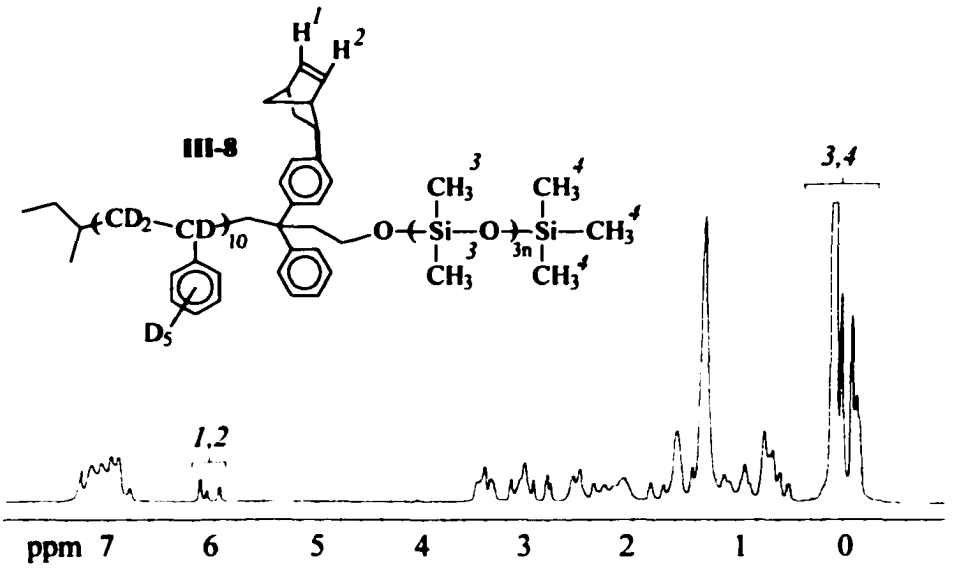

Figure 3-9. ^{1}H NMR spectrum of diblock macromonomer **III-8**.

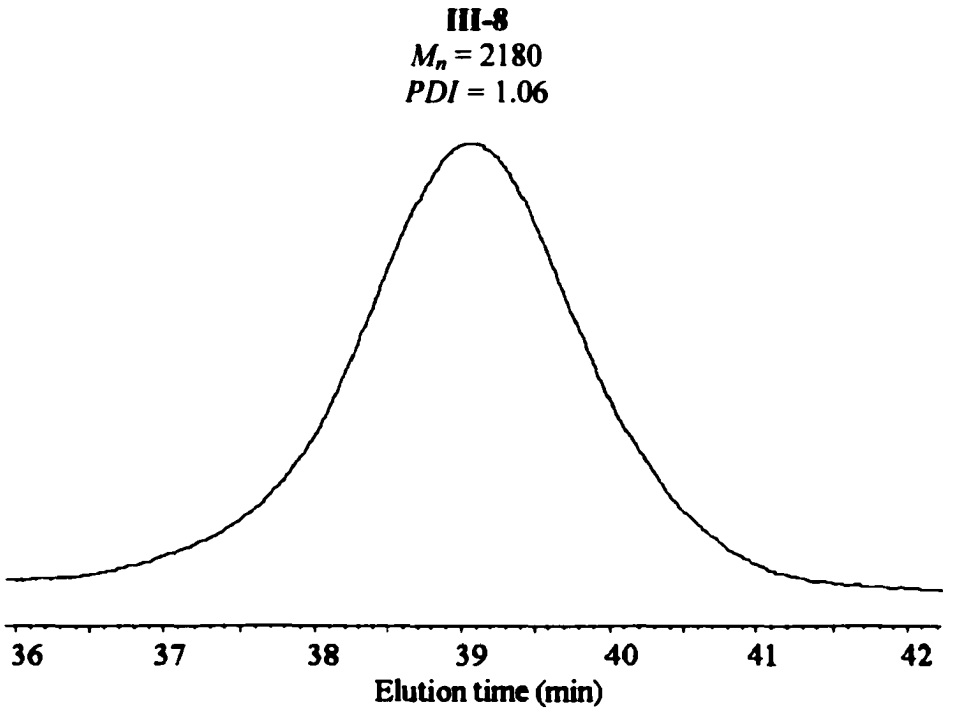

Figure 3-10. GPC curve of diblock macromonomer **III-8**.

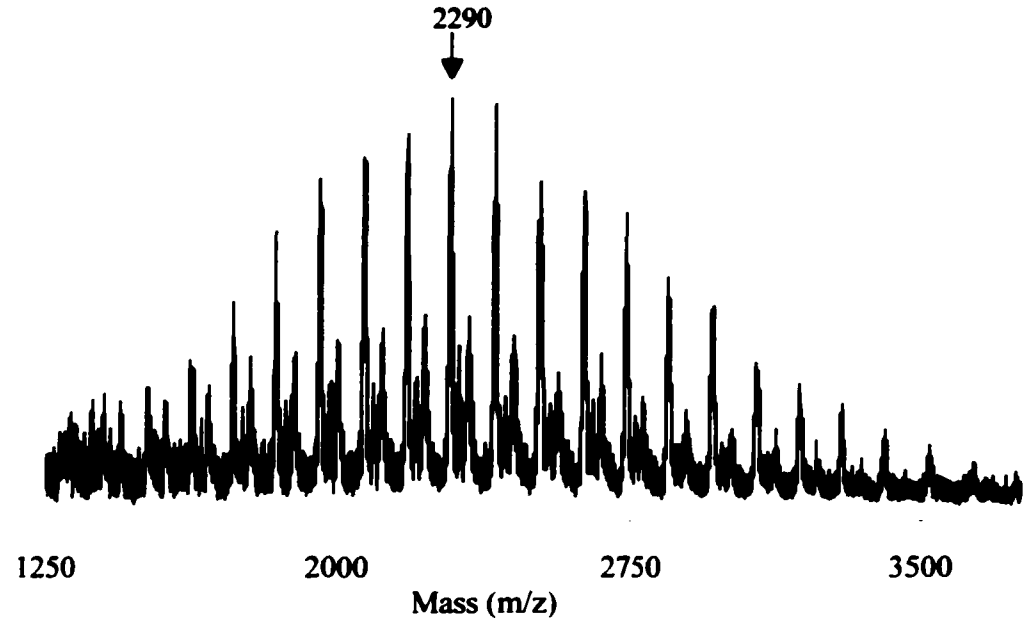

Figure 3-11. MALDI spectrum of macromonomer **III-8**.

1,1-diphenylhexyllithium (DPHLi) was used to initiate anionic ring-opening polymerization of D_3.

Preparation of **III-2** from **III-3** by deprotonation with DPHLi was carried out in THF at -78 °C. DPHLi solution was added dropwise into **III-3** solution. Because DPHLi has characteristic red color in solution and the deprotonation is a very fast process, the addition was stopped as soon as slight red color appeared in the reaction solution stably, indicating the end-point of deprotonation with the quantitative formation of **III-2**. After warming the solution of **III-2** to room temperature, 10.7 equivalents of D_3 relative to **III-2** was dissolved in THF and was added into **III-2** solution, with an initial concentration of D_3 of 0.55 M. Before the termination with chlorotrimethylsilane, polymerization of D_3 was allowed for only 30 min to avoid side reactions which can occur at a considerable level at high conversion of D_3 and result in ill-defined product [*68, 69*].

Different from all other diblock macromonomers synthesized, diblock macromonomer **III-8** was viscous liquid instead of solid, presumably because of the very low glass transition temperature of its poly(dimethylsiloxane) (PDMS) block. Well-controlled formation of its PDMS block was verified by ^{1}H NMR, GPC, and MALDI analyses. As shown in **Figure 3-9**, strong resonances of methyl protons of PDMS block from 0.23 to -0.37 ppm were presented on the ^{1}H NMR spectrum of **III-8**. Based on their intensities relative to the resonance intensities of norbornenyl alkene protons, a DP_n of D_3 of 1.67 was determined. Such an experimental DP_n value corresponds to a monomer conversion of 16% in the polymerization and a M_n of 2060 for **III-8**. Because each D_3 monomer forms three dimethylsiloxane structure units, the DP_n of PDMS block in **III-8** was 5.0. A very low polydispersity of 1.06 was obtained from monomodal GPC curve of **III-8** (**Figure 3-10**), indicating no significant occurrence of side reactions during polymerization. At the same time, because the peak position of GPC curve of **III-3** is at elution time of 41.3 min, if there is significant amount of polymer species that have no D_3 monomer unit incorporated and just was end-capped with trimethylsilyl group, a GPC peak corresponding would appear just before the peak position for **III-3**. Therefore, the symmetrical, monomodal, narrow GPC curve of **III-8** also suggests that essentially polymer species of **III-3** have (at least one) D_3 monomer unit(s) incorporated. Thus, considering the DP_n of D_3 of only 1.67, it can be further inferred that initiation was significantly faster than propagation during polymerization. High resolution MALDI spectrum of **III-8**, obtained using dithranol matrix, confirmed the relatively narrow monomodal molecular weight distribution of **III-8** (**Figure 3-11**). It confirmed no significant amount of polymer species without D_3 monomer unit. The MALDI signals

with maximum intensities appeared at the molecular weight around 2290, in good agreement with the M_n of 2060 obtained by ^{1}H NMR.

3-3e **Summary of Structural Parameters of Diblock Macromonomers.** Experimental structural parameters of the five types of diblock macromonomers synthesized were summarized in **Table 3-1**. All diblock macromonomers have the same parameters for the first poly(styrene-d_8) block, with a calculated DP_n of 10. Because GPC analysis could not be considered as accurate for the short poly(styrene-d_8) block and MALDI analysis showed maximum signal corresponding to a DP_n of 10, the actual DP_n of the first block was considered as 10 in following calculations. Experimental DP_n values of the second block of diblock macromonomers were obtained by ^{1}H NMR analysis. Based on 600 MHz ^{1}H NMR quantitative analysis, the experimental DP_n values were considered to be reasonably accurate. The experimental M_n values of diblock macromonomers were obtained based on either GPC or ^{1}H NMR. Because GPC instrument was calibrated with linear polystyrenes that theoretically must differ from diblock macromonomers in relationship between molecular weight and hydrodynamic volume, $M_{n,GPC}$ values obtained were considered as representatives of hydrodynamic volumes of macromonomers rather than creditable M_n. The $M_{n,H\text{-}NMR}$ values, which were calculated using experimental DP_n values of the second block by ^{1}H NMR and considering DP_n values of the first block as 10, were generally in good agreement of peak *MW* values obtained by MALDI analysis and considered to be reasonably accurate, and was used in further calculation. The molecular weight information obtained by MALDI could not be used to deduce M_n or *PDI* due to no suitable processing method available to

us. Polydispersities of macromonomers were determined only by GPC calibrated with linear polystyrene.

Table 3-1. Structural Parameters of Diblock Macromonomers

	first block			second block		entire macromonomer			
	DP_n		DP_{peak}	DP_n		$M_n(10^3)$		$M_{peak}(10^3)$	PDI
Entry	calcd	GPC[a]	MALDI	calcd	^{1}H NMR	GPC[a]	^{1}H NMR[b]	MALDI	GPC[a]
III-4	10	9.4	10	10	11	2.29	2.72	2.4-2.6	1.06
III-5	10	9.4	10	10	10	2.57	2.90	2.7-3.0	1.10
III-6	10	9.4	10	10	10.4	2.36	2.70	2.77	1.05
III-7	10	9.4	10	26	28	2.84	2.85	2.85-2.9	1.06
III-8	10	9.4	10	-	5.0[c]	2.06	2.18	2.18-2.4	1.06

[a] Relative to linear non-deuterated polystyrenes. [b] Considering DP_n of first block as 10 in calculation. [c] Relative to dimethylsiloxane structure unit.

3-4 ROMP of Diblock Macromonomers with Block Junctions Carrying Norbornenyl Functionality

3-4a **Synthetic Design and General Results.** Ring-opening metathesis polymerization (ROMP) experiments of diblock macromonomers **III-4**, **III-5**, **III-6**, **III-7**, and **III-8** were carried out using a Grubbs initiator in $CDCl_3$ for the synthesis of poly(macromonomer)s **III-9**, **III-10**, **III-11**, **III-12**, and **III-13** (**Scheme 3-6**).

Scheme 3-6

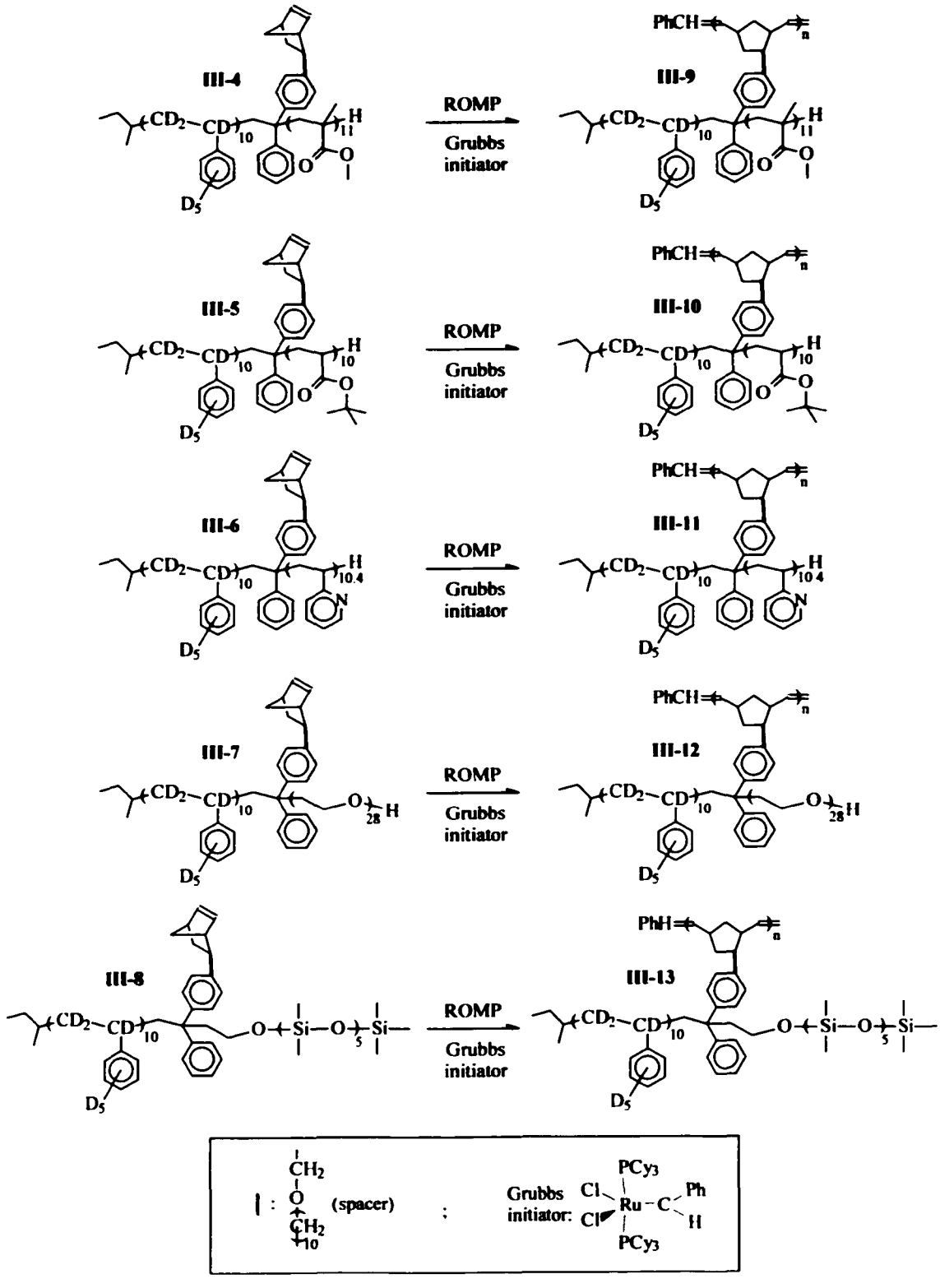

Table 3-2. ROMP of Diblock Macromonomers Using Grubbs Initiator

			^{1}H NMR observance				GPC determination [a]					
		$[M]_0$	t	conv	DP_n		t	conv	DP_n		M_n	
Entry	M	$[I]_0$	(h)	(%)	calcd.	exptl.	(h)	(%)	calcd.	exptl.[b]	(10^3)	*PDI*
III-9a	**III-4**	10	4	98	9.8	10	12	98	9.8	9.5	21.6	1.10
III-9b	**III-4**	25	4	75	18.8	20.6	12	90	22.5	22.2	50.8	1.14
III-9c	**III-4**	50	6	80	40	40	12	91	46	37.3	85.4	1.17
III-10a	**III-5**	10	4	99	9.9	9.9	12	99	9.9	9.2	23.6	1.14
III-10b	**III-5**	25	4	79	19.8	20.2	12	91	22.8	17.9	46.1	1.14
III-10c	**III-5**	50	6	80	40	38.6	12	89	44	37.0	95.8	1.17
III-11a[c]	**III-6**	10	4	94	9.4	-	12	94	9.4	5.1	11.7	1.15
III-11b[c]	**III-6**	25	4	88	22	-	12	88	22	8.7	20.4	1.13
III-11c[c]	**III-6**	50	6	77	38.5	-	12	81	40.4	17.2	40.6	1.19
III-12a	**III-7**	10	4	98	9.8	9.8	12	96	9.6	4.6	13.1	1.11
III-12b[d]	**III-7**	25	4	93	23.3	22.3	12	-	-	-	-	-
III-12c[d]	**III-7**	50	6	99	49.5	37	12	-	-	-	-	-
III-13a	**III-8**	10	4	100	10	9.4	12	96	9.6	7.7	16.7	1.15
III-13b	**III-8**	25	4	95	22.5	22.5	12	95	22.5	16.4	35.7	1.13
III-13c[e]	**III-8**	50	6	>95	>47.5	-	12	94	47	32.1	69.9	1.23

[a] linear polystyrenes standards. [b] $DP_{n,det} = M_{n,polymacromonomer,GPC} / M_{n,macromonoemr,GPC}$.

[c] DP_n cannot be determined by ^{1}H NMR due to overlapping characteristic resonances.

[d] GPC analysis unsuccessful. [e] DP_n cannot be determined by ^{1}H NMR due to insufficient resolution of characteristic resonances.

Theoretically, with backbone stiffened gradually by increased side-chains densely grafted, poly(macromonomer)s have morphologies changing from flexible star-shaped sphere to rigid cylinder-brush with increased length ratio of backbone to side-chain. Therefore, initial feed ratios of macromonomer to Grubbs initiator were 10, 25, and 50 to target a range of length ratio of backbone to side-chain of poly(macromonomer)s produced. Because of the special structures of macromonomers, all poly(macromonomer)s densely grafted with two types of polymer chains were also double-brush copolymers. The ROMP results are summarized in **Table 3-2.**

3-4b **^{1}H NMR in Situ Analysis.** Polymerization solutions were analyzed by ^{1}H NMR 4-6 h after the start of ROMP, for in situ observation of conversion of macromonomer and DP_n of poly(macromonomer)s yielded. ^{1}H NMR analysis verified that ROMP of the diblock macromonomers was a well-controlled process, yielding poly(macromonomer)s with relatively high macromonomer conversion and well-controlled DP_n of backbone. For all trials, high macromonomer conversion (no less than 75%) was reached within 4-6 h. For the trials with initial molar feed ratio of macromonomer to initiator, $[M]_0/[I]_0$, of 10, nearly complete macromonomer conversion (94-100%) was obtained. Moreover, for those trials with DP_n of poly(macromonomer) measured by ^{1}H NMR, the experimental DP_n values of poly(macromonomer)s obtained generally were in excellent agreements with the DP_n values calculated based on macromonomer conversion and $[M]_0/[I]_0$, indicating the living characteristics of the ROMP process. Typical ^{1}H NMR spectra of the polymerization solutions were shown in **Figure 3-12** (for **III-9**), **Figure 3-13** (for **III-10**), **Figure 3-14** (for **III-11**), **Figure 3-15**

(for **III-12**), and **Figure 3-16** (for **III-13**). Because of the Grubbs initiator used, each poly(macromonomer) molecule formed has a PhCH=CH- group at its α-chain-end of backbone. For poly(macromonomer)s **III-9**, **III-10**, **III-12**, and **III-13**, the ^{1}H NMR resonances of the α-proton (proton *1*) and the β-proton (proton *2*) relative to the phenyl ring of the chain-end group were identified at 6.43-6.29 ppm and 6.29-6.12 ppm respectively, and the resonances from the α-proton have quantitative intensities under the characterization conditions, and therefore were used for quantitative analysis in most cases. Unreacted macromonomers showed characteristic ^{1}H NMR resonances in the regions of 6.10 (resonance *a*; for both *exo* and *endo*), 6.04 (for *exo* only), and 5.92 (resonance *b*; for *endo* only) ppm for their norbornenyl alkene protons. Macromonomer conversion was deduced from comparisons of these resonance intensities with the resonance intensities of the chain-end α-proton of poly(macromonomer)s, and $[M]_0/[I]_0$. Moreover, the backbone of poly(macromonomer)s formed by ROMP has characteristic ^{1}H NMR resonances at 5.5-5.0 ppm for its in-chain alkene protons (protons *3* and *4*). Thus, the DP_n of the backbone of poly(macromonomer)s was also obtained, based on the ratios of the resonance intensities for these backbone-in-chain protons to the resonance intensities of the backbone-chain-end α-proton of poly(macromonomer)s. For all trials of **III-9**, **III-10**, **III-12**, and **III-13**, except **III-12c** and **III-13c**, very close agreements between calculated DP_n and experimental DP_n values were observed. ^{1}H NMR determination of DP_n for **III-12c** was affected by relatively broad resonances of backbone-in-chain protons; ^{1}H NMR determination of DP_n for **III-13c** could not be performed because the resonances of backbone-chain-end α-proton for that trial had relatively poor resolution and could not be quantitatively analyzed. For

poly(macromonomer) **III-11**, the resonances of its backbone-chain-end protons overlapped with the resonances of aromatic protons of 2-VP monomer unit, therefore ^{1}H NMR determination of DP_n for **III-11** trials could not be performed. The ^{1}H NMR determination of macromonomer conversion for **III-11** was based on the comparison of resonance intensities of backbone-in-chain protons at 5.5-5.0 ppm for poly(macromonomer) with resonance intensities of methyl protons of *s*-BuLi fragment at 0.77-0.50 ppm for both poly(macromonomer) and remaining macromonomer.

^{1}H NMR characterization of the polymerization solutions also verified that macromonomers with *exo*-norbornenyl groups have a significantly faster polymerization rate than macromonomers with *endo*-norbornenyl groups [*42*], presumably due to higher reactivity of *exo*-norbornenyl group resulting from less steric hindrance for the carbon-carbon double bond. The macromonomers have comparable *exo*- and *endo*-norbornenyl groups presented (*exo*/*endo* = 43/57) based on characteristic ^{1}H NMR resonances of one of the two alkene protons at 6.04 ppm for *exo*-norbornenyl groups and at 5.92 ppm for *endo*-norbornenyl groups. However, as shown in **Figure 3-12**, **Figure 3-13**, **Figure 3-15**, and **Figure 3-16**, nearly no resonances at 6.04 ppm could be observed for the trials with $[M]_0/[I]_0$ of 10, suggesting that essentially all macromonomers with *exo*-norbornenyl groups were consumed. For all other trials with higher $[M]_0/[I]_0$, much weaker resonances at 6.04 ppm than resonances at 5.92 ppm were detected, suggesting again faster consumption of macromonomers with *exo*-norbornenyl groups. It can be further inferred that macromonomers with increased size of polymer blocks can also be polymerized by ROMP with reasonably high yield if they have exclusive *exo*-norbornenyl groups.

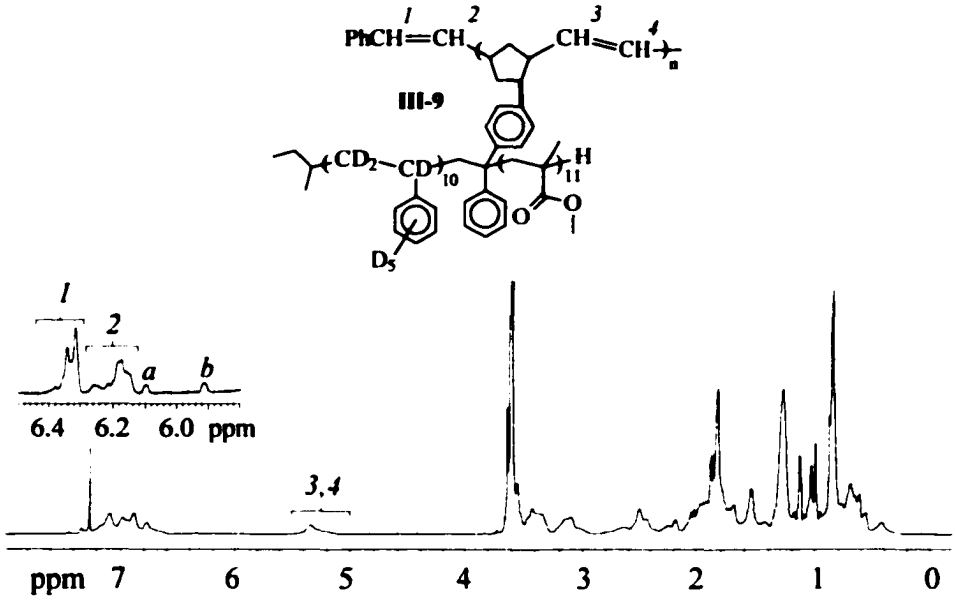

Figure 3-12. ^{1}H NMR spectrum of polymerization solution **III-9a** at reaction time of 4 h.

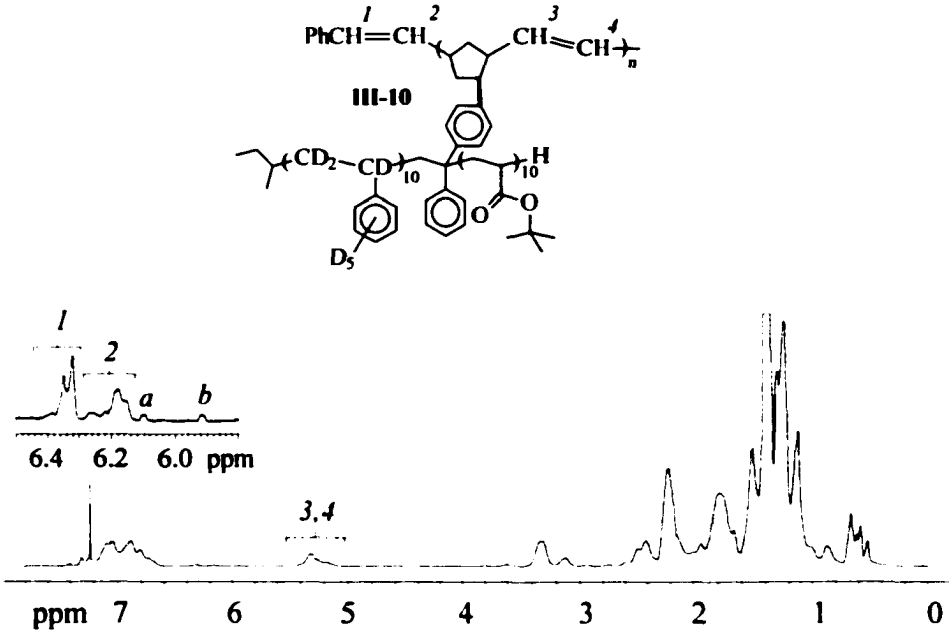

Figure 3-13. ^{1}H NMR spectrum of polymerization solution **III-10a** at reaction time of 4 h.

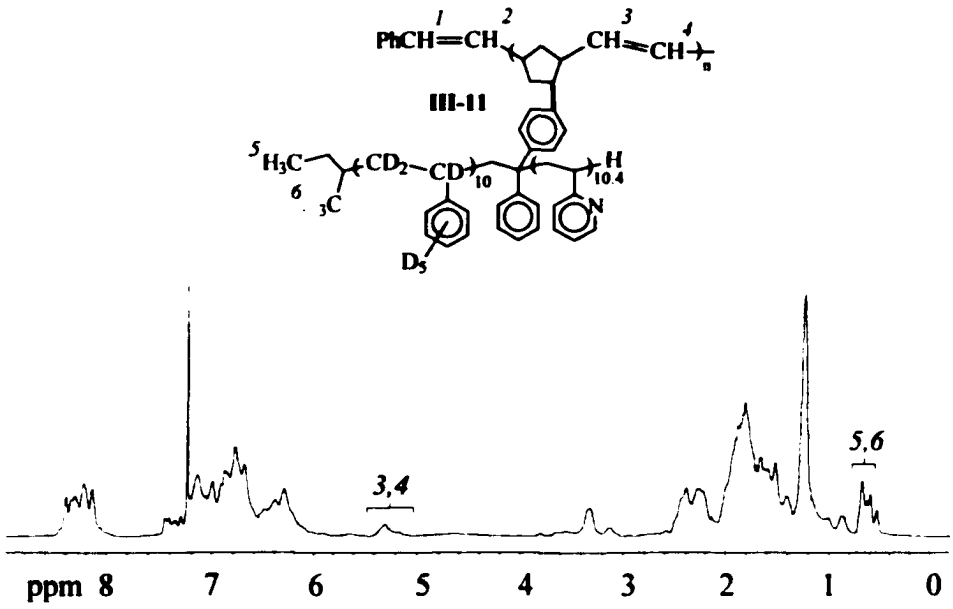

Figure 3-14. ^{1}H NMR spectrum of polymerization solution **III-11a** at reaction time of 4 h.

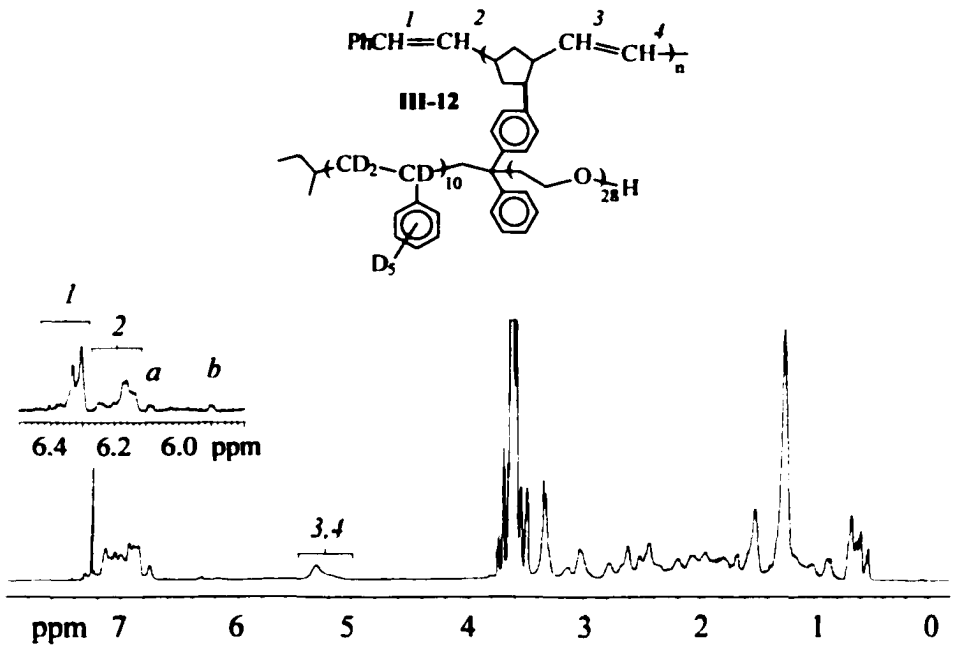

Figure 3-15. ^{1}H NMR spectrum of polymerization solution **III-12a** at reaction time of 4 h.

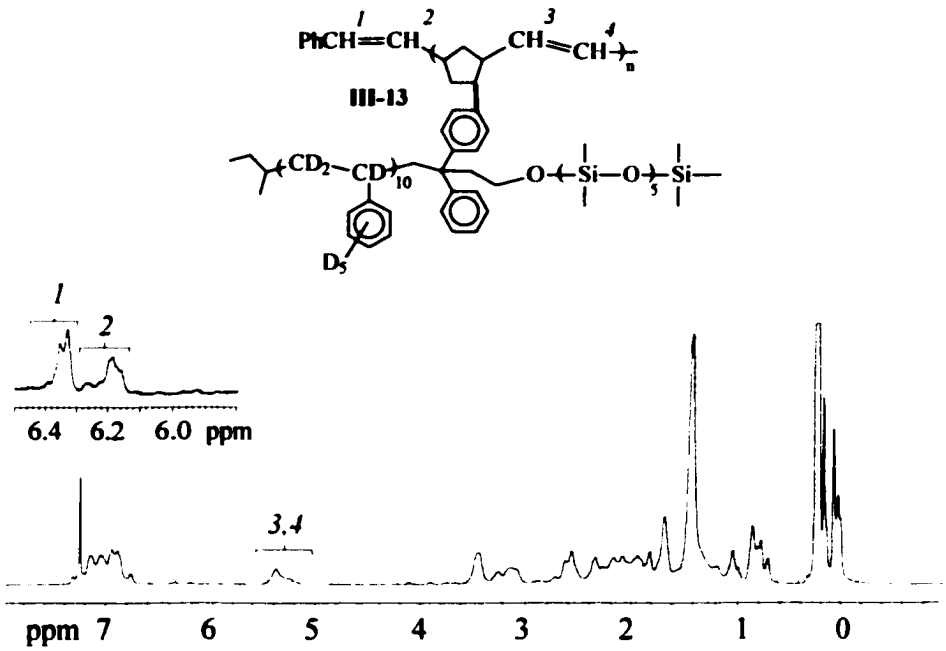

Figure 3-16. ^{1}H NMR spectrum of polymerization solution **III-13a** at reaction time of 4 h.

3-4c **GPC Analysis and Solution Morphology Discussion.** ROMP of macromonomers was terminated with ethyl vinyl ether about 12 h after the start of polymerization for each trial, and then polymerization solutions were analyzed by GPC. The GPC analysis of poly(macromonomer)s is still a subject not yet well-developed [*3*]. Depending on factors such as molecular weight and size-ratio of backbone to graft, the macromolecule can be assumed to have star or cylinder-brush shape. Further complications arise due to the divergent properties of the connected diblocks. The use of linear polystyrene standards to obtain reliable information on poly(macromonomer)s require extremely carefully considerations. At this time, polymer parameters from measurement such as viscosity and light scattering are not available. Our present GPC analyses can only be considered as tentative and qualitative.

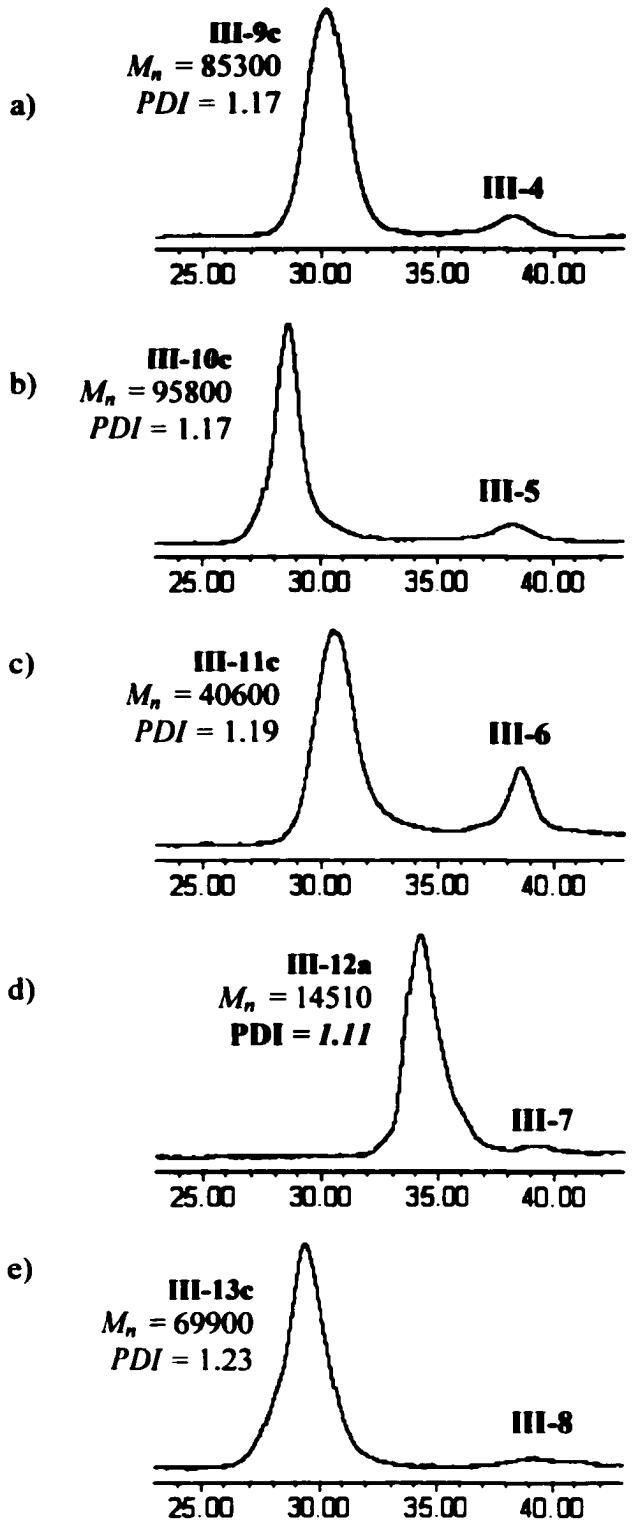

Figure 3-17. GPC curves of ROMP solutions with reaction time of 12 h: a) **III-9c**; b) **III-10c**; c) **III-11c**; d) **III-12a**; e) **III-13c**. (X-scale: elution time (min))

Typical GPC curves for the polymerization solutions were shown in **Figure 3-17**. GPC curves for all trials where GPC analysis is applicable indicated the formation of poly(macromonomer)s and high macromonomer conversions. GPC determination of macromonomer conversion was performed by comparing the integration area of the GPC peak of poly(macromonomer) with the sum of integration areas of GPC peaks of poly(macromonomer) and macromonomer. Nearly complete macromonomer conversions (94-99%) were found for all trials with the molar feed ratio of macromonomer to initiator, $[M]_0/[I]_0$, of 10. High macromonomer conversions (>88%) were found for all trials with $[M]_0/[I]_0$ of 25. Even for the trials with $[M]_0/[I]_0$ of 50, macromonomer conversion was also reasonably high (>80%), indicating the formation of poly(macromonomer)s with backbones (having five carbon atoms per repeating unit on main-chain) much longer than side chains.

The monomodal narrow GPC peaks of poly(macromonomer)s have no or only very slight overlap with macromonomers, suggesting that initiation rate was higher than or at least comparable to propagation rate during the ROMP process. Relatively low polydispersities of poly(macromonomer)s were further determined by GPC with calibration using linear polystyrenes. With side-chains densely carried by rigid backbones, poly(macromonomer)s are expected to have quite different relationship of hydrodynamic volume and elution time with linear polystyrenes. Therefore, the polydispersity determination of poly(macromonomer)s could not be considered as accurate and the polydisperity values obtained are underestimated. For the same reasons, molecular weights of poly(macromonomer)s determined by GPC are also underestimated.

The ratio of M_n of poly(macromonomer) to M_n of macromonomer by GPC represents the hydrodynamic volume ratio of poly(macromonomer) to macromonomer based on linear polystyrene calibration, and we defined it as experimental $DP_{n,GPC}$. Because it has been established by ^{1}H NMR analyses that the DP_n values of the backbones of poly(macromonomer)s generally were in very close agreement with the calculated DP_n values, the ratio of calculated DP_n to experimental $DP_{n,GPC}$ represents the extent of hydrodynamic volume contraction due to polymerization to form poly(macromonomer). We defined this ratio as volume contraction ratio (VCR), and it reflects the combined effects on solution morphology of poly(macromonomer) from its grafted architectures, and its intramacromolecular interaction under the characterization conditions (THF as solvent, 40 °C).

Table 3-3. Hydrodynamic Volume Contraction of Poly(macromonomer)s [a]

	VCR (backbone DP_n)			solubility parameter δ [(cal/cm^3)$^{1/2}$] [b]		
entry	short backbone → long backbone			THF	poly(St-d_8)	2nd side-chain
III-9	1.0 (9.8)	1.0 (22.5)	1.2 (46)	9.1	8.9 (±0.2)	9.3 (±0.2)
III-10	1.1 (9.9)	1.3 (22.8)	1.2 (44)	9.1	8.9 (±0.2)	8.95 (±0.15)
III-11	1.8 (9.4)	2.5 (22)	2.4 (40.4)	9.1	8.9 (±0.2)	12.35
III-12	2.1 (9.6)	-	-	9.1	8.9 (±0.2)	9.9 (±1)
III-13	1.2 (9.6)	1.4 (22.5)	1.5 (44)	9.1	8.9 (±0.2)	7.45 (±0.15)

[a] In THF at 40 °C. [b] Based on reference [*70*].

VCR values of poly(macromonomer)s, along with (calculated) backbone DP_n values and solubility parameter δ values are listed in **Table 3-3**. All poly(macromonomer)s are densely grafted, with two short hetero-side-chains (generally having DP_n around 10) connected to backbone norbornene unit (with five main-chain carbons) through a $-CH_2O(CH_2)_{10}-$ spacer. With a defined chain length of heterografts, poly(macromonomer)s are expected, in principle, to change from flexible star-like morphology (without significant hydrodynamic volume contraction) to rigid rod-like morphology with increasing backbone length (as well as significant hydrodynamic volume contraction). Intramacromolecular interaction of poly(macromonomer) involves two types of divergent side-chains and solvent. The influence of the backbone and spacers essentially can be neglected here, because they are only small parts and are confined by steric restrictions. Typically, strong intramacromolecular attraction results in significant hydrodynamic volume contraction. With the moderately polar solvent used, we judge the interaction (attraction) tendency between any two of the three members based on their solubility parameter δ [*70*]. Theoretically, other parameters, such as the Huggins polymer-solvent interaction parameter χ, can also be used. However, for the current systems, availability of these parameters is insufficient.

For poly(macromonomer) **III-9**, based on the close δ values, its poly(styrene-d_8) and poly(MMA) side-chains have no strong repulsion to each other, and both of them can be readily dissolved by THF. A VCR ratio of 1.0 was observed for the first two trials (DP_n values of the backbone were about 10 and 22 respectively), suggesting that the corresponding **III-9a** and **III-9b** were solvated very well and essentially may take a flexible star-like morphology in solution. However, a VCR of 1.2 for long-backbone **III-**

9c with calculated backbone DP_n of 37.3 (about 190 carbon atoms on the backbone main-chain) suggests that with many side-chains densely carried by backbone, **III-9c** should be different from **III-9a** and **III-9b** in solution morphology, and might take a rigid rod-like morphology in solution.

Similar to **III-9**, poly(macromonomer) **III-10** also has δ values close for its divergent side-chains that should not have strong repulsion for each other, and both of the side-chains can be readily dissolved by THF. However, to have remarkable hydrodynamic volume contraction, **III-10** macromolecules require shorter backbone than **III-9** macromolecules according to their VCR values, suggesting that the backbone length needed for **III-10** to assume rigid rod-like conformation is significantly shorter than that for **III-9**. Because **III-10** differs from **III-9** in the second type of side-chain mainly in macromolecular architectures, it is expected that the poly(*t*-BA) side-chains with bulky *tert*-butyl ester group on **III-10** can play a more important role than poly(MMA) side-chains in stiffening the corresponding densely grafted architectures.

For poly(macromonomer) **III-11**, its poly(styrene-d_8) and poly(2-VP) side-chains have a big difference in δ values, suggesting they may have very strong repulsion to each other. At the same time, based on its δ value, THF is a better solvent for poly(styrene-d_8) than for poly(2-VP). Therefore, it is expected that poly(styrene-d_8) side-chains on **III-11** can be well-solvated in THF, while solvation of poly(2-VP) side-chains is not so efficient. In other words, poly(2-VP) side-chains on **III-11** are expected to have strong attraction among them. As expected, a high VCR value of 1.8 was observed for **III-11** with even a short backbone DP_n of 9.4, suggesting a possible micelle morphology with poorly solvated poly(2-VP) segments as a relatively tight core and well-solvated

poly(styrene-d_8) side-chains stretching out. With a long backbone, **III-11** exhibited an even higher VCR, suggesting the formation of rigid rod-like morphology with core-shell structure, which has poly(2-VP) segments as core and well-solvated poly(styrene-d_8) segments as shell.

Poly(macromonomer) **III-12** has poly(styrene-d_8) and poly(ethylene oxide) side-chains. THF is a good solvent for both of them. However, with significant difference in δ values for the two types of side-chains, it is expected that attraction among the same type of side-chain is stronger than the attraction among different types of side-chains. Thus, intramacromolecular self-assembly of the two types of side-chains is possible. At the same time, compared with all other types of side-chains in all poly(macromonomer)s synthesized, the poly(ethylene oxide) side-chains are not only the longest but also the most flexible. Thus, in principle, intramacromolecular interaction (entanglement) between or among **III-12** macromolecules may take place through their poly(ethylene oxide) side-chains.

GPC characterization could only be carried out effectively for the first trial of **III-12**, i.e. **III-12a** (**Figure 3-18**). When the solution containing 2.0 mg dried polymerization mixture of **III-12a** per mL of THF was analyzed, a bimodal GPC curve for poly(macromonomer) was observed. But when the solution containing 0.6 mg dried polymerization mixture of **III-12a** per mL of THF was analyzed, monomodal GPC peak for the polymacromonomer appeared at a slightly longer elution time. Such results suggest that significant intermacromolecular interaction occurred for **III-12a** in the first GPC measurement using a higher sample concentration. Based on the second GPC measurement, a high VCR of 2.1 suggests that intramacromolecular interaction for

III-12a is also significant. GPC measurement of **III-12b** was tried twice but failed. The first measurement was carried out just after the polymerization solution of **III-12b** was terminated. It was found that poly(macromonomer) **III-12b** had an even longer elution time than **III-12a**, although **III-12b** was expected to have a DP_n at least twice as high as DP_n of **III-12a**. Weeks later, the dried polymerization mixture of **III-12b** was redissolved in THF and measured again, but no GPC peak of polymacromonomer **III-12b** could be

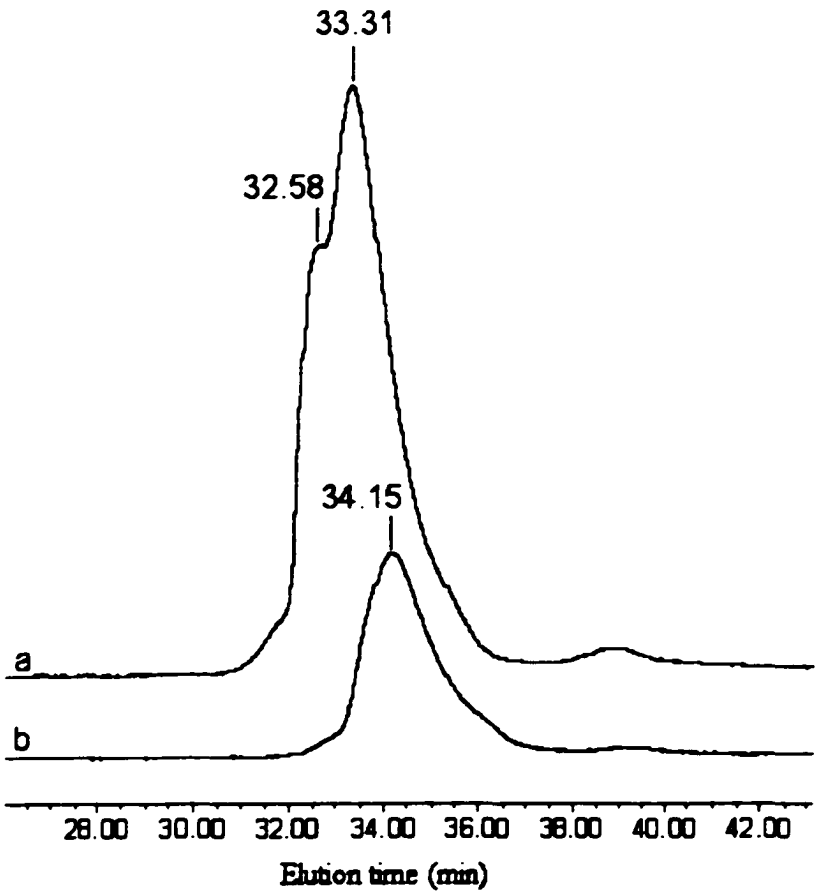

Figure 3-18. GPC curves for **III-12a**: a) 2.0 mg/ml, and b) 0.6 mg/ml. (Concentration is referred to dried polymerization mixtures in THF; injection volume is 100 μl.)

be observed within the characterization time. For polymerization solution of **III-12c** with an expected DP_n of 50 for the backbone of the polymacromonomer, GPC analysis could not be carried out because the polymerization solution was gel-like and could be swollen readily but could not be dissolved. Such results suggest that intermacromolecular interaction (attraction) was strengthened greatly with increased backbone length of **III-12** through cooperative effects and could not be destroyed by solvation.

Poly(macromonomer)s **III-13** have both poly(styrene-d_8) and PDMS side chains. Based on δ values, THF is a better solvent for poly(styrene-d_8) than for PDMS, and at the same time, the two types of side-chains may not have significant tendency to interact with one another. Thus, similar to **III-11**, **III-13** might have solution morphology changing from micelle to rigid rod-like core-shell structures with poorly solvated shorter PDMS segments as core and better solvated poly(styrene-d_8) as shell, as indicated by VCR values. Considering the short size of PDMS blocks with DP_n of only 5.0 relative to dimethylsiloxane structure unit, the VCR values of 1.2, 1.4, and 1.5 with increasing backbone size actually are relatively remarkable.

3-4d **Polymerization Kinetics Discussion.** Differences among macromonomers in their polymerization kinetics in ROMP process can be observed by the comparison of macromonomer conversion determined by in situ ^{1}H NMR analysis at the polymerization time of 4-6 h and macromonomer conversion determined by GPC analysis of the terminated polymerization solution with polymerization time of 12 h. For the trials of **III-9b**, **III-9c**, **III-10b**, **III-10c** with either **III-4** or **III-5** used as macromonomer, macromonomer conversion reached 75-80% by ^{1}H NMR determination, and with longer

polymerization time, significant increase in macromonomer conversion was observed, suggesting the propagation of poly(macromonomer) backbone was continued after the first several hours of polymerization. On the other hand, when **III-6**, **III-7**, or **III-8** was used as macromonomer, typically higher macromonomer conversion could be observed by ^{1}H NMR analysis for the trials with an initial molar feed ratio of macromonomer to initiator of 25 or 50, suggesting a generally faster polymerization rate than the corresponding polymerization systems using **III-4** or **III-5** as macromonomer in the first several hours. However, except the trials using **III-7** as macromonomer that showed exceptionally fast polymerization rate and approached complete conversion within 4-6 hours of polymerization time, the trials using **III-6** or **III-8** as macromonomer did not show further significant increase in macromonomer conversion with increased polymerization time after the first several hours, although generally considerable amounts of macromonomers remaining.

The above differences among macromonomers in their polymerization kinetics of the ROMP process could be explained through the tendency of intermacromolecular interaction of macromonomers, and intra- and/or intermacromolecular interaction of the poly(macromonomer)s formed. The solubility parameter δ of $CDCl_3$, the solvent used in all trials, can be estimated as 9.3 $(cal/cm^3)^{1/2}$, the same as that of $CHCl_3$. When macromonomer **III-4** or **III-5** was used as macromonomer, because both polystyrene blocks and poly(MMA) or poly(*t*-BA) blocks have comparable affinity (based on δ values) and can be well solvated by $CDCl_3$. No specific interaction among macromonomers could be expected, and there would be essentially random steric distribution of macromonomer molecules in solution. At the same time, without strong

interactions expected with the formation of micelle-like structures, the poly(macromonomer)s yielded should have sterically accessible propagation centers even with a number of macromonomer molecules incorporated. Therefore the corresponding ROMP of macromonomer should be a gradual process, and macromonomer conversion increased hour by hour (**Figure 3-19a**). On the other hand, with two types of side-chains with quite different δ values from polymerization solvent $CDCl_3$, macromonomers **III-6**, **III-7**, and **III-8** are expected to have some level of self-assembled structures in solution leading to relatively high local concentrations of the norbornenyl group of macromonomer molecules. At the same time, initiated ROMP living center can also approach the norbonenyl group readily by assistance from self-assembly. Therefore, relatively fast polymerization rate could be observed in the ROMP of these macromonomers in the first hours. The formed poly(macromonomer)s should also have some degree of self-assembly of their two types of side-chains. If such self-assembly predominantly depends on intramacromolecular interaction, then with the formation of structures similar to unimolecular micelle, the steric accessibility of propagating living center on poly(macromonomer) would be decreased greatly or essentially lost with the increased *DP* of its backbone. Thus, after the initial hours, the polymerization of macromonomer would become very slow or just stop. The above rationalization agrees with the experimental observation of polymerization kinetics for the trials using **III-6** (with poly(styrene-d_8) and poly(2-VP) side-chains) and **III-8** (with poly(styrene-d_8) and PDMS side-chains) as macromonomer (**Figure 3-19b**). Alternatively, if the self-assembly of poly(macromonomer) macromolecules also significantly depends on intramacromolecular interaction, then with the formation of structures similar to lamellar

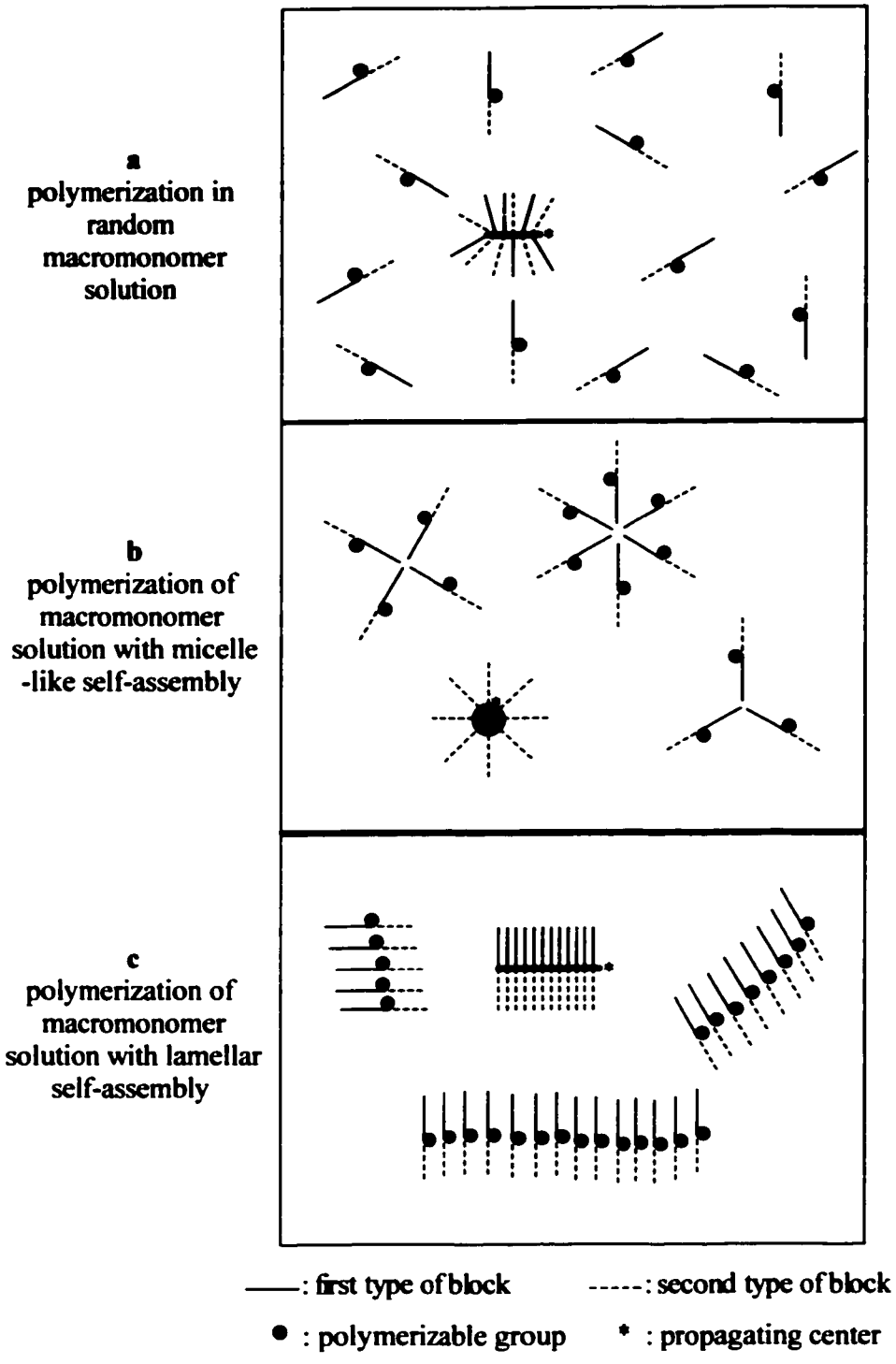

Figure 3-19. Schematic representations of expected systems of ROMP of diblock macromonomers.

structures, the steric accessibility of a propagating living center on poly(macromonomer) would not be decreased significantly with the increased *DP* of its backbone. Thus, the polymerization of macromonomer would be relatively fast until near complete macromonomer conversion is reached. Such rationalization is in line with the experimental observation of polymerization kinetics for the trials using **III-7** (with poly(styrene-d_8) and poly(ethylene oxide) side-chains) as macromonomer (**Figure 3-19c**).

Further investigations such as neutron and light scattering are required to provide solid evidence for the involvement of self-assembly in polymerization.

3-5 Perspective

The nanostructure characterization of the poly(macromonomer)s produced is of importance. As double-brush copolymers, these poly(macromonomer)s are expected to exhibit unique intramacromolecular self-assembled nanostructures. The nanostructures theoretically would change with the backbone to side-chain length ratios, as well as the divergent properties of the hetero-side-chains. At the same time, intermacromolecular self-assembly can also be among the key factors that determine properties of poly(macromonomer)s. Investigation of the nanostructures of the poly(macromonomer)s has been scheduled. Such an investigation potentially will provide the foundation for developing new types of nanomaterials.

Initial work on the synthesis and ROMP of diblock macromonomers with block junction carrying norbornenyl group has been well done. However, based on what we

have accomplished, further synthetic work, by copolymerization of different types of diblock macromonomers or copolymerization of diblock macromonomer with homopolymer-based macromonomer, can yield a variety of novel poly(macromonomer)s with unique and very interesting macromolecular architectures, as shown in **Figure 3-20.**

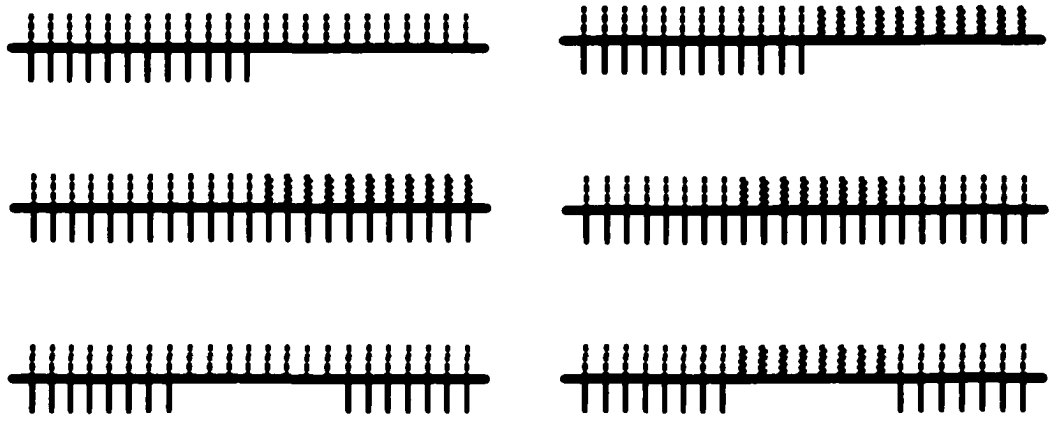

Figure 3-20. Schematic representations of some poly(macromonomer)s obtainable

3-6 Experimental

Materials. Grubbs catalyst $RuCl_2(CHC_6H_5)[P(C_6H_{11})_3]_2$ (Strem), *sec*-butyllithium (*s*-BuLi; 1.3 *M* in cyclohexane, Aldrich), and lithium chloride (99.99%, Aldrich) were used as received. Nitrogen (>99.999%, Welco) was used as inert atmosphere for all reactions without further purification. Styrene-d_8 (98%, Polymer Source) was distilled over CaH_2 and then distilled over sodium. Methyl methacrylate (MMA; 99%, Aldrich), *tert*-butyl acrylate (*t*-BA; 99%, TCI), and 2-vinylpyridine (2-VP; 97%, Aldrich) were diluted with toluene, distilled over CaH_2, and then distilled from triethylaluminum.

Ethylene oxide (99.5%, Aldrich) was distilled over CaH_2 and then distilled from *n*-butyllithium. Hexamethylcyclotrisiloxane (D_3; 98%, Aldrich) was distilled over CaH_2 and then dissolved in THF. Benzene (99.9%, Acros) was distilled over CaH_2 and then distilled from 1,1-diphenylhexyllithium. Tetrahydrofuran (THF; 99.9%, Acros) was refluxed overnight over CaH_2 and then distilled from sodium naphthalene. Chloroform-*d* ($CDCl_3$; 99.8%, Acros) and ethyl vinyl ether (99%, Aldrich) were distilled over CaH_2. Chlorotrimethylsilane (>99%, Aldrich) was distilled. 1,1-Diphenylhexyllithium (DPHLi) was prepared by the reaction of *n*-butyllithium with an equivalent of freshly-distilled 1,1-diphenylethylene in THF. DPE-potassium adduct was prepared by the reaction of 1,1-diphenylethylene with an excess of potassium in THF overnight. The synthesis of **II-1** was described in Chapter 2.

Norbornene-Functionalized Poly(St-d_8)-Based 1,1-Diphenylalkyllithium III-1. All chemicals were transferred with dry syringes, and all reactions were carried out in a pre-flamed glass bottle with magnetic stirring. Styrene-d_8 was added dropwise into *s*-BuLi in benzene at room temperature, with the molar feed ratio of styrene-d_8 to *s*-BuLi of 10. The reaction time was 30 min. Then the resulting poly(styryl)lithium was added slowly into an excess of **II-1** in THF at -78 °C. Red THF solution of **III-1** was formed with quantitative yield within 1 h and then was stored at -78 °C.

Norbornene-Functionalized Poly(St-d_8)-Based Alcohol III-3. Part of **III-1** solution prepared was reacted with an excess of ethylene oxide in THF at -78 °C. Then the reaction solution was precipitated in acidified methanol to give **III-3** as white solid. ^{1}H NMR spectrum of **III-3** was shown in **Figure 3-2**.

Diblock Macromonomer with Norbornenyl Group Connected by Block Junctions of Poly(St-d_8)-*b*-poly(MMA), III-4. All chemicals were transferred with dry syringes, and the reaction was carried out in a pre-flamed glass bottle with magnetic stirring. MMA was added slowly into the THF solution of **III-1** in the presence of lithium chloride at -78 °C, with the molar feed ratio of MMA to **III-1** of 10. The reaction time was 1 h to complete monomer conversion. After termination with methanol, the reaction mixture was separated using flash column chromatography eluted with dichloromethane-methanol to give **III-4** as white solid. ^{1}H NMR spectrum of **III-3** was shown in **Figure 3-4a**.

Diblock Macromonomer with Norbornenyl Group Connected by Block Junctions of Poly(St-d_8)-*b*-poly(*t*-BA), III-5. The synthesis and purification of **III-5** followed the same procedure as the synthesis and purification of **III-4**, except using *t*-BA as monomer. ^{1}H NMR spectrum of **III-3** was shown in **Figure 3-4b**.

Diblock Macromonomer with Norbornenyl Group Connected by Block Junctions of Poly(St-d_8)-*b*-poly(2-VP), III-6. The synthesis of **III-6** followed the same procedure as the synthesis of **III-4**, except using 2-VP as monomer. The reaction mixture was precipitated in pentane to give **III-6** as white solid. ^{1}H NMR spectrum of **III-3** was shown in **Figure 3-4c**.

Diblock Macromonomer with Norbornenyl Group Connected by Block Junctions of Poly(St-d_8)-*b*-poly(ethylene oxide), III-7. All chemicals were transferred with dry syringes, and the reaction was carried out in a pre-flamed glass bottle with magnetic stirring. A THF solution of 1,1-diphenylhexyllithium was added dropwise into a THF solution of **III-3** at -78 °C. The addition was stopped as soon as the red color of

reaction solution disappeared. Then 25 equivalents of ethylene oxide relative to **III-3** were added. The temperature of the reaction solution was allowed to increase very slowly to 40 °C in hours, and then was kept at 40 °C for 24 h. After termination with acidified methanol, the reaction mixture was separated using flash column chromatography eluted with dichloromethane-methanol to give **III-7** as a pale yellow solid. ^{1}H NMR spectrum of **III-7** was shown in **Figure 3-7**.

Diblock Macromonomer with Norbornenyl Group Connected by Block Junctions of Poly(St-d_8)-*b*-poly(dimethylsiloxane), III-8. All chemicals were transferred with dry syringes, and the reaction was carried out in a pre-flamed glass bottle with magnetic stirring. A THF solution of DPE-potassium adduct was added dropwise into a THF solution of **III-3** at -78 °C. The addition was stopped as soon as the red color of reaction solution disappeared. After warming the reaction solution to room temperature, 10.7 equivalents of D_3 in THF relative to **III-3** were added. After termination with chlorotrimethylsilane 30 min later, the reaction mixture was precipitated in methanol to give **III-7** as a pale yellow viscous liquid. ^{1}H NMR spectrum of **III-8** was shown in **Figure 3-9**.

Ring-Opening Metathesis Polymerization. Macromonomers **III-4**, **III-5**, **III-6**, **III-7**, and **III-8** were added into NMR tubes, and then were repeatedly dissolved with $CDCl_3$ followed by evaporation under reduced pressure to remove impurities with low boiling points. After the macromonomers were finally dissolved by $CDCl_3$, a $CDCl_3$ solution of the Grubbs initiator was added into each macromonomer solution followed by vigorous mixing using a Vortex Genie for each reaction tube. Poly(macromonomer)s **III-9**, **III-10**, **III-11**, **III-12**, and **III-13** were produced from macromonomers **III-4**, **III-5**,

III-6, **III-7**, and **III-8** respectively. The ^{1}H NMR spectra of the polymerization solutions were shown in **Figure 3-12**, **Figure 3-13**, **Figure 3-14**, **Figure 3-15** and **Figure 3-16**. For all trials, polymerization was allowed to proceed for 12 h, and then terminated with ethyl vinyl ether.

Characterization. ^{1}H NMR analyses were carried out at room temperature on a Varian 600 MHz spectrometer in $CDCl_3$, using tetramethylsilane as reference. For each spectrum, 64 to 128 transients were collected with pulse angle of 39° and delay time of 3 s. Quantitative results were supported by the observations that the spectra obtained with delay time of 10 s were identical to the spectra obtained with delay time of 3 s.

GPC analyses were performed at 40 °C on a Waters-150C GPC instrument equipped with a refractive index detector, four Styragel columns (HR1, HR3, HR4, HR5E), using THF as eluent at 1.0 mL/min. The instrument was calibrated with narrow-disperse linear polystyrene standards.

Positive MALDI-TOF mass spectra were recorded in the linear mode, using a Voyager-DE STR instrument, equipped with a laser emitting at 337 nm, with a 2 ns pulse width. 2,5-Dihydroxybenzoic acid or dithranol was used as matrix. THF was used as solvent for polymers. Accelerating voltage was 20KV. The number of laser shots is 100 per spectrum.

3-7 Conclusions

A series of well-defined diblock macromonomers with block junction carrying a norbornenyl group were synthesized by anionic polymerization of norbornene-

functionalized DPE agent with norbornenyl group intact. ROMP of these diblock macromonomers with limited size of each block using a Grubbs initiator yielded a series of poly(macromonomer)s with well-controlled DP_n and high macromonomer conversion. Kinetics of the ROMP process might be affected by self-assemblies of macromonomers and polymacromonomers occurring under the polymerization conditions. With diblock heterografts densely grafted to backbone, the poly(macromonomer)s are structurally also double-brush copolymers. The synthetic strategy developed here is especially suitable for the synthesis of double-brush copolymers with relatively short heterografts. Because the two types of heterografts have very different properties, the double-brush copolymers, i.e. poly(macromonomer)s, are expected to have novel self-assemblied morphologies and application, which will be investigated in near future.

3-8 General Summary for Double-Brush Copolymer

3-8a **Comparison between the Two Synthetic Strategies**. Because the two strategies, i.e. macroinitiator strategy and macromonomer strategy, have already been investigated, comparison between them is made here.

Macroinitiator strategy (using polystyrene-grafted polyfunctional macroinitiators) is suitable for the synthesis of double-brush copolymers with relatively big dimensions. The backbone can be very long, with DP_n of hundreds. The first type of graft, i.e. polystyrene graft, can have DP_n over one hundred. The second type of graft can have very high DP_n, as well as block structures by sequential addition of different monomers.

A variety of topological features (**Figure 2-13**) can be manipulated into macromolecular architectures of double-brush copolymers.

Macromonomer strategy (ROMP of diblock macromonomer with non-terminal norbornenyl functionality) is suitable for the synthesis of double-brush copolymers with small dimensions. Neither type of graft can be long. The backbone can be significantly longer than grafts, but cannot reach the maximum length that is available using the macroinitiator strategy. However, compared with the macroinitiator strategy, macromonomer can allow more choices for the second type of graft, and at the same time, a variety of well-defined, very interesting topological features (**Figure 3-20**) can be targeted through copolymerization of macromonomers.

3-8b **Composition Range**. No matter which synthetic strategy is selected, the backbone of the double-brush copolymers synthesized is polynorbornene-based in the present work. Because in all cases, the backbone is only a small part, but both types of heterografts consist of the major parts of double-brush copolymers, the composition of grafts is crucial.

Although the first type of heterograft is confined to polystyrene (or substituted polystyrene), there are a broad range of choices for the second type of heterograft. By macroinitiator strategy, polymethacrylates, poly(*t*-BA), and very likely poly(2-VP) can be introduced as the second type of heterograft. By the macromonomer strategy, more choices, including many types of polymers from cyclic monomers suitable for anionic ring-opening polymerization, can be used for the second type of heterograft. Thus, as shown in **Table 3-4**, heterografts with contrasting properties (non-polar vs. polar,

hydrophobic vs. hydrophilic, non-ionic vs. cationic/anionic, insulator vs. conductor, non-biodegradable vs. biodegradable, high surface energy vs. low surface energy, or plastic vs. rubber) can be combined into the grafted architectures of double-brush copolymers.

Table 3-4. Structure and Property Comparison of Heterografts of Double-Brush Copolymers

1st type of heterograft	PS [a]		nonpolar, hydrophobic, nonionic, insulator, nonbiodegrable, T_g ~ 100°C (plastic)
choices of 2nd type of heterograft	PMMA [b,c]	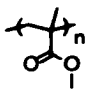	polar, hydrophobic
	P(*t*-BA) [b,c]	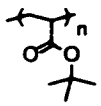	polar, hydrophobic $\xrightarrow{H^+/H_2O}$ hydrophilic $\xrightarrow{MtOH}$ anionic
	P(DMAEMA) [b,c]	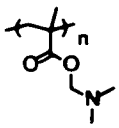	highly polar $\xrightarrow{MeI}$ cationic
	P(2-VP) [c,d]		highly polar, high surface-attaching capacity
	PEO [c]	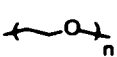	hydrophilic $\xrightarrow{LiI}$ ionic conductor
	PDMS [d]	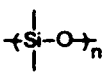	low surface energy, low T_g (rubber)
	PCL [e]	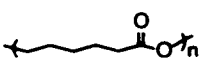	biodegradable

[a] Can also be substituted polystyrene. [b] Obtained by macroinitiator strategy (Chapter 2). [c] Obtained by macromonomer strategy (Chapter 3). [d] Obtainable by macroinitiator strategy (Chapter 2). [e] Obtainable by macromonomer strategy (Chapter 3).

***3-8c* Nanostructures and Potential Applications.** Although comprehensive characterization of nanostructures of double-brush copolymers has not completed yet, the theoretical analysis of their self-assembled nanostructures presented in Chapter 2 (section *2-6a*; **Table 2-6**) is suitable for all types of double-brush copolymers.

As summarized in **Table 3-5**, with novel self-assembled nanostructures and well-organized components with divergent properties, double-brush copolymers are expected to have broad potential applications in areas including nanoparticle and nanocomposite preparation, surface and interface modification, drug and gene delivery, etc.

Table 3-5. Potential Applications of Double-Brush Copolymers Based on Their Expected Nanostructures and Obtainable Components with Divergent Properties

nanostructure [a]	potential applications (constrasting properties of heterografts [b])
a	surface or interface modification (all except ni/c, ni/a)
b	core-shell nanoparticle (all except ni/c, ni/a); drug delivery (hb/hl)
$\mathbf{c_1}$	novel nanoparticle (all except ni/c, ni/a)
$\mathbf{c_2}$	surface or interface modification (all except ni/c, ni/a)
d	nanocomposite (hb/hl, ni/c, ni/a); gene delivery (ni/c)

[a] Correspondent to **Table 2-6**.

[b] Including: np/p (non-polar vs. polar); hb/hl (hydrophobic vs. hydrophilic); hse/lse (high surface energy vs. low surface energy); il/ic (insulator vs. ionic conductor); p/r (plastic vs. rubber); ni/c (non-ionic vs. cationic); ni/a (non-ionic vs. anionic).

Chapter 4

Synthesis and Ring-Opening Metathesis Polymerization of Homopolymer-Based α-Norbornenyl Macromonomers

Abstract: Well-defined poly(MMA)-based, and poly(β-butyrolactone)-based α-norbornenyl macromonomers were synthesized by anionic polymerization and anionic ring-opening polymerization respectively using norbornenyl-functionalized initiators. Their quantitative norbornenyl functionality, well-controlled DP_n, and low polydispersities were verified by ^1H NMR, GPC and MALDI analyses. Ring-opening metathesis polymerization of these macromonomers using a Grubbs catalyst was investigated. Nearly complete conversion (97-100%) was observed for ROMP of poly(MMA)-based macromonomers, and relatively high conversion (79-96%) was also observed for ROMP of poly(β-butyrolactone)-based macromonomers, suggesting that the Grubbs catalyst is very effective catalyst for macromonomers. Well-controlled backbone DP_n and low polydispersities of poly(macromonomer)s synthesized were supported by ^1H NMR and GPC respectively, indicating living characteristics of ROMP of macromonomers. Additionally, GPC analytic results also suggest that the size of macromonomer has a key influence on the solution morphology of the corresponding poly(macromonomer)s.

4-1 Introduction

This is another chapter on synthesis and polymerization of macromonomers with norbornenyl functionality. The background of synthesis and polymerization of macromonomers has been presented in the introduction section of Chapter 3. In this chapter we introduce the general aspects, directly related to the research described in this chapter, on synthesis and ring-opening metathesis polymerization (ROMP) of macromonomers with norbornenyl functionality.

Following the development of well-defined metathesis catalysts, especially the molybdenum-based family [*1*, *2*], the research on the norbornenyl-functionalized macromonomer polymerized by ROMP based on metathesis reaction has gained increasing importance in recent years.

Typically, norbornenyl-functionalized macromonomers are synthesized based on living polymerization techniques to exert good control over macromonomer structures. Because norbornenyl functionality is inert under typical anionic conditions, most reported norbornene-functionalized macromonomers were synthesized by anionic polymerization, including anionic ring-opening polymerization, using norbornene-functionalized initiator or terminating agent. The formed macromonomers reported are based either on homopolymers, including polystyrene [*3-8*], poly(ethylene oxide) [*9*], polybutadiene [*10*] and poly(ε-caprolactone) [*11*], or on diblock copolymers, including polystyrene-*b*-poly(ethylene oxide) [*12*], and polystyrene-*b*-polybutadiene [*13*]. Very recently, other methods for the synthesis of norbornenyl-functionalized macromonomers have also been reported. Polyphosphazene-based macromonomer [*14*] and poly(δ-valerolactone)-based

macromonomer [*15*] were synthesized by cationic ring-opening polymerization using norbornenyl-functionalized terminating agent and initiator respectively, suggesting certain level of stability of norbornenyl functionality under cationic conditions. Polynorbornene-based macromonomer was synthesized through ROMP using a functionalized terminating agent followed by ω-chain-end modification [*16*]. Because norbornenyl functionality can be polymerized by radical polymerization [*17-19*], no synthesis of norbornenyl-functionalized macromonomer based on radical polymerization has been reported. For all types of macromonomers reported, only one type of polystyrene-based macromonomer has in-chain norbornenyl functionality [*4*], and all others have terminal norbornenyl functionality.

It has been well established that, like ROMP of a conventional monomer, ROMP with norbornenyl-functionalized macromonomer typically also exhibit living characteristics [*20*]. Due to the unusual structures and properties of poly(macromonomer)s, ROMP of macromonomer without conventional monomer feed has been investigated extensively [*4-14*, 16]. With generally well-controlled synthetic results, it has been recognized as an exceptionally good strategy for the synthesis of well-defined poly(macromonomer)s. Relatively high M_n up to 10 000, typically not allowed for other types of macromonomers for effective polymerization, can be targeted for norbornene-functionalized macromonomers to give poly(macromonomer)s via ROMP [*6, 8, 13, 14, 16*], presumably because the formed poly(macromonomer)s have lower grafting density than most other types of poly(macromonomer)s based on number of intervening chemical bonds on the main-chain backbone. Up to now, molybdenum-based Schrock catalysts have been used predominantly as the initiator of ROMP of

norbornenyl-functionalized macromonomer [*4-10, 12-14, 16*], mainly because of its high reactivity. A ruthenium-based multi-component catalyst system, not capable of leading to living polymerization, was used in one report [*11*]. Surprisingly, well-defined ruthenium-based Grubbs catalysts [*21, 22*], used widely in other metathesis reaction systems, have not yet been used generally for ROMP of norbornenyl-functionalized macromonomer. Although Grubbs catalysts have lower metathesis reactivity than Schrock catalysts, Grubbs catalysts have important merits that are not possessed by Schrock catalysts, including higher functional group tolerance [22], affordable price [*23*], as well as non-stringent preparation, storage, and application conditions [*24*].

There are two main reasons for our interest in ROMP of norbornenyl-functionalized macromonomer using Grubbs catalysts. First, in principle, Grubbs catalysts can tolerate a broad range of functional groups on macromonomers, therefore it can be expected that a wide variety of poly(macromonomer)s can be prepared by ROMP of macromonomers using Grubbs catalysts. Second, even for macromonomers with only functional groups allowed by Schrock catalyst, very small amount of impurities in macromonomers potentially can effectively poison Schrock catalysts.

In the following sections, we will present our investigation on synthesis and ROMP, using a Grubbs catalyst, of two new types of macromonomers, i.e. poly(methyl methacrylate)-based and poly(β-butyrolactone)-based α-norbornenyl macromonomers. Our related research work of diblock macromonomers with non-terminal norbornenyl functionality has been presented in Chapter 3.

Poly(MMA)-based α-norbornenyl macromonomer was synthesized by anionic polymerization using norbornenyl functionalized initiator, based on DPE-norbornene

bifunctional agent **II-1**. Poly(β-butyrolactone)-based α-norbornenyl macromonomer was synthesized by anionic ring-opening polymerization using norbornenyl-functionalized initiator. Noteworthily, with Chapter 3 as a reference, a broad variety of norbornenyl-functionalized macromonomers based on homopolymers of polystyrene, poly(*tert*-butyl acrylate), poly(2-vinyl pyridine), poly(ethylene oxide), and poly(dimethyl siloxane) can also be readily prepared using **II-1**. Further research work, especially on new macromonomers based on poly(2-vinyl pyridine) and poly(dimethyl siloxane), is of importance, but will not be covered in this dissertation.

4-2 Synthesis and ROMP of Poly(MMA)-Based α-Norbornenyl Macromonomers

4-2a **Synthesis of Poly(MMA)-Based α-Norbornenyl Macromonomers.** Poly(MMA)-based α-norbornenyl macromonomer **IV-2** was synthesized, following **Scheme 4-1**, using anionic polymerization initiated by norbornenyl-functionalized 1,1-diphenylalkyllithium **IV-1**. Anionic polymerization was carried out in THF at -78 °C in the presence of lithium chloride. Initiator **IV-1** was in situ prepared by the reaction of *sec*-butyllithium with 1.2 equivalents of DPE-norbornene bifunctional agent **II-1** (*exo*/*endo* = 43/57) for 30 min. Characteristic red color of 1,1-diphenylalkyllithium appeared as soon as *sec*-butyllithium was added into a THF solution of **II-1**, indicating a very fast reaction between *sec*-butyllithium and the DPE functionality of **II-1**. Because it has been well-established that the reaction of alkyllithium with DPE unit is quantitative

and norbornenyl group is inert under typical anionic polymerization conditions [*25, 26*], with an excess of **II-1** used, it can be assumed that the molar amount of the initiator **IV-1** formed was equal to the feed molar amount of *sec*-butyllithium. A small amount of **II-1** remaining in the system did not interfere with either **IV-1** or the subsequent anionic polymerization of MMA, because both its DPE functionality and norbornenyl functionality do not have considerable reactivity with either 1,1-diphenylalkyllithium or poly(MMA) living anion. In principle, 1,1-diphenylalkyllithiums are among the most useful initiators for anionic polymerization of methacrylates and *tert*-butyl acrylate [*25, 26*], as well as 2-vinylpyridine [*27*]. In current work, norbornenyl-functionalized 1,1-diphenylalkyllithium **IV-1** prepared was only used for MMA.

Scheme 4-1

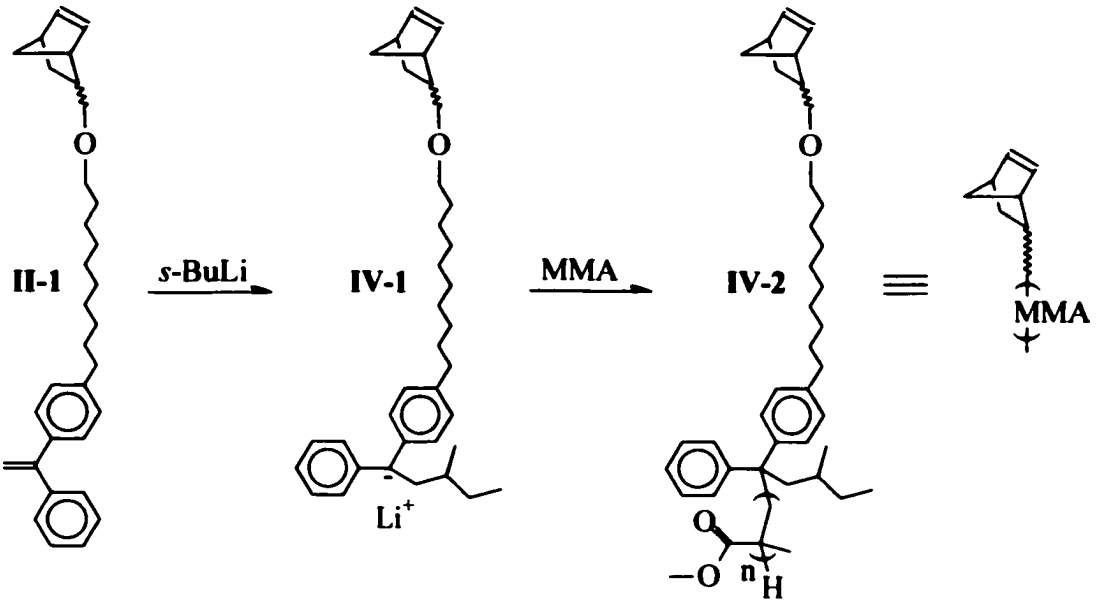

Anionic polymerization of MMA was started by adding MMA dropwise to the reaction system. With 10 equivalents of lithium chloride relative to initiator **IV-1** in the system to improve the ratio of initiation rate to propagation rate [*28*], the characteristic red color of **IV-1** disappeared when less than 2 equivalents of MMA relative to **IV-1** were introduced, indicating a fast initiation relative to propagation. Polymerization was allowed to proceed for 1 h to complete monomer conversion before termination with methanol. Then polymerization solutions were first precipitated in cold pentane to remove small amounts of **II-1**, and then the precipitated polymers were dissolved in dichloromethane-methanol (20:1) and filtered through a column packed with silica gel to remove lithium chloride and lithium methoxide (formed by methanol termination). With the molar feed ratio of monomer to initiator, $[MMA]_0/[\textbf{IV-1}]_0$, of 10, 20, and 40, poly(MMA)-based α-norbornenyl macromonomers, i.e. macromonomers **IV-2**, with different poly(MMA) chain length were obtained. Due to the living characteristics of the anionic polymerization system, macromonomers **IV-2** have well-defined structures that were verified by ^{1}H NMR, GPC, and MALDI analyses. The synthetic results of **IV-2** were summarized in **Table 4-1**.

Table 4-1. Synthesis of Poly(MMA)-Based α-Norbornenyl Macromonomers [a]

entry	$[MMA]_0/[\textbf{IV-1}]_0$	$DP_{n,H\text{-}NMR}$	$M_{n,H\text{-}NMR}$	$M_{n,GPC}$ [b]	$M_{p,MALDI}$	PDI_{GPC} [b]
IV-2a	10	13	1800	1990	1938	1.06
IV-2b	20	23	2800	3040	2839	1.05
IV-2c	40	43	4800	5070	-	1.05

[a] THF as solvent; $[LiCl]_0/[\textbf{IV-1}]_0 = 10$; -78 °C. [b] Calibrated with linear polystyrenes.

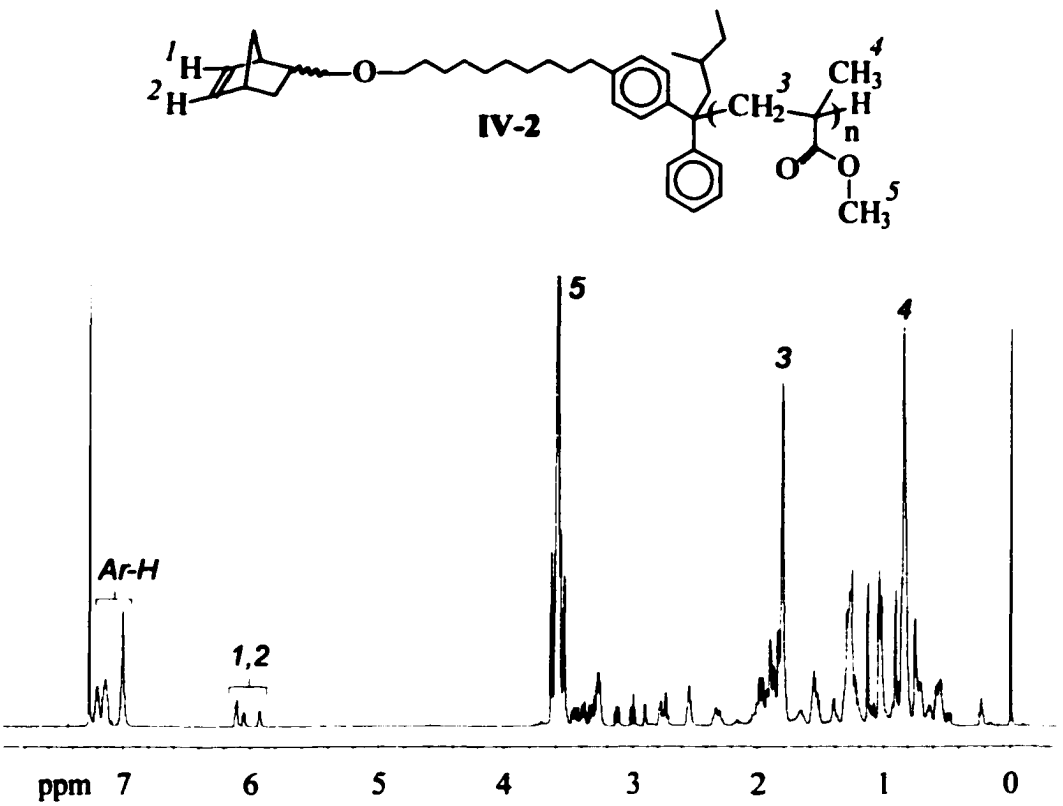

Figure 4-1. ^{1}H NMR spectrum of PMMA-based α-norbornenyl macromonomer **IV-2**.

^{1}H NMR analysis of macromonomer **IV-2** verified their chemical structures. Characteristic resonances of both norbornenyl functionality and MMA monomer unit are presented in the ^{1}H NMR spectrum of **IV-2** (**Figure 4-1**). The norbornenyl group on **IV-2** was established through resonances of its alkene protons at 6.15-5.87 ppm. Poly(MMA) chain on **IV-2** was verified through strong resonances concentrated at 3.59, 1.81, and 0.84 ppm, corresponding to the protons of methoxyl, methylene, and α-methyl groups of MMA monomer units respectively. Moreover, quantitative resonance intensities of aromatic protons (7.25-6.90 ppm) from the DPE site relative to resonance intensities of norbornenyl alkene protons suggest that each poly(MMA) chain formed via the initiation of 1,1-diphenylalkyllithium initiator site was connected with a norbornenyl group. The

resonances of methoxyl protons of MMA monomer unit (centered at 3.59 ppm) have no significant overlap with other resonances, and therefore their intensities were compared with the resonance intensities of norbornenyl alkene protons (6.15-5.87 ppm) to give experimental DP_n values of macromonomer **IV-2**. For macromonomer **IV-2c** which has the longest PMMA chain, nearly quantitative initiation using **IV-1** was indicated by the excellent agreement between the experimental DP_n value and the molar feed ratio of monomer to initiator, i.e. $[MMA]_0/[\textbf{IV-1}]_0$. For macromonomer **IV-2b** with poly(MMA) chain of intermediate length, a good agreement between the experimental DP_n value and $[MMA]_0/[\textbf{IV-1}]_0$ was observed. For macromonomer **IV-2a** with the shortest poly(MMA) chain, experimental DP_n value of PMMA chain of 13 is remarkably higher than the $[MMA]_0/[\textbf{IV-1}]_0$ of 10, presumably because a considerable amount of polymer species of **IV-3a** with relatively low molecular weights could not be recovered by precipitation. Based on weights of macromonomers finally obtained, up to 10% of **IV-2a**, and several percent of **IV-2b** were lost by precipitation; polymer loss in precipitation is not noticeable for **IV-2c**.

Very low polydispersities (1.05-1.06) of macromonomer **IV-2** samples were determined by GPC analysis. As shown in **Figure 4-2**, **IV-2a**, **IV-2b**, and **IV-2c** all have very narrow, symmetrical molecular weight distributions. The M_n values of **IV-2** samples by GPC were in good agreements with the M_n values based on ^{1}H NMR analysis. At the same time, M_n values obtained by ^{1}H NMR were considered as more accurate, because the relationship between hydrodynamic volume and elution time for **IV-2** differs from that for linear polystyrenes used for GPC calibration.

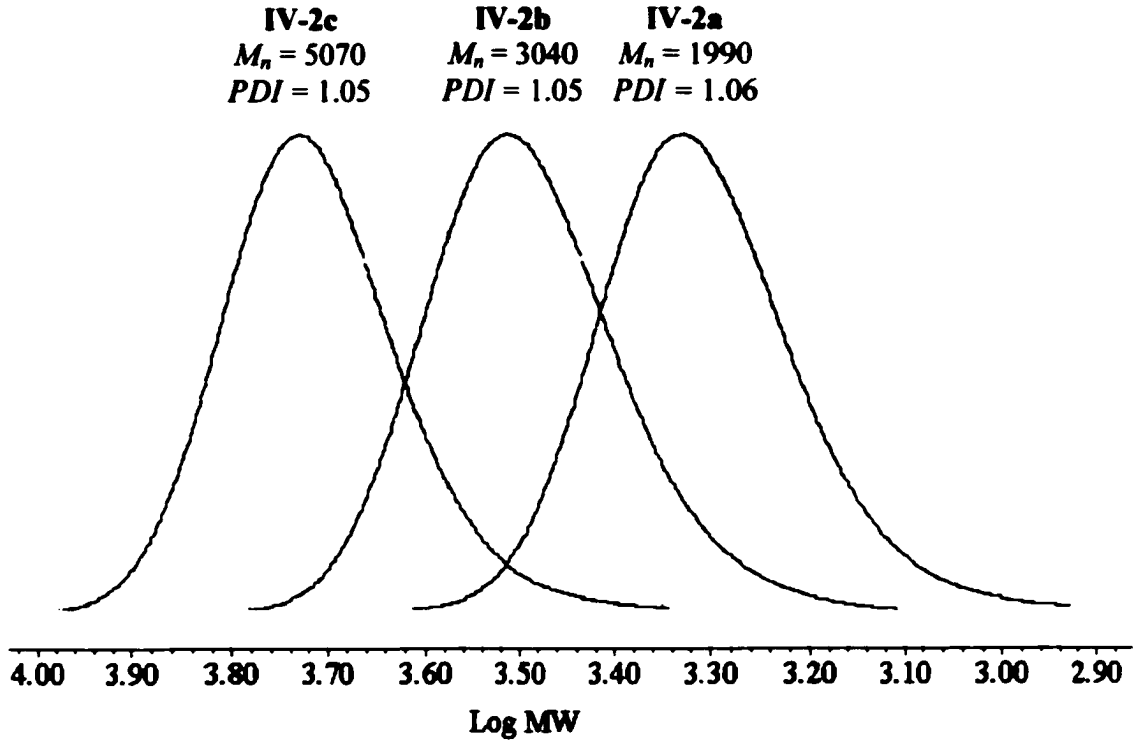

Figure 4-2. Molecular weight distributions of **IV-2** samples determined by GPC. (GPC was calibrated with linear polystyrenes)

Concerning the possibly significant experimental error in GPC determination for **IV-2a** and **IV-2b** due to their relatively low molecular weights, MALDI characterization using 2,5-dihydroxybenzoic acid as matrix was further performed. As shown in **Figure 4-3**, both **IV-2a** and **IV-2b** show a narrow molecular weight distribution, with maximum intensities at 1938 (*DP* of 14) and 2839 (*DP* of 23) respectively [*29*]. The excellent agreement of peak molecular weight, M_P, by MALDI with the M_n by ^{1}H NMR (and GPC) further confirmed the well-defined structures of macromonomers **IV-2**. Macromonomer **IV-2c** was also measured by MALDI, but the spectrum obtained has poor resolution. At

the same time, based on a M_n of 4800 by ^{1}H NMR, GPC determination for **IV-2c** can be considered as reasonable estimation.

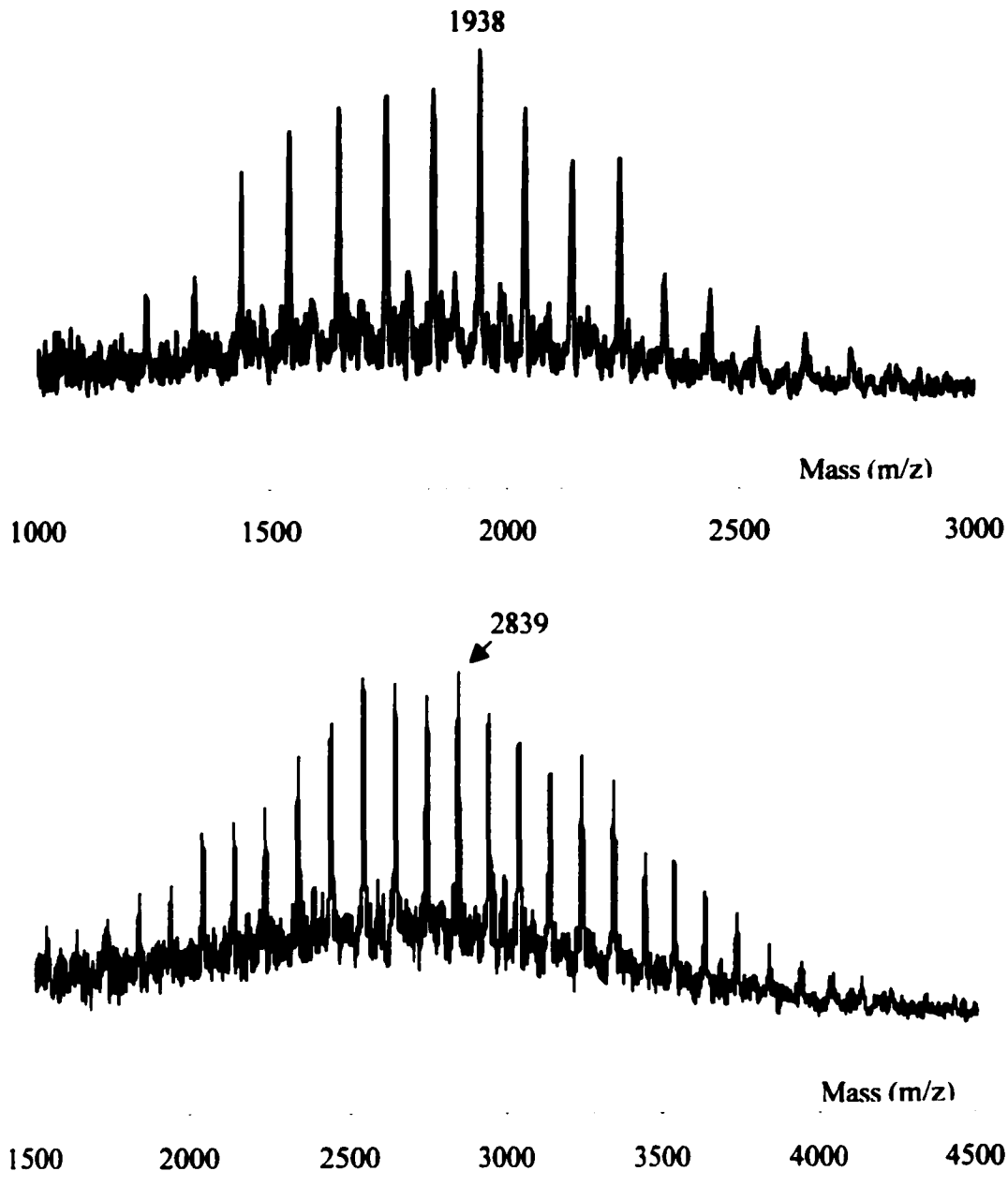

Figure 4-3. MALDI spectra of macromonomers a) **IV-2a** and b) **IV-2b**.

***4-2b* ROMP of Poly(MMA)-Based α-Norbornenyl Macromonomers.** Ring-opening metathesis polymerization (ROMP) of macromonomer **IV-2** was carried out using a Grubbs catalyst in $CDCl_3$, following **Scheme 4-2**. The molar feed ratio of macromonomer to the Grubbs catalyst ranged from 10 to 80 to target poly(**IV-2**), i.e. poly(macromonomer) **IV-3**, with different backbone lengths. Polymerization time was 6 h, and ethyl vinyl ether was used to terminate polymerization. Just before termination, in situ ^1H NMR analysis was performed for all trials to determine macromonomer conversion, backbone DP_n of **IV-3**, and $M_{n,H\text{-}NMR}$ of **IV-3**. Poly(macromonomer) **IV-3** finally obtained was analyzed by GPC for polydispersity and $M_{n,GPC}$ determinations. It was found that the synthesis was surprisingly successful. Macromonomer conversion was nearly complete for all trials. Poly(macromonomer) **IV-3** yielded also has a well-defined macromolecular structure. The synthetic results were summarized in **Table 4-2**.

Scheme 4-2

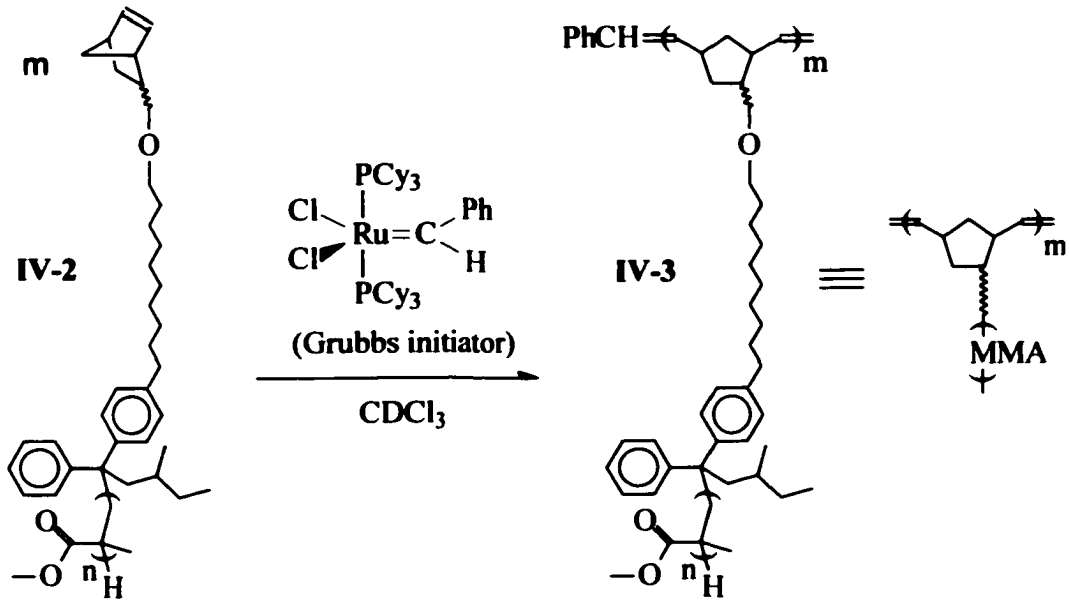

Table 4-2. ROMP of Poly(MMA)-Based α-Norbornenyl Macromonomers [a]

		$[IV\text{-}2]_0$	conv [b]	DP_n		M_n (10^3)		PDI
entry	IV-2	$[I]_0$	(%)	calcd.	^{1}H NMR	^{1}H NMR	GPC [c]	(GPC[c])
IV-3a1	**IV-2a**	20	100	20	20	36.4	26.9	1.13
IV-3a2	**IV-2a**	40	99	39	38	68.2	46.8	1.15
IV-3a3	**IV-2a**	80	97	77	79	142	102	1.34
IV-3b1	**IV-2b**	10	100	10	10	28.1	19.0	1.13
IV-3b2	**IV-2b**	20	99	20	20	56.1	35.7	1.12
IV-3b3	**IV-2b**	40	99	40	39	109	55.0	1.12
IV-3c1	**IV-2c**	10	100	10	8.2	39.5	26.9	1.10
IV-3c2	**IV-2c**	20	98	20	14	67.3	47.6	1.10
IV-3c3	**IV-2c**	40	99	40	-	-	60.9	1.12

[a] Using Grubbs initiator in $CDCl_3$. [b] By ^{1}H NMR. [c] Calibrated with linear polystyrenes.

Nearly complete conversion (97-100%) of macromonomer **IV-2** was determined by ^{1}H NMR analysis. A typical ^{1}H NMR spectrum (of **IV-3b2**) obtained by in situ monitoring of the polymerization solution is shown in **Figure 4-4**. The norbornenyl alkene protons of **IV-2** have ^{1}H resonances concentrated at 6.11 (resonance *a*; for one proton of both *exo* and *endo*), 6.03 (for the other proton of *exo*), and 5.92 ppm (resonance *b*; for the other proton of *endo*). Conversion of macromonomer **IV-2** was determined based on comparison of their resonance intensities with the resonance intensities of the alkene protons of the poly(norbornene) backbone at 5.0-5.5 ppm. The nearly complete conversion was beyond our expectation based on the general notion that Grubbs catalyst

has good functional group tolerance other than very high reactivity. It is possible that with many pendent ester groups whose oxygen atoms have nonbonding electron-pairs, the presence of poly(MMA) chains on macromonomer **IV-2** and poly(macromonomer) **IV-3** may activate, to certain extent, the ruthenium-based initiating and propagating sites by their interaction (as ligands) with the ruthenium atoms. Of course, further investigation is needed to clarify the high reactivity of Grubbs catalyst in the current system. Additionally, for all trials, no characteristic alkene proton resonances concentrated at 6.03 ppm for *exo*-norbornenyl group of macromonomer **IV-2** could be observed, indicating complete conversion of macromonomers with *exo*-norbornenyl functionality due to their higher reactivity [*8*].

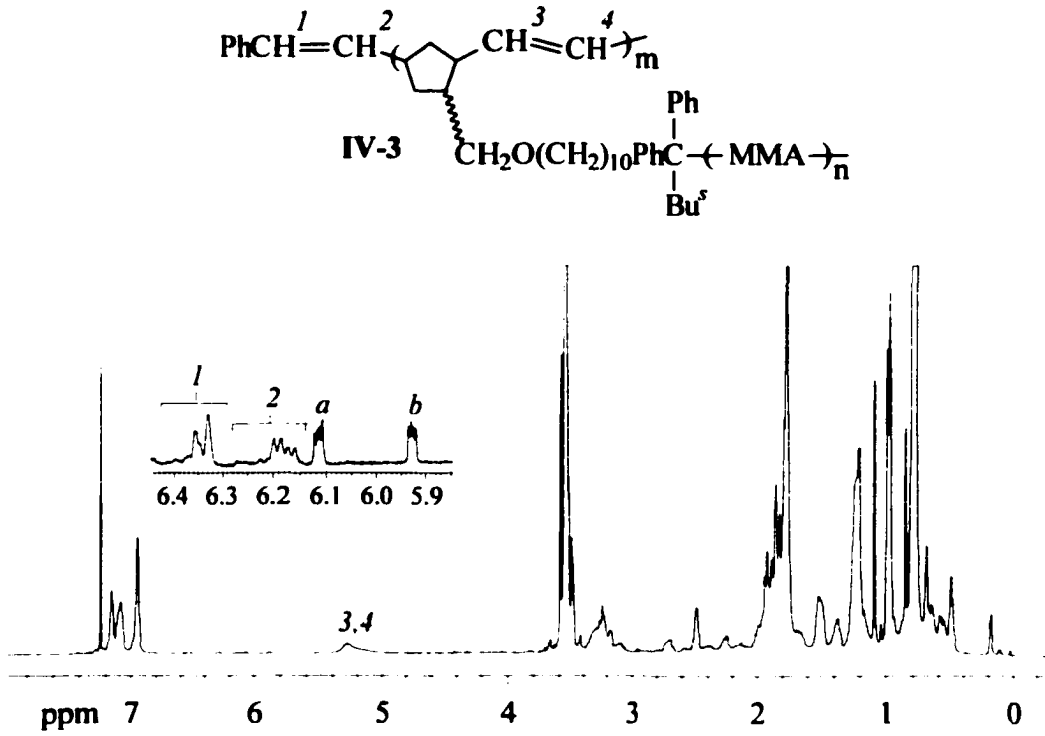

Figure 4-4. ^{1}H NMR spectrum of polymerization solution of **IV-3b2**.

Well-controlled backbone DP_n of poly(macromonomer) **IV-3** was also verified by ^{1}H NMR analysis, indicating the living characteristics of ROMP of macromonomers **IV-2** using Grubbs catalyst. The α-chain-end of backbone of **IV-3** has a quantitative concentration of PhCH- fragment from the Grubbs initiator, and the benzyl proton showed characteristic ^{1}H NMR resonances at 6.43-6.29 ppm. Therefore, the DP_n of poly(norbornene)-based backbone of polymacromonomer **IV-3** was determined based on comparison of their resonance intensities with the resonance intensities of backbone alkene protons at 5.5-5.0 ppm. Excellent agreements between experimental DP_n values and the DP_n values calculated based on macromonomer conversion and the molar feed ratio of macromonomer to initiator were obtained for the trials using macromonomer **IV-2a** or **IV-2b**, suggesting quantitative initiation using Grubbs catalyst in the current system. But for the trials using macromonomer **IV-2c** having the longest poly(MMA) chain among macromonomers, DP_n values of poly(macromonomer) backbones measured by ^{1}H NMR were significantly below the calculated values, presumably because intensities of relatively broad resonance from backbone alkene protons were underestimated to some extent due to the rigid backbone of the resulting poly(macromonomer) with relatively long side-chains.

With macromonomer conversion measured by ^{1}H NMR with reasonable confidence in our current work, GPC analysis was used mainly to determine polydispersities of poly(macromonomer) **IV-3** produced. Low polydisperisities, as well as monomodal molecular weight distribution, of **IV-3** samples were verified for all trials. **Figure 4-5** shows the GPC curves for poly(macromonomer) samples prepared from macromonomer **IV-2a**. With increased molar feed ratio of macromonomer to initiator,

the formed poly(macromonomer) had decreased elution time, indicating increasing molecular weight and backbone length. Among all poly(macromonomer)s yielded, **IV-3a3** (*PDI* = 1.34) was the only one with polydispersity over 1.15, presumably because for that trial, the small amount of initiator solution could not be mixed with viscous macromonomer solution very sufficiently within seconds.

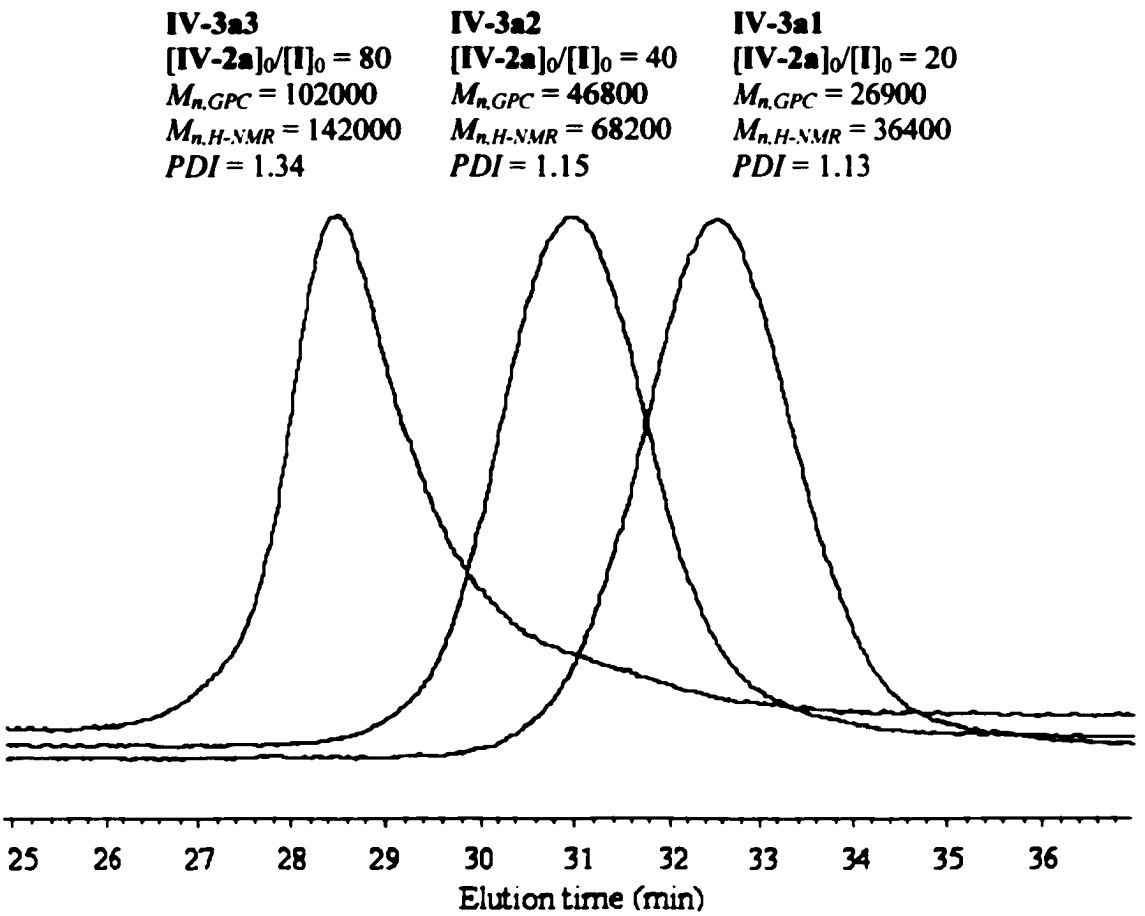

Figure 4-5. GPC curves of poly(macromonomer)s **IV-3a1**, **IV-3a2**, and **IV-3a3**.

With calibration using linear polystyrenes, the M_n of poly(macromonomer) **IV-3** obtained by GPC could not be considered as accurate, and obviously were

underestimated because with densely grafted architectures, poly(macromonomer)s typically have smaller hydrodynamic volume than polystyrenes with the same molecular weights. The M_n values obtained based on DP_n of poly(macromonomer) backbones determined by ^{1}H NMR were considered as reasonably accurate. Additionally, it is also expected that polydispersities of **IV-3** were underestimated somewhat because typically the hydrodynamic volume of poly(macromonomer)s is less sensitive to molecular weight than linear polystyrenes.

4-3 Synthesis and ROMP of Poly(β-butyrolactone)-Based α-Norbornenyl Macromonomers

4-3a **Synthesis of Poly(β-butyrolactone)-Based α-Norbornenyl Macromonomers.** Poly(β-butyrolactone)-based α-norbornenyl macromonomer **IV-4** was synthesized by anionic ring-opening polymerization initiated by potassium 5-norbornene-2-carboxylate in the presence of 18-crown-6, following **Scheme 4-3**.

Scheme 4-3

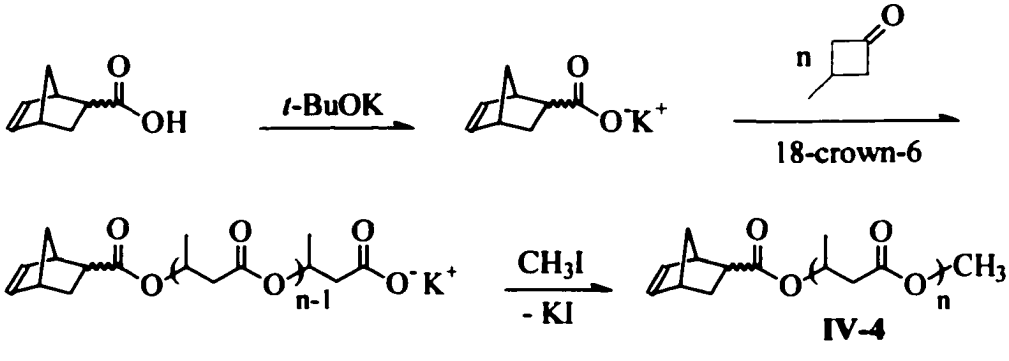

Table 4-3. Synthesis of Poly(β-butyrolactone)-Based α-Norbornenyl Macromonomers [a]

entry	$[\beta\text{-BL}]_0/[I]_0$	$DP_{n,H\text{-}NMR}$	$M_{n,H\text{-}NMR}$	$M_{n,GPC}$ [b]	$M_{p,MALDI}$	PDI_{GPC} [b]
IV-4a	9.4	9.3	952	1130	949	1.16
IV-4b	18.8	18.5	1740	2310	1809	1.10
IV-4c	28.1	26.0	2390	3260	2326	1.07
IV-4d	37.6	35.2	3180	4230	3014	1.06

[a] Initiator (I): NBCOOK; $[18\text{-crown-6}]_0/[I]_0 = 1.0$; solvent: THF; room temperature; polymerization time: 40 h; conversion: ~100%. [b] Calibrated with linear polystyrenes.

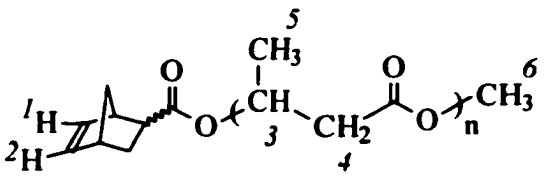

IV-4

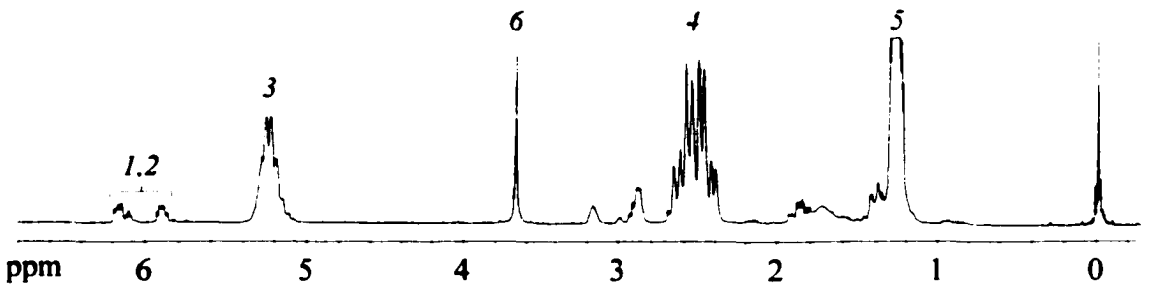

Figure 4-6. ^{1}H NMR spectrum of poly(β-BL)-based α-norbornenyl macromonomer **IV-4a**

Initiator potassium 5-norbornene-2-carboxylate was prepared by the reaction of 5-norbornene-2-carboxylic acid (*exo/endo* mixture) with potassium *tert*-butoxide. A

slight excess of 18-crown-6 relative to potassium 5-norbornene-2-carboxylate was then used to form a complex with potassium 5-norbornene-2-carboxylate to activate and increase the solubility of the latter [*30*]. Anionic ring-opening polymerization of β-butyrolactone (β-BL) was carried out in THF at room temperature. Polymerization was allowed to proceed for 40 h, and ^{1}H NMR analysis of polymerization solution showed that nearly complete conversion was reached for each trial. Polymerization was then terminated with iodomethane. Potassium iodide formed and 18-crown-6 were removed by filtration and extraction. With the molar feed ratio of monomer to initiator, $[\beta\text{-BL}]_0/[\mathbf{I}]_0$, of 10, 20, 30, and 40, α-norbornenyl poly(β-BL) samples, i.e. macromonomer **IV-3**, with different poly(β-BL) chain length were obtained. The macromonomer **IV-4** synthesized was viscous liquid at room temperature because of low glass transition temperature (~-2 °C) of their poly(β-BL) chains [*30*]. ^{1}H NMR, GPC, and MALDI analyses were used to characterize macromonomer **IV-2** and its well-defined structure was verified. The synthetic results of **IV-4** were summarized in **Table 4-3.**

^{1}H NMR analysis (200 MHz) was used to verify the chemical structure and determined DP_n of macromonomer **IV-4**. As shown in **Figure 4-6**, characteristic resonances of both norbornenyl functionality and β-BL monomer unit were present in the ^{1}H NMR spectrum of **IV-4**. The norbornenyl group on **IV-4** was established through the resonances of its alkene protons at 6.23-5.80 ppm. Poly(β-BL) chain on **IV-4** was verified through strong resonances concentrated at 5.42-4.97, 2.74-2.27, and 1.51-1.04 ppm, which correspond to the protons of methine, methylene, and methyl of β-BL monomer units respectively. The ω-methyl group was also verified through its resonances centered at 3.65 ppm. The resonances of methine protons of β-BL monomer

unit (5.42-4.97 ppm) do not have considerable overlap with other resonances, and therefore their intensities were compared with the resonance intensities of norbornenyl alkene protons (6.23-5.80 ppm) to give the experimental DP_n values of macromonomers **IV-4**. For all trials, experimental DP_n values were very close to the molar feed ratios of monomer to initiator, indicating very good initiation efficiency and well-controlled poly(β-BL) chain length of macromonomers **IV-4**.

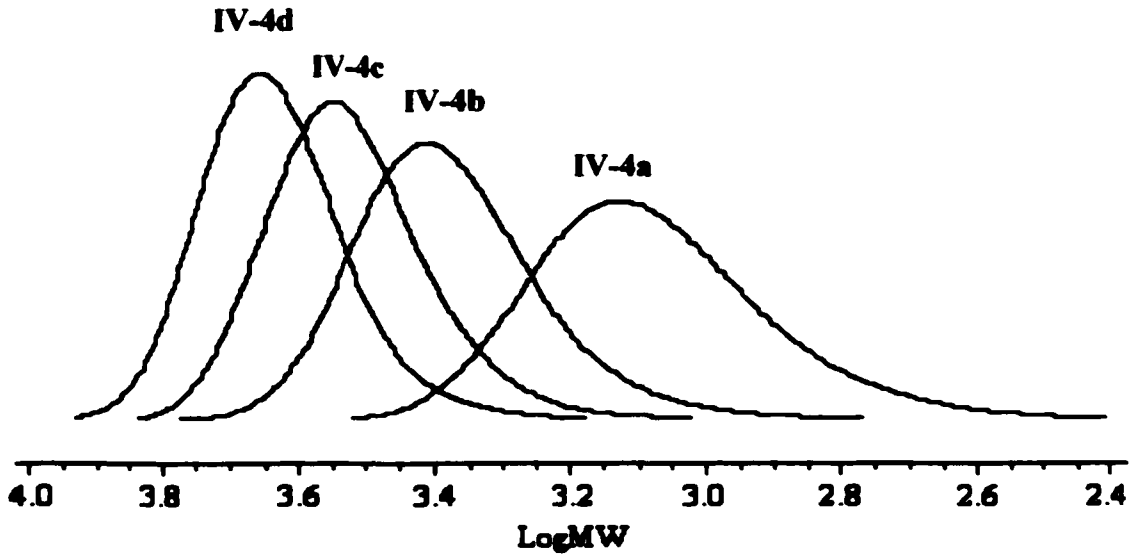

Figure 4-7. Molecular weight distributions of **IV-4** samples determined by GPC.

Low polydispersities of macromonomers **IV-4** were indicated by GPC analysis. As shown in **Figure 4-7**, each **IV-4** sample has narrow, monomodal molecular weight distribution. With increased $[\beta\text{-BL}]_0/[I]_0$ ratio, **IV-4** has increased molecular weight but decreased polydispersity (from 1.16 to 1.06), suggesting no significant occurrence of side reactions in the polymerization system and well-defined structure of macromonomer **IV-4**. On the other hand, because linear polystyrenes that were used for GPC calibration

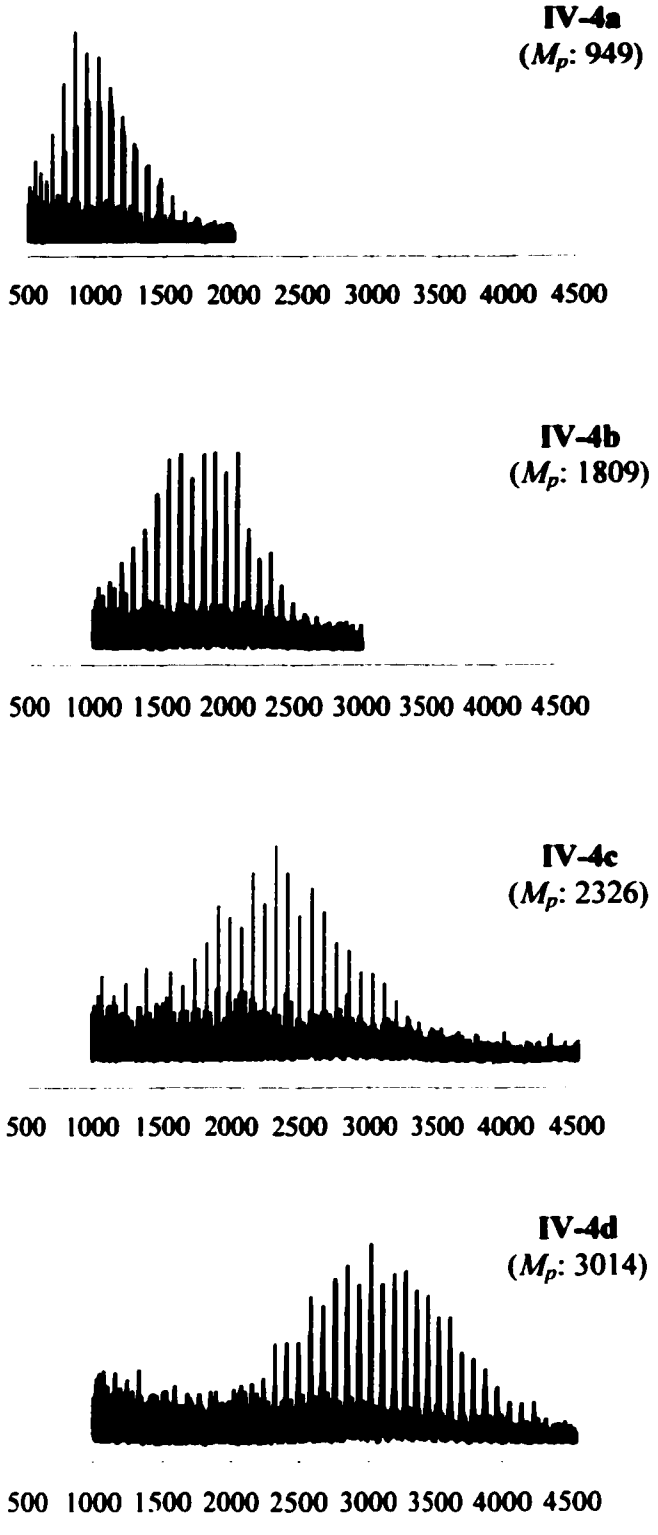

Figure 4-8. MALDI spectra of **IV-4** samples

must differ from macromonomer **IV-4** in the relationship between molecular weight and elution time, it is obvious that M_n values of **IV-2** obtained by GPC cannot be considered as very reliable. At the same time, because all samples of **IV-2** have quite low M_n values (<5000), GPC measurement could not be considered as accurate.

Therefore MALDI analysis, using 2,5-dihydroxybenzoic acid as matrix, was used to further examine molecular weight and molecular weight distribution of macromonomer **IV-4**. As shown in **Figure 4-8**, narrow molecular weight distributions for all samples were verified by MALDI. Macromonomer **IV-4** has increased molecular weight with increasing $[\beta\text{-BL}]_0/[\text{I}]_0$ in polymerization. Moreover, excellent agreements between the maximum peak molecular weight (M_p) values of macromonomers **IV-4** and their M_n values based on DP_n determined by ^{1}H NMR further provide strong evidence for well-controlled poly(β-BL) chain length for macromonomers as well as their well-defined structures [*31*].

In summary, all characterization results, including well-controlled DP_n and narrow molecular weight distribution, suggest that macromonomer **IV-4** has a well-defined structure and anionic ring-opening polymerization of β-BL used for the synthesis of **IV-4** can be considered as living polymerization.

4-3b **ROMP of Poly(β-butyrolactone)-Based α-Norbornenyl Macromonomers.** Ring-opening metathesis polymerization (ROMP) of macromonomer **IV-4** was carried out using a Grubbs catalyst in $CDCl_3$ (**Scheme 4-4**). The molar feed ratio of macromonomer to the Grubbs catalyst ranged from 10 to 80, to target poly(macromonomer) **IV-5**, i.e. poly(**IV-4**), with different backbone lengths.

Polymerization time was 6 h, and ethyl vinyl ether was used to terminate polymerization. The synthetic results are summarized in **Table 4-4**.

Scheme 4-4

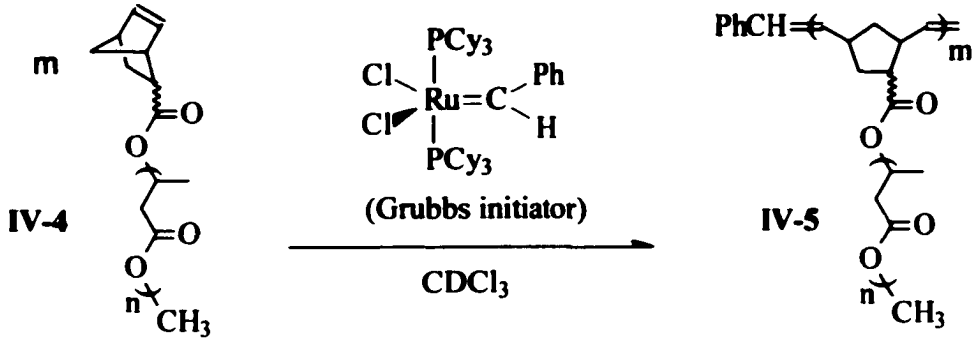

Macromonomer conversion and molecular weight of the poly(macromonomer) **IV-5** were determined by GPC analysis of terminated polymerization solution. Relatively high macromonomer conversion (79-96%) was obtained based on comparison of the integration area of the poly(macromonomer) and the sum of integration areas of both poly(macromonomer) and macromonomer remaining. Typical GPC curves of polymerization solutions were shown in **Figure 4-9**. With major amounts of macromonomer polymerized for all trials, compared with the GPC peaks for poly(macromonomer)s **IV-5**, the GPC peaks corresponding to macromonomer **IV-4** remaining after 6 h of polymerization are relatively small. Such high yield indicates that Grubbs catalyst used is a very effective initiator for poly(β-BL)-based macromonomer **IV-4**. For the trials using the same macromonomer **IV-4** sample, with increased poly(macromonomer) backbone DP_n value calculated based on macromonomer conversion and the molar feed ratio of macromonomer to initiator, the

poly(macromonomer) has decreased elution time and increased molecular weight as expected. At the same time, low polydispersities (1.11-1.30) of poly(macromonomer) IV-5 samples were also obtained by GPC analysis.

Table 4-4. ROMP of Poly(β-BL)-Based α-Norbornenyl Macromonomers [a]

		$[IV\text{-}2]_0$	conv [b]	DP_n [c]		M_n (10^3)			
entry	IV-2	$[I]_0$	(%)	calcd	GPC [b]	calcd	GPC [b]	PDI [b]	VCR [d]
IV-5a1	**IV-2a**	10	96	9.6	7.1	9.24	7.99	1.16	1.36
IV-5a2	**IV-2a**	20	95	19	14.4	18.2	16.3	1.24	1.32
IV-5a3	**IV-2a**	40	91	36.4	28.1	34.8	31.8	1.30	1.29
IV-5a4	**IV-2a**	80	94	75.2	55.4	71.7	62.6	1.22	1.36
IV-5b1	**IV-2b**	10	95	9.5	5.6	16.6	13.1	1.17	1.70
IV-5b2	**IV-2b**	20	91	18.2	12.3	31.8	28.5	1.20	1.48
IV-5c1	**IV-2c**	10	83	8.3	6.3	19.9	20.6	1.15	1.32
IV-5c2	**IV-2c**	20	86	17.2	9.3	41.2	30.4	1.18	1.85
IV-5c3	**IV-2c**	40	89	35.6	17.3	85.2	56.3	1.13	2.06
IV-5c4	**IV-2a**	80	80	64	27.3	153	88.9	1.18	2.34
IV-5d1	**IV-2d**	10	87	8.7	6.8	27.8	28.6	1.12	1.29
IV-5d2	**IV-2d**	20	86	17.2	10.2	54.8	43.1	1.11	1.69
IV-5d3	**IV-2d**	40	82	32.8	15.3	104	64.8	1.15	2.14
IV-5d4	**IV-2d**	80	79	63.2	23.9	201	101	1.12	2.64

[a] Using Grubbs initiator in $CDCl_3$. [b] By GPC calibrated with linear polystyrenes.

[c] For backbone of **IV-5**; $DP_{n,GPC} = M_{n,GPC,IV\text{-}5} / M_{n,GPC,IV\text{-}4}$. [d] $DP_{n,calcd} / DP_{n,GPC}$.

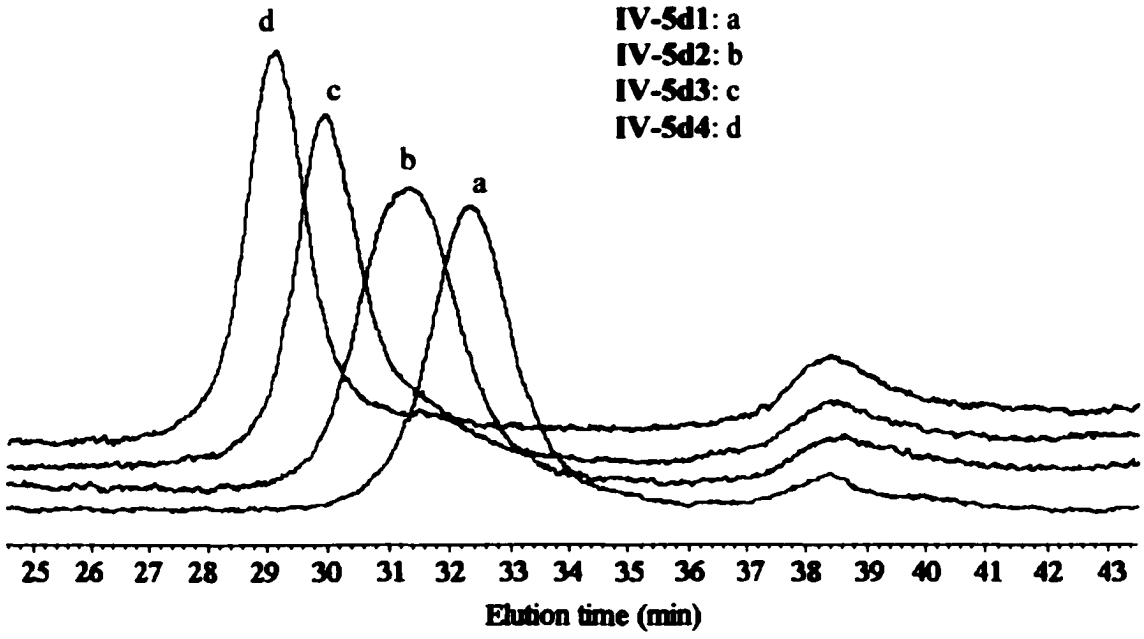

Figure 4-9. GPC curves of polymerization solutions for **IV-5d** (poly(**IV-4d**)) series.

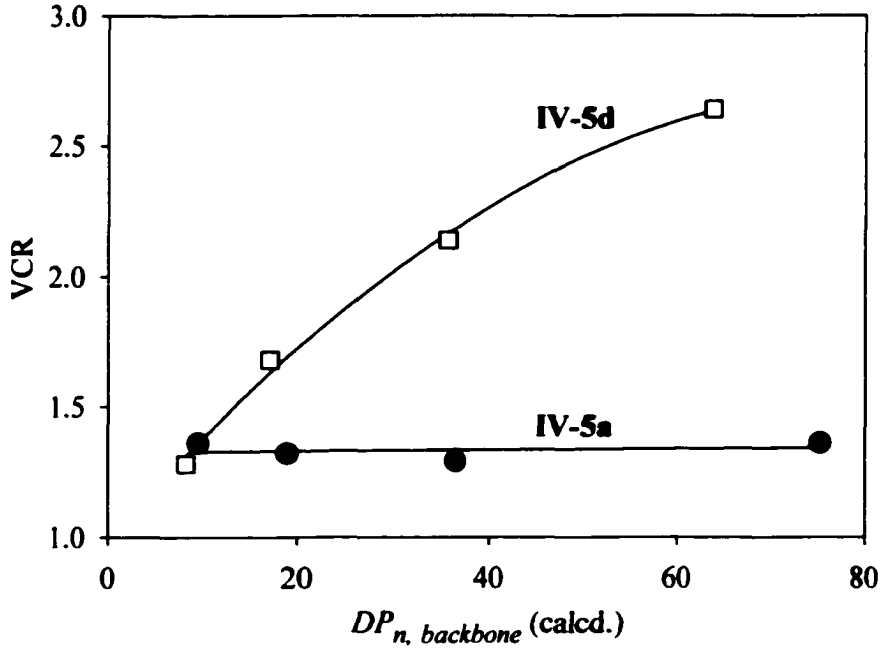

Figure 4-10. Hydrodynamic volume contraction ratio (VCR) dependence on backbone DP_n of **IV-5a** (●; poly(**IV-4a**)) and **IV-5d** (□; poly(**IV-4d**)) series.

On the other hand, because linear polystyrenes used for GPC calibration must differ from poly(macromonomer) **IV-5** in the relationship between molecular weight and elution time, it is obvious that, in general, M_n values of **IV-5** determined by GPC could not agree very well with calculated values. At the same time, polydispersities of **IV-5** samples obtained by GPC are expected to be underestimated for some extent due to their densely grafted architectures. However, significant information on solution morphology of poly(macromonomer) **IV-5** can be deduced from GPC analysis. Because GPC analysis is based on hydrodynamic volume dependence on molecular weight, the ratio of $M_{n,GPC}$ value of **IV-5** to $M_{n,GPC}$ value of corresponding **IV-4** represents hydrodynamic volume of **IV-5** relative to hydrodynamic volume of **IV-4** under the GPC characterization conditions, and here we define this ratio as $DP_{n,GPC}$. Furthermore, the ratio of calculated DP_n to $DP_{n,GPC}$ reflects the extent of hydrodynamic volume contraction of poly(macromonomer) **IV-5** relative to the corresponding macromonomer **IV-4**, and the higher the ratio is, the more significant the contraction is. Therefore, we define this ratio as volume contraction ratio (VCR). On **Figure 4-10**, the VCR dependence on poly(macromonomer) backbone DP_n was plotted for poly(macromonomer) **IV-5a** and **IV-5d** series where **IV-4a**, the macromonomer sample with the shortest chain, and **IV-4d**, the macromonomer sample with the longest chain, were polymerized respectively. No significant change on VCR ratio relative to backbone DP_n was observed for **IV-5a** series. It indicates that the size of side-chains ($DP_{n,\beta\text{-BL}}$ = 9.3) is too small to stiffen the poly(macromonomer) backbone significantly, and suggests that similar to typical linear polymers, poly(macromonomer) **IV-5a** samples have relatively flexible morphology in solution. On the other hand, the fast increase of VCR ratio relative to backbone DP_n was

observed for **IV-5d** series. It indicates that the size of side-chains ($DP_{n,\beta\text{-BL}}$ = 35.2) is bulky enough to stiffen the poly(macromonomer) backbone, and suggests that backbone of poly(macromonomer) **IV-5d** became more and more stiffened with increasing backbone DP_n (and length). Thus, it can be further expected, poly(macromonomer) **IV-5d** with short backbone length, such as **IV-5a1** (backbone with a DP_n of 8.7, corresponding to an average of about 44 carbon atoms on the backbone main-chain), would take flexible star-like morphology in solution. However, **IV-5d** with long backbone, such as **IV-5a4** (backbone with a DP_n of 63.2, corresponding to an average of about 320 carbon atoms on the backbone main-chain), would assume rigid rod-like morphology in solution.

Although it can not be judged through GPC results whether the poly(macromonomer) **IV-5** have well-controlled backbone length and entire molecular weights, the well-controlled ROMP process for **IV-5** synthesis was supported by ^{1}H NMR evidence. ^{1}H NMR analysis was performed just before termination of polymerization. As shown in ^{1}H NMR spectrum of polymerization solution of **IV-5a1** (**Figure 4-11**), the resonances of backbone α-chain-end benzyl proton (from a fragment of the Grubbs catalyst) were identified at 6.44-6.29 ppm. Their intensities relative to intensities of other protons were in excellent agreement with calculated values based on quantitative initiation, suggesting that poly(macromonomer) **IV-5** yielded by ROMP of macromonomer **IV-4** has well-controlled backbone DP_n, as well as molecular weight. Such ^{1}H NMR analytic results, coupled with low polydispersities of **IV-5** samples demonstrated by GPC analysis, further illustrate that poly(macromonomer) **IV-5** has a well-defined macromolecular structure.

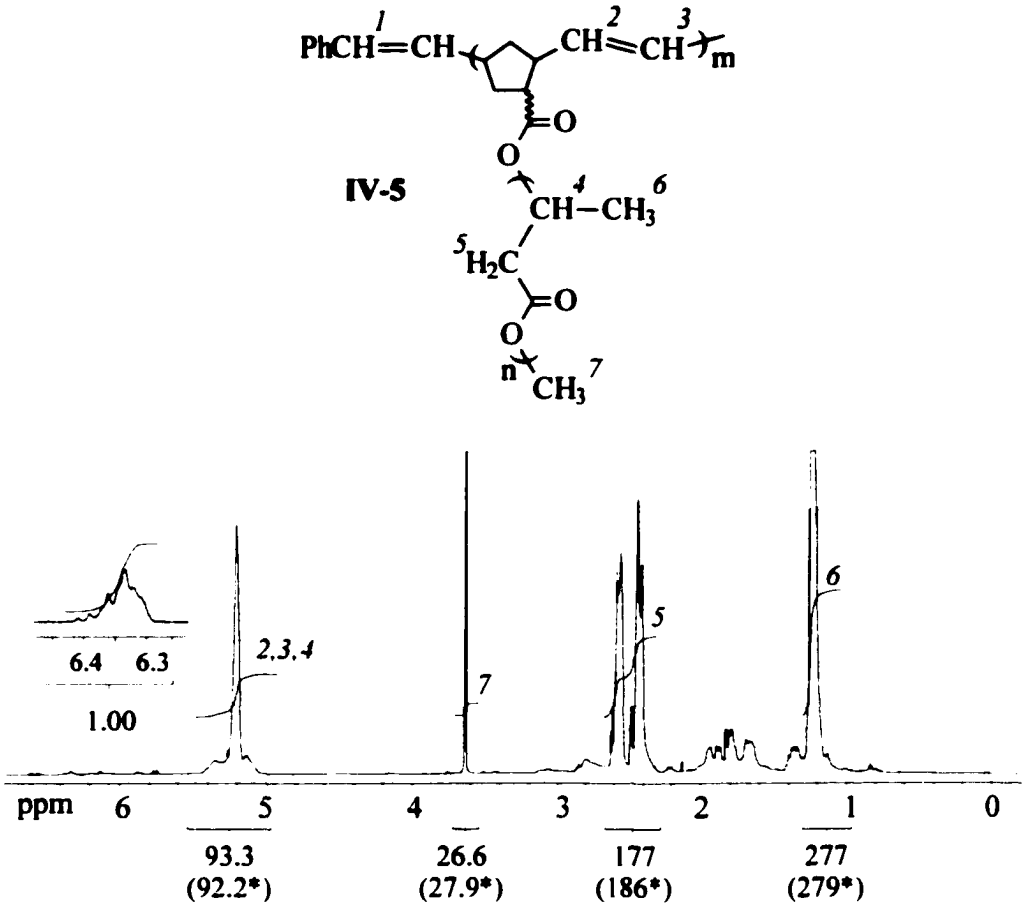

Figure 4-11. ^{1}H NMR spectrum of polymerization solution of **IV-5a1**

(*calculated value)

4-4 Experimental

Materials. Grubbs catalyst $RuCl_2(CHC_6H_5)[P(C_6H_{11})_3]_2$ (Strem), *sec*-butyllithium (*s*-BuLi; 1.3 *M* in cyclohexane, Aldrich), lithium chloride (99.99%, Aldrich), ethyl vinyl ether (99%, Aldrich), and iodomethane (99%, Acros) were used as received. Nitrogen (>99.999%, Welco) was used as inert atmosphere for all reactions without further purification. Methyl methacrylate (MMA; 99%, Aldrich) was diluted with toluene,

distilled over CaH_2 and then distilled from triethylaluminum. β-Butyrolactone (β-BL; >98%, Aldich) was distilled over CaH_2, and then distilled over dispersed sodium before use. Tetrahydrofuran (THF; 99.9%, Acros) was refluxed overnight over CaH_2 and then distilled from sodium naphthalene. 5-Norbornene-2-carboxylic acid (98%, mixture of *endo* and *exo*, Aldrich) was distilled. Potassium *tert*-butoxide (95%, Aldrich) was sublimed. 18-Crown-6 (>99.5%, Aldrich) was recrystallized from pentane twice. Chloroform-*d* ($CDCl_3$; 99.8%, Acros) was distilled over CaH_2. Synthesis of **II-1** was described in Chapter 2.

Poly(MMA)-Based α-Norbornenyl Macromonomer IV-2. All chemicals were transferred with dry syringes, and reactions were carried out in a pre-flamed glass bottle with magnetic stirring. *s*-BuLi was added slowly into 1.2 equivalents of **II-1** in THF in the presence of 10 equivalents of lithium chloride at -78 °C, and the reaction was allowed to proceed for 30 min to give solution of **IV-2** with red color. MMA was then slowly added to induce anionic polymerization. One hour later, polymerization was terminated with methanol. Polymerization solutions were precipitated in cold pentane. The polymers recovered were redissolved in dichloromethane/methanol (20:1), and the formed solutions were filtered through a short column packed with silica gel. After evaporating solvents under reduced pressure, **IV-2** was obtained as a white solid. ^1H NMR spectrum of **IV-2** was shown in **Figure 4-1**.

Potassium 5-Norbornene-2-carboxylate. 5-Norbornene-2-carboxylic acid (4.17 g, 30.0 mmol) was added into potassium *tert*-butoxide (3.03 g, 27.0 mmol) in THF. Potassium 5-norbornene-2-carboxylate immediately was washed by THF for several times. After recrystallization from THF/ethanol, it was dried under vacuum at 40 °C for

48 h. ^{1}H NMR (200 MHz, $CDCl_3$) δ: 6.20-5.85 (m, 2H), 3.12 (s, 1H), 2.80 (m, 2H), 1.83 (m, 1H), 1.30 (m, 3H).

Complex of Potassium 5-Norbornene-2-carboxylate and 18-Crown-6. Potassium 5-norbornene-2-carboxylate (2.18 g, 12.4 mmol) was dissolved in dry methanol, and then 18-crown-6 (3.31 g, 12.6 mmol) was added. After evaporation of solvent, THF was added and evaporated successively to remove traces of methanol. Finally, about 400 ml of THF was added, and complex solution was obtained after filtration. The concentration of complex was determined based on weight of solute measured after removing solvent.

Poly(β-butyrolactone)-Based α-Norbornenyl Macromonomer IV-4. Anionic ring-opening polymerization of β-butyrolactone was carried out in a pre-flamed flask at room temperature under nitrogen. After adding the THF solution of the complex of potassium 5-norbornene-2-carboxylate and 18-crown-6, β-butyrolactone was introduced by dry syringe. Polymerization was allowed to proceed for 40 h for nearly complete conversion, and then was terminated with excess iodomethane. One day after the addition of iodomethane, THF and MeI remaining were removed under reduced pressure. The polymers obtained were redissolved in CH_2Cl_2, and the formed solutions were extracted several times with water to remove crown ether and salt. The polymer solutions were then dried over $MgSO_4$, and evaporated to dryness, giving **IV-2** as a pale yellow viscous liquid. ^{1}H NMR spectrum of **IV-2** was shown in **Figure 4-1**.

Ring-Opening Metathesis Polymerization. Macromonomers **IV-2** and **IV-4** were added into glass tubes, and then were repeatedly dissolved with $CDCl_3$ followed by evaporation under reduced pressure to remove impurities with low boiling points. After

the macromonomers were finally dissolved in $CDCl_3$, a $CDCl_3$ solution of Grubbs initiator was added into each macromonomer solution followed by vigorous mixing using a Vortex Genie for each reaction tube. Poly(macromonomer)s **IV-3** and **IV-5** were yielded from macromonomers **IV-2** and **IV-4** respectively. The ^1H NMR spectra of the polymerization solutions recorded at a polymerization time of 6 h were shown in **Figure 4-4** and **Figure 4-11**. Then polymerization was terminated with ethyl vinyl ether.

Characterization. ^1H NMR analyses were carried out at room temperature on a Varian 600 MHz or 200 MHz spectrometer with $CDCl_3$ as solvent and tetramethylsilane as internal reference. For each spectrum, 64 to 128 transients were collected with pulse angle of 39° and delay time of 3 s. Quantitative results were supported by the observations that the spectra obtained with delay time of 10 s were identical to the spectra obtained with delay time of 3 s.

GPC analyses were performed at 40 °C on a Waters-150C GPC instrument equipped with a refractive index detector, four Styragel columns (HR1, HR3, HR4, HR5E), using THF as eluent at 1.0 mL/min. The instrument was calibrated with narrow-disperse linear polystyrene standards.

Positive MALDI-TOF mass spectra were recorded in linear mode, using a Voyager-DE STR instrument, equipped with a laser emitting at 337 nm, with a 2 ns pulse width. 2,5-Dihydroxybenzoic acid was used as the matrix. THF was used as solvent for the polymers. Accelerating voltage was 20 KV. Number of laser shots was 100 per spectrum.

4-5 Conclusions

Using norbornenyl-functionalized initiators, well-defined poly(MMA)-based and poly(β-butyrolactone)-based α-norbornenyl macromonomers can be synthesized by anionic polymerization and anionic ring-opening polymerization respectively. Grubbs catalyst is very effective initiator for ring-opening metathesis polymerization (ROMP) of these macromonomers, and can lead to high yield of poly(macromonomer)s with well-controlled macromolecular architectures.

Following the same strategy but using different monomers for the synthesis of poly(MMA)-based α-norbornenyl macromonomer, a variety of new types of macromonomers with α-norbornenyl group can be expected to lead to new types of poly(macromonomer)s.

Chapter 5

Synthesis of Grafted Copolymers Based on Well-Defined Polyfunctional Macroinitiators for Stable Free Radical Polymerization

Abstract: An ensemble of grafted copolymers with controlled architectures were synthesized by the strategy of combined living anionic polymerization and stable free radical polymerization (SFRP). Polyfunctional SFRP macroinitiators were synthesized by anionic polymerization with an alkoxyamine-functionalized methacrylate monomer. These macroinitiators, with homopolymer, block and statistical copolymer structures, have well-controlled number-average alkoxyamine functionalities, chain-length, low polydispersities, suggesting that alkoxyamine functionality is stable under the anionic polymerization conditions used. SFRP using these macroinitiators yielded grafted copolymers with well-controlled backbone, graft, graft number, entire molecular weights, and low polydispersities. Block structures of grafts were obtained readily through the sequential SFRP process. Besides nonpolar and polar components incorporated into grafted copolymers by polymerization, hydrophilic and ionic polymeric components can also be introduced into grafted copolymers readily through subsequent modification reactions. With well-organized components of divergent polarities, these grafted copolymers exhibited a series of well-defined self-assembled surface nanopatterns.

5-1 Introduction

Living radical polymerization (LRP) has been well established for the synthesis of well-defined polymers in last decade [*1-3*]. Up to now, three important types of LRP techniques, including stable free radical polymerization (SFRP) [*4*], atom transfer radical polymerization (ATRP) [*5, 6*], and reversible addition fragmentation transfer (RAFT) [*7*], have been developed. Among them, SFRP has attracted our major attention due to its good compatibility with anionic polymerization [*8, 9*].

SFRP is based on reversible termination by mediation of radical chain carrier with stable radical. The mediation effects of a variety of stable radicals on radical polymerization have been investigated [*10*]. However, currently only when nitroxide is used as mediation radical, SFRP can yield well-defined polymers. SFRP with nitroxide mediation typically is also referred to as nitroxide-mediated radical polymerization (NMRP).

Although the preliminary work using nitroxide to mediate radical polymerization can be tracked to the 1980s [*11*], SFRP was not established as a living polymerization technique until the mid-1990s. Georges et al. synthesized narrow-disperse polymers [*12*] and investigated SFRP mechanism using ESR [*13*]. However, the bimolecular initiating system (i.e. a conventional radical initiator, with the addition of free nitroxide) they used cannot lead to good control over molecular weights of polymers yielded, and also is not suitable for the synthesis of polymers with complex architectures. Hawker then modified SFRP system by using unimolecular alkoxyamine-based initiators [*14*], and finally established the general strategy for well-controlled polymer synthesis by SFRP.

For all nitroxide-mediated radical polymerization systems, the nitroxide used has key influence on polymerization results [*4*]. 2,2,6,6-Tetramethylpiperidinooxy (TEMPO) is the most used nitroxide because it is commercially available, but only few monomers, such as styrenes and 4-vinylpyridine, can be converted into well-defined polymers by TEMPO-mediated radical polymerization. Additional monomers, such as acrylates, acrylamides, and 1,3-dienes, can be polymerized with good structural control by using new types of nitroxides [*15-18*]. However, compared with ATRP or RAFT, currently SFRP has a quite narrow range of applicable monomers, and this significantly restricts the application potentials of SFRP.

The synthesis of grafted polymers using alkoxyamine-functionalized polyfunctional macroinitiators is an important aspect of SFRP research [*19-22*]. Well-defined polyfunctional SFRP macroinitiators with statistically distributed alkoxyamine functionality have been synthesized by Hawker et al. via coupling reaction between a well-defined polymer (prepared by ATRP) and a small molecule alkoxyamine agent [*19*]. More efforts have been made to prepare polyfunctional SFRP macroinitiators by polymerization of alkoxyamine-functionalized monomer. Several alkoxyamine-based monomers have been reported by Hawker [*20*], Gravert et al. [*21*], and Stehling et al [*22*]. However, because typical free radical polymerization (with AIBN as initiator) and coordination polymerization adopted for polymerizing the monomers were not living, the resulting polymers, i.e. polyfunctional SFRP macroinitiators, were not well-defined.

This chapter describes our finding of living anionic polymerization of alkoxyamine-functionalized monomer as a general synthetic strategy for the synthesis of well-defined SFRP polyfunctional macroinitiators, as well as controlled synthesis of

grafted copolymer using the macroinitiators produced. Well-defined surface nanopatterns exhibited by the grafted copolymers synthesized are also to be discussed. Considering good stability of alkoxyamine functionality under anionic polymerization conditions as our work illustrated, a wide variety of polymers with complex macromolecular architectures can be further synthesized by combined anionic polymerization and alkoxyamine-based SFRP.

5-2 General Synthetic Design

Scheme 5-1

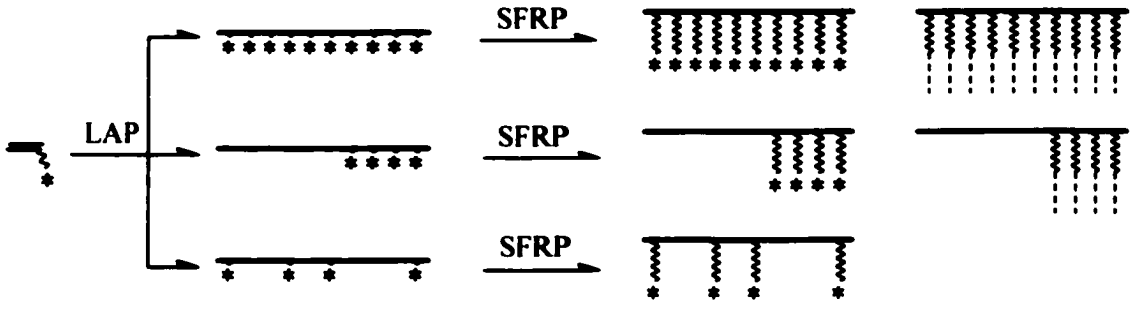

* : alkoxyamine (SFRP initiator site).

The general synthetic strategy used in this chapter is shown in **Scheme 5-1**. An alkoxyamine-functionalized vinyl monomer was synthesized first. Three types of well-defined alkoxyamine-functionalized polymers, with homopolymer, block and statistical copolymer structures, were synthesized by living polymerization with the monomer. Using these polymers as polyfunctional NMRP macroinitiators, a variety of grafted copolymers with controlled architectures but different structural features were

synthesized, and some of them have grafts with block structures. By modification of the grafted copolymers, new types of grafted copolymers were also further obtained.

5-3 Synthesis of Well-Defined Polyfunctional Alkoxyamine-Functionalized Macroinitiators

1-Methacryloyloxy-2-phenyl-2-(2',2',6',6'-tetramethyl-1'-piperidinyloxyl)ethane (**V-1**) [*21*], an alkoxyamine-functionalized methacrylate monomer, was synthesized following **Scheme 5-2**. Because anionic polymerization of methacrylates can yield polymers with accurate structural control, we investigated the anionic polymerization with **V-1**. Three types of well-defined polymers with alkoxymaine functionalities were synthesized by anionic homopolymerization of **V-1**, anionic block copolymerization of MMA and **V-1**, and anionic statistical copolymerization of *tert*-butyl methacrylate (*t*-BMA) with **V-1** respectively.

Scheme 5-2

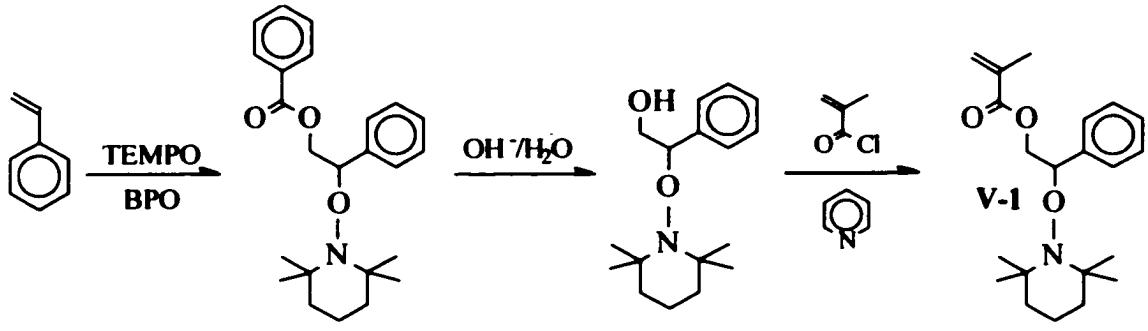

Scheme 5-3

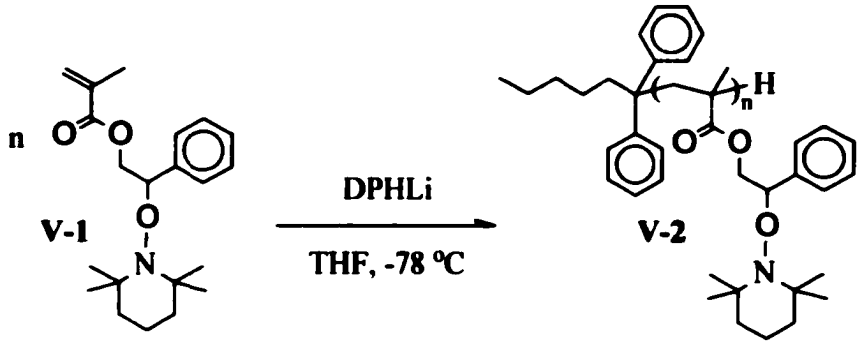

Anionic polymerization of **V-1** was carried out in THF at -78 °C using 1,1-diphenylhexyllithium (DPHLi) [*23*] as initiator under nitrogen atmosphere (**Scheme 5-3**). Five equivalents of lithium chloride relative to DPHLi were used as an additive to improve the ratio of initiation rate to propagation rate [*24*], and the polymerization time was 1 h. As a result, well-defined poly(**V-1**), that is, **V-2**, was yielded (**Table 5-1**).

Table 5-1. Synthesis of Macroinitiator V-2 by Anionic Polymerization of V-1

	$[V\text{-}1]_0$	conv	DP_n		M_n	PDI	
entry	$[DPHLi]_0$	(%)	calcd	NMR	(NMR)	GPC [a]	GPC [b]
V-2a	6.0	100	6.0	6.4	2450	1.11	1.28
V-2b	12	100	12	11	4030	1.10	1.18
V-2c	24	90	22	23	8170	1.10	1.05
V-2d	48	78	37	35	12300	1.07	1.05

[a] Calibrated with linear polystyrene standards. [b] Calibration based on M_n of **V-2** determined by ^{1}H NMR.

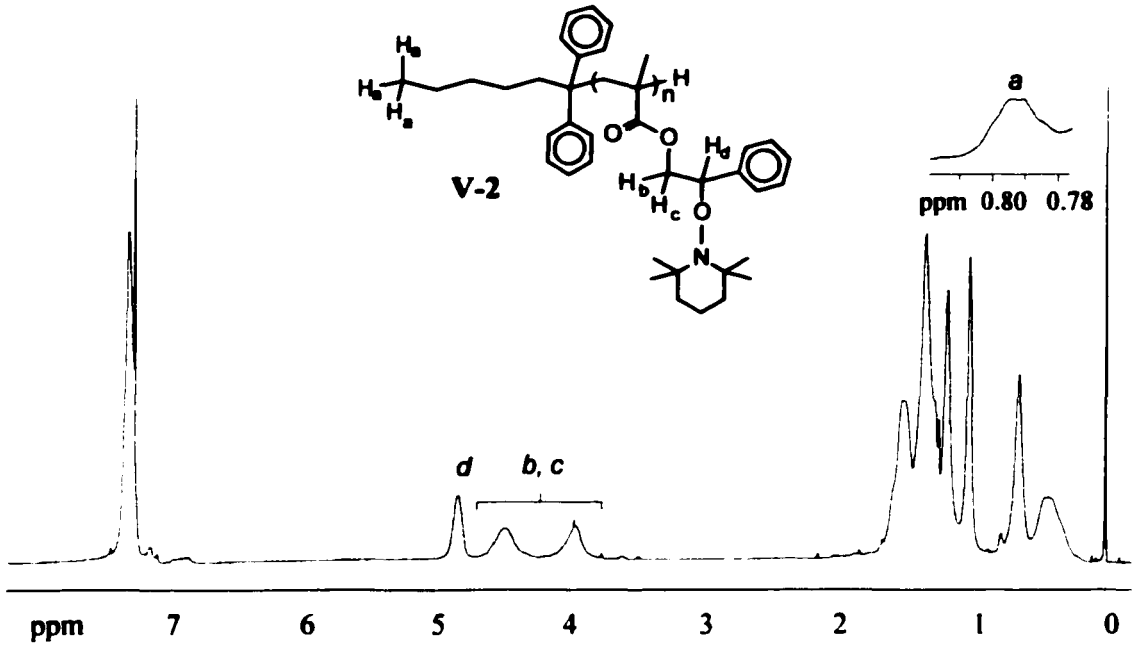

Figure 5-1. ^{1}H NMR spectrum of SFRP polyfunctional macroinitiators **V-2**

^{1}H NMR characterization verified the molecular structures of **V-2** (**Figure 5-1**). The quantitative ^{1}H NMR measurement of α and β protons of the phenyl ring in the monomer unit of **V-1** (*b*, *c*, and *d*; centered at 3.96, 4.50, and 4.82 ppm) not only verified the existence of an alkoxyamine functionality per monomer unit, but also was used to determine the number-average degree of polymerization (DP_n) by comparing the area of their signals with that of the signal due to the chain-end methyl proton (*a*; from DPHLi, centered at 0.79 ppm) [*25*]. The experimental DP_n values were very close to the DP_n values calculated from monomer conversion and the initial feed ratio of monomer to initiator, $[\text{V-1}]_0/[\text{DPHLi}]_0$, indicating well-controlled number-average alkoxyamine functionality on **V-2**.

Although typically MALDI analysis is suitable for polydispersity measurement for narrow-dispersed polymers with relatively small M_n values, it cannot be used to analyze

V-2 due to the instability of its alkoxyamine functionalities under the analytical conditions [*26*]. MALDI measurement was performed using different types of matrices and different accelerating voltages. But in all trials, besides peaks with mass values corresponding to complete **V-2** polymer species, numerous peaks with mass values corresponding to **V-2** polymer species losing one or more TEMPO moieties, or α-chain-end 1,1-diphenylhexyl group were observed; the occurence of bimacromolecular coupling during analysis was also indicated by bimodal molecular weight distributions observed in some trials.

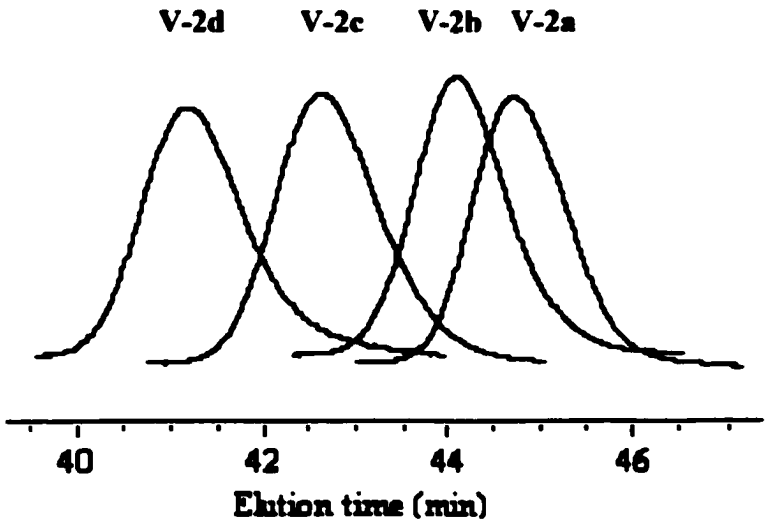

Figure 5-2. GPC curves of polyfunctional SFRP macroinitiators **V-2**

The polydispersities of **V-2** were finally analyzed by GPC. The GPC instrument equipped with a high resolution column for low molecular weight analysis (Styragel HR 3; effective molecular weight range: 500-30 000) in addition to three Ultrastyragel columns allows sufficient resolution for all samples of **V-2**. As shown in **Figure 5-2**, each sample showed a very narrow peak on its GPC curve. The GPC curves were first

calibrated with linear polystyrene standards and low polydispersities (*PDI* = 1.07-1.11) were obtained for all samples of **V-2**. Because the relationship between molecular weight and elution time of **V-2** must differ from that for linear polystyrene, a second calibration was constructed, assuming that eluting species of **V-2** on the peak maxima of GPC curves have the number-average molecular weight (M_n) values from ^{1}H NMR measurement. Because a linear relationship between *logMW* and elution time does not hold for the entire molecular weight range of **V-2** (M_n = 2450-12 300; $M_n = 238 + 345DP_n$), a third-order fit was chosen for the calibration. GPC results from the second calibration further confirm the low polydispersities of **V-2** (*PDI* = 1.05-1.28). The polydispersities of **V-2** decrease with the increasing degree of polymerization and the two samples of **V-2** with the highest DP_n values, **V-2c** and **V-2d**, are nearly monodispersed. All the above results demonstrate that the alkoxyamine functionality of **V-1** is stable under the anionic polymerization conditions used, and the anionic polymerization of **V-1** has the characteristics of living polymerization. The polymerization rate of **V-1** was relatively slow because the steric hindrance from the bulky alkoxyamine-based ester alkyl group of **V-1** decreases the reactivity of both its methacryloyl vinyl functionality and the poly(**V-1**) propagating anion. After 1 h of polymerization time, incomplete conversion of **V-1** in synthesizing **V-2c** and **V-2d** was detected by ^{1}H NMR analysis of polymerization solution through the existence of the resonance of alkene protons of **V-1** at 5.47 and 5.98 ppm. Longer polymerization time is required for complete monomer conversion of the two trials.

Anionic block copolymerization of MMA and **V-1** was carried out in THF at -78 °C using DPHLi as initiator in the presence of lithium chloride under nitrogen

atmosphere (**Scheme 5-4**). MMA was chosen as the first monomer because poly(MMA) anion is more reactive than poly(V-1) anion. The polymerization time of MMA was 30 min for complete conversion, and the polymerization time of V-1 was 1 h. As a result, well-defined poly(MMA)-*block*-poly(V-1), that is, V-3, was produced (**Table 5-2**).

Scheme 5-4

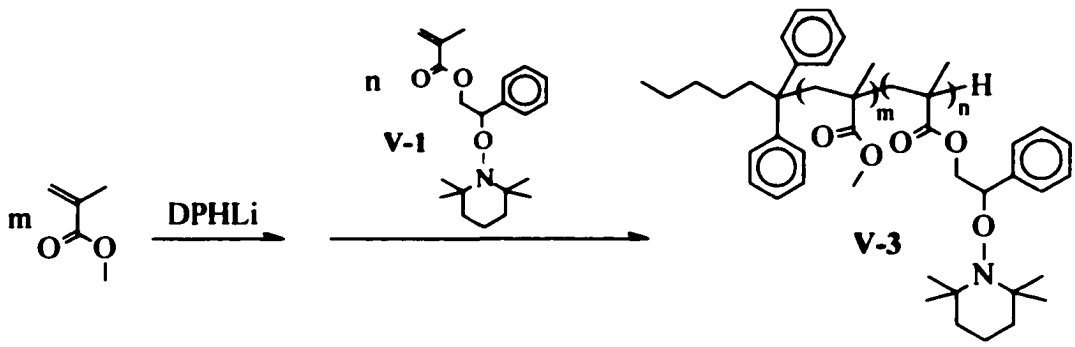

Table 5-2. Synthesis of Macroinitiator V-3 by Anionic Sequential Polymerization of MMA and V-1

	$[MMA]_0$	$[V\text{-}1]_0$	conv (%)		$DP_{n,\,MMA}$		$DP_{n,V\text{-}1}$		M_n	
entry	$[DPHLi]_0$	$[DPHLi]_0$	MMA	V-1	calcd	NMR	calcd	NMR	(NMR)	PDI^a
V-3a	240	12	100	100	240	210	12	11	25000	1.03
V-3b	120	24	100	~100	120	130	24	26	19300	1.08

[a] By GPC relative to linear polystyrene standards.

The DP_n values of blocks of MMA and V-1 were determined by ^1H NMR (600 MHz) through comparing the area of the signal due to chain-end methyl proton (from DPHLi, centered at 0.79 ppm) with that of the signals from ester methyl proton of MMA

unit (centered at 3.60 ppm) and that of the signals from α and β protons of the phenyl ring in **V-1** unit (centered at 3.96, 4.50, and 4.82 ppm). The close agreement between the experimental DP_n values and the calculated DP_n values for blocks of MMA and **V-1**, together with the low polydispersities of **V-3** (*PDI* = 1.03-1.08) ascertained by GPC, indicates that **V-3** has well-defined block structures with controlled number-average alkoxyamine functionality.

Scheme 5-5

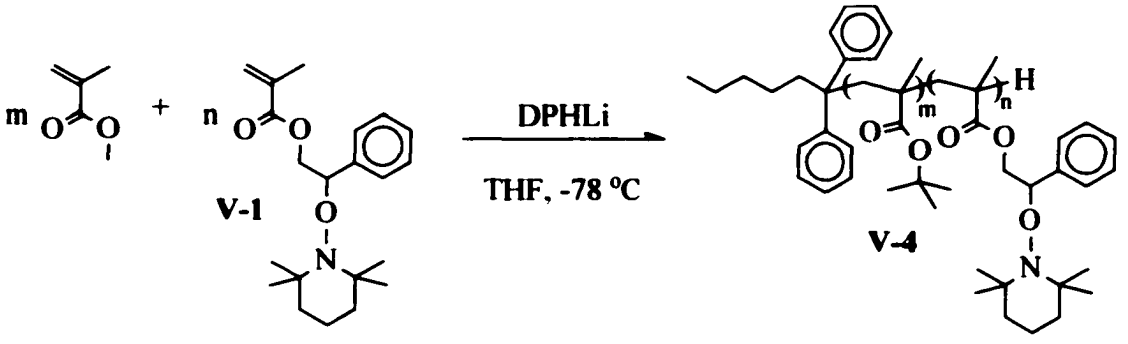

Anionic statistical copolymerization of *t*-BMA with **V-1** was carried out in THF at -78 °C for 3 h using DPHLi as initiator in the presence of lithium chloride under nitrogen atmosphere (**Scheme 5-5**). The feed ratio of **V-1** to *t*-BMA was kept quite low (1/20-1/80) to obtain copolymers with low density of alkoxyamine functionality. As a result, well-controlled poly(*t*-BMA-*stat*-**V-1**), that is, **V-4**, was yielded (**Table 5-3**). The composition of **V-4** was determined by ^{1}H NMR analysis from the area of signals from *tert*-butyl protons of *t*-BMA unit (1.24-1.63 ppm) and the area of signals due to the α and β protons of the phenyl ring **V-1** unit (centered at 4.01, 4.41, and 4.83 ppm) [*27*]. The monomer conversion was calculated from composition and weight of copolymer

recovered. Complete conversion of V-1 and high conversion of *t*-BMA (80%-97%) were obtained. Twenty minutes after the copolymerization for synthesizing V-4c was induced, a small amount of copolymerization solution was withdrawn for analysis. The monomer conversion of 87% for V-1 and 59% for *t*-BMA further illustrates that although V-1 was consumed faster than *t*-BMA, their polymerization rates were still comparable. Therefore the alkoxyamine functionalities of copolymer yielded were distributed along the copolymer chain rather than confined to the initial chain-end.

Table 5-3. Synthesis of Macroinitiator V-4 by Anionic Statistical Copolymerization of *t*-BMA and V-1

		conv (%)		$DP_{n,\text{V-1}}$		$DP_{n,t\text{-BMA}}$		M_n (10^3)		
entry	$[B]_0/[\text{V-1}]_0/[I]_0$[a]	*t*-BMA	V-1	calcd	exptl[b]	calcd	exptl[c]	calcd[d]	exptl[e]	*PDI*[e]
V-4a	100/5/1	97	100	5.0	5.0	97	94.2	15.8	15.3	1.04
V-4b	200/5/1	81	100	5.0	5.1	162	172	25.0	24.2	1.03
V-4c	200/10/1	92	100	10.0	10.9	184	191	29.6	32.0	1.07
V-4d	400/5/1	80	100	5.0	6.6	320	304	47.4	45.7	1.03
V-4e	400/10/1	87	100	10.0	11.7	348	385	53.1	59.0	1.06

[a] $[t\text{-BMA}]_0/[\text{V-1}]_0/[\text{DPHLi}]_0$. [b] $DP_{n,\text{V-1}}$ (exptl) = M_n(exptl) × $w_{\text{V-1}}$ / 345; $w_{\text{V-1}}$: weight-fraction of V-1 units in V-4, determined by ^{1}H NMR. [c] $DP_{n,t\text{-BMA}}$ (exptl) = M_n(exptl) × $w_{t\text{-BMA}}$ / 345; $w_{t\text{-BMA}}$: weight-fraction of *t*-BMA units in V-4, determined by ^{1}H NMR.

[d] M_n (calcd) = 238 + (345 × $[\text{V-1}]_0/[\text{DPHLi}]_0$) + (142 × $[t\text{-BMA}]_0/[\text{DPHLi}]_0$).

[e] Determined by GPC relative to linear polystyrene standards.

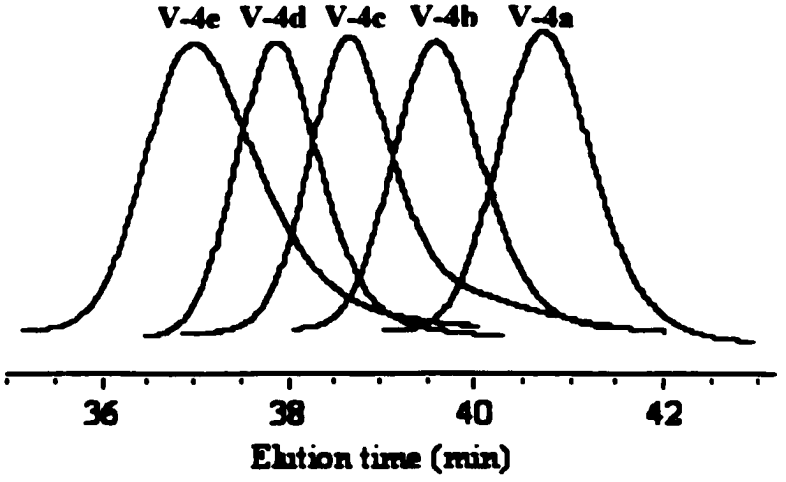

Figure 5-3. GPC curves of polyfunctional SFRP macroinitiators **V-4**

The number-average molecular weight (M_n) values of **V-4** were determined by GPC, and are close to the M_n values calculated from monomer to initiator ratio and monomer conversions, indicating well-controlled molecular weights of **V-4**. Because the ^{1}H NMR resonances of chain-end methyl proton (from DPHLi) overlapped with other resonances and could not be quantitatively determined, the experimental DP_n values for both monomers were obtained from experimental composition and M_n of **V-4**. The excellent agreement between the experimental and the calculated DP_n values for both monomers further verifies the well-controlled number-average alkoxyamine functionality (F_n; $F_n = DP_{n,V\text{-}1}$) on **V-4**, as well as the average chain length of **V-4**. Moreover, the very low polydispersities (1.03-1.07) of **V-4** from GPC suggest nearly uniform chain length for each sample of **V-4** (**Figure 5-3**). All the above results demonstrate that **V-4** has a well-defined structure.

Polymers **V-2**, **V-3**, and **V-4** all are well-defined polyfunctional alkoxyamine-functionalized macroinitiators. The successful synthesis of them suggests that a wide variety of well-defined polyfunctional SFRP macroinitiators can be prepared by the strategy of anionic polymerization with alkoxyamine-functionalized monomer.

With high functionality group density of alkoxyamine on poly(**V-1**) block, **V-2** and **V-3** can be used respectively for the syntheses of graft and block-graft copolymers with high graft density via SFRP. With alkoxyamine functionalities sparsely distributed on poly(*t*-BMA)-based polymer chain, **V-4** can be used to prepare grafted copolymers with low graft density via NMRP. With differences in grafted architectures, densely grafted copolymers and sparsely grafted copolymers require different considerations not only in characterization but also in synthetic control. Therefore they are discussed separately.

5-4 Synthesis of Densely Grafted Copolymers Based on Well-Defined Polyfunctional Alkoxyamine-Functionalized Macroinitiators

5-4a Controlled Synthesis of Copolymers with Dense Polystyrene Grafts.

With TEMPO-based alkoxyamine functionality in each repeating unit of poly(**V-1**) segments, macroinitiators **V-2** and **V-3** can initiate graft SFRP polymerization of styrene to yield copolymers with dense polystyrene grafts (**Scheme 5-6**). The poly(MMA) block of **V-3** has no important effects on SFRP process, but the copolymers yielded have block-graft architectures with a poly(MMA) branch connected with densely polystyrene-grafted backbone. To establish the SFRP behavior in the synthesis of densely grafted

copolymersd, investigation was first carried out by using **V-2b** (poly(**V-1**), DP_n = 11, PDI = 1.18) as macroinitiator.

Scheme 5-6

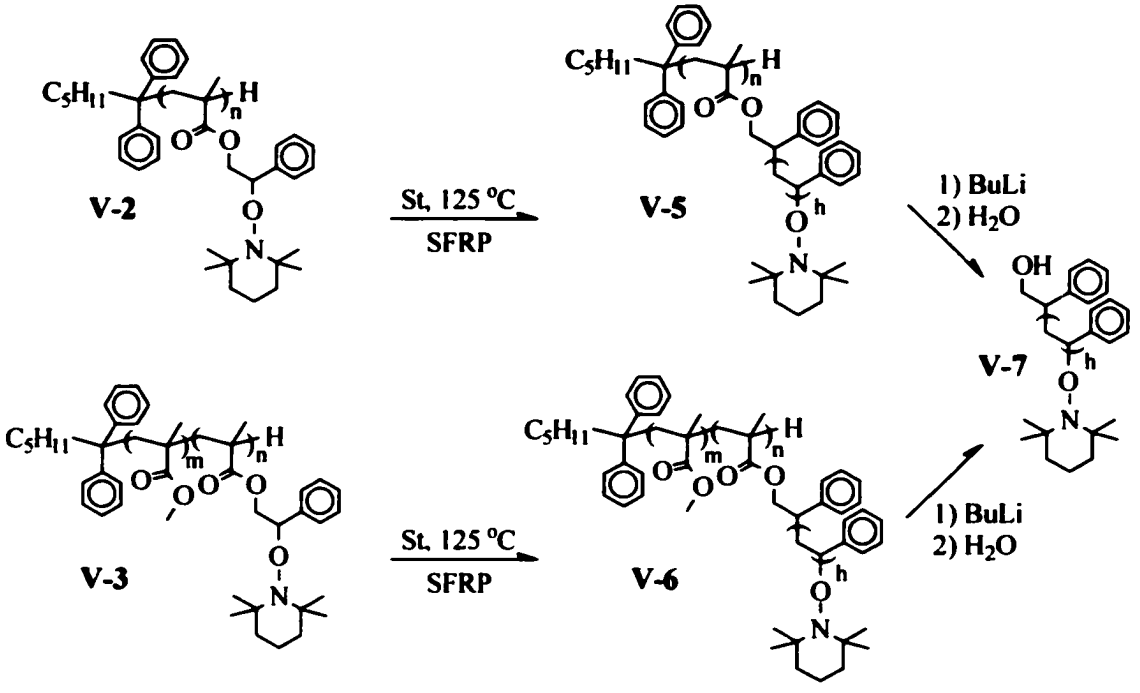

A series of bulk polymerization of styrene were carried out at 125 °C using with an initial feed of 192 equivalents of styrene per alkoxyamine functionality of **V-2b**. The polymerization times were 0.8 h, 2 h, 3.6 h, 6 h, and 12 h, and complete consumption of initial alkoxyamine functionalities on **V-2b** was verified by the disappearance of their characteristic ^{1}H NMR resonance at 4.82 ppm for all trials. The resulting graft copolymer poly(**V-1**-*graft*-styrene), that is **V-5**, has polystyrene grafts densely connected to the backbone by the ester group. No detachment of polystyrene grafts from backbone was detected by GPC analysis after refluxing for 24 h a THF-water (19:1) solution of **V-5**

with hydrochloric acid or sodium hydroxide as catalyst. The grafted architectures of **V-5** finally were ascertained by detaching polystyrene grafts from the backbone with *n*-butyllithium, a strong nucleophilic agent, to yield linear polystyrene **V-7**. Well-controlled graft formation of **V-5** was verified by DP_n and polydispersity analyses of grafts (**Figure 5-4**). Experimental DP_n values of grafts were obtained from GPC measurement of **V-7** and ^{1}H NMR (600 MHz) analysis of **V-5** (**Figure 5-5**). The DP_n from NMR is based on the ratio of the area of signals from terminal benzylic proton [*28*] (*a*; centered at 3.99, 4.42, 4.55 ppm) to that from aromatic protons (6.30-7.31 ppm) of polymerized styrene units of grafts, assuming that all grafts are quantitatively end-capped by alkoxyamine functionalities. The excellent agreement between the two sets of DP_n values establishes alkoxyamine functionality at the graft-ends. Moreover, both sets of DP_n values have a linear relationship with monomer conversion and are close to the calculated DP_n values, indicating well-controlled average graft length and graft number, as well as excellent grafting efficiency. Meanwhile, the low polydispersities of **V-7** (PDI = 1.08-1.20) verified by GPC illustrate narrow graft length distribution. The molecular weights and polydispersities of graft copolymer **V-5** were analyzed by GPC. All the samples of **V-5** showed a single peak with half-height width comparable to linear polystyrene standards, implying a good control over intermolecular biradical coupling. Therefore, M_n values of **V-5** can be estimated from the detected graft length of **V-5** and the number-average alkoxyamine functionality on macroinitiator **V-2b**, and the estimated values are close to the calculated M_n values of **V-5** (**Figure 5-6**). On the other hand, with GPC measurement calibrated with linear polystyrene standards, the experimental M_n values of **V-5** were significantly lower than the calculated M_n values because grafted copolymers have smaller

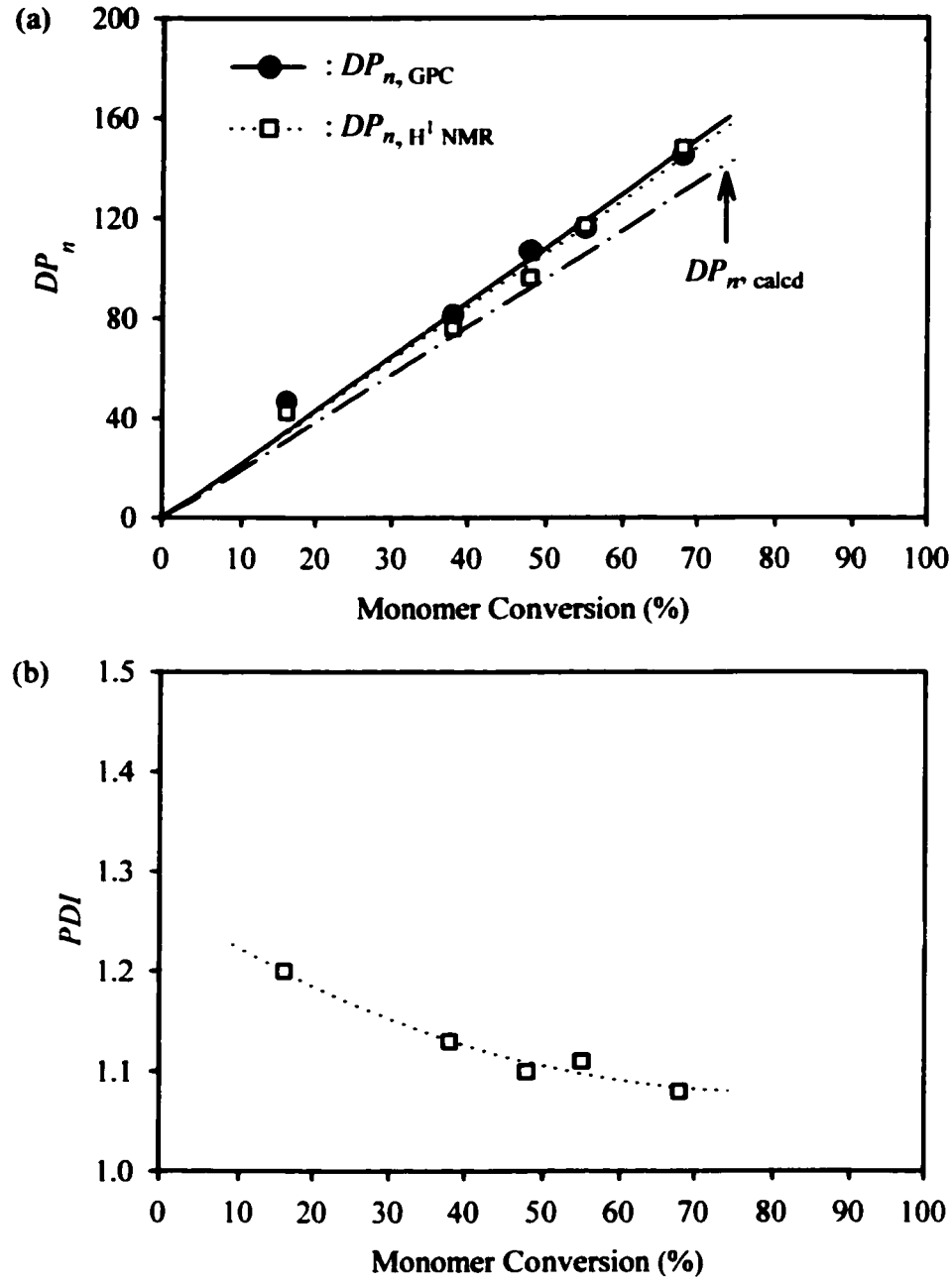

Figure 5-4. Analysis of polystyrene graft of grafted copolymer **V-5**: (a) DP_n of polystyrene grafts versus monomer conversion; (b) *PDI* of polystyrene grafts (detected from **V-7** by GPC) versus monomer conversion.

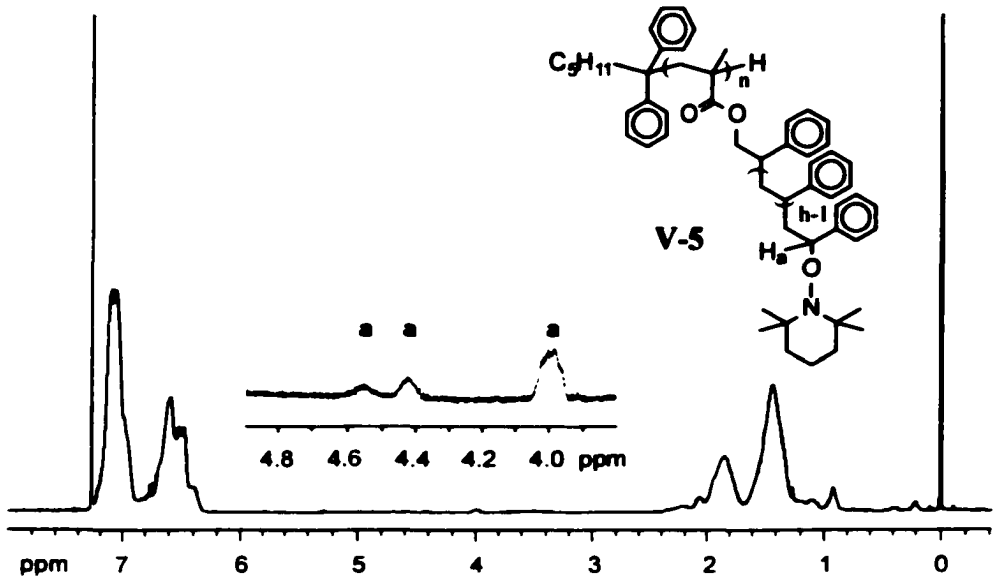

Figure 5-5. ^{1}H NMR spectrum of **V-5** (from **V-2b**).

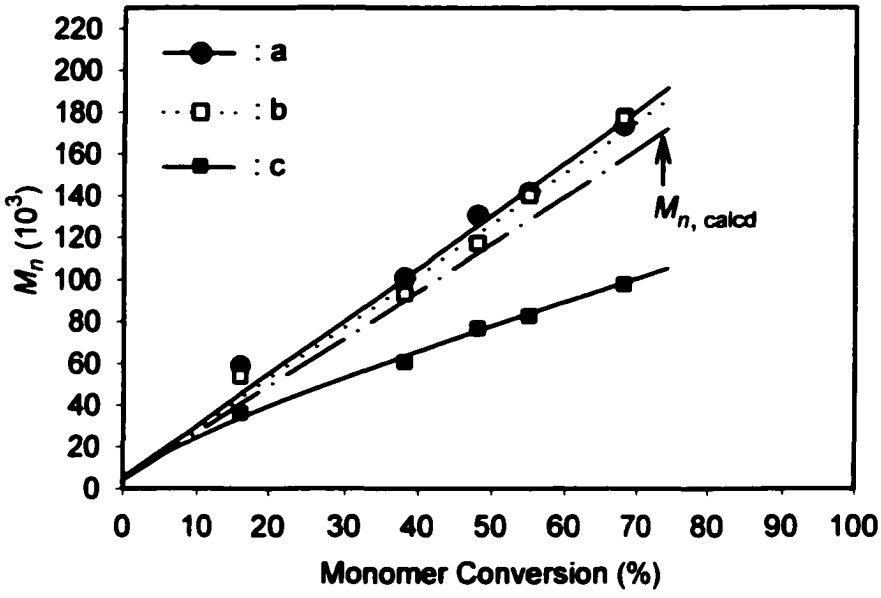

Figure 5-6. M_n of **V-5** versus monomer conversion: a) $M_{n,V\text{-}5}$ estimated from $M_{n,V\text{-}7}$ by GPC, $M_{n,V\text{-}5} = 238 + 11(68 + M_{n,V\text{-}7})$; b) $M_{n,V\text{-}5}$ estimated from $DP_{n,graft}$ by ^{1}H NMR, $M_{n,V\text{-}5} = 238 + 11(345 + 104DP_{n,graft})$; c) $M_{n,V\text{-}5}$ detected by GPC based on calibration with linear polystyrene standards.

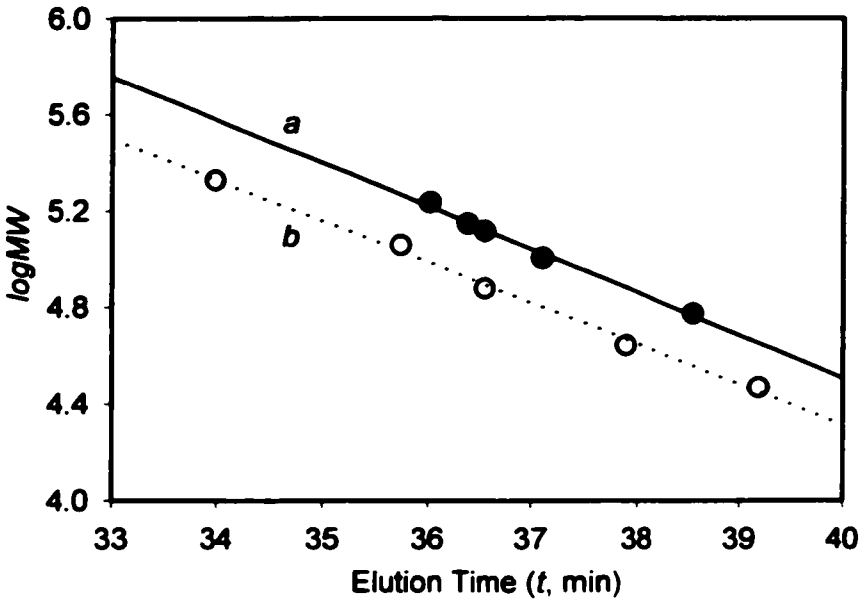

Figure 5-7. Comparison between calibration curve *a* based on graft copolymer **V-5** (*logMW* = 11.6 – 0.178*t*) and the linear plot *b* of *logMW* versus elution time for linear polystyrene standards (*logMW* = 11.1 – 0.169*t*).

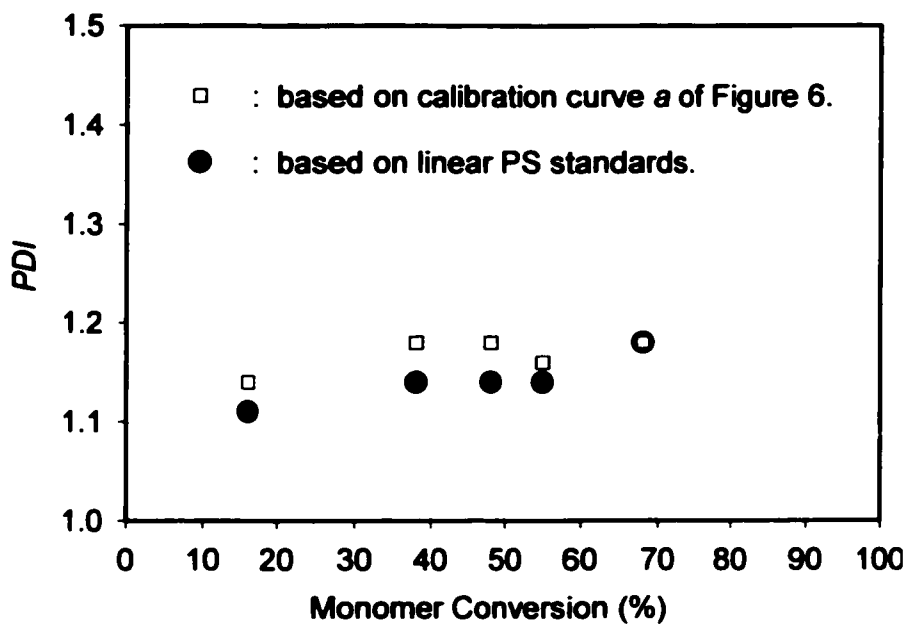

Figure 5-8. Dependence of polydispersity of **V-5** (from **V-2b**) on monomer conversion.

hydrodynamic volume than the corresponding linear polymers with the same molecular weights, and the experimental polydispersity values (1.11-1.18) of **V-5** were also considered as estimations. Therefore, an additional calibration was constructed (**Figure 5-7**), assuming that eluting species of **V-5** on the peak maxima of the GPC curves have the molecular weights estimated based on graft length detected from GPC traces of corresponding **V-7**, that is, $MW_{peak,V\text{-}5} = 238 + [11 \times (68 + M_{n,V\text{-}7})]$. Because the linear relationship between *logMW* and elution time holds well for the molecular weight range of **V-5**, a first-order curve fit was chosen for the calibration. Compared with linear polystyrene, **V-5** shows a slightly higher slope for the *logMW* versus elution time plot, indicating, as expected, a smaller α value of Mark-Houwink equation for densely grafted copolymer **V-5**. The polydispersities of **V-5** from the new calibration remain low (*PDI* = 1.14-1.18, **Figure 5-8**). All the above results demonstrate that **V-5** has well-controlled densely grafted macromolecular architecture.

A collection of well-defined polyfunctional macroinitiators **V-2** and **V-3** were used to initiate the bulk polymerization of styrene at 125 °C (**Table 5-4**). The resulting well-defined graft copolymer **V-5** and block-graft copolymer **V-7** have polystyrene grafts densely grafted from the poly(**V-1**) segments of the macroinitiators. The DP_n values of grafts were determined using GPC analysis of corresponding **V-7** and ^{1}H NMR (600 MHz) analysis of **V-5** and **V-6** based on the resonance intensities of the terminal benzylic proton of grafts (centered at 3.99, 4.42, 4.55 ppm). The good agreement between the two sets of experimental DP_n values and the calculated DP_n values indicates well-controlled graft length and well-defined alkoxyamine functionality at graft-ends. Compared with ^{1}H NMR analysis, the GPC analysis showed slightly higher DP_n values of the grafts, and this

Table 5-4. Synthesis of Well-Defined Densely Grafted Copolymer V-5 and Block-Graft Copolymer V-6 by SFRP

						PS graft				entire copolymer				
	macroinitiator			t	conv	DP_n			PDI	M_n (10^3)			PDI	
entry	no.	F^a	$DP_{n,MMA}$	(h)	(%)	calcd	GPC[b]	NMR	GPC[b]	calcd	GPC[b]	GPC[c]	GPC	GPC[c]
V-5a	**V-2a**	6.4	-	6	49	94	103	99	1.14	65	56	93	1.12	1.16
V-5b	**V-2b**	11	-	6	55	106	117	117	1.11	128	83	-	1.14	1.16
V-5c	**V-2c**	23	-	2	32	61	76	67	1.19	155	97	169	1.19	1.22
V-5d	**V-2d**	35	-	2	29	56	64	58	1.19	215	123	217	1.22	1.24
V-6a	**V-3a**	11	210	6	52	100	109	104	1.11	140	91	157	1.12	1.13
V-6b	**V-3b**	26	130	2	31	60	74	65	1.19	183	117	205	1.16	1.30

[a] The number-average alkoxyamine functionality of macroinitiator. [b] By GPC relative to linear polystyrene standards. [c] Based on calibration curve *a* of **Figure 5-7**.

possibly was caused by minute loss of low molecular weight species of **V-7** during precipitation. The narrow graft length distribution of **V-5** and **V-6** was verified through the low polydispersities of **V-7** determined by GPC. The molecular weights and polydispersities of the entire graft copolymers **V-5** and block-graft copolymer **V-6** were also analyzed by GPC. When calibration using linear polystyrene standards was adopted, experimental M_n values were lower than calculated values for all of the **V-5** and **V-6** samples. For **V-5** and **V-6** from macroinitiators with higher number-average alkoxyamine functionality, a greater extent of difference between the experimental and calculated M_n values was observed. When calibration based on **V-5** (from **V-2b**, curve *a* in **Figure 2-7**) was adopted, the experimental molecular weights obtained were much closer to the

calculated values except for **V-5a**, the graft copolymer with the smallest average graft number. The polydispersities of **V-5** and **V-6** were also calculated using both sets of calibration. With the calibration using linear polystyrene samples, the experimental *PDI* values range from 1.12 to 1.22. With calibration based on **V-5** (from **V-2b**, curve *a* in **Figure 5-7**), the polydispersities of **V-5** and **V-6** were slightly higher (1.16-1.30). Based on the level of agreement between the experimental and calculated M_n values, the second set of polydispersities was considered as more accurate except for **V-5a**.

***5-4b* Polymerization Conditions for Graft Structural Control.** Different from living polymerization systems, controlled free radical polymerization systems may involve various side reactions, although their occurrence can be suppressed by proper mediation. Appropriate polymerization conditions are crucial for structural control of macromolecular architecture through controlled polymerization. Thus, we investigated the influences of polymerization conditions on graft structural control in our system.

Although the molecular weights of polystyrene can be well controlled up to 30 000 in the nitroxide-mediated free radical polymerization system using monofunctional initiator, the polystyrene grafts of densely grafted copolymers need to be controlled to a smaller size to obtain low polydispersities of grafted copolymers formed. A series of bulk polymerization of styrene were carried out using **V-2b** as initiator at 125 °C for 6 h, with the molar ratios of styrene to alkoxyamine functionality of 192, 384, 576, and 768. The monomer conversions were 55%, 56%, 62%, and 56%, corresponding to the calculated DP_n of polystyrene grafts of 106, 215, 357, and 430 respectively. The polydispersities of grafted copolymers increase markedly with the increasing graft size (**Figure 5-9**). In the

latter two trials, although the experimental molecular weights for the main peaks were very close to calculated values [*29*], minor peaks appeared on the high molecular weight side of their GPC curves, giving evidences for the occurrence of intermolecular biradical coupling. The occurrence of intermolecular biradical coupling increases with the number of alkoxyamine functionalities on the macroinitiator used, as well as the graft length reached, therefore grafts with limited size should be targeted for our polymerization system using a macroinitiator with higher number-average alkoxyamine functionality.

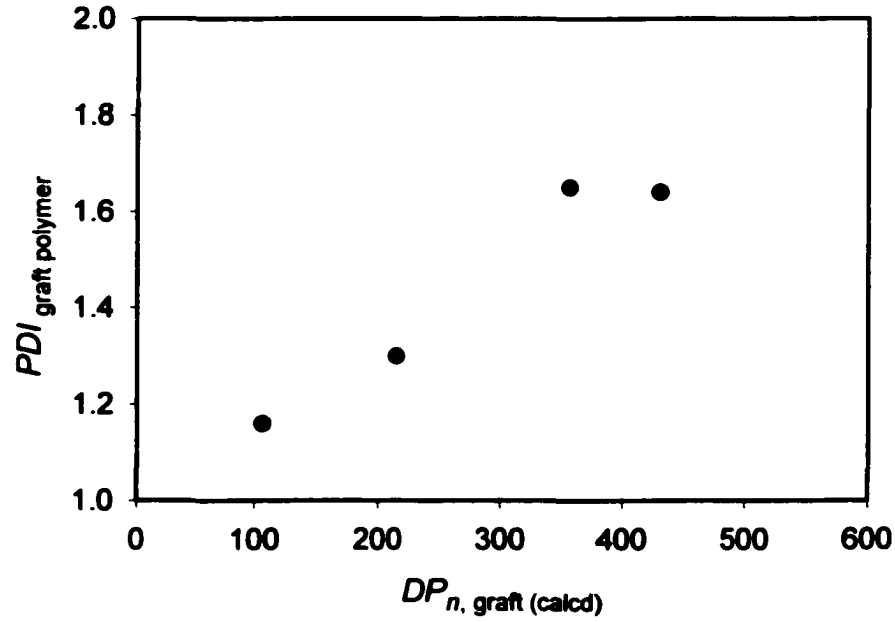

Figure 5-9. Dependence of polydispersity (by GPC using the calibration curve *a* of Figure 2-5) of graft copolymers on calculated DP_n of grafts. The graft copolymers were prepared from macroinitiator **V-2b**.

Similar to polymerization system using monofunctional initiator, nitroxide-mediated free radical polymerization using polyfunctional macroinitiators can reach

moderate monomer conversion within hours. But then the polymerization rate decreases greatly due to the high local viscosity with the formation of grafted copolymer, thus hindering the accessibility of monomer by propagating graft-end. Extended polymerization time leads to little further improvement in monomer conversion but causes increasing occurrence of side reactions. For example, bulk polymerization of styrene using macroinitiator **V-2b** was carried out at 125 °C with 192 equivalents of styrene per alkoxyamine functionality for 45 h. The monomer conversion was 77%, and the polydispersity of graft polymer yielded was 1.22 by GPC based on calibration curve *a* of **Figure 5-7**. But the ^{1}H NMR (600 MHz) analysis showed that the number of alkoxyamine functionalities decreased significantly, and only about 70% of the grafts have the alkoxyamine end-group according to the resonance intensities of the terminal benzylic protons (centered at 3.99, 4.42, 4.55 ppm). At the same time, the formation of considerable amount of linear polystyrene due to thermal autopolymerization was detected by GPC analysis.

All samples of **V-5** and **V-6** reported here as well-defined graft and block-graft copolymers were synthesized with the targeted DP_n of grafts below 150 and moderate monomer conversion within hours of polymerization. However, well-defined graft and block-graft copolymers with longer grafts can be synthesized, in principle, with the addition of external nitroxide to further suppress side reactions. Then, the polymerization rate would be relatively slow and polymerization time required would be prolonged. Moreover, fractionation is required to remove linear polymers formed by thermal autopolymerization.

***5-4c* Synthesis of Copolymers with Dense Polystyrene-*b*-Poly(DMAEMA) Grafts.** Because of their alkoxyamine graft-ends, **V-5** and **V-6** can still serve, in turn, as second generation of macroinitiators for SFRP. With accurate structural control suggested by their low *PDI* values (1.12-1.16), **V-5a**, **V-5b** and **V-6a** were selected to initiate a series of bulk polymerization of 2-(dimethylamino)ethyl methacrylate (DMAEMA) at 125 °C (**Scheme 5-7**). As a result, graft copolymer and block-graft copolymers with dense diblock polystyrene-*b*-poly(DMAEMA) grafts, that is, **V-8** and **V-9**, were produced (**Table 5-5**).

Scheme 5-7

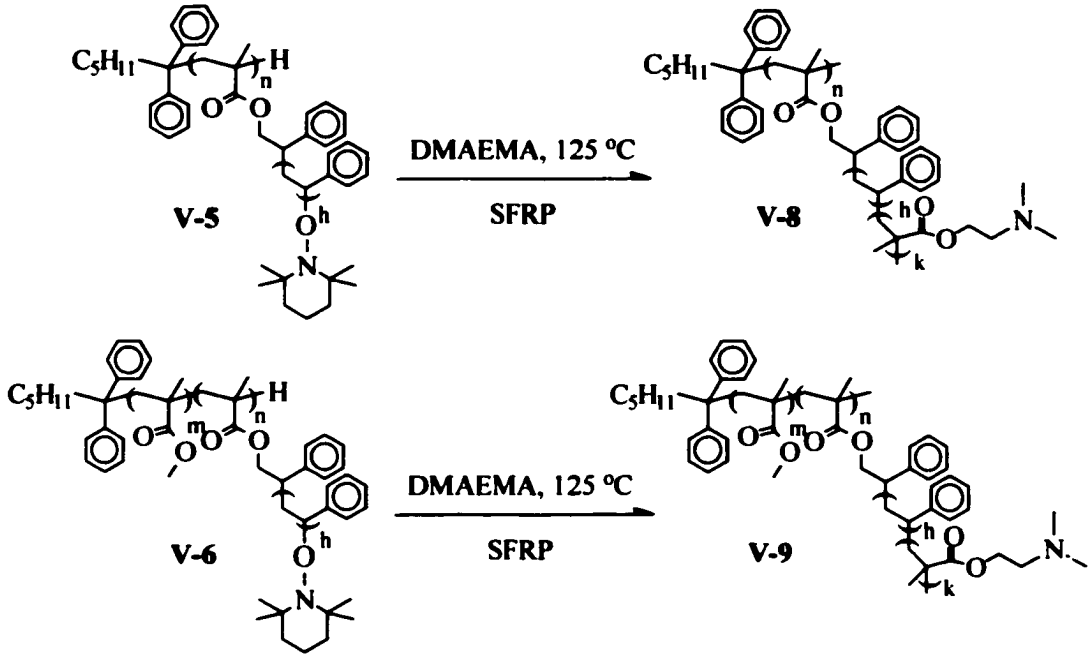

^{1}H NMR analysis verified the existence of DMAEMA monomer units in **V-8** and **V-9**. A typical ^{1}H NMR spectrum of **V-8** was shown in **Figure 5-10**. Different with **V-8**, **V-9** has a poly(MMA) chain connecting its grafted backbone segment, and therefore **V-9**

Table 5-5. Synthesis of Copolymers V-8 and V-9 with Dense Diblock Polystyrene-*b*-poly(DMAEMA) Grafts

	macroinitiator[a]		$[D]_0$[b]	time	conv	diblock graft		$M_n(10^3)$			*PDI*	
entry	1st	2nd	$[A]_0$	(h)	(%)	$DP_{n,St}$	$DP_{n,DMAEMA}$	calcd	GPC[d]	GPC[c]	GPC[d]	GPC[c]
V-8a	**V-2a**	**V-5a**	479	2	11	109	51	126	84	135	1.18	1.21
V-8b	**V-2a**	**V-5a**	615	2	16	109	95	170	107	169	1.17	1.22
V-8c	**V-2b**	**V-5b**	696	2	5.6	117	39	201	101	163	1.10	1.11
V-9a	**V-3a**	**V-6a**	778	2	11	103	81	261	161	267	1.13	1.15
V-9b	**V-3a**	**V-6a**	1094	2	9.2	103	100	291	173	289	1.13	1.15

[a] 1st: 1st generation of macroinitiator; 2nd: 2nd generation of macroinitiator. [b] The molar feed ratio of DMAEMA monomer to alkoxyamine functionality of 1st generation of macroinitiator. [c] By GPC calibrated with linear polystyrene standards.

[d] Based on calibration curve *a* of **Figure 5-7**.

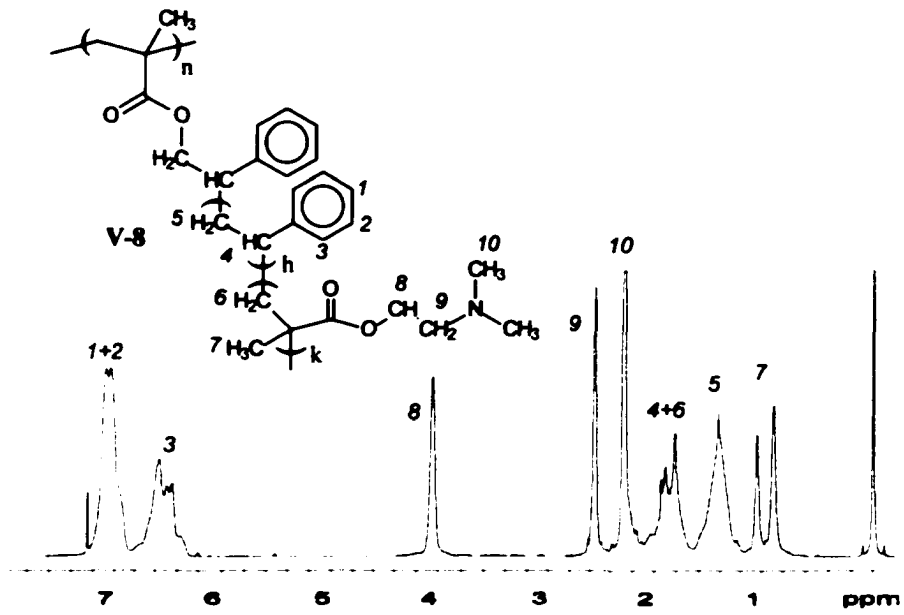

Figure 5-10. ^{1}H NMR spectrum of **V-8**

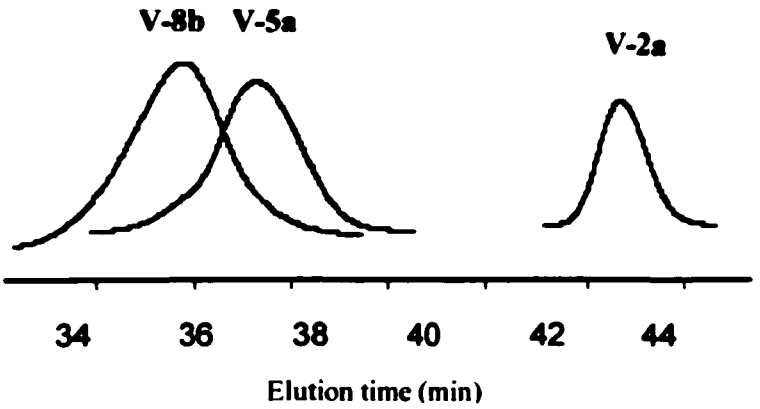

Figure 5-11. GPC curves of macroinitiator **V-2a**, graft copolymer **V-4a** (from **V-2a**), and graft copolymer **V-8b** (from **V-4a**) with diblock polystyrene-*b*-poly(DMAEMA)

also has resonances of protons of MMA monomer units. Because it has been reported that bulk polymerization of DMAEMA initiated by linear polystyrene-TEMPO adduct yielded narrow-disperse copolymers with mono-modal molecular weight distribution [*30*], the DP_n values of DMAEMA on the diblock grafts of **V-8** and **V-9** were determined by ^{1}H NMR with the assumption of complete initiation from the alkoxyamine initiator sites on macroinitaiators. GPC analysis showed the formation of new grafted copolymer **V-8** and **V-9** from macroinitiators (**Figure 5-11**). No matter whether calibration relative to linear polystyrenes or calibration based on **V-5** (from **V-2b**, curve *a* in **Figure 5-7**) was used, the *PDI* values (1.13-1.22) of **V-8** and **V-9** obtained by GPC were relatively low. Low polydispersities, coupled with mono-modal GPC curves, suggests that irreversible biradical coupling reaction was negligible. Therefore, the M_n values of **V-8** and **V-9** can be estimated based on graft size of diblock graft and number-average alkoxyamine

functionalities on macroinitiators. These calculated M_n values have good agreement with the experimental M_n values obtained by GPC using calibration based on **V-5**.

However, SFRP of DMAEMA could not be considered as living polymerization. Only low monomer conversion (<20%) of DMAEMA was obtained in all trials, suggesting that irreversible chain termination took place for grafts after limited amounts of DMAEMA monomer were propagated. The time dependence of monomer conversion was investigated by a series of experiments carried out under the same polymerization conditions as **V-8c** synthesis but with different polymerization times (4min, 10min, 20min, 30 min, 1h), and it was found that no significant increase of monomer conversion could be detected after the first 10 minutes of polymerization, suggesting relatively fast occurrence of irreversible termination. ^{1}H NMR analysis further demonstrated that β-hydrogen transfer reaction was a major termination reaction [*31*], according to the resonances of methylene unsaturation at 5.52 and 6.21 ppm for **V-8** and **V-9**. Because the termination reactions could not take place simultaneously, the *PDI* values of poly(DMAEMA) block in the diblock grafts are expected to be broad, although experimental determination of them cannot be made.

5-4d **Synthesis of Copolymers with Diblock Grafts Containing Polymeric Ionic Components.** Polymers with pendent quaternary ammonium salts are applicable to a wide scope of products such as water-soluble polymers, polyelectrolytes, polyampholytes, and hydrogels [*32-34*]. Therefore, the synthesis of grafted copolymers having diblock grafts consisted of blocks with pendent quaternary ammonium salts is of both academic and practical interests. Amine functionality in DMAEMA monomer unit

can be readily quaternized to give cationic quaternary ammonium species [*35*]. Therefore, the poly(DMAEMA) blocks of diblock polystyrene-*b*-poly(DMAEMA) graft of **V-8** and **V-9** can be converted into polymeric cationic blocks, with the formation of new grafted copolymers **V-10** and **V-11** (**Scheme 5-8**).

Scheme 5-8

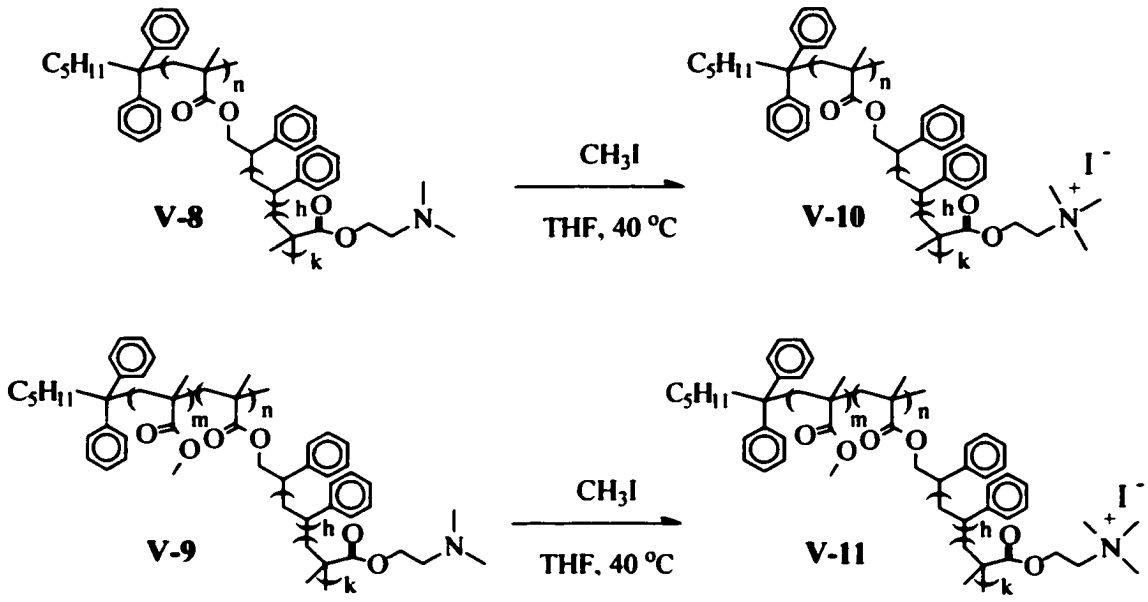

The quaternization reaction of amine functionalities of **V-8** and **V-9** was carried out by employing excessive amounts of methyl iodomethane in THF at 40 °C for 24 h, yielding **V-10** and **V-11** as yellow precipitates. However, **V-10** and **V-11** can be dissolved by dimethyl sulfoxide (DMSO) and *N*,*N*-dimethylformamide (DMF). ^{1}H NMR analysis in DMSO-d_6 verified that the quaternization reaction was complete, and all amine functionalities in the poly(DMAEMA) blocks were converted into cationic quaternary ammonium species. ^{1}H NMR spectrum of **V-10** is shown in **Figure 5-12**. The

^{1}H NMR spectrum of **V-11** is similar to that of **V-10** except that resonances of MMA monomer unit are also present on spectrum of **V-11** due to its poly(MMA) branch connected to the grafted segment of backbone.

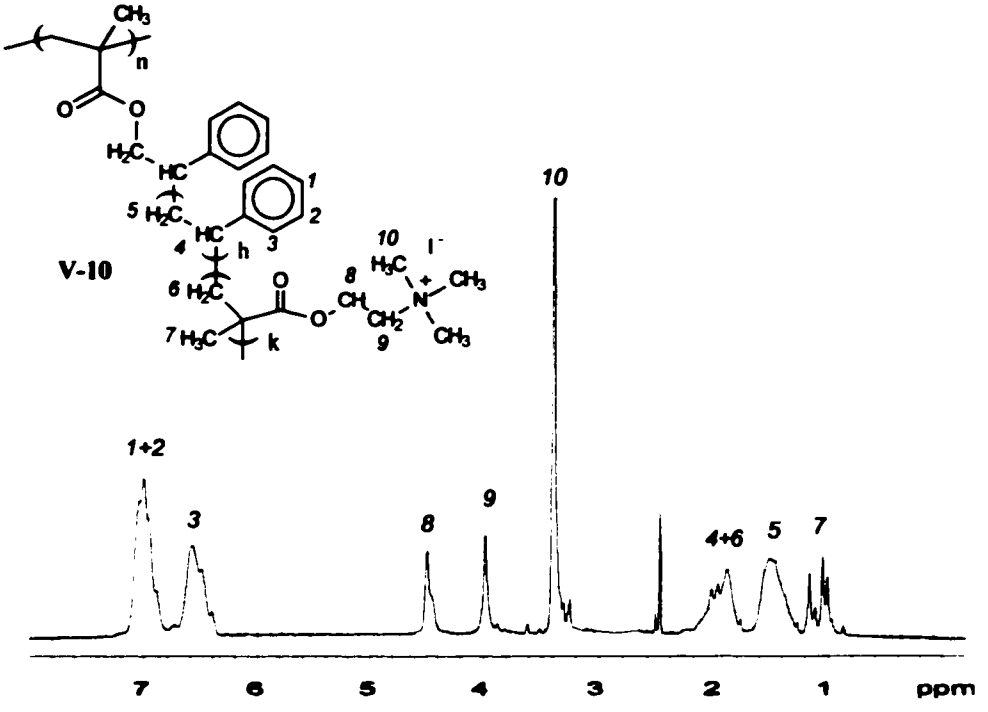

Figure 5-12. ^{1}H NMR spectrum of **V-10**

5-5 Synthesis of Sparsely Grafted Copolymers Based on Well-Defined Polyfunctional Alkoxyamine-Based Macroinitiators

***5-5a* Controlled Synthesis of Sparsely Grafted Copolymers.** According to the sum of DP_n for **V-1** and *t*-BMA units (ΣDP_n = 99.2-397) in copolymer **V-4**, the density of alkoxyamine functionality (F_n = 5.0-11.7; $F_n/\Sigma DP_n$ = 5.05-2.12%) in **V-4** is relatively low. Therefore with well-controlled number-average alkoxyamine functionality, well

controlled chain-length, and low polydispersities, **V-4** can be used for controlled synthesis of grafted copolymers with low graft density by SFRP (**Scheme 5-9**).

Scheme 5-9

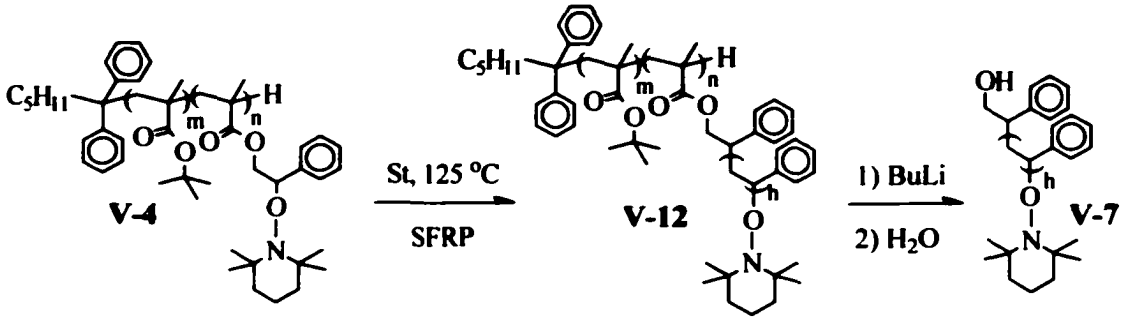

A series of bulky polymerization of styrene with **V-4** as macroinitiator were carried out at 125 °C (**Table 5-6**). Especially under low monomer conversion, the current system had a slower polymerization rate than the polymerization system using small molecule alkoxyamine initiators, because the presence of poly(*t*-BMA)-based backbone leads to a relative low local monomer concentration around the alkoxyamine functionalities. The formation of grafted copolymer poly(*t*-BMA-*stat*-**V-1**)-*graft*-polystyrene, that is **V-12**, from **V-4** was detected by GPC measurement (**Figure 5-13**). Well-controlled molecular weights of **V-12** based on close agreement between experimental M_n values by GPC and the calculated values, together with the low polydispersities of **V-12** (1.11-1.33) obtained from their symmetrical GPC curves, indicates that side reactions, especially biradical intermolecular coupling, were under good control in the polymerization conditions used. Grafted copolymer **V-12** was also characterized by ^{1}H NMR. Complete consumption of initial alkoxyamine functionality on

V-12 was verified by the disappearance of its characteristic resonance at 4.83 ppm; the formation of new alkoxyamine functionality on polystyrene graft-ends of **V-12** was detected through the resonance of terminal benzylic proton at 3.98, 4.40, and 4.53 ppm (*a*; **Figure 5-14**) [*28*]. The existence of alkoxyamine functionality on graft-ends suggests that **V-12** can still serve as polyfunctional SFRP macroinitiator for further graft growth, and new grafted copolymers having graft with block structures can be prepared from **V-12**.

Table 5-6. Synthesis of Well-Defined Sparsely Grafted Copolymer V-12 by SFRP

							PS graft			entire copolymer		
	macroinitiator			$[St]_0$[c]	t	conv	DP_n			$M_n(10^3)$		
entry	no.	F_n[a]	ΣDP_n[b]	$[A]_0$	(h)	(%)	calcd	exptl[d]	PDI[d]	calcd	exptl[d]	PDI[d]
V-12a	**V-4a**	5.0	99.2	192	2	13	26	30	1.38	28.6	28.9	1.11
V-12b	**V-4a**	5.0	99.2	192	6	47	90	94	1.19	62.2	60.8	1.15
V-12c	**V-4a**	5.0	99.2	192	24	76	146	145	1.20	91.2	88.4	1.16
V-12d	**V-4a**	5.0	99.2	384	6	50	192	177	1.18	115	117	1.17
V-12e	**V-4b**	5.1	177	192	6	57	109	124	1.21	121	114	1.17
V-12f	**V-4c**	10.9	202	192	6	44	84	98	1.18	68.5	67.5	1.14
V-12g	**V-4d**	6.6	311	192	6	47	90	116	1.20	161	160	1.33
V-12h	**V-4e**	11.7	397	192	6	48	92	98	1.17	136	114	1.22

[a] Number-average alkoxyamine functionality of macroinitiator. [b] $\Sigma DP_n = DP_{n,V\text{-}I} + DP_{n,t\text{-}BMA}$. [c] The molar feed ratio of styrene to alkoxyamine functionality of macroinitiator. [d] By GPC calibrated with linear polystyrenes.

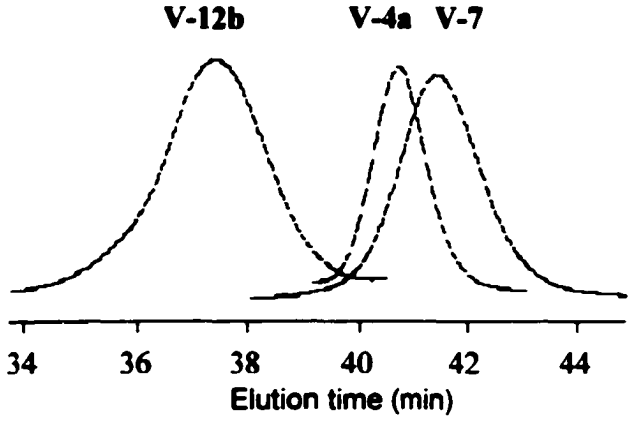

Figure 5-13. GPC curves of macroinitiator **V-4a** (M_n = 15 300, PDI = 1.04), grafted copolymer **V-12b** (from **V-4a**; M_n = 60 800, PDI = 1.15), and detached polystyrene graft **V-7** (from 3-b; M_n = 10 100, PDI = 1.19). The polydispersities of **V-4a** and **V-7** reflect the length distribution of backbone and graft of **V-12b** respectively.

GPC calibrated with linear polystyrene standards.

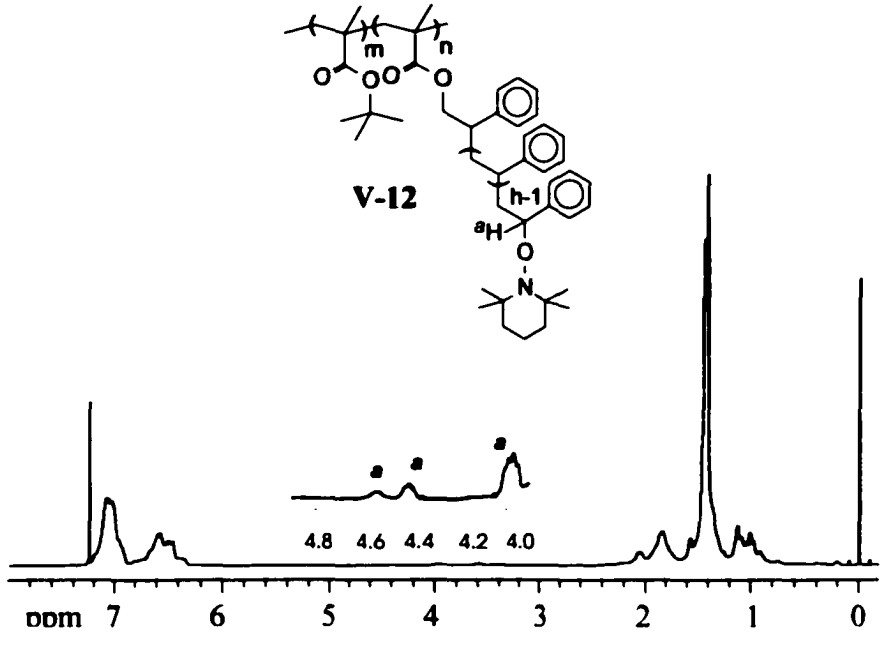

Figure 5-14. ^{1}H NMR spectrum of **V-12**

To understand the structural details of grafts, grafted copolymer **V-12** was treated with an excess of a strong nucleophilic agent *n*-butyllithium (five equivalents relative to the sum of ester groups in **V-12**) to break the linkage of ester group between its backbone and graft. Representing the polystyrene graft of **V-12**, the linear polystyrene **V-7** thus produced was analyzed by GPC to give experimental polydispersities and molecular weights. The low polydispersities of **V-7** (1.17-1.38) reflect the narrow length distribution of grafts. The DP_n values of polystyrene grafts obtained from M_n of **V-7** ($DP_{n,expt(PS\ graft)} = (M_{n,V\text{-}7} - 277) / 104$) close to the DP_n values calculated based on monomer conversion, indicating well-controlled average graft length, graft number, and excellent grafting efficiency. The average graft length of **V-12** can be manipulated by monomer conversion, as well as the molar feed ratio of monomer to initial alkoxyamine functionality.

5-5b **Controlled Synthesis of Amphiphilic Copolymers.** As well-defined grafted copolymer with low graft density, **V-12** has two kinds of ester groups. One is the tertiary alkyl ester group on the poly(*t*-BMA)-based backbone; the other is the primary alkyl ester group connecting polystyrene grafts and the backbone. In principle, the tertiary alkyl ester group can undergo a hydrolysis reaction much more readily than the primary alkyl ester group. Thus, amphiphilic grafted polymers with hydrophilic poly(mathacrylic acid)-based backbone and hydrophobic polystyrene grafts can be expected to be synthesized through the conversion of the former into a carboxylic acid functionality with the latter intact by choosing appropriate hydrolysis conditions. Acid hydrolysis of **V-12** was investigated at first. Although selective acid hydrolysis towards

tertiary alkyl ester group can undergo readily for linear polymers [*36*], it is not feasible for grafted copolymer **V-12**. When the THF-water (50/1) solution of **V-12** was refluxed at 67 °C overnight with trifluoro-acetic acid as catalyst, no occurrence of hydrolysis was detected by ^{1}H NMR analysis possibly because the hydrophobic polystyrene grafted prevented water and catalyst from approaching backbone. On the other hand, when the DMSO-water (25/1) solution of **V-12** was heated at 140 °C with *p*-toluenesulfonic acid as catalyst overnight, hydrolysis occurred with an unselective manner and the formation of linear polystyrene was detected by GPC analysis.

Scheme 5-10

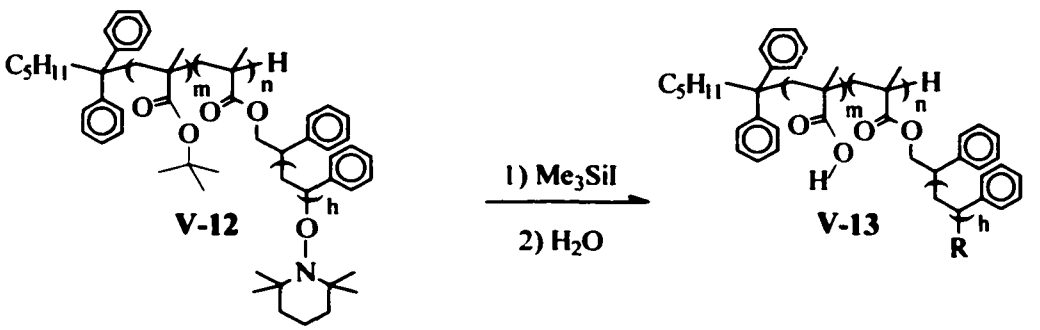

Iodotrimethylsilane (Me_3SiI) was finally employed to selectively convert the *tert*-butyl ester group into carboxylic acid functionalities with the primary backbone-graft ester linkage intact (**Scheme 5-10**) [*37, 38*]. Excess amounts of Me_3SiI (ten equivalents relative to the sum of both kinds of ester group) reacted with all **V-12** samples in toluene at room temperature for 24 h, and then the reaction mixtures were treated with water, resulting in corresponding amphiphilic grafted copolymer poly(methacrylic acid-*stat*-**V-1**)-*graft*-polystyrene, that is, **V-13**. The primary alkyl ester group of **V-12** was not

affected under the reaction conditions used, according to the lack of formation of linear polystyrene as detected by GPC for all trials.

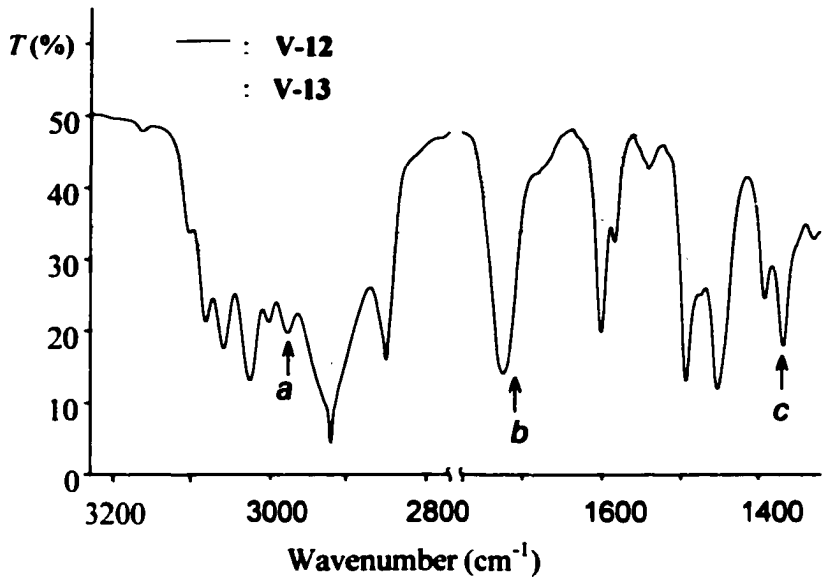

Figure 5-15. Comparison of FT-IR spectra of **V-12** and **V-13**

The formation of carboxylic acid functionalities from *tert*-butyl ester groups was verified by FT-IR. The FT-IR analysis (**Figure 5-15**) shows that compared with **V-12**, **V-13** presents no characteristic C-H stretching absorption at 2875 cm^{-1} (region *a*) and only weak C-H bending absorption at 1340-1410 cm^{-1} (region *c*) for methyl group, indicating the absence of *tert*-butyl group in the conversion of **V-13** from **V-12**; **V-13** also exhibits significantly lower transmittance at 2500-3300 cm^{-1} for O-H stretching and a broad absorption at 1640-1780 cm^{-1} for C=O stretching of carboxylic acid group (region *b*) instead of a narrow absorption at 1725 cm^{-1} for C=O stretching of ester group, giving the evidence of the formation of carboxylic acid group from ester group.

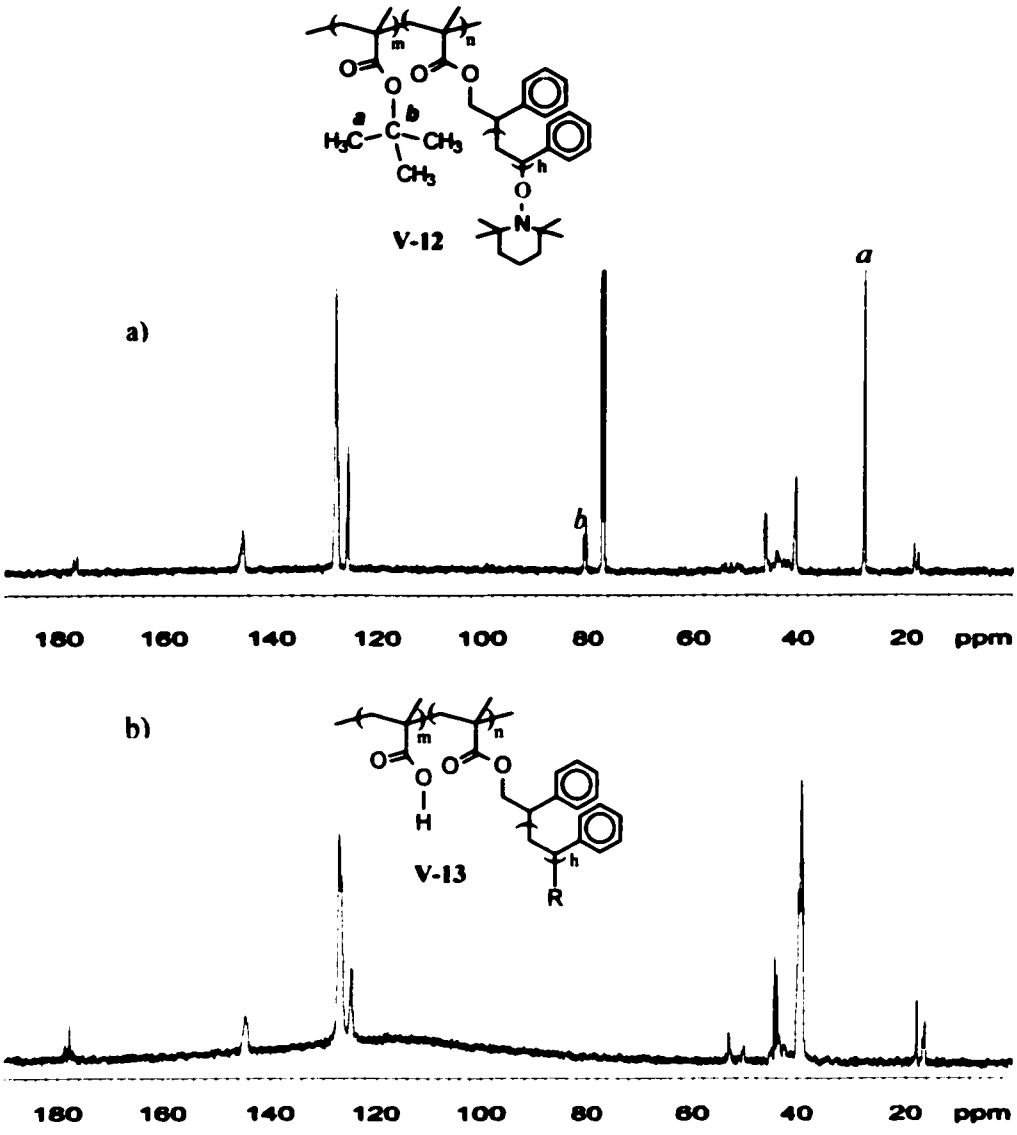

Figure 5-16. Comparison of ^{13}C NMR spectra of a) **V-12** and b) **V-13.**

NMR analysis verified complete conversion of *tert*-butyl ester group. Because $CDCl_3$ cannot dissolve poly(methacrylic acid)-based backbone well, all NMR analysis of **V-13** was carried out at 120 °C in DMSO-d_6, a good solvent for both poly(methacrylic acid)-based backbone and polystyrene grafts at elevated temperature. Compared with the very strong ^1H NMR resonances of **V-12** at 1.18-1.68 ppm for its *tert*-butyl protons on

poly(methacrylic acid)-based backbone and methylene protons on polystyrene grafts, much weak resonances of **V-13** in that region was observed due to the loss of *tert*-butyl group. Unambiguous proof of absence of *tert*-butyl ester group in **V-13** was from ^{13}C NMR analysis (**Figure 5-16**). **V-12** showed characteristic resonances of *tert*-butyl methyl carbons at 27.8 ppm and characteristic resonances of *tert*-butyl quaternary carbon at 80.7 ppm, but no such resonances were present in ^{13}C NMR spectra of **V-13**.

5-5c **Solubility Study of Grafted Copolymers.** With the conversion of *t*-BMA monomer units on backbone into methacrylic acid monomer units, amphiphilic grafted copolymer **V-13** yielded has different properties with its parent grafted copolymer **V-12**. As a basic physical property, solubility of **V-13** samples and their parent **V-12** samples was investigated (**Table 5-7**). Because the solubility parameters of polystyrene and poly(*t*-BMA) are close, although **V-12** samples differ with each other in components and grafting features, they exhibit similar solubility in most solvents used except acetone. Acetone is a solvent for poly(*t*-BMA) blocks but a nonsolvent for polystyrene blocks at room temperature, and therefore **V-12** samples with higher molar fraction of *t*-BMA generally showed better solubility in acetone. On the other hand, compared with ether poly(*t*-BMA) or polystyrene, poly(methacrylic acid) has very different solubility, therefore conversion of poly(*t*-BMA)-based backbone into poly(methacrylic acid)-based backbone dramatically changed the solubility of grafted copolymer. **V-13** cannot be dissolved in diethyl ether and acetone any more. At the same time, because of different mole fractions of methacrylic acid and structural parameters, **V-13** samples showed marked differences in solubility in a series of solvents including toluene, chloroform,

methylene chloride, and DMSO at room temperature. Noteworthily, aprotic solvents, such as THF and DMF, can dissolve all **V-12** and **V-13** samples, and DMSO can also dissolve all these samples above 50 °C. However, even though **V-13** samples have a hydrophilic backbone, none of them still can be dissolved by protic solvents such as ethanol and methanol, presumably because the mole fraction of methacrylic acid in **V-13** is not high enough.

Table 5-7. Comparison of Solubility between **V-12** and **V-13** at Room Temperature

		solubility of **V-12** / solubility of **V-13** [c,d]					
V-12/V-13 [a]	F_1 [b]	Et_2O	toluene	$CHCl_3$	CH_2Cl_2	acetone	DMSO
V-12a/V-13a	0.39	s/i	s/i	s/s	s/s	s/i	i/i
V-12b/V-13b	0.17	s/i	s/s	s/s	s/s	i/i	i/i
V-12c/V-13c	0.12	s/i	s/s	s/s	s/s	i/i	i/i
V-12d/V-13d	0.10	s/i	s/s	s/s	s/s	i/i	i/i
V-12e/V-13e	0.21	s/i	s/s	s/s	s/s	s/i	i/s
V-12f/V-13f	0.15	s/i	s/s	s/s	s/s	i/i	i/i
V-12g/V-13g	0.28	s/i	s/i	s/i	s/i	s/i	i/s
V-12h/V-13h	0.25	s/i	s/i	s/i	s/i	s/i	i/i

[a] **V-12** sample / the corresponding **V-13** sample. [b] Mole fraction of *t*-BMA in **V-12** and methacrylic acid in **V-13**. [c] s: soluble; i: insoluble. [d] All samples of **V-12** and **V-13** are soluble in THF and DMF, but are insoluble in ethanol and methanol.

5-6 Self-Assembled Surface Morphologies of Grafted Copolymers

Based on well-defined polyfunctional SFRP macroinitiators **V-2**, **V-3**, and **V-4**, eight types of grafted copolymers, including **V-5**, **V-6**, **V-8**, **V-9**, **V-10**, **V-11**, **V-12**, and **V-13**, were synthesized. According to principles of self-assembly, these grafted copolymers, with polymeric components of divergent polarities as illustrated by **Figure 5-17**, are expected to possess interesting nano-phase segregated morphologies leading to their potential applications based on their novel morphologies. Due to the lack of instruments required for bulk morphology analysis, we used AFM to study their surface morphologies. The Langmuir-Blodgett (L-B) technique was used to prepare a monomolecular layer of grafted copolymers for AFM characterization.

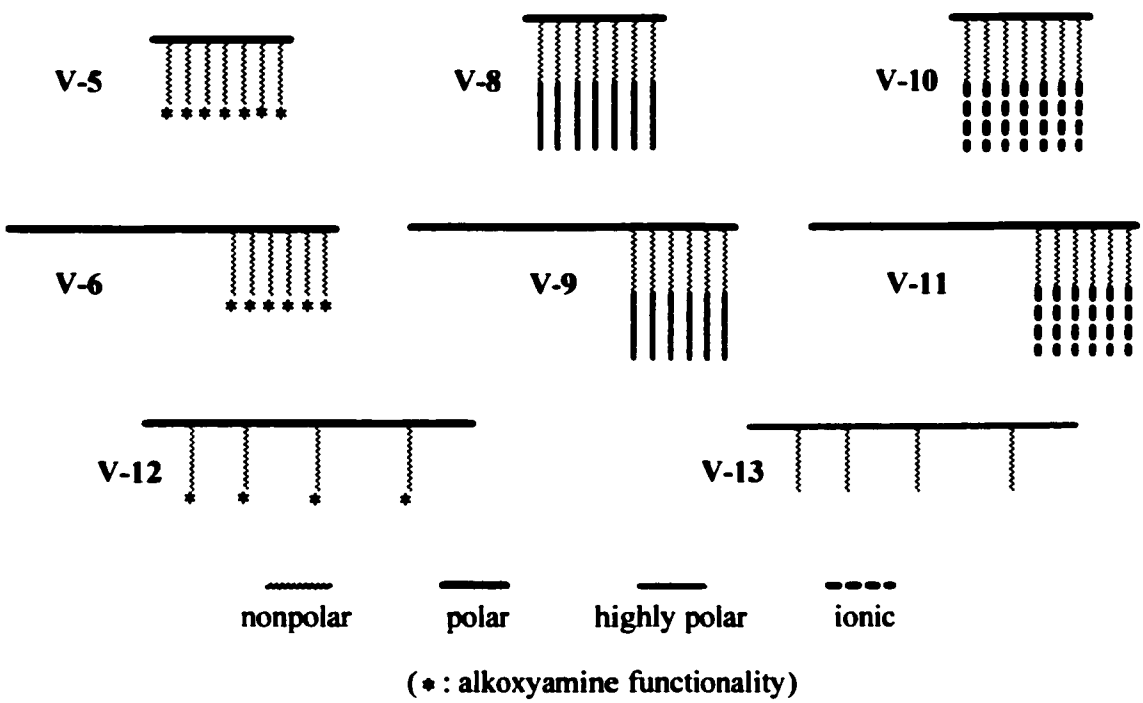

Figure 5-17. Schematic representations of grafted copolymers

Grafted copolymer **V-5** could not form a L-B film because it does not have balanced divergent components, and its highly confined polar polymethacrylate-based backbone is only a very small part of entire polymer. Grafted copolymers **V-10** and **V-11** also could not form L-B film, because both of them contain significant amounts of polymer ionic components with quaternized DMAEMA as repeating unit, and are insoluble in hydrophobic solvents. Grafted copolymers **V-8** and **V-9**, having comparable nonpolar and highly polar components, could form a L-B film. However, because the highly polar poly(DMAEMA) blocks on their amphiphilic polystyrene-*b*-poly(DMAEMA) diblock grafts strongly restrict intermacromolecular aggregation of nonpolar polystyrene components, the surface nanopatterns on their L-B films have dimensions just around the resolution of our AFM measurement, and cannot be clearly recognized. Therefore, the discussion of self-assembled surface morphologies is focused on grafted copolymers **V-6**, **V-12**, and **V-13**.

In all cases, silica wafer was dipped in water and moved up to take on a L-B film of grafted copolymers formed on air-water interface. Therefore, for grafted copolymers **V-6**, **V-12**, and **V-13**, their nonpolar polystyrene aggregations are expected to present on the top of the L-B film and appear as bright regions on AFM images. At the same time, the aggregations formed by their polar, or hydrophilic components are expected to locate on the bottom of the L-B film.

Block-graft copolymers **V-6**, i.e. poly(MMA)-*block*-poly(**V-1**-*graft*-styrene), have a relatively long polar poly(MMA) chain connected with a nonpolar polystyrene densely grafted segment. The self-assembled surface morphologies of **V-6** depend mainly on the weight ratio of polystyrene components to poly(MMA) components, i.e. W_{PS}/W_{PMMA}. As

shown in **Figure 5-18**, with increased W_{PS}/W_{PMMA} ratio from 0.69 to 2.7, to 13.7, the surface pattern of the bright regions changed from micelle, to consecutive micelle, and then to ribbon, suggesting that, with decreased poly(MMA) weight fraction, polystyrene components from more and more macromolecules tend to aggregate together.

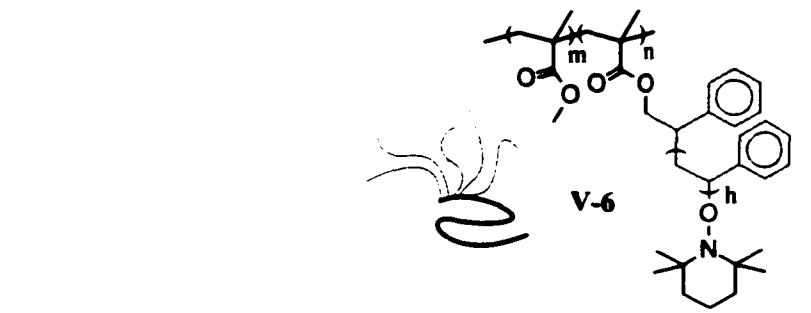

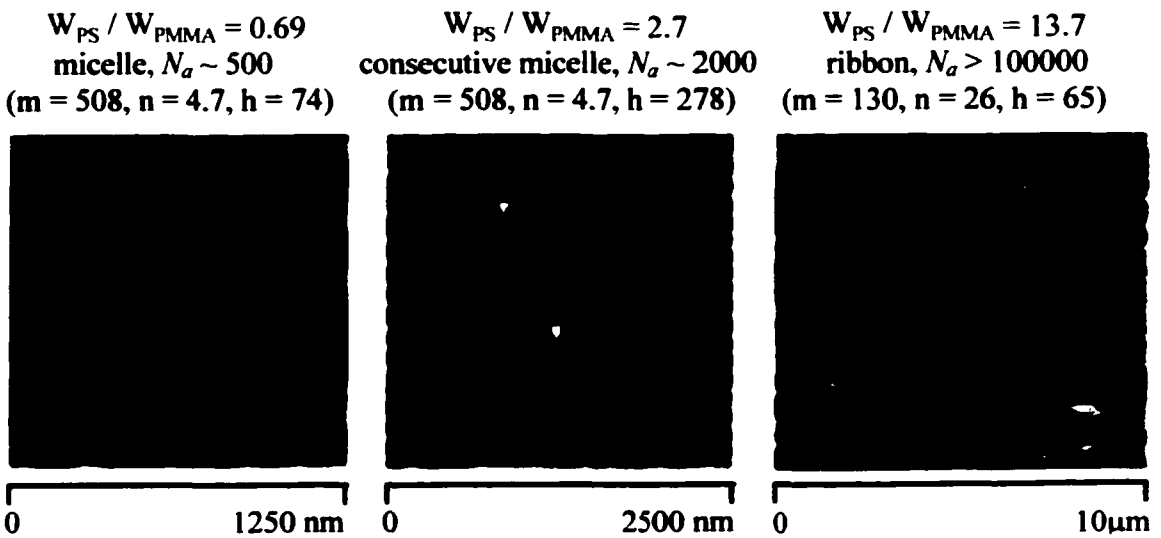

Figure 5-18. AFM images of L-B films of grafted copolymer **V-6**

(N_G: aggregation number, i.e. the number of grafted copolymer macromolecules aggregated with their polystyrene components to present the average size of polystyrene surface domain; estimated from polystyrene domain size)

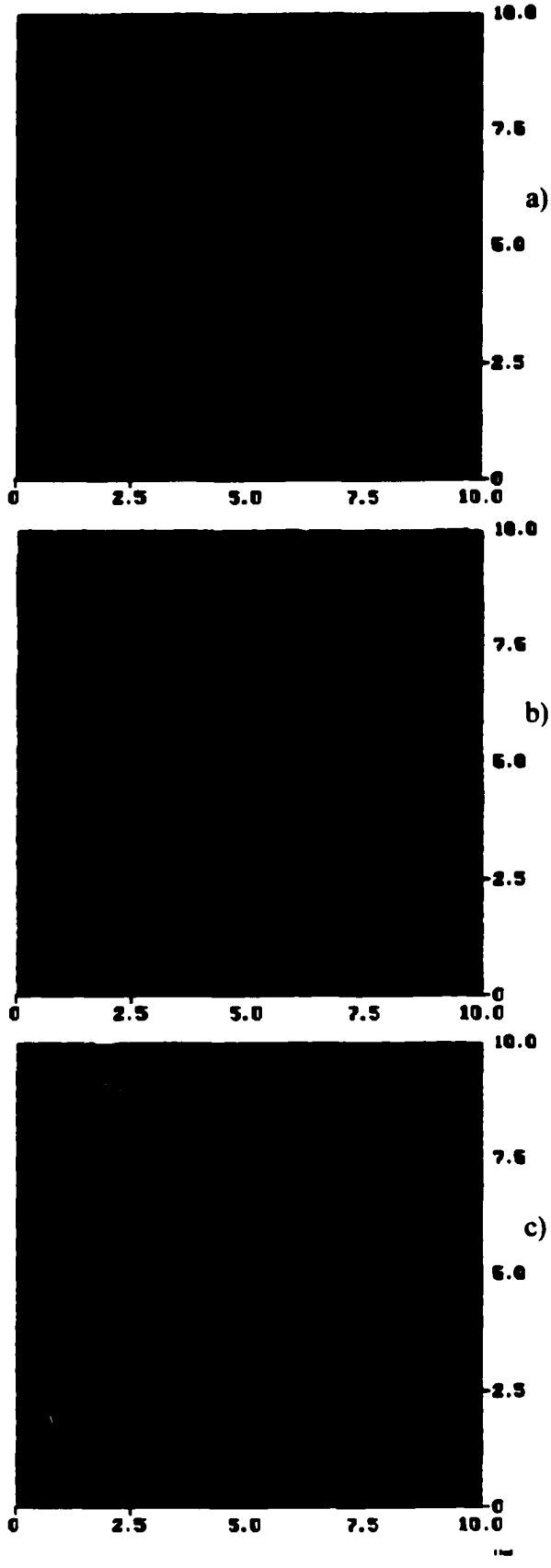

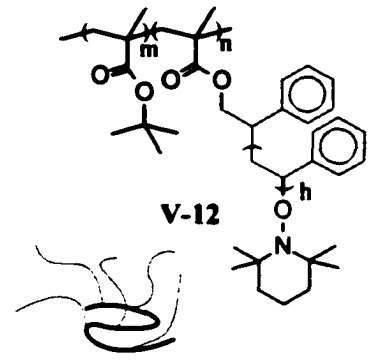

Figure 5-19. AFM images of L-B films of grafted copolymer **V-12**

a. $W_{PS} / W_{PBMA} = 2.1$
m = 172
n = 5.1
h = 98

b. $W_{PS} / W_{PBMA} = 4.1$
m = 191
n = 11.7
h = 116

c. $W_{PS} / W_{PBMA} = 5.6$
m = 94
n = 5
h = 145

(10 μm × 10 μm for all images)

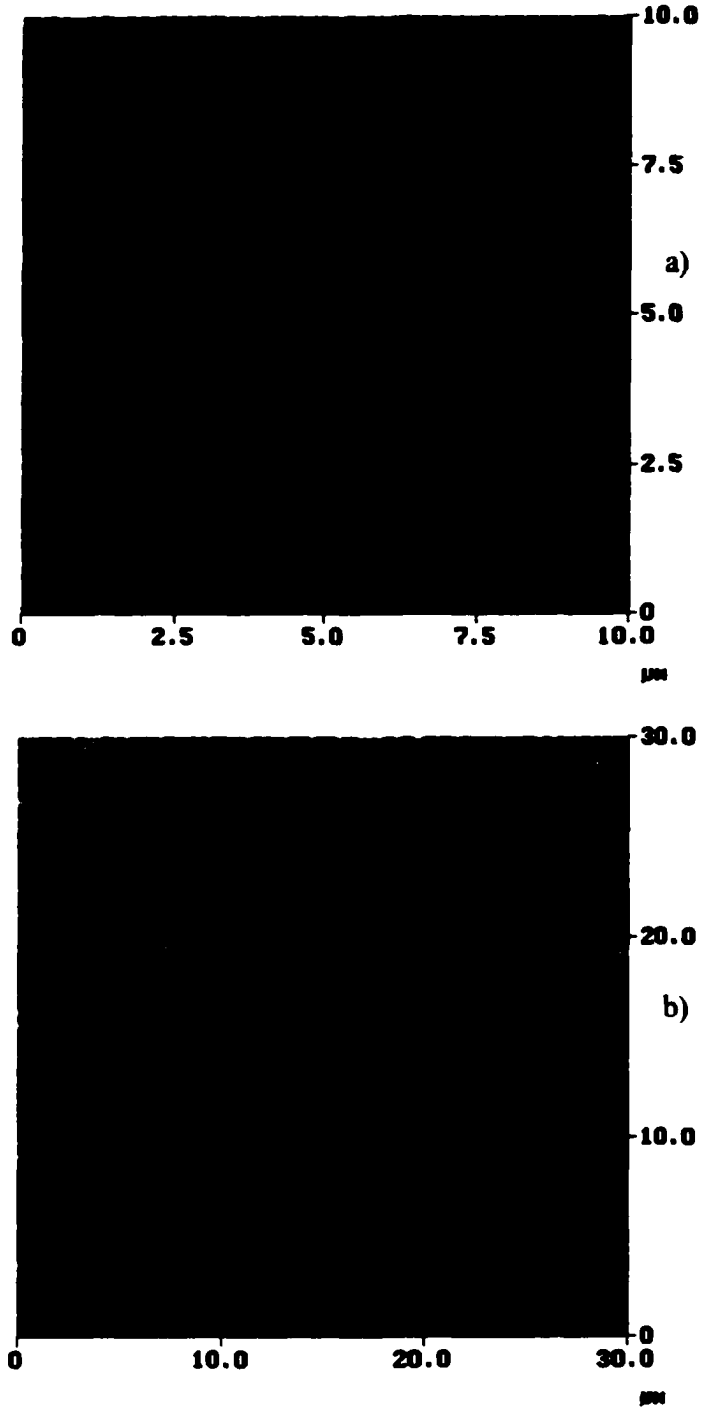

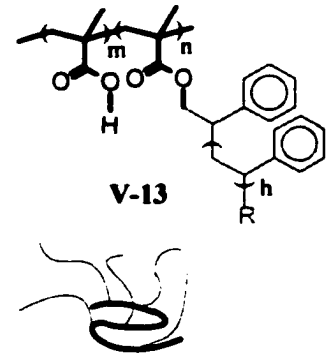

V-13

Figure 5-20. AFM images of L-B films of grafted copolymer **V-13**

$W_{PS} / W_{PMA} = 5.6$
m = 94
n = 5
h = 145

a) 10 μm × 10 μm
b) 30 μm × 30 μm

Grafted copolymers **V-12**, i.e. poly(*t*-BMA-*stat*-**V-1**)-*graft*-polystyrene, have a polar poly(*t*-BMA)-based backbone sparsely grafted with a number of nonpolar

polystyrene side-chains. As shown in **Figure 5-19**, grafted copolymers **V-12**, with different structural parameters, exhibit a variety of well-defined surface self-assembled morphologies. However, a number of variables, such as weight ratio of polystyrene components to poly(*t*-BMA) components (W_{PS}/W_{PBMA}) and grafting density, potentially can influence their surface morphologies. Moreover, different from the homopolymer of poly(MMA), homopolymer poly(*t*-BMA) can form a L-B film [*39*]. With poly(*t*-BMA)-based backbone of **V-12** as a special factor, surface morphologies of **V-12** can be further complicated, resulting in self-assembled surface morphologies of **V-12** not readily explainable in detail at this time.

Grafted copolymers **V-13**, i.e. poly(methacrylic acid-*stat*-**V-1**)-*graft*-polystyrene, have a hydrophilic poly(methacrylic acid)-based backbone sparsely grafted with a number of nonpolar polystyrene side-chains. Because **V-13** was derived from grafted copolymer **V-12**, they have the same structural parameters except a different backbone monomer unit. However, their self-assembled surface morphologies were very different. As shown in **Figure 5-20**, a **V-13** sample showed two types of surface aggregations on its AFM images. One type is surface nano-sized micelles, and the other type is a nanowire with a length up to tens of microns; neither of them is similar to the surface patterns of the parent **V-12** sample shown in **Figure 5-19, c**.

5-7 Experimental

Materials. *n*-Butyllithium (2.0 M solution in cyclohexane, Aldrich), iodomethane (99%, Acros), iodotrimethylsilane (Me_3SiI; 97%, Aldrich), methacryloyl chloride (97%,

Acros), and pyridine (99%, Aldrich) were used as received. Nitrogen (>99.999%, Welco) was used as the atmosphere for all reactions without further purification. Tetrahydrofuran (THF; 99.5%, Acros) was refluxed overnight over CaH_2 and then distilled from sodium naphthalene before use. Methyl methacrylate (MMA; 99%, Acros) and *tert*-Butyl methacrylate (*t*-BMA; 99%, Acros) were distilled over CaH_2 and then distilled from triisobutylaluminum before use. Styrene (99%, Acros) and 2-(dimethylamino)ethyl methacrylate (DMAEMA; 98%, Aldrich) were distilled over CaH_2 before use. Lithium chloride (99.99%, Aldrich) was dried at 120 °C overnight and dissolved in THF before use. 1,1-Diphenylhexyllithium (DPHLi) was prepared from the reaction of *n*-butyllithium with an equivalent of freshly-distilled 1,1-diphenylethylene in THF before use. 1-Hydroxy-2-phenyl-2-(2',2',6',6'-tetramethyl-1'-piperidinyloxyl)ethane was prepared following the literature [*40*].

1-Methacryloyloxy-2-phenyl-2-(2',2',6',6'-tetramethyl-1'-piperidinyloxyl)eth-ane, V-1. Methacryloyl chloride (2.50 g, 23.9 mmol) and pyridine (1.80 g, 22.8 mmol) were simultaneously added dropwise to a solution of 1-hydroxy-2-phenyl-2-(2',2',6',6'-tetramethyl-1'-piperidinyloxyl)ethane (6.28 g, 22.6 mmol) in THF (20 mL) at room temperature. The reaction mixture was kept at 40 °C for 5 h and then evaporated to dryness and partitioned between water (50 mL) and dichloromethane (50 mL). After the aqueous layer was extracted with dichloromethane (3 × 30 mL), the combined organic layers were dried with magnesium sulfate and evaporated to dryness. The crude product was purified by flash column chromatography eluting with dichloromethane to give **V-1** (5.20 g, 15.1 mmol) as a pale yellow solid in 67% yield. The last traces of dichloromethane were removed from **V-1** by three successive additions and

cyrodistillations of THF, and then **V-1** was dissolved in THF before use. Mp: 45 °C; ^{1}H NMR (200 MHz, $CDCl_3$, δ): 7.38-7.19 (m, 5H, Ar-H), 5.98 (s, 1H, =CH*H*), 5.47 (s, 1H, =C*H*H), 4.96 (t, 1H, CH), 4.63 (dd, 1H, CH*H*), 4.34 (dd, 1H, C*H*H), 1.85 (s, 3H, CH_3), 1.60, 1.48, 1.41, 1.33, 1.19, 1.04, 0.71 (each br s, 18H, 3 × CH_2 and 4 × CH_3).

Polyfunctional Macroinitiator Poly(V-1), V-2. Anionic polymerization of **V-1** was carried out in a pre-flamed round bottom glass flask under magnetic stirring. All chemicals were transferred with dry syringes. After THF, a THF solution of lithium chloride, and a THF solution of DPHLi were added, the flask was cooled to -78 °C in a methanol-dry ice bath. The polymerization was induced by the addition of a THF solution of **V-1**, and was terminated 1 h later using methanol. After withdrawing a small amount of polymerization solution for monomer conversion analysis with 200 MHz ^{1}H NMR, the rest of polymerization solution was precipitated into a large amount of methanol to give **V-2** as a white solid. ^{1}H NMR (600 MHz, $CDCl_3$, δ): 7.56-6.78 (m, 5H, Ar-H), 4.82 (s, 1H, CH), 4.50 (s, 1H, CH*H*), 3.96 (s, 1H, C*H*H), 1.51, 1.36, 1.26, 1.20, 1.03 (each br s, 17H, 4 × CH_2 and 3 × CH_3), 0.78 (s, chain-end CH_3), 0.65, 0.42 (each br s, 6H, 2 × CH_3); ^{13}C NMR (600 MHz, $CDCl_3$) *δ*: 176.4, 148.9, 141.1, 127.9, 125.4, 83.9, 66.6, 60.2, 59.7, 54.2, 44.3, 40.4, 34.3, 34.1, 29.7, 22.6, 20.3, 17.2, 16.3, 14.2.

Polyfunctional Macroinitiator Poly(MMA)-*block*-poly(V-1), V-3. II-3 was prepared following the same procedure for **V-2** except that in the preparation of **V-3**, MMA was added 30 min before the addition of **V-1**. ^{1}H NMR (600 MHz, $CDCl_3$, δ): 7.56-6.78 (m, 5H, Ar-H of **V-1**), 4.82 (s, 1H, CH of **V-1**), 4.50 (s, 1H, CH*H* of **V-1**), 3.96 (s, 1H, C*H*H of **V-1**), 3.60 (s, OCH_3 of MMA), 2.00-1.76 (m, CH_2 of MMA and **V-1**),

1.51, 1.36, 1.26, 1.20, 1.03 (each br s, 17H, 4 × CH_2 and 3 × CH_3 of **V-1**), 0.86 (s, CH_3 of MMA), 0.78 (s, chain-end CH_3), 0.65, 0.42 (each br s, 6H, 2 × CH_3 of **V-1**).

Polyfunctional Macroinitiator Poly(*t*-BMA-*stat*-V-1), V-4. **V-4** was prepared following the same procedure for **V-2** except that in the preparation of **V-4**, the polymerization was induced by the addition of mixture of *t*-BMA and **V-1**, polymerization time was 3 h, and copolymerzation solution was precipitated into cold methanol or methanol/water (80/20). ^{1}H NMR (600 MHz, $CDCl_3$, δ): 7.56-6.78 (m, 5H, Ar-H of **V-1**), 4.82 (s, 1H, CH of **V-1**), 4.50 (s, 1H, CH*H* of **V-1**), 3.96 (s, 1H, C*H*H of **V-1**), 2.27-1.57 (m, CH_2 of *t*-BMA), 1.57-1.20 (m, 9H, *t*-C_4H_9 of *t*-BMA), 1.20-0.80 (m, 3H, CH_3 of *t*-BMA). All ^{1}H NMR resonances of **V-1** at 2.27-0.80 ppm were covered by resonances of *t*-BMA.

Grafted Copolymer Poly(V-1-*graft*-styrene), V-5. **V-2** was dissolved in styrene under nitrogen in a pre-flamed glass tube. After sealing the tube with a flame, polymerization was induced by heating the styrene solution of **V-2** in an oil bath at 125 °C. After the designated time, the polymerization was quenched by removing the sealed tube from the oil bath and cooling it to room temperature. After diluted with THF, the polymerization solution was precipitated into a large amount of methanol to give **V-5** as a white solid. ^{1}H NMR (600 MHz, $CDCl_3$, δ): 7.31-6.87 (m, 3H, Ar-H), 6.87-6.30 (m, 2H, Ar-H), 4.55, 4.42, 3.99 (graft terminal benzylic CH), 2.44-1.71 (m, 1H, CH), 1.42 (br s, 2H, CH_2).

Block-Graft Copolymer Poly(MMA)-*block*-poly(V-1-*graft*-styrene), V-6. **V-6** was prepared following the same procedure for **V-5** except that in the preparation of **V-6**, the macroinitiator used was **V-3**, instead of **V-2**. ^{1}H NMR (600 MHz, $CDCl_3$, δ): 7.31-

6.86 (m, 3H of Ar-H of styrene), 6.87-6.30 (m, 2H of Ar-H of styrene), 4.55, 4.42, 3.99 (graft terminal benzylic CH), 3.60 (s, 3H of OCH_3 of MMA), 2.44-1.71 (m, 2H of CH_2 of MMA, 1H of CH of St), 1.42 (br s, 2H of CH_2 of styrene), 0.86 (s, 3 H of CH_3 of MMA).

Detachment of Polystyrene Graft. A THF solution of **V-5**, **V-6**, or **V-12** reacted with an excess of cyclohexane solution of *n*-butyllithium at room temperature under nitrogen overnight. After the addition of a small amount of water, the reaction mixture was precipitated into a large amount of methanol to give detached polystyrene graft **V-7** as a white solid for GPC analysis.

Graft-Block Copolymer Poly(V-1-*graft*-styrene/DMAEMA), V-8. **V-5** was dissolved in DMAEMA under nitrogen in a pre-flamed glass tube. After sealing the tube with a flame, polymerization was induced by heating the styrene solution of **V-5** in an oil bath at 125 °C. After the designated time, the polymerization was quenched by removing the sealed tube from oil bath and cooling it to room temperature. After diluted with THF, the polymerization solution was precipitated into a large amount of hexane to give **V-8** as a white solid. ^{1}H NMR (600 MHz, $CDCl_3$, δ): 7.31-6.87 (m, 3H of Ar-H of styrene), 6.87-6.30 (m, 2H of Ar-H of styrene), 4.05 (s, 2H of OCH_2 of DMAEMA), 2.56 (s, 2H of NCH_2 of DMAEMA), 2.28(s, 6H of 2 × NCH_3 of DMAEMA), 2.10-1.66 (m, 1H of CH of styrene, 2H of CH_2 of DMAEMA), 1.43 (br s, 2H of CH_2 of styrene), 1.18-0.71 (m, 3H of CH_3 of DMAEMA).

Block-Graft-Block Copolymer Poly(MMA)-*block*-Poly(V-1-*graft*-styrene/ DMAEMA), V-9. **V-9** was prepared following the same procedure for **V-8** except that in the preparation of **V-9**, the macroinitiator used was **V-6**, instead of **V-5**. ^{1}H NMR (600 MHz, $CDCl_3$, δ): 7.31-6.87 (m, 3H of Ar-H of styrene), 6.87-6.30 (m, 2H of Ar-H of

styrene), 4.05 (s, 2H of OCH_2 of DMAEMA), 3.60 (s, 3H of OCH_3 of MMA), 2.56 (s, 2H of NCH_2 of DMAEMA), 2.28(s, 6H of 2 × NCH_3 of DMAEMA), 2.10-1.65 (m, 2H of CH_2 of MMA, 1H of CH of styrene, 2H of CH_2 of DMAEMA), 1.43 (br s, 2H of CH_2 of styrene), 1.18-0.71 (m, 3H of CH_3 of MMA, 3H of CH_3 of DMAEMA).

Graft-Block Copolymer Poly(MMA)-*block*-Poly(V-1-*graft*-styrene/ quaternized DMAEMA), V-10. A THF solution of **V-8** was reacted with an excess of iodomethane at 40 °C for 24 h. The yellow precipitate formed was collected and dried to give **V-10** as a yellow solid. ^{1}H NMR (600 MHz, DMSO-d_6, δ): 7.31-6.87 (m, 3H of Ar-H of styrene), 6.87-6.30 (m, 2H of Ar-H of styrene), 4.50 (s, 2H of OCH_2 of quaternized DMAEMA), 3.99 (s, 2H of NCH_2 of quaternized DMAEMA), 3.39 (s, 9H of 3 × NCH_3 of quaternized DMAEMA), 2.36-1.74 (m, 1H of CH of styrene, 2H of CH_2 of quaternized DMAEMA), 1.50 (br s, 2H of CH_2 of styrene), 1.24-0.90 (m, 3H of CH_3 of quaternized DMAEMA).

Block-Graft-Block Copolymer Poly(MMA)-*block*-Poly(V-1-*graft*-styrene/ quaternized DMAEMA), V-11. A THF solution of **V-9** was reacted with an excess of iodomethane at 40 °C for 24 h. The yellow precipitate formed was collected and dried to give **V-11** as a yellow solid. ^{1}H NMR (600 MHz, DMSO-d_6, δ): 7.31-6.87 (m, 3H of Ar-H of styrene), 6.87-6.30 (m, 2H of Ar-H of styrene), 4.50 (s, 2H of OCH_2 of quaternized DMAEMA), 3.99 (s, 2H of NCH_2 of quaternized DMAEMA), 3.60 (s, 3H of OCH_3 of MMA), 3.39 (s, 9H of 3 × NCH_3 of quaternized DMAEMA), 2.36-1.74 (m, 2H of CH_2 of MMA, 1H of CH of styrene, 2H of CH_2 of quaternized DMAEMA), 1.50 (br s, 2H of CH_2 of styrene), 1.24-0.73 (m, 3H of CH_3 of MMA, 3H of CH_3 of quaternized DMAEMA).

Poly(*t*-BMA-*stat*-V-1)-*graft*-polystyrene, V-12. **V-12** was prepared following the same procedure for **V-5** except that in the preparation of **V-12**, the macroinitiator used was **V-4**, instead of **V-2**. ^{1}H NMR (600 MHz, $CDCl_3$, δ): 7.31-6.86 (m, 3H of Ar-H of styrene), 6.87-6.30 (m, 2H of Ar-H of styrene), 2.53-1.68 (m, 1H of CH of St, 2H of CH_2 of *t*-BMA), 1.68-1.19 (m, 2H of CH_2 of styrene, 9H of *t*-C_4H_9 of *t*-BMA), 1.19-0.80 (m, CH_3 of *t*-BMA).

Poly(methacrylic acid-*stat*-V-1)-*graft*-polystyrene, V-13. A toluene solution of **V-12** was reacted with an excess of Me_3SiI (ten equivalents relative to the sum of ester groups in **V-12**) at room temperature for 24 h, then the reaction mixture was concentrated by solvent evaporation and redissolved in THF. The THF solution of the reaction mixture was precipitated in 0.1 *M* HCl aqueous solution containing $Na_2S_2O_3$ (discoloring agent). The polymer recovered was purified by repeated precipitation from THF into water followed by from THF into hexane to give **V-13** as a white solid. ^{1}H NMR (600 MHz, DMSO-d_6, δ): 7.50-6.69 (m, 3H of Ar-H of styrene), 6.69-5.97 (m, 2H of Ar-H of styrene), 2.53-1.71 (m, 1H of CH of St, 2H of CH_2 of methacrylic acid), 1.71-1.19 (m, 2H of CH_2 of styrene), 1.19-0.80 (m, CH_3 of methacrylic acid).

Characterization. ^{1}H NMR and ^{13}C NMR spectra were obtained at room temperature on a Varian 600 MHz spectrometer with $CDCl_3$ or DMSO-d_6 as solvent and tetramethylsilane as internal reference. For each spectrum, 64 to 128 transients were collected with pulse angle of 39° and delay time of 3 s.

FT-IR spectra were obtained at room temperature on a Nicolet Magna-IR 550 spectrometer. Minimum amounts of dichloromethane or THF were used to dissolve

samples. A polyethylene-based IR card was used as substrate. Dissolved samples on IR cards were dried under vacuum at room temperature before measurement.

All GPC measurements were performed at 40 °C on a Waters-150C GPC instrument equipped with a refractive index detector, three Ultrastyragel columns (10^4, 10^5, 10^6 Å) and a Styragel HR 3 column, using THF as eluent at 1.0 mL/min. Unless otherwise stated, GPC analyses were based on the calibration using fifteen linear monodisperse polystyrene standards (*MW*: 760, 2360, 3700, 8300, 13 700, 18 700, 29 300, 44 000, 75 700, 114 200, 212 400, 382 100, 679 000, 935 000, and 1 880 000; Aldrich). The calibration curve has a fourth order fit for the broad molecular weight range.

AFM images were recorded with a Nanoscope III instrument operating in the contact mode, using tip with radius of about 20 nm. The samples were prepared by the Langmuir-Blodgett (L-B) technique. Each polymer sample was dissolved in chloroform at 1 mg/mL before spreading on the water. Each solution was spread using a micro-syringe at ambient temperature. A computer controlled KSV3000 double barrier L-B trough was used. Measurement of surface pressure-area (π-A) diagram was followed by the transfer of monolayers, i.e. L-B films, onto hydrophilic silicon wafers at 15 dyne/cm. The barrier and film transferring speed were 5 mm/min and 2 mm/min respectively. Distilled and deionized water was used as the subphase.

5-8 Conclusions

An ensemble of well-defined polyfunctional alkoxyamine-based macroinitiators were synthesized by living anionic polymerization with alkoxyamine-based monomer. These macroinitiators have well-controlled number-average and density of alkoxyamine groups, chain length, and low polydispersities. Besides homopolymer structures, block structures and copolymer structures were also incorporated into the macroinitiators. Graft SFRP of styrene using these macroinitiators yielded well-defined grafted copolymers with controlled graft formation and predetermined graft density. Block structures of grafts were further obtained by SFRP of other monomers via alkoxyamine groups on the graft-ends of the resulting graft copolymers. Polymeric hydrophilic component and ionic component were also introduced into graft architectures via modification reactions to give amphiphilic grafted copolymers.

Extending the above strategy to include proper structural design of alkoxyamine, judicious selection of comonomers, and additional routes of modification reactions, a broad range of well-defined grafted architectures with controlled length and composition of the backbone as well as the graft can be achieved.

Chapter 6

Radical Polymerization Mediated by Stable Carbon-Centered Radical

Abstract: Radical polymerization mediated by tri-(*p*-*t*-butylphenyl)methyl stable carbon-centered radical (TBPM•) was investigated. Thermal initiators that can simultaneously release active radical and TBPM• at elevated temperature were synthesized. In all trials of radical polymerization using these TBPM-based initiators, thermal decomposition of initiators was slow, resulting in slow initiation. Radical polymerization of styrene yielded polystyrenes with increasing DP_n with monomer conversion and monomodal molecular weight distribution, suggesting living characteristics due to mediation of TBPM•. Mediation effects of TBPM• were further supported by ω-TBPM functionality of polystyrenes synthesized (verified by ^{1}H NMR) and the initiating capacity of TBPM-PS adduct, but the slow initiation using TBPM-PS as initiator indicated that mediation from TBPM• cannot be sufficient to obtain a typical living radical polymerization system. Radical polymerization of MMA yielded poly(MMA)s with DP_n independent of monomer conversion, suggesting no mediation effects of TBPM• on radical polymerization of MMA. Predominant ω-unsaturation of poly(MMA) produced (verified by ^{1}H NMR) further suggests relatively high reactivity of TBPM• in β-hydrogen transfer reaction in the polymerization system.

6-1 Introduction

The synthesis of polymers with well-defined macromolecular architectures is a major aspect in modern polymer synthetic chemistry. Living radical polymerization (LRP) has been utilized to prepare a wide variety of well-defined macromolecular architectures from a broad range of monomers [*1-3*]. The key improvement of living radical polymerization relative to conventional radical polymerization is to introduce mediating species to average the reaction courses of radical chain carriers and to avoid the major occurrence of irreversible termination during the polymerization time. Three important LRP techniques, including stable free radical polymerization (SFRP) [*4*], atom transfer radical polymerization (ATRP) [*5, 6*], and reversible addition fragmentation transfer (RAFT) [*7*], have been developed by using different types of mediating species. However, no broad industrial application of these LRP techniques has taken place. Based on reversible termination, ATRP currently uses toxic and electrically conductive paramagnetic metal salts as mediating species, but no economical method has been developed to remove the metal-based species from the polymers produced. RAFT is based on reversible chain transfer, therefore its major application is to synthesize linear polymers, and at the same time, because currently dithioestera are used as the major mediating species, the polymers synthesized generally have dithioester groups, which have associated odors and colors. As a LRP technique, SFRP is based on reversible termination through (metal-free) stable radical mediation, and can be applied to the synthesis of polymers with complex macromolecular architectures. However SFRP, currently using nitroxide as the major mediating species, can only be applied to a narrow

range of monomers, because of unavoidable disadvantages associated with nitroxides, especially their tendency to abstract β-hydrogen of initiating or propagating radicals. Therefore, one of our major interests in LRP is to investigate mediation effects of new types of stable radicals other than nitroxides, exploring the possibility of developing LRP systems with broad applications. This chapter describes our study of radical polymerization of styrene and methyl methacrylate (MMA) mediated by a stable carbon-centered radical.

Research on stable carbon-centered radical mediated radical polymerization can be traced back to the pioneering work of Ostu et al. in the 1980s [*8, 9*]. Their study of radical polymerization of methacrylates initiated by phenylazotriphenylmethane (PAT), as a so-called thermal "iniferter", can be considered as one of the earliest attempts to develop a LRP system based on stable radical mediation (**Scheme 6-1**). During polymerization at elevated temperature, PAT decomposed to give equimolar amounts of active phenyl radical as the initiating radical, and stable trityl radical as the mediating radical. They did observe increasing molecular weights of resulting polymers with monomer conversion, and even block copolymers were further obtained. However, all conversions reported were below 30%, and polydispersities of resulting polymers increased with monomer conversion and multiple-modal molecular weight distributions with polydispersities as high as 5.54 were detected, suggesting very severe occurrence of undesirable side reactions. The most concerned side reactions proposed are related to the *para* positions of phenyl rings of trityl radical, where the carbon with the least steric hindrance has radical properties due to electron delocalization. These side reactions were expected to decrease the concentration of trityl radical and/or to give polymers with only

very weak reactivity for reinitiation (**Scheme 6-2**), causing polymerization gradually out of control. Ostu et al. [*10, 11*], Braun et al. [*12*], Nuyken et al. [*13-15*], and others [*16-19*] also studied radical polymerization involving substituted diphenylmethyl radicals, which might have weak but observable initiating capacity and therefore would further complicate polymerization behavior.

Based on the seminal research of Ostu et al., as well as recent progress in LRP providing solid foundation for further study, we rediscovered tri-(*p-t*-butylphenyl)methyl

Scheme 6-1

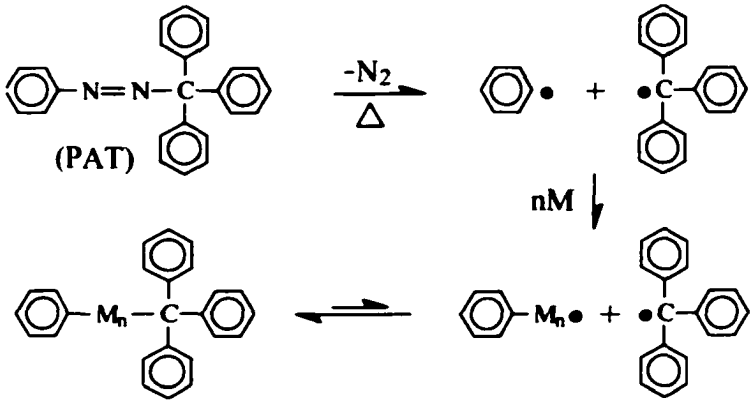

Scheme 6-2

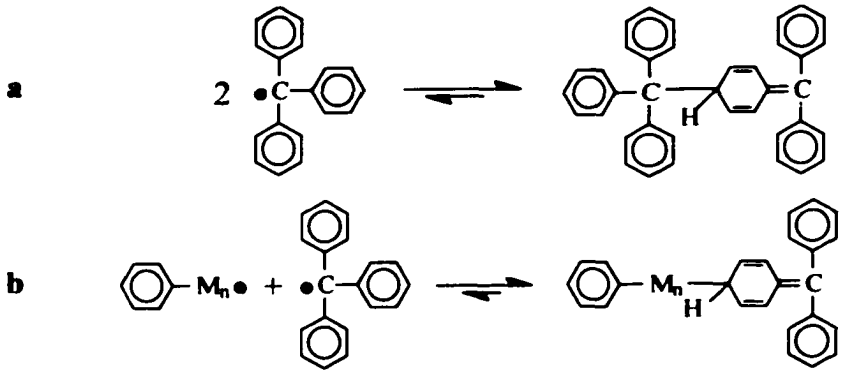

Scheme 6-3

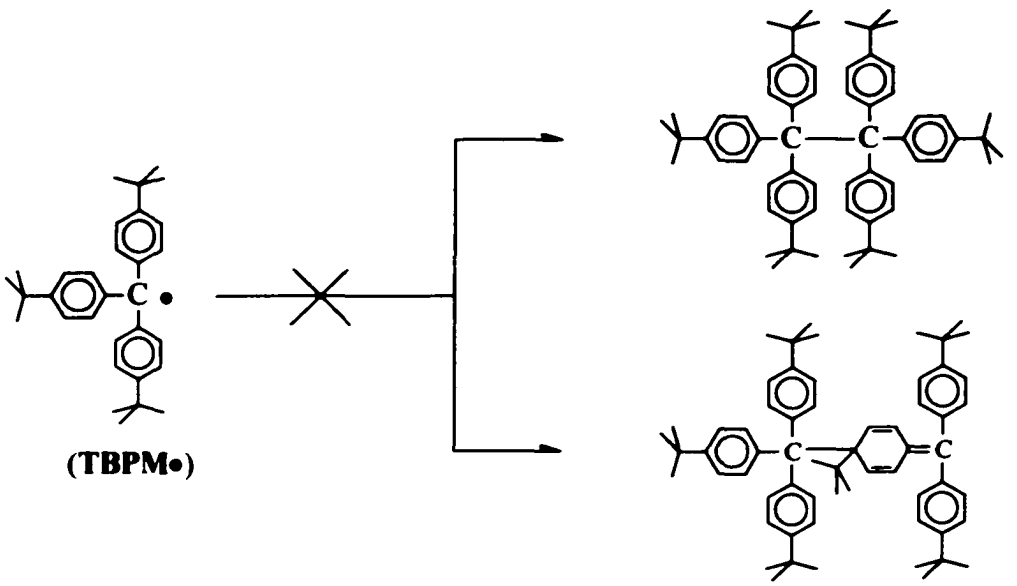

(TBPM•) stable radical [*20*], synthesized three types of TBPM-based thermal initiators, and investigated radical polymerization using these initiators. Typically, triarylmethyl radicals are in equilibrium with their dimers [*21*], and as shown in **Scheme 6-2a**, the *para* position of triarylmethyl radicals is a key reaction site for dimerization [*22*]. However, described in an early report, TBPM• concentration has no dependence on temperature, suggesting that TBPM• has no dimerization (**Scheme 6-3**), or its dimmerization only ocuurs at a negligible level [*20*]. Thus, it can be further expected that the pathway of side reactions occurring at the *para* positions is essentially blocked by bulky *tert*-butyl groups with the reactivity of the tertiary carbon radical less affected. Thus, our study of radical polymerization mediated by the selected TBPM• would provide some insight into the general mediation effects of stable carbon-centered radical on radical polymerization.

Besides triarylmethyl radicals, there are also other stable carbon-centered radicals reported [*21, 23-25*], typically with great steric hindrance around radical center. Due to

steric reasons, they generally are not expected to have significant mediation function for radical polymerization; no corresponding investigation has been reported by others and it is not of our current concern. Additionally, the studies on addition of carbon-centered radicals to alkenes performed by others are not directly related to our current work, but do provide helpful insight into reactivity of carbon-centered radicals [*26*].

6-2 Synthesis of TBPM-Based Thermal Initiators

Monofunctional TBPM-based thermal initiators, R-TBPM, are expected to undergo homolytic dissociation at elevated temperature, releasing equimolar amounts of initiating radical R• and stable carbon-centered radical TBPM•. The major concern in the structure design of TBPM-based thermal initiators is that the initiating radical R• needs to have balanced reactivities. It must be reactive enough to efficiently initiate monomers. But at the same time, it should not be too reactive, because otherwise the tendency of homolytic dissociation of initiator would be relatively weak. Thus, three types of monofunctional TBPM-based thermal initiators **VI-1**, **VI-2**, and **VI-3** were designed and synthesized. Initiator **VI-1** is designed to release $Ph(CH_3)CH•$ as initiating radical; initiator **VI-2** is designed to release $CH_3OOC(Ph)CH•$ as initiating radical; initiator **VI-3** is designed to release polystyrene radical as initiating radical. Based on resonance effects, $Ph(CH_3)CH•$ from **VI-1** and polystyrene radical from **VI-3** are expected to be more reactive than $CH_3OOC(Ph)CH•$ from **VI-2**. But on the other hand, **VI-2** is expected to have faster homolytic dissociation than **VI-1** and **VI-3** under the same reaction conditions.

Scheme 6-4

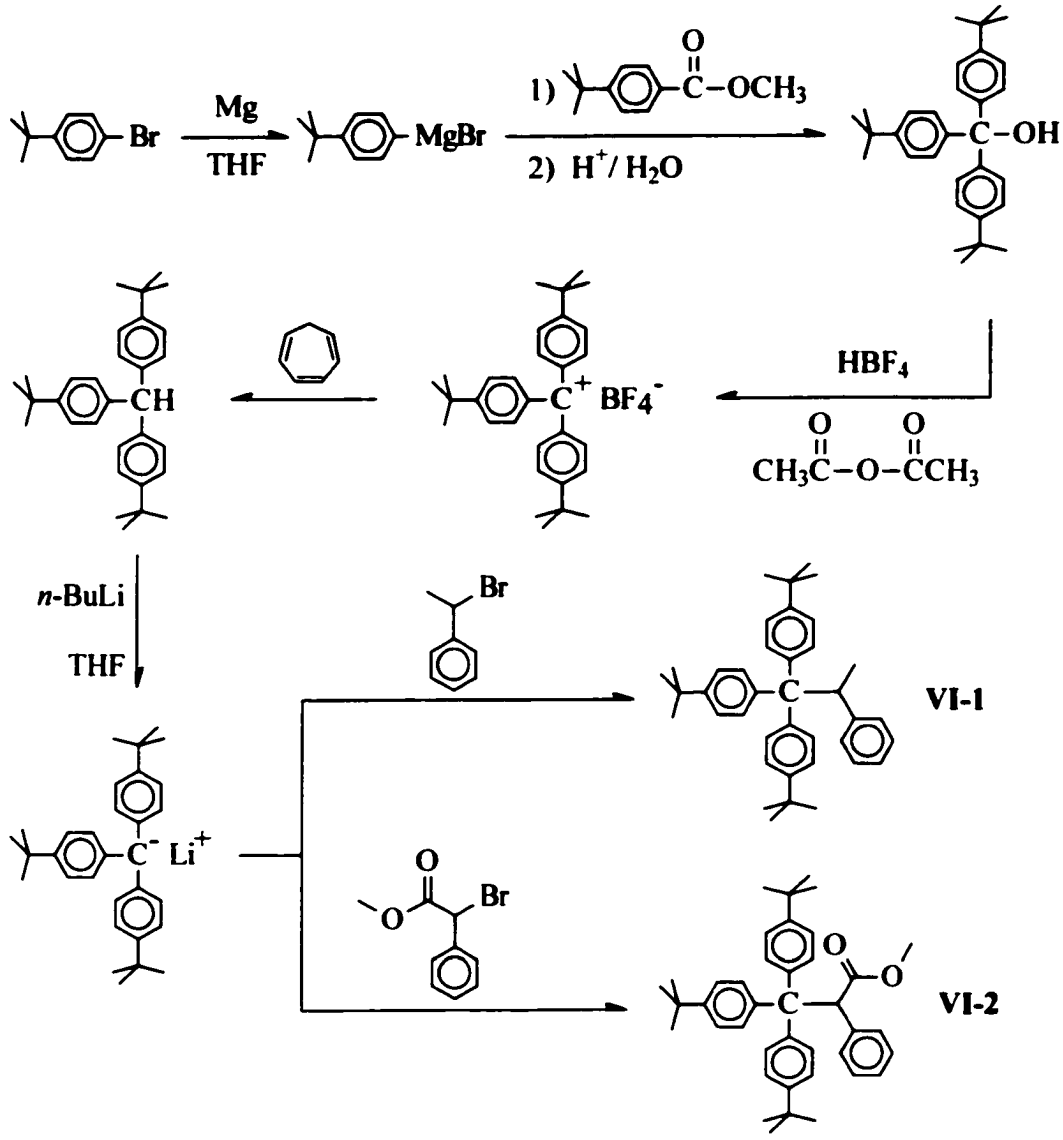

Both **VI-1** and **VI-2** are small molecular compounds, and their synthetic routes are shown in **Scheme 6-4**. First, tri-(*p-t*-butylphenyl)methanol was synthesized by typical Grignard reaction. Grignard reagent prepared from 1-bromo-4-*tert*-butylbenzene and magnesium was used to react with methyl 4-*tert*-butylbenzoate in THF, and tri-(*p-t*-butylphenyl)methanol was formed in 79% yield. Then tri-(*p-t*-butylphenyl)methane was

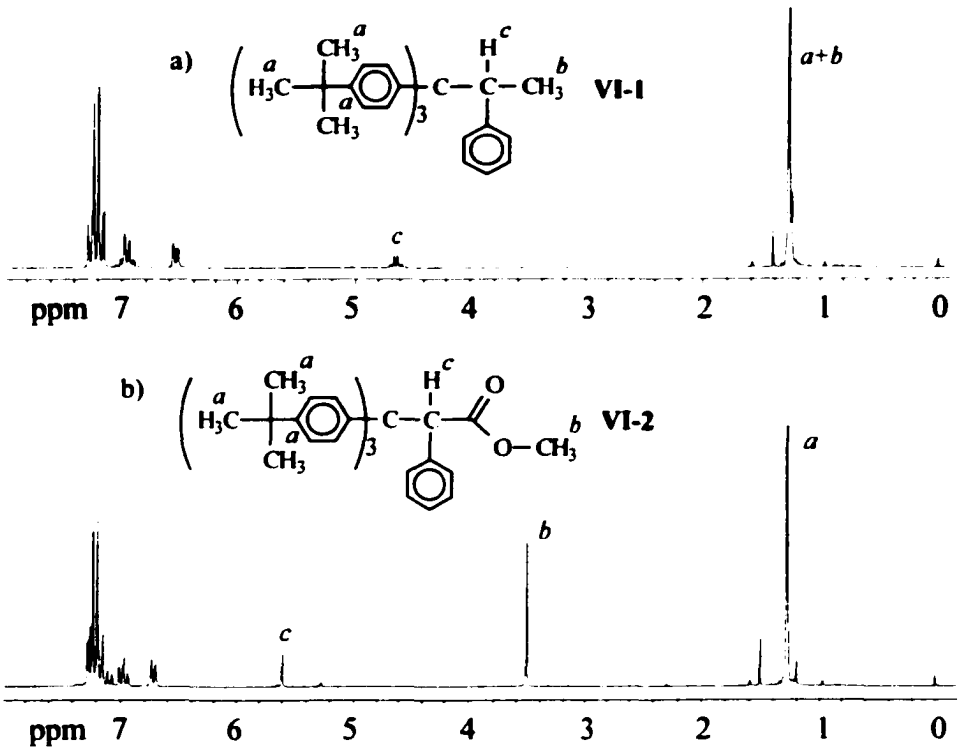

Figure 6-1. ^{1}H NMR spectra of a) **VI-1** and b) **VI-2**.

prepared from tri-(*p*-*t*-butylphenyl)methanol in 85% yield through reaction of tri-(*p*-*t*-butylphenyl)methanol with fluoroboric acid in the presence of acetic anhydride to generate the salt of fluoroborate of tri-(*p*-*t*-butylphenyl)methyl carbocation, followed by treating the salt with cycloheptatriene which loses a proton to tri-(*p*-*t*-butylphenyl)methyl carbocation [*27*]. As the last step, tri-(*p*-*t*-butylphenyl)methane was reacted with a strong nucleophilic reagent *n*-butyllithium, then the resulting tri-(*p*-*t*-butylphenyl)methyl anion was used to react with excesses of (1-bromoethyl)benzene and methyl *α*-bromophenylacetate to yield **VI-1** and **VI-2** respectively. In this step, a polar solvent, such as THF, must be used; otherwise, tri-(*p*-*t*-butylphenyl)methyl anion cannot be formed. Relative to the amount of tri-(*p*-*t*-butylphenyl)methane used, the yield of **VI-2** (24%) is slightly lower than the yield of **VI-1** (29%), presumably due to the occurrence of

side reaction between tri-(*p*-*t*-butylphenyl)methyl anion and the ester group of methyl *α*-bromophenylacetate in the synthesis of **VI-2**. The structures of **VI-1** and **VI-2** were verified by ^{1}H NMR analyses. As shown in **Figure 6-1**, **VI-1** has characteristic resonances of its benzyl proton at 4.62 ppm; **VI-2** has characteristic resonances of its benzyl proton at 5.60 ppm and its ester methyl protons at 3.52 ppm. For both of them, the characteristic resonances for *tert*-butyl methyl protons are centered at 1.27 ppm.

Scheme 6-5

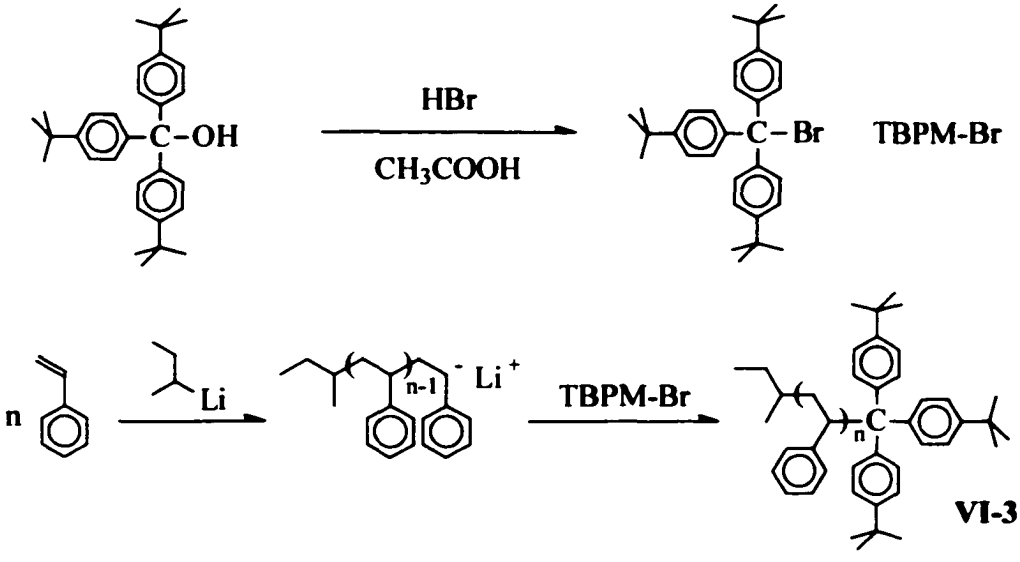

To synthesize polystyrene-TBPM adduct **VI-3**, poly(styryl)lithium, with a number-average degree of polymerization (DP_n) of styrene of 30, was prepared by *sec*-butyllithium-initiated anionic polymerization in benzene at room temperature and was terminated using an excess of tri-(*p*-*t*-butylphenyl)methyl bromide (**Scheme 6-5**). Tri-(*p*-*t*-butylphenyl)methyl bromide used was synthesized by the reaction of tri-(*p*-*t*-butylphenyl)methanol with a strong acid and nucleophile, hydrobromic acid, in acetic acid with 92% yield.

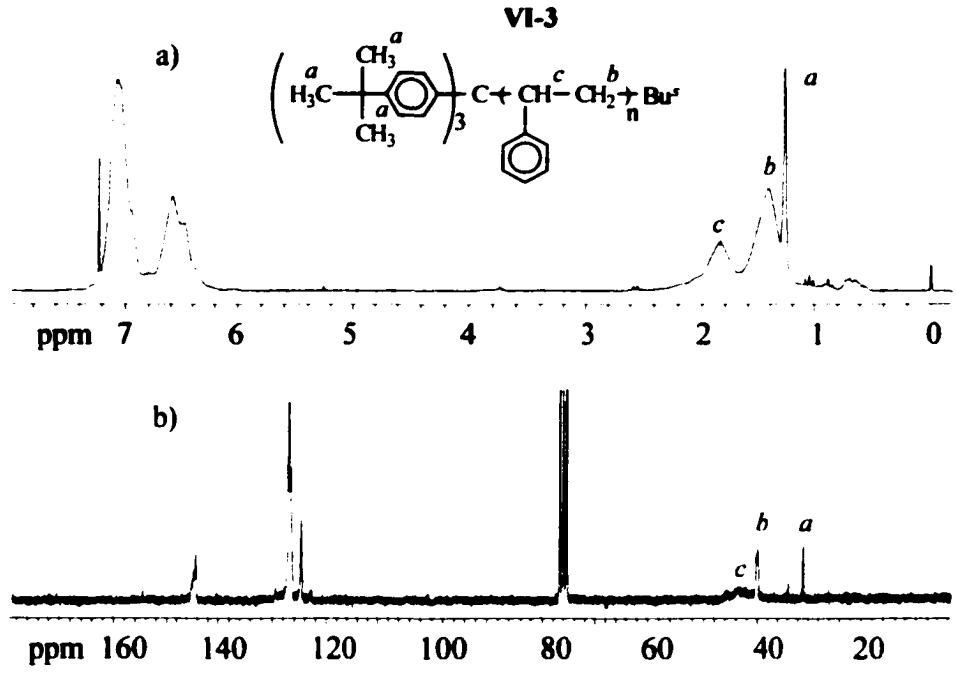

Figure 6-2. a) ^{1}H NMR and b) ^{13}C NMR spectra of PS-TBPM, **VI-3**.

GPC analysis of the product obtained showed that it has TBPM-functionalized polystyrene (M_{peak} = 3728; corresponding to $(St)_{30}$-TBPM) as major component with 83% in weight, and dimeric unfunctionalized polystyrene (M_{peak} = 6632; corresponding to $(St)_{60}$) as minor component with 17% in weight. Both components are nearly monodisperse. NMR analysis verified the TBPM functionalities in the product through characteristic ^{1}H NMR resonances of its *tert*-butyl methyl protons at 1.27 ppm and ^{13}C NMR resonances of its *tert*-butyl methyl carbons at 31.3 ppm (**Figure 6-2**). Based on the integration area ratio of all ^{1}H NMR resonances of aromatic protons and all ^{1}H NMR resonances of aliphatic protons, it was further estimated that desired TBPM-functionalized polystyrene was formed in 82% yield and unfunctionalized polystyrene was formed in 18% yield, in excellent agreement with GPC analysis. Because typically

chain transfer to polymer is negligible, unfunctionalized polystyrene can be considered as inert to radical polymerization, therefore it was not removed but was kept as reference to estimate the consumption percentage of polystyrene-TBPM when it was used as initiator for radical polymerization.

Efforts were also made to synthesize poly(MMA)-TBPM adduct but failed (**Scheme 6-6**). Poly(MMA) living anion was prepared by 1,1-diphenylhexyllithium-initiated anionic polymerization of MMA in THF at -78 °C. Then an excess of tri-(*p*-*t*-butylphenyl)methyl bromide, employed as a terminating agent, was add into the THF solution of poly(MMA) living anion. However, ^{1}H NMR analysis showed no TBPM functionality in product, indicating that no occurrence of coupling reaction between tri-(*p*-*t*-butylphenyl)methyl bromide and poly(MMA) living anion. Although compared with polystyrene living anion, poly(MMA) living anion is less reactive, it can react with typical benzyl bromides quite efficiently [*28*]. Thus, the failure of the synthesis of poly(MMA)-TBPM may suggest that the covalent bond between poly(MMA) and TBPM moiety cannot be formed due to insuperable steric hindrance.

Scheme 6-6

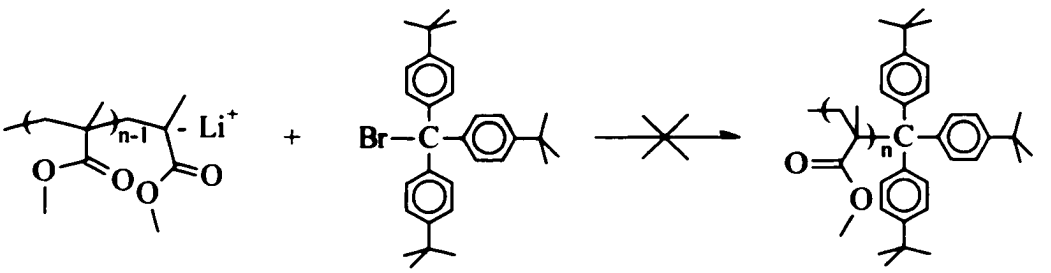

6-3 Radical Polymerization of Styrene Initiated by TBPM-Based Thermal Initiators

According to the structures of **VI-1**, **VI-2**, and **VI-3**, directly employing them as thermal initiators in radical polymerization at elevated temperature results in radical polymerization systems with TBPM• stable carbon-centered radical as mediating species. Radical polymerization of styrene initiated by these TBPM-based thermal initiators (**Scheme 6-7**) was investigated to study the mediation effects of TBPM•. Because triarylmethyl radicals (including TBPM•) are sensitive to light [*21*], all trials of polymerization were carried out in dark at 100 °C or 125 °C. The polymerization results are shown in **Table 6-1**.

Because mediation effects of stable radical on radical polymerization essentially is based on reversible termination of polymer propagating radicals with stable radical, it is crucial to investigate whether polystyrene **VI-4** yielded has ω-TBPM functionality and whether polystyrene-TBPM adduct has initiating capacity in order to establish mediation function of TBPM• on radical polymerization. The ω-TBPM functionality of **VI-4** was verified by ^{1}H NMR (**Figure 6-3**) based on the characteristic resonances of *tert*-butyl protons of TBPM functionality at 1.27 ppm. The close agreement between **VI-4** and **VI-3** in ^{1}H NMR, especially exactly the same position and shape of signals of *tert*-butyl protons of TBPM functionality, indicates that **VI-4** is also polystyrene-TBPM adduct with TBPM functionality connected to polystyrene chain through its central benzyl carbon other than its phenyl *para* positions with bulky *tert*-butyl substitution. Thus, **VI-4**

Scheme 6-7

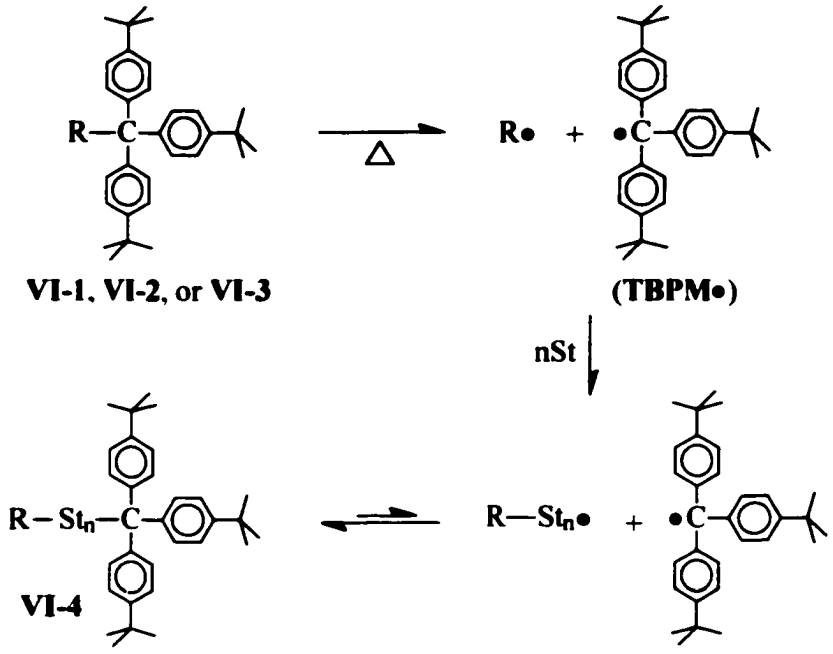

R: $Ph(CH_3)CH$ for **VI-1**, $CH_3OCO(Ph)CH$ for **VI-2**, ^{s}Bu-PSt for **VI-3**.

and **VI-3** essentially have the same chemical structures except α-chain end, chain length, and polydispersity. Because of the relatively high polydispersities of **VI-4** (1.72-3.42, by GPC), **VI-3** with nearly monodisperse polystyrene-TBPM was used as macroinitiator to unambiguously identify and analyze polystyrenes yielded by radical polymerization initiated by polystyrene-TBPM adduct. As a result, **VI-3**, representing dormant species in radical polymerization mediated by TBPM•, exhibited its initiation capacity with the formation of polystyrene **VI-4c**. On the other hand, mediation effects of TBPM• on radical polymerization of styrene were not sufficiently strong as indicated by the incomplete initiation of all TBPM-based initiators, especially **VI-3**. GPC analysis showed that all polystyrene **VI-4** samples had relatively high polydispersities (1.72-3.42) and relatively long tails to the low molecular weight sides, indicating gradual generation of

Table 6-1. Radical Polymerization of Styrene Initiated by TBPM-Based Initiators [a]

entry	initiator	T (°C)	time (h)	conv (%)	$DP_{n,\,calcd}$ [b]	$DP_{n,\,GPC}$ [c]	PDI [c]	I_e (%) [d]
VI-4a	**VI-1**	100	2	6.1	12.2	2480	2.15	0.5
VI-4b1	**VI-2**	100	13	63	126	427	1.95	30
VI-4b2	**VI-2**	125	0.5	12	24	176	1.90	14
VI-4b3	**VI-2**	125	1	20	40	196	2.00	20
VI-4b4	**VI-2**	125	2	43	86	203	2.02	42
VI-4b5	**VI-2**	125	3.6	72	144	225	2.52	64
VI-4b6	**VI-2**	125	6	96	192	283	3.42	68
VI-4c	**VI-3**	125	2	21	42	1450[e]	1.72	2.9

[a] $[St]_0 / [initiator]_0 = 200$. [b] DP_n calculated based on assumption of quantitative initiation and no bimolecular termination. [c] By GPC calibrated with linear polystyrenes.

[d] Initiation efficiency (estimated) = $DP_{n,\,calcd} / DP_{n,\,GPC}$.

[e] Increased DP_n relative to the initial DP_n of **VI-3**.

VI-4

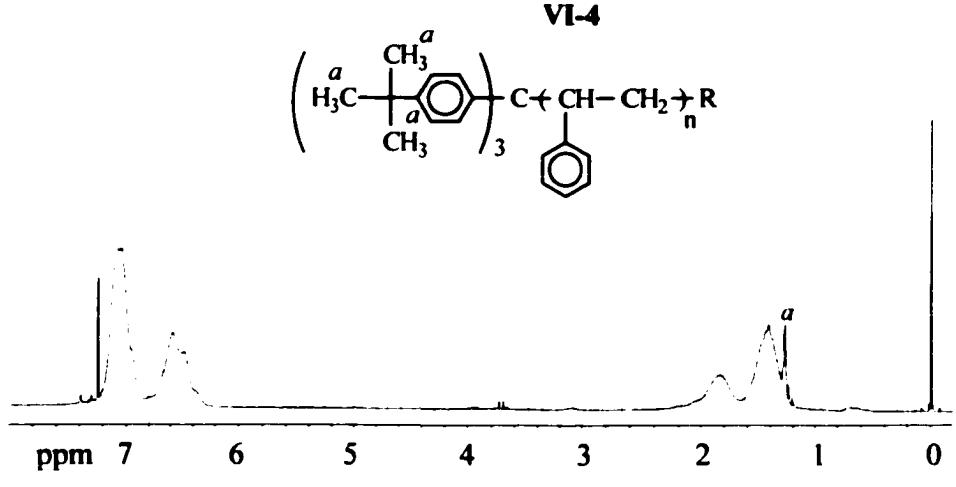

Figure 6-3. ^1H NMR spectrum of polystyrene **VI-4 (VI-4b3)**.

initiating radicals in all trials. Experimental DP_n values of all **VI-4** samples determined by GPC were much or relatively higher than the DP_n values calculated based on the feed ratio of monomer to initiator and monomer conversion with the assumption of complete initiation, suggesting very or relatively low initiation efficiency (I_e), $DP_{n,\,calcd.}$ / $DP_{n,\,GPC}$, during polymerization time. Very low initiation efficiency of **VI-1** (0.5%, 100 °C) and **VI-3** (2.9%, 125 °C) relative to polymerization time of 2 h suggested their very slow thermal homolytic dissociation, and relatively strong GPC peaks corresponding to **VI-1** and **VI-3** were also detected by GPC analyses of the polymerization solutions for the syntheses of polystyrenes **VI-4a** and **VI-4c**. Because it is the fast equilibrium between dormant species and propagating polymer radical that greatly averages the reaction courses of radical chain carriers and decides the major polymerization behavior of typical LRP systems, the slow initiation by polystyrene-TBPM adduct (**VI-3**) further suggested that mediation by TBPM• on radical polymerization is not sufficient to provide a typical LRP system.

Compared with **VI-1** and **VI-3**, **VI-2** showed much higher initiation efficiency than **VI-1** and **VI-3** under the same conditions. Because the initiating radical $CH_3OOC(Ph)CH$• from **VI-2** is not as reactive as the initiating radicals from either **VI-1** or **VI-3** based on resonance effects, such results indicated that, in all trials, the initiation rate depends on homolytic dissociation of TBPM-based initiator, presumably because homolytic dissociation rate was slower than the rate of initiation by initiating radical in all cases. Besides fast equilibrium between dormant species and propagating polymer radical, significant concentration of mediation radical is also required to build up persistent radical effect for typical LRP systems. Due to the faster homolytic dissociation

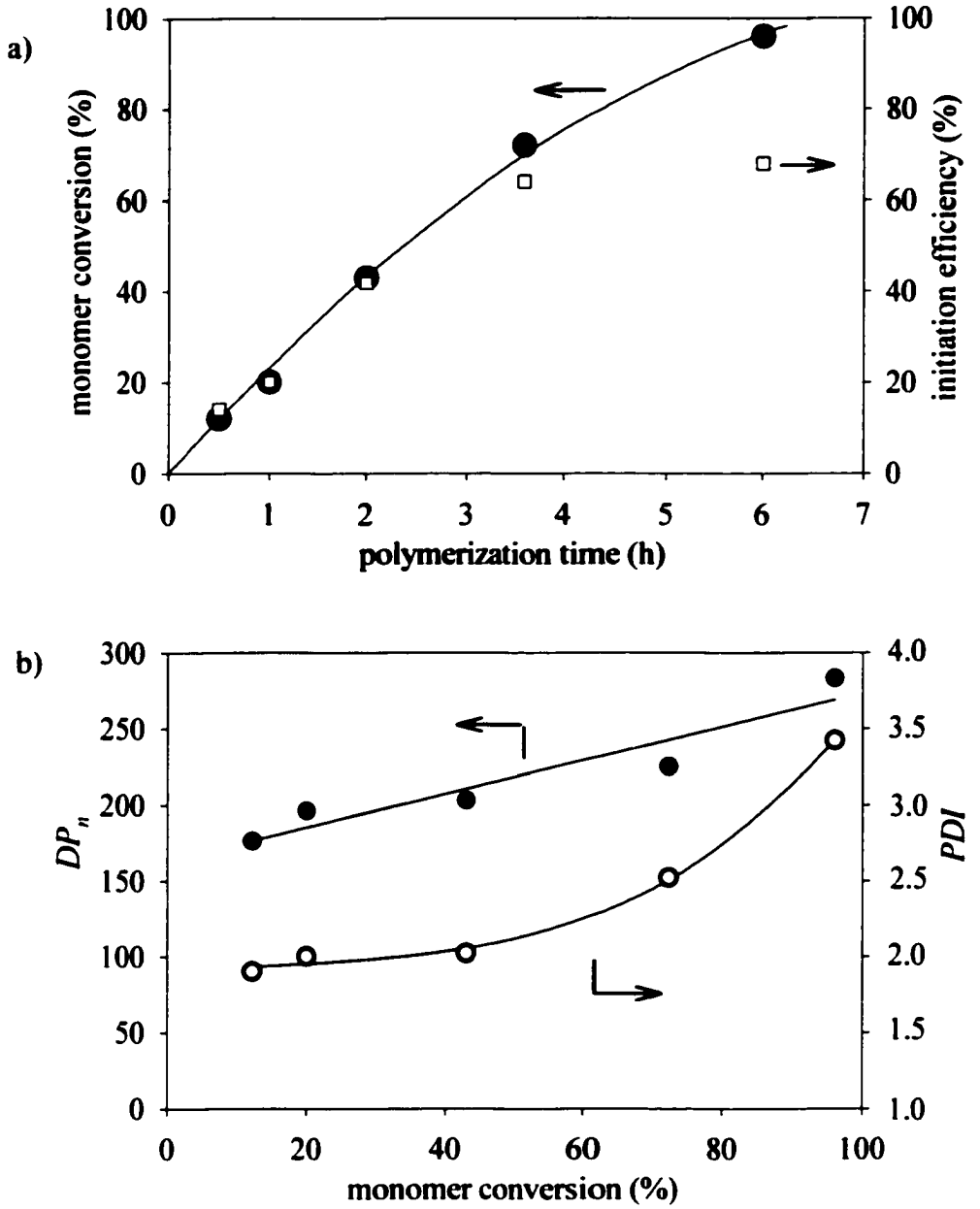

Figure 6-4. Polymerization characteristics of radical polymerization of styrene initiated by **VI-2** at 125 °C, with $[St]_0/[\textbf{VI-2}]_0 = 200$.

a) Polymerization time versus monomer conversion and initiation efficiency.

b) Monomer conversion versus DP_n and polydispersity.

of **VI-2** relative to **VI-1** and **VI-3**, the concentration of TBPM• required for the persistent radical effect is most likely to be obtained by using **VI-2** as initiator. Therefore, the study then was focused on the polymerization system initiated by **VI-2**.

Polymerization characteristics of radical polymerization of styrene initiated by **VI-2** was investigated through a series of polymerization experiments at 125°C with initial molar feed ratio of styrene to initiator of 200 (**VI-4b2**, **VI-4b3**, **VI-4b4**, **VI-4b5**, and **VI-4b6**). As shown in **Figure 6-4**, the monomer conversion increased steadily with polymerization time, and nearly completed within 6h. Initiation efficiency was also increased gradually with polymerization time, indicating the gradual occurrence of thermal homolytic dissociation of **VI-2** during the polymerization. For the first three trials with polymerization time of 0.5 h, 1 h, and 2 h, the GPC analyses of corresponding polymerization solutions showed evident GPC peaks of initiator **VI-2**. The final calculated initiation efficiency of 68% at polymerization time may be somewhat lower than the real value, because significant amounts of **VI-2** might decompose after most monomer was consumed, yielding polymer species with quite low DP_n that could be lost readily by precipitation. Because the gradual occurrence of thermal homolytic dissociation of **VI-2**, polymers were produced from polymerization system gradually, and the longer the polymerization time, the more different reaction courses of radical chain carriers would be expected. Therefore, **VI-4** yielded has increased polydispersity with polymerization time and monomer conversion. However, the increasing DP_n of **VI-4** with monomer conversion and monomodal molecular weight distribution for **VI-4** suggests that the polymerization system has some living characteristics due to TBPM• mediation.

6-4 Radical Polymerization of MMA Initiated by TBPM-Based Thermal Initiators

Radical polymerization of MMA initiated by TBPM-based thermal initiators VI-1, VI-2, and VI-3 was investigated to study the mediation effects of TBPM• in the polymerization system. Surprisingly, in contrast to certain degree of mediation of TBPM•

Schene 6-8

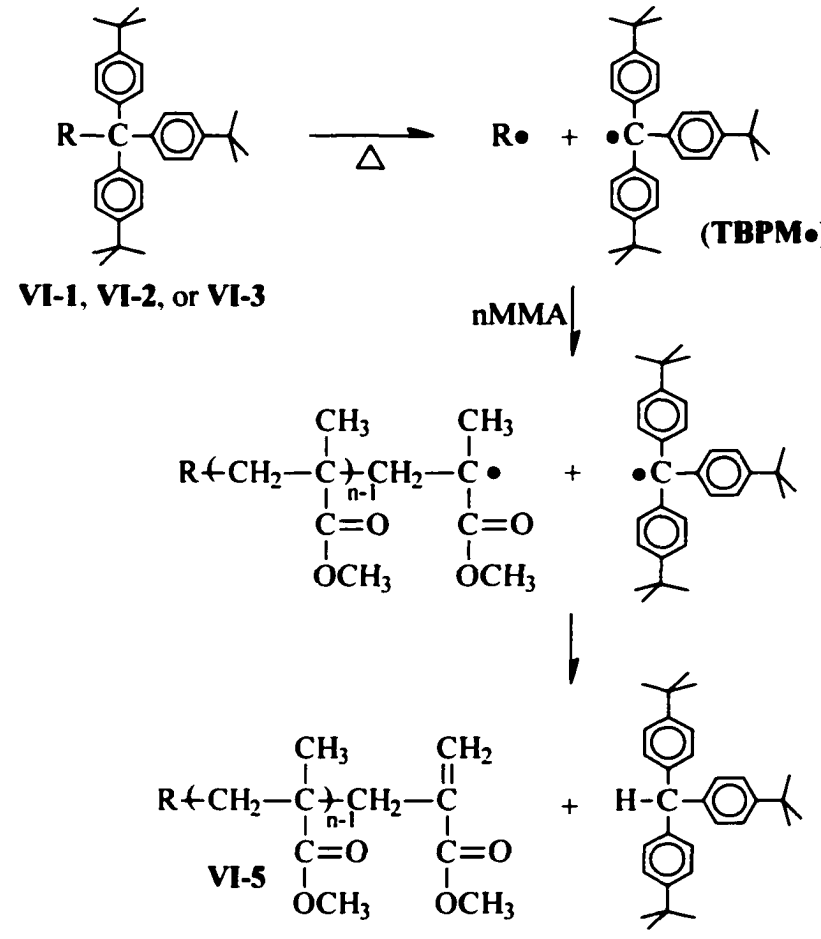

R: $Ph(CH_3)CH$ for VI-1, $CH_3OCO(Ph)CH$ for VI-2, ^{s}Bu-PSt for VI-3.

to radical polymerization of styrene, no mediation of TBPM• to radical polymerization of MMA can be detected. On the other hand, the obvious role that TBPM• can play in radical polymerization of MMA is to abstract β-hydrogen of propagating poly(MMA) radical, yielding PMMA **VI-5** with ω-unsaturation (**Scheme 6-8**).

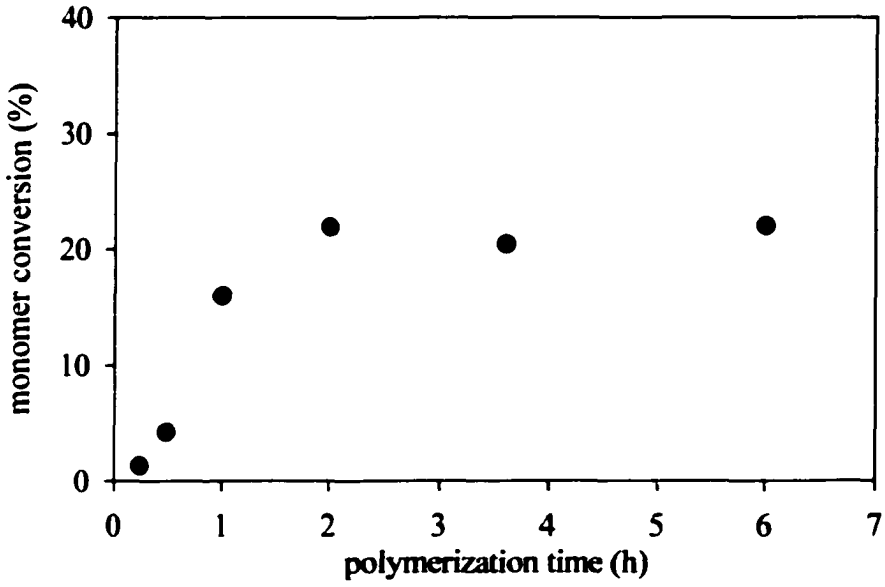

Figure 6-5. The relationship between polymerization time and monomer conversion for radical polymerization of MMA initiated by **VI-2** at 125 °C with $[MMA]_0/[VI\text{-}2]_0$ of 200.

A series of radical polymerization experiments of MMA initiated by **VI-2**, which has much faster thermal homolytic dissociation than **VI-1** and **VI-3**, were carried out at 125 °C with the molar feed ratio of MMA to **VI-2** of 200. Polymerization times were 0.25 h, 0.5 h, 1 h, 2 h, 3.6 h, and 6 h. As shown in **Figure 6-5**, monomer conversion increased with polymerization time only in about first 2 h, and then polymerization actually stopped at conversion around 20%, and no considerable increasing in conversion

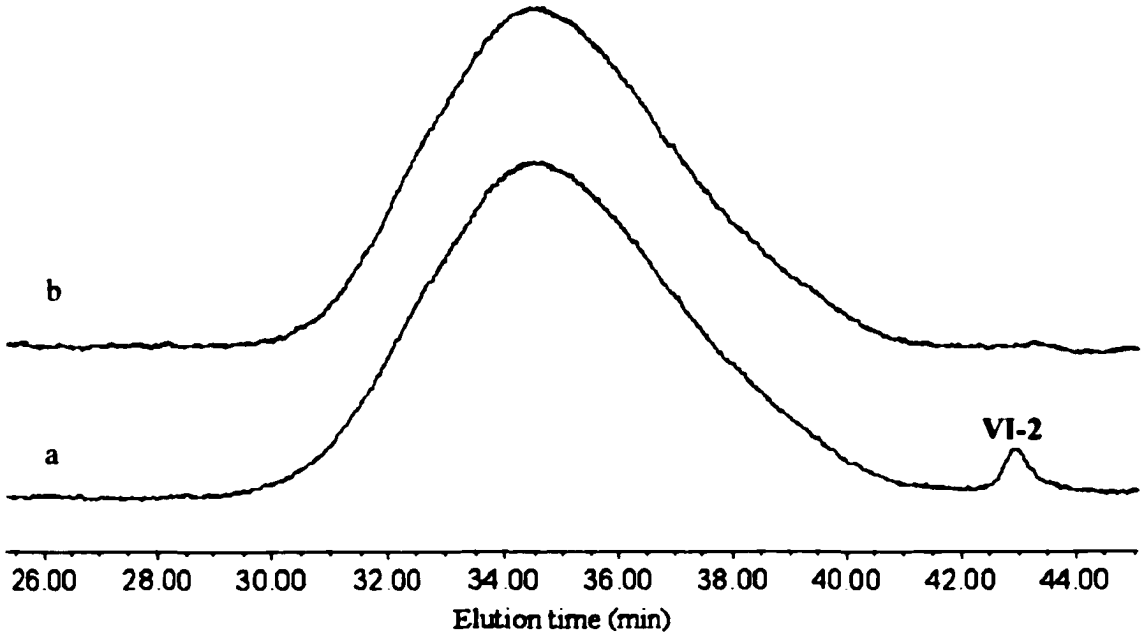

Figure 6-6. GPC curves of **VI-5** synthesized by radical polymerization of MMA initiated by **VI-2** at 125 °C with $[MMA]_0/[VI\text{-}2]_0$ of 200.

a) Polymerization time: 0.25h; M_n = 6560; DP_n = 64.0; PDI = 1.79.

b) polymerization time: 6h; M_n = 6580; DP_n = 64.2; PDI = 1.73.

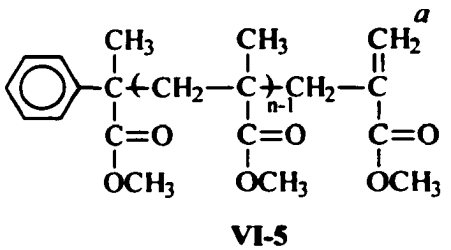

VI-5

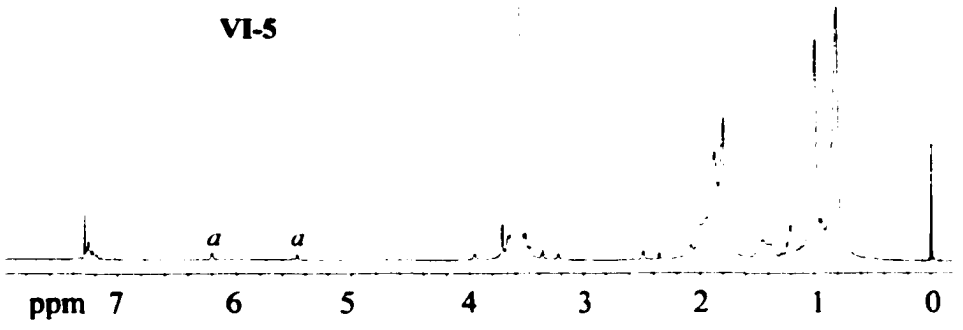

Figure 6-7. ^1H NMR spectrum of **VI-5** (synthesized by using **VI-2** as initiator)

can be detected for prolonged polymerization time. GPC analysis further indicated that no observable change in DP_n or polydispersity of poly(MMA) **VI-5** relative to polymerization time. As shown in **Figure 6-6**, two **VI-5** samples produced at polymerization times of 0.25 h and 6 h respectively had very close polydispersities, very similar shapes of GPC curves, and nearly the same, relatively low M_n and DP_n values. All the above results suggest that the existence of TBPM• in the polymerization system had no detectable mediation effects but promoted severe occurrence of side reactions, and such suggestions were supported by ^{1}H NMR analysis of **VI-5** (**Figure 6-7**). Poly(MMA) **VI-5** has no ω-TBPM functionality based on the absence of characteristic resonance at 1.27 ppm for its *tert*-butyl methyl protons, suggesting that (reversible) termination of propagating poly(MMA) radical with TBPM• by coupling required for mediation cannot be obtained. This further indicates the possibility that the covalent bond proposed between poly(MMA) and TBPM moiety cannot be formed due to insuperable steric hindrance (**Scheme 6-9**). On the other hand, on ^{1}H NMR spectra of **VI-5**, small resonances at 6.15 and 5.41 ppm were observed and were assigned to polymer chain-end alkene protons. Based on DP_n of **VI-5** determined by GPC, quantitative ^{1}H NMR analysis further showed that **VI-5** has ω-unsaturation predominantly. Because ordinary bimolecular termination of polymer radical must yield some saturated ω-chain-ends, the exclusive ω-unsaturation of **VI-5** indicated that TBPM• played the key role in termination of propagating poly(MMA) radicals by seizing its β-hydrogen, and such β-hydrogen abstraction was the key chain-breaking event in the radical polymerization system. At the same time, the formed tri-*p*-*t*-butylphenylmethane is not a very effective chain transfer agent, otherwise significant amounts of **VI-5** would have ω-saturation.

Thus, potentially TBPM• can be used to synthesize macromonomers by β-hydrogen abstraction [*29-31*].

Scheme 6-9

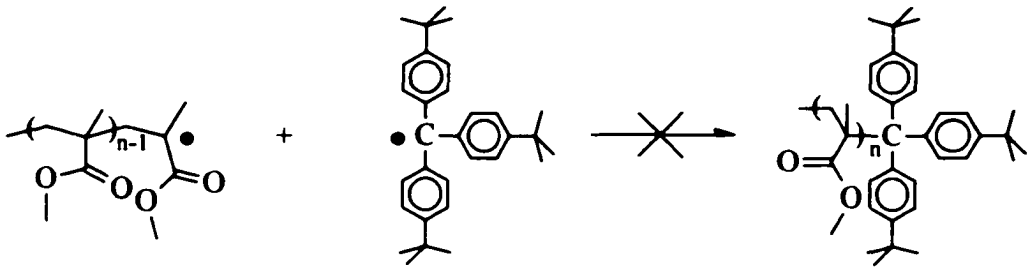

Table 6-2. Radical Polymerization of MMA Initiated by TBPM-Based Initiators [a]

entry	initiator	time(h)	conv(%)	DP_n [a]	PDI [a]
VI-5a	**VI-1**	2	10.5	3340	3.97
VI-5b	**VI-2**	13	~100	1130	2.22
VI-5c	**VI-3**	2	8.6	1110	1.91

[a] $[MMA]_0/[initiator]_0 = 200$. [b] By GPC relative to linear polystyrenes.

Although TBPM• is relatively reactive for β-hydrogen abstraction, poly(MMA) with high DP_n values can still be synthesized using TBPM-based thermal initiators. The key of such synthesis is to suppress the concentration of TBPM• in the polymerization system through relatively slow thermal decomposition of initiators. As shown in **Table 6-2**, by choosing a lower polymerization temperature (100 °C) for polymerization using **VI-2** as initiator, poly(MMA) **VI-5b** with high DP_n and monomodal molecular weight distribution was formed with nearly complete yield. Poly(MMA) **VI-5a** and **VI-5c** with

high DP_n were also produced using **VI-1** and **VI-3** as initiator respectively. Due to the very slow thermal homolytic decomposition of **VI-1** and **VI-3**, low yields of poly(MMA) were obtained within polymerization time of 2 h for the two trials. But because most initiators were not consumed in the polymerization systems, according to GPC analyses of polymerization solution, and the yields were expected to be improved by prolonged polymerization time. Noteworthily, because the initiator **VI-3** is polystyrene-TBPM adduct, **VI-5c** formed actually was a diblock copolymer of styrene and MMA. With relatively high molecular weights, quantitative ^{1}H NMR analysis of ω-end-group cannot be performed accurately. However, because the concentration of TBPM• was not significantly high, ordinary bimolecular termination of propagating poly(MMA) radicals was expected to occur at a considerable level, yielding significant amounts of polymers without ω-unsaturation.

Compared with Ostu's report on radical polymerization of MMA initiated by PAT which showed weak mediation from trityl radical, current observation of no mediation effects from TBPM• stable radical on MMA suggest two possibilities. One is as indicated before, it is the steric hindrance from the three *tert*-butyl substitution that inhibits the tertiary radical site of TBPM•, and prevents it from coupling with poly(MMA) radical. The other possibility is the limited mediation from trityl radical to radical polymerization of MMA might actually be realized by (irreversible) termination poly(MMA) radical with trityl radical through its *para* position as shown in **Scheme 6-2b**. Further investigation is required to establish the nature of the reaction between trityl radical and poly(MMA) radical.

6-5 Experimental

Materials. Nitrogen (99.998%, Welco) was used as protecting atmosphere for reactions. Acetic acid (>99.7%, Aldrich), acetic anhydride (98%, Aldrich), hydrobromic acid (48%, Aldrich), tetrafluoroboric acid (54% in ether, Aldrich), cycloheptatriene (90%, Aldrich), *n*-butyllithium (2.0 M in cyclohexane, Aldrich) and *sec*-butyllithium (1.3 *M* in cyclohexane, Aldrich) were used as received. Tetrahydrofuran (THF; 99.9%, Acros) was refluxed overnight over CaH_2 and then distilled from sodium naphthalene. Benzene (99.9%, Acros) was distilled over CaH_2 and then distilled from 1,1-diphenylhexyllithium. Styrene (>99.5%, Acros) was dried over CaH_2 and then distilled from sodium. Methyl methacrylate (MMA; 99%, Aldrich), 1-bromo-4-*tert*-butylbenzene (98%, Aldrich), methyl 4-*tert*-butylbenzoate (99%, Aldrich), and (1-bromoethyl)benzene (97%, Aldrich) were distilled over CaH_2. Methyl α-bromophenylacetate (97%, Aldrich) was dried with CaH_2 and degassed. Magnesium (98%, turnings, Aldrich) was heated at 120 °C for 12 h before use.

Synthesis of Tri-(*p*-*t*-butylphenyl)methanol. Grignard reagent was prepared by reacting 1-bromo-4-*tert*-butylbenzene (25.0 g, 117 mmol) with magnesium (2.85 g, 117 mmol) in THF. Methyl 4-*tert*-butylbenzoate (7.96 g, 41 mmol) was diluted with THF, and then added into the solution of Grignard reagent. After refluxing for 3 h, the reaction solution was cooled down, and most THF was removed under reduced pressure. Aqueous ammonium chloride solution was added gradually until the reaction solution became neutral. Reaction solution was extracted with CH_2Cl_2, and the organic phase collected was dried with $MgSO_4$, evaporated to dryness, and separated by flash column

chromatography (pentane-dichloromethane gradient) to give tri-(*p*-*t*-butylphenyl)methanol (14.3 g, 33 mmol, 79% yield). ^{1}H NMR (200 MHz, $CDCl_3$, δ): 7.39-7.11 (m, 12H, Ar-H), 2.74 (s, 1H, OH), 1.30 (s, 27H, 9 × CH_3).

Synthesis of Tri-(*p*-*t*-butylphenyl)methane. Tetrafluoroboric acid (3 mL of ether solution, 22 mmol) was added to 50 mL of acetic anhydride. Then tri-(*p*-*t*-butylphenyl)methanol (6.13 g, 14 mmol) was introduced. The mixture was heated at 70 °C to give a dark red solution of tri-(*p*-*t*-butylphenyl)methyl fluoroborate. Cycloheptatriene (2.40 g, 26 mmol) was added. The red color of solution faded with the formation of tropilium fluoroborate precipitate. After cooling the reaction mixture and removing precipitate by filtration, the filtrate was extracted with CH_2Cl_2, and the organic phase collected was dried with $MgSO_4$, evaporated to dryness, and separated by flash column chromatography (pentane-dichloromethane gradient) to give tri-(*p*-*t*-butylphenyl)methane (4.98 g, 12 mmol, 85% yield). ^{1}H NMR (200 MHz, $CDCl_3$, δ): 7.32-6.98 (m, 12H, Ar-H), 5.40 (s, 1H, CH), 1.27 (s, 27H, 9 × CH_3).

Synthesis of Tri-(*p*-*t*-butylphenyl)methyl Bromide. Tri-(*p*-*t*-butylphenyl)methanol (3.33 g, 7.8 mmol) was dissolved in 100 mL acetic acid at 70 °C, followed by addition of 10 mL of hydrobromic acid (47 wt.%). After heating the solution at 100 °C for 5 min, the solution was cooled in ice. The solid product collected by filtration was recrystallized from toluene-*n*-hexane to give tri-(*p*-*t*-butylphenyl)methyl bromide (3.53 g, 7.2 mmol, 92% yield). ^{1}H NMR (200 MHz, $CDCl_3$, δ): 7.33-7.13 (m, 12H, Ar-H), 1.32 (s, 27H, 9 × CH_3).

Synthesis of 1,1,1-tri-(*p*-*t*-butylphenyl)-2-phenyl-2-methylethane (VI-1). An excess of *n*-butyllithium was added into the THF solution of tri-(*p*-*t*-butylphenyl)methane

(0.445 g, 1.08 mmol) at −78 °C under nitrogen. The reaction solution was allowed to gradually warm to room temperature to give a dark red tri-(*p*-*t*-butylphenyl)lithium solution within 90 min. Then (1-bromoethyl)benzene was added dropwise into the solution until its red color disappeared. Solvent was removed from the solution under reduced pressure. Water and CH_2Cl_2 were added into the reaction mixture followed by extraction. The organic phase collected was dried with $MgSO_4$, evaporated to dryness, and separated by flash column chromatography (pentane-dichloromethane gradient) to give **VI-1** (0.16 g, 0.31 mmol, 29% yield). ^{1}H NMR (200 MHz, $CDCl_3$, δ): 7.36-6.45 (m, 17H, Ar-H), 4.65 (q, 1H, CH), 1.33-1.24 (m, 30H, 10 × CH_3).

Synthesis of Methyl α-Tri-(*p*-*t*-butylphenylmethyl)phenylacetate (VI-2). Synthesis followed the procedure used in the synthesis of **VI-1** but using methyl α-bromophenylacetate instead of (1-bromoethyl)benzene as a reactant, to give **VI-2** in 24% yield. ^{1}H NMR (200 MHz, $CDCl_3$, δ): 7.44-6.63 (m, 17H, Ar-H), 5.60 (s, 1H, CH), 3.52 (s, 3H, CH_3), 1.27 (s, 27H, 9 × CH_3).

Synthesis of Polystyrene-TBPM Adduct (VI-3). Anionic polymerization of styrene (2 mL, 1.91 g, 18.4 mmol) using *sec*-butyllithium (0.54 mmol) as initiator was carried out in benzene at room temperature for 30 min. Then excess of tri-(*p*-*t*-butylphenyl)methyl bromide was added. The reaction solution was precipitate into methanol to give **VI-3** as a white solid. ^{1}H NMR (200 MHz, $CDCl_3$, δ): 7.37-6.12 (m, all Ar-H), 1.85 (br, CH of St), 1.43 (br, CH_2 of St), 1.27 (s, CH_3 of TBPM). ^{13}C NMR (200 MHz, $CDCl_3$, δ): 145.2, 127.9, 127.5, 125.6, 43.7, 40.3, 34.1, 31.3 (*t*-butyl methyl carbons of TBPM).

Radical Polymerization. After standing under vacuum for hours, initiator (**VI-1**, **VI-2**, or **VI-3**) was dissolved in styrene or MMA in a glass tube under nitrogen. The contents were degassed and sealed. Then the tube was wrapped with aluminum film to keep its contents in the dark, and was heated in an oil bath. After the designated time, the polymerization was quenched by removing the tube from oil bath and cooling it to room temperature. The polymerization solution, which was diluted with THF if solidified or too viscous, was precipitated in methanol or pentane to give the polymer product **VI-4** or **VI-5**. ^{1}H NMR (**VI-4**) (200 MHz, $CDCl_3$, δ): 7.37-6.12 (m, all Ar-H), 1.85 (br, CH of St), 1.43 (br, CH_2 of St), 1.27 (s, CH_3 of TBPM). ^{1}H NMR (**VI-5**, from **VI-2**) (200 MHz, $CDCl_3$, δ): 7.40-6.97 (m, 5H of Ar-H from **VI-2**), 6.20 (1H of =CH*H*), 5.48 (1H of =C*H*H), 3.60 (s, 3H of OCH_3 of MMA), 2.26-1.42 (m, 2H of CH2 of MMA), 1.42-0.66 (m, CH_3 of MMA).

Characterization. ^{1}H NMR and ^{13}C NMR analyses were carried out at room temperature on a Varian 200 MHz spectrometer with $CDCl_3$ as solvent and tetramethylsilane as internal reference. For each spectrum, 64 transients were collected with pulse angle of 31.5° and delay time of 2 s.

GPC analyses were performed at 40 °C on a Waters-150C GPC instrument equipped with a refractive index detector, four styragel columns (HR1, HR3, HR4, HR5E), using THF as eluent at 1.0 mL/min. The instrument was calibrated with narrow-disperse linear polystyrene standards.

6-6 Conclusions

TBPM-based compounds can be applied as thermal initiator for radical polymerization, releasing an active radical as initiating radical and TBPM• stable carbon-centered radical as mediating radical. TBPM• has no detectable mediation effects on radical polymerization of MMA presumably due to steric hindrance, but has relatively high reactivity for hydrogen transfer to result in poly(MMA) with predominate ω-unsaturation. TBPM• has observable mediation effects on radical polymerization of styrene, indicated by ω-TBPM functionality in the polystyrene yielded, the initiating capacity of PS-TBPM adduct, and the increased DP_n with monomer conversion. However, sufficient mediation, which is required for typical LRP system to effectively average the reaction courses of chain carriers, could not be obtained in the radical polymerization system.

To develop successful LRP system based on mediation using stable carbon-centered radical, further structure design of stable radical is needed. Severe steric hindrance around radical center should be avoided. Stability of carbon-centered radical needs to be improved based on enthalpic effects (other than steric effects), in order to specifically increase the thermal homolytic dissociation reactivity of the labile bond in dormant species, which is responsible for releasing initiating/propagating radical and stable carbon-centered radical.

Chapter 7

Investigation of Stable Free Radical Polymerization of Methacrylates Initiated by PS-TEMPO Adduct

Abstract: To reconcile conflicting reports on stable free radical polymerization (SFRP) of methacrylates initiated by PS-TEMPO adduct, a series of polymerization experiments of MMA and *n*-BMA were carried out in bulk at 130 °C under argon without initial addition of TEMPO, following exactly the reaction conditions used by Yousi (*Macromolecules* 2000, *33*, 4745). In contrast to reported successes, the polymerization showed no living characteristics, and polymers were formed with very low monomer conversion, relatively high polydispersities, and bimodal molecular weight distribution. Polymerization actually stopped within relatively short polymerization time, presumably due to severe occurrence of undesirable side reactions. Occurrence of β-hydrogen abstraction was supported by ^{1}H NMR evidence of ω-unsaturation. However, the observation of only about 40% of polymer chains with ω-unsaturation further suggests that other chain-breaking processes, such as hydroxylamine termination, should also occur at a significant level. The major polymerization characteristics of SFRP of *n*-BMA from our results agreed well with data obtained under similar reaction conditions by Burguière et al. (*Macromolecules* 1999, *32*, 3883).

7-1 Introduction

Stable free radical polymerization (SFRP) of methacrylate monomers is of significant research interests for many polymer synthetic chemists [*1*]. Hawker et al. reported the synthesis of well-defined random copolymers of methacrylate and styrene by nitroxide-mediated radical copolymerization with high feed fractions of styrene [*2, 3*], and the synthetic strategy was further applied to synthesize poly(styrene-*b*-(styrene-*co*-*n*-butyl methacrylate)) block copolymer by Butz et al. [*4*]. The kinetics of nitroxide-mediated radical copolymerization of butyl methacrylate with styrene was investigated by Cuervo-Rodriguez et al. [*5*]. However, many attempts to homopolymerize methacrylates by SFRP using nitroxide as mediating radical yielded polymers with very low conversions [*6-9*]. Such results generally were ascribed to the degradation of propagating radicals via β-hydrogen abstraction by nitroxide (**Scheme 7-1**), followed by the resulting hydroxylamine acting as a chain terminating agent for a second propagating chain with nitroxide recovered [*1, 10*]. Most recently, White et al. reported high conversions in SFRP of methacrylates based on new types of mediating radicals, but the polydispersities of polymers produced were relatively high (1.6-2.17) [*11*].

Scheme 7-1

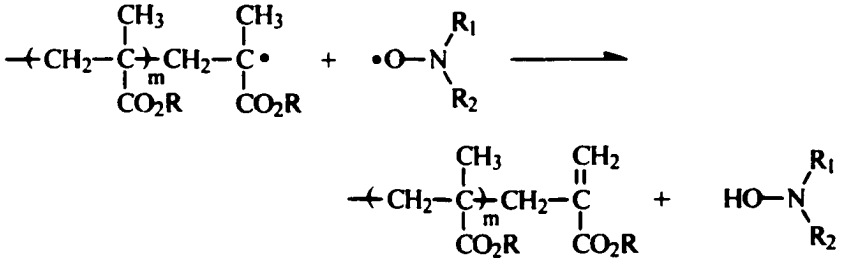

Surprisingly, without consideration of β-hydrogen abstraction, Yousi reported typical living radical polymerization characteristics for SFRP of methacrylates initiated by PS-TEMPO adduct [*12*]. Well-defined diblock copolymers with high conversions and low polydispersities were described as products for bulk polymerization of a variety of methacrylate monomers, including methyl methacrylate (MMA), ethyl methacrylate (EMA), *n*-butyl methacrylate (*n*-BMA), and *n*-octyl methacrylate (*n*-OMA). These data do not agree with the results of others obtained for the same monomers under very similar reaction conditions. Steenbock et al. reported that polymerization of MMA initiated by PS-TEMPO adduct was only observed in the presence of camphorsulfonic acid in the polymerization system, yielding polymers with bimodal molecular weight distribution; otherwise, no polymerization of MMA could be detected by GPC analysis [*6*]. Burguière et al. studied the polymerization of *n*-BMA initiated by PS-TEMPO adduct, but found that conversion was very low and the polydispersities of polymers formed could be relatively high [*9*]. Based on MALDI and ^{1}H NMR analyses, they further identified that poly(styrene-*b*-*n*-butyl methacrylate) block copolymers possessed ω-unsaturation exclusively and therefore concluded that the main chain-breaking event is the β-hydrogen abstraction. The present investigation is an attempt to reconcile the above conflicting reports. We carried out a series of polymerization experiments of MMA and *n*-BMA following the methods and the exact reaction conditions used by Yousi. However, in contrast to data reported by Yousi, our polymerization results showed no living polymerization characteristics at all for the polymerization systems. On the other hand, our results generally agreed well with those of Burguière et al., and had explainable differences with the results of Steenbock et al.

7-2 Results and Discussion

PS-TEMPO adduct was synthesized following the method used by Yousi, and was characterized by GPC and ^{1}H NMR. GPC analysis showed that it has a number-average molecular weight (M_n) of 4830 and a low polydispersity of 1.14. ^{1}H NMR analysis verified its TEMPO-functionalized chain-end through the resonance (4.01, 4.43, 4.56 ppm) of its benzylic methine proton of the styrene monomer unit bonded to the piperidinyloxyl group [*13*]. Initiating capacity of the PS-TEMPO adduct was demonstrated by polystyrene chain extension experiment, which was carried out by bulk polymerization of styrene at 130 °C using the adduct as macroinitiator. Quantitative TEMPO-based alkoxyamine functionality on the PS-TEMPO adduct was deduced based on the complete disappearance of its GPC peak on the GPC curve of its chain-extended product (**Figure 7-1**). Well-controlled molecular weight ($M_{n,calcd.}$ = 25 700; $M_{n,\,GPC}$ = 27 400) and low polydispersity (1.24) of the chain-extended product further illustrated that the polymerization procedure and conditions used were suitable for SFRP experiments.

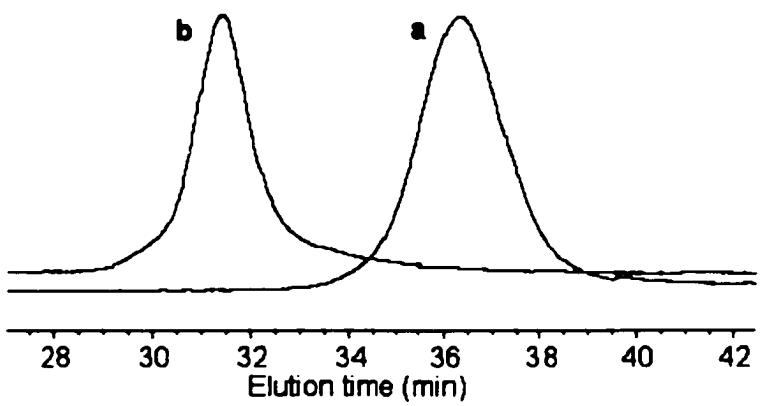

Figure 7-1. GPC curves of PS-TEMPO adduct (**a**), and its chain-extended product (**b**).

Table 7-1. SFRP of MMA and *n*-BMA initiated by PS-TEMPO [a]

			conversion (%)		M_n	*PDI*	$N_{methacrylate}$ [e]
entry [b]	$[M]_0/[I]_0$ [c]	time (h)	exptl	calcd	(GPC[d])	(GPC[d])	(GPC[d])
PS-M1	290	0.5	6.7	5.1(6.2[f])	6160	1.56	14.9(18.1[f])
PS-M2	290	1	6.7	4.9	6080	1.57	14.1
PS-M3	290	2	6.7	5.3	6200	1.52	15.3
PS-M4	290	3.8	7.2	5.1	6140	1.52	14.7
PS-M5	290	5	6.8	4.8	6070	1.59	14.0
PS-B1	290	0.5	6.9	4.7	6600	2.01	13.6
PS-B2	290	5	7.5	5.4	6902	1.85	15.7
PS-B3	396	2	6.2	4.7 (5.0[f])	7330	1.75	18.7 (19.9[f])

[a] Bulk polymerization; 130 °C; argon atmosphere. [b] MMA: the monomer used for PS-M series; *n*-BMA: the monomer used for PS-B series. [c] Molar feed ratio of monomer to PS-TEMPO adduct. [d] Calibrated with linear polystyrenes. [e] Average number of MMA or *n*-BMA monomer units in polymer. [f] By ^{1}H NMR.

A series of SFRP experiments of MMA and *n*-BMA initiated by PS-TEMPO adduct were carried out following exactly the reaction conditions reported by Yousi, and the results were shown in **Table 7-1**. Very low monomer conversion of only few percent for polymerization of MMA and *n*-BMA was observed in all trials. Moreover, no significant change in monomer conversion was observed with polymerization time ranging from 0.5 to 5 h. It can be inferred that, similar to SFRP of 2-(dimethylamino)ethyl methacrylate initiated by PS-TEMPO adduct [*8*], polymerization of

MMA and *n*-BMA actually stopped within a relatively short polymerization time (0.5 h), presumably due to severe occurrence of undesirable side reactions.

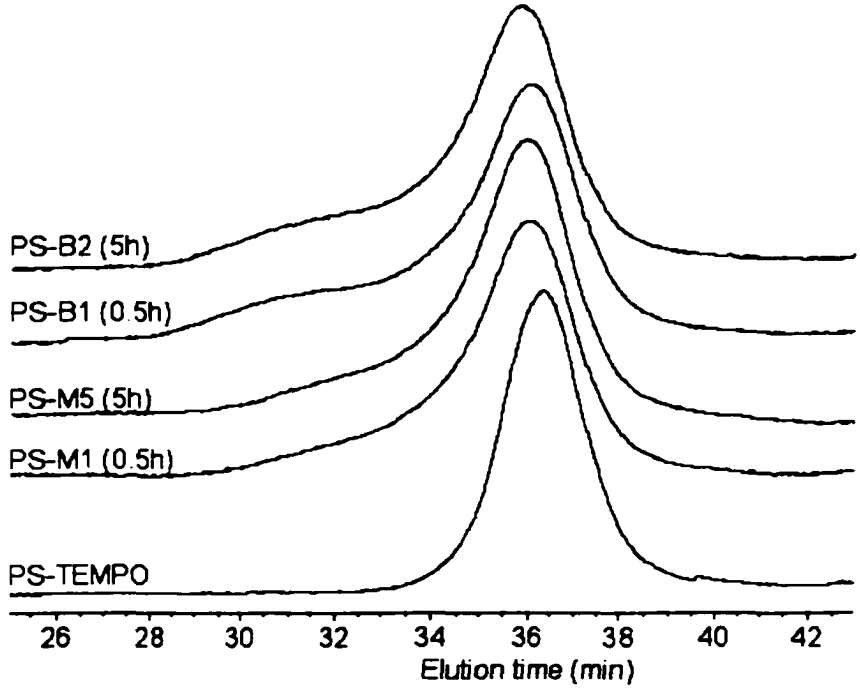

Figure 7-2. GPC curves of the products of polymerization of MMA and *n*-BMA, compared with the GPC curve of PS-TEMPO adduct used as macroinitiator.

Relatively high polydispersities (1.52-1.59 for MMA; 1.75-2.01 for *n*-BMA) and bimodal GPC curves were also observed for the trials (**Figure 7-2**). The molecular weights corresponding to the major GPC peaks are only slightly higher than the molecular weight for the GPC peak of the PS-TEMPO adduct, indicating that most polymer chains lost activity with at most a few methacrylate monomer units incorporated. Meanwhile, long tails to high molecular weight side were observed in all trials, illustrating that small amounts of polymer chains formed have relatively long

polymethacrylate block. Because the occurrence of important side reactions, especially β-hydrogen abstraction, depend on the concentration of nitroxide in the polymerization system, these small amounts of polymers with many methacrylate monomer units are expected to be formed at the initial stage of polymerization before concentration of TEMPO was significantly built up.

In the 600 M Hz ^{1}H NMR spectra of the polymers formed, we could not observe any characteristic ^{1}H NMR resonances for the methyl protons of TEMPO moiety that were claimed by Yousi, indicating essentially the absence of TEMPO-based alkoxyamine functionality in polymers we obtained. On the other hand, for both MMA or *n*-BMA used as monomer, small resonances around 5.46 and 6.19 ppm, which were not described by Yousi but reported by Burguière et al. for polymerization of *n*-BMA, were always observed by us. These resonances were assigned to the two protons of the terminal methylene unsaturation of polymers, suggesting the occurrence of β-hydrogen abstraction during polymerization (**Figure 7-3**). Quantitative analysis based on the intensities of these resonances showed that nearly 40% of polymer chains have ω-unsaturation, suggesting that besides β-hydrogen abstraction, other chain-breaking processes, especially termination of propagating chain with hydroxylamine formed by β-hydrogen, could also be important in our polymerization systems. This ^{1}H NMR result apparently differs from the MALDI result of Burguière et al. which showed that the polymers that they synthesized by polymerization of *n*-BMA have ω-unsaturation exclusively. However, the MALDI data they presented were for the polymers synthesized from polymerization systems with initial addition of TEMPO, which could have significantly promoted the occurrence of β-hydrogen abstraction.

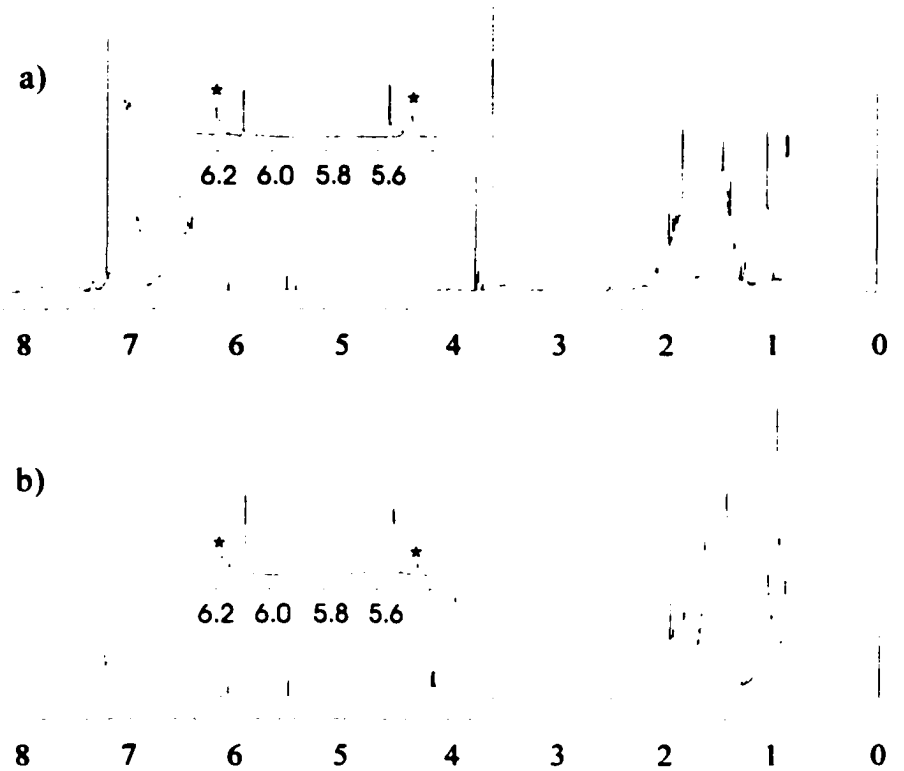

Figure 7-3. ^{1}H NMR spectra of a) PS-M1 and b) PS-B3.

(Resonances marked with star are around 5.46 and 6.19 ppm; sharp resonances at 5.55 and 6.10 ppm are for alkene protons of traces of methacrylate monomer in polymers)

7-3 Experimental

Materials. Argon (99.998%, Welco) was used as protecting atmosphere for all reactions. 2,2,6,6-Tetramethylpiperidinooxy (TEMPO, 98%, Acros) and benzoyl peroxide (BPO, 97%, Aldrich) were used without further purification. Styrene (>99.5%, Acros), methyl methacrylate (MMA; 99%, Aldrich), and *n*-butyl methacrylate (*n*-BMA; 99%, Acros) were distilled over CaH_2 before use.

Synthesis of PS-TEMPO Adduct. BPO (0.52 g, 2.14 mmol) and 1.2 equivalents of TEMPO (0.40 g, 2.56 mmol) were dissolved in styrene (22.4 g, 0.235 mol). The reaction mixture was first heated at 95 °C for 3 h, and then heated at 125 °C for 20 h. The polymerization solution was precipitated in methanol, and the polymer recovered was dissolved in THF and precipitated in methanol twice to remove traces of TEMPO. Finally 8.14 g of the final product was obtained in 33% yield.

Polystyrene Chain Extension from PS-TEMPO. After standing under vacuum for hours, PS-TEMPO adduct (0.145 g) was dissolved in styrene (1 mL, 0.905 g) in a glass tube under argon. The contents were degassed, sealed, and then heated at 130 °C in an oil bath for 5.6 h. The polymerization was quenched by removing the sealed tube from oil bath and cooling it to room temperature. The polymerization solution was diluted with THF, and then was precipitated in methanol to give product (0.772 g, 69% yield).

Polymerization of Methacrylates. Polymerization followed the procedure used in polystyrene chain extension from PS-TEMPO but using MMA or *n*-BMA as monomer with different polymerization times. To avoid underestimating monomer conversion by the precipitation process, monomer remaining in the polymerization solution was removed under vacuum at 70 °C for 48 h, and monomer conversion was determined based on the weights of polymers thus obtained and occasionally was also checked by ^{1}H NMR.

Characterization. ^{1}H NMR analyses were carried out at room temperature on a Varian 600 MHz spectrometer with $CDCl_3$ as solvent and tetramethylsilane as internal reference. For each spectrum, 64 transients were collected with pulse angle of 39° and delay time of 3 s.

GPC analyses were performed at 40 °C on a Waters-150C GPC instrument equipped with a refractive index detector, four Styragel columns (HR1, HR3, HR4, HR5E), using THF as eluent at 1.0 mL/min. The instrument was calibrated with narrow-disperse linear polystyrene standards.

7-4 Conclusions

Following exactly the reaction conditions described in Yousi's report, we could not succeed in SFRP of methacrylates, and our results drastically differed in main aspects from Yousi's results which include high conversion, low polydispersities, monomodal molecular weight distribution, steady increase in conversion over hours, and ^{1}H NMR evidence of alkoxyamine functionality in polymers. We found that SFRP of MMA and *n*-BMA initiated by PS-TEMPO adduct was a very sluggish process, yielding polymers with very low monomer conversion, relatively high polydispersities, and bimodal molecular weight distribution. The polymerization actually stopped within relatively short polymerization time, presumably due to severe occurrence of undesirable side reactions, including β-hydrogen abstraction and hydroxylamine termination. Under similar reaction conditions, our results of SFRP of *n*-BMA agreed well with the results from Burguière et al. in major polymerization characteristics, but our results of SFRP of MMA have significant differences from the results from Steenbock et al. Their observation of no polymerization of MMA detected by GPC in the absence of camphorsulfonic acid might result from insufficient degassing or significant concentration of free TEMPO in PS-TEMPO adduct.

References and Notes

Chapter 1

1. Odian, G. *Principles of Polymerization*, 4th ed.; Wiley: New York, 2003, in press.

2. Jenkins, A. D.; Kratochvil, P.; Stepto, R. F. T.; Suter, U. W. *Pure Appl. Chem.* **1996**, *68*, 1591.

3. Szwarc, M. *J. Polym. Sci. Part A: Polym. Chem.* **1998**, 36.

4. Darling, T. R.; Davis, T. P.; Fryd, M.; Gridnev, A. A.; Haddleton, D. M.; Ittel, S. D.; Matheson, R. R.; Moad, G.; Rizzardo, E. *J. Polym. Sci. Part A: Polym. Chem.* **2000**, 1707.

5. Webster, O. W. *Science* **1991**, *251*, 887.

6. Szwarc, M. *Nature* **1956**, *178*, 1168.

7. Tahada, N.; Inoue, S. *Makromol. Chem.* **1978**, *179*, 1377.

8. Doi, Y.; Ueki, S.; Keii, T. *Macromolecules* **1979**, *12*, 814.

9. Otsu, T.; Yoshida, M. *Makromol. Chem., Rapid Commun.* **1982**, *3*, 127.

10. Webster, O. W.; Hertler, W. R.; Sogah, D. Y.; Farnham, W. B.; Rajanbabu, T. V. *J. Am. Chem. Soc.* **1983**, *105*, 5706.

11. Miyamoto, M.; Sawamoto, M.; Higashimura, T. *Macromolecules* **1984**, *17*, 265.

12. Gilliom, L. R.; Grubbs, R. H. *J. Am. Chem. Soc.* **1986**, *108*, 733

13. Sogah, D. Y.; Webster, O. W. *Macromolecules* **1986**, *19*, 1775

14. Georges, M. K.; Veregin, R. P. N.; Kazmaier, P. M.; Hamer, G. K. *Macromolecules* **1993**, *26*, 2987.

15. Hawker, C. J. *J. Am. Chem. Soc.* **1994**, *116*, 11185.

16. Kato, M.; Kamigaito, M.; Sawamoto, M.; Higashimura, T. *Polym. Prepr. Jpn.* **1994**, *43*, 1792.

17. Wang, J. S.; Matyjaszewski, K. *J. Am. Chem. Soc.* **1995**, *117*, 5614.

18. Chiefari, J.; Chong, Y. K.; Ercole, F.; Krstina, J.; Jeffery, J.; Le, T. P. T.; Mayadunne, R. T. A.; Meijs, G. F.; Moad, C. L.; Moad, G.; Rizzardo, E.; Thang, S. H. *Macromolecules* **1998**, *31*, 5559.

19. Morton, M. *Anionic Polymerization: Principles and Practice*; Academic Press: New York, 1983.

20. Hsieh, H. L.; Quirk, R. P. *Anionic Polymerization: Principles and Practical Applications*; Marcel Dekker: New York, 1996.

21. Hadjichristidis, N.; Pitsikalis, M.; Pispas, S.; Iatrou, H. *Chem. Rev.* **2001**, *101*, 3747.

22. Truett, W. L.; Johnson, D. R.; Robinson, I. M.; Montague, B. A. *J. Am. Chem. Soc.* **1960**, *82*, 2337.

23. Schrock, R. R.; Murdzek, J. S.; Bazan, G. C.; Robbins, J.; DiMare, M.; O'Regan, M. *J. Am. Chem. Soc.* **1990**, *112*, 3875.

24. Trnka, T. M.; Grubbs, R. H. *Acc. Chem. Res.* **2001**, *34*, 18.

25. Buchmeiser, M. R. *Chem. Rev.* **2000**, *100*, 1565.

26. *Controlled Radical Polymerization*; Matyjaszewski, K., Ed.; American Chemical Society: Washington, DC, 2000; Vol. 685.

27. *Controlled/Living Radical Polymerization: Progress in ATRP, NMP, and RAFT*; Matyjaszewski, K., Ed.; American Chemical Society: Washington, DC, 2000; Vol. 768.

28. Ostu, T.; Yoshida, M.; Tazaki, T. *Makromol. Chem., Rapid Commun.* **1982**, *3*, 133.

29. Solomon, D. H.; Rizzardo, E.; Cacioli, P. U.S. Patent, 4,581,429, 1986.

30. Hawker, C. J.; Bosman, A. W.; Harth, E. *Chem. Rev.* **2001**, *101*, 3661.

31. Matyjaszewski, K.; Xia, J. *Chem. Rev.* **2001**, *101*, 2921.

32. Kamigaito, M.; Ando, T.; Sawamoto, M. *Chem. Rev.* **2001**, *101*, 3689.

33. Fischer, H. *Chem. Rev.* **2001**, *101*, 3689.

34. Davis, K. A.; Matyjaszewski, K. *Adv. Polym. Sci.* **2002**, *159*, 1.

35. Kickelbick, G.; Paik, H.-j.; Matyjaszewski, K. *Macromolecules* **1999**, *32*, 2941.

36. Personal discussion with Dr. Jin-Shan Wang, one of the polymer chemists with fundamental contribution to ATRP (see ref. 17).

37. No devoted review focusing on combination of living polymerization techniques has been published. But ref. 1, 32, 34 have portions on the discussion of this topic.

38. Feldthusen, J.; Ivan, B.; Muller, A. H. E. *Macromolecules* **1998**, *31*, 578 and references therein.

39. No review paper focusing on this topic has been published yet. But ref. 34 has a portion for the discussion of this topic.

40. Ryu, S. W.; Hirao, A. *Macromolecules* **2000**, *33*, 4765 and references therein.

41. Ito, K.; Kawaguchi, S. *Adv. Polym. Sci.* **1999**, *142*, 129.

42. Grubbs, R. B.; Hawker, C. J.; Dao, J.; Fréchet, J. M. J. *Angew Chem., Int. Ed. Engl.* **1997**, *36*, 270.

43. Beers, K. L.; Gaynor, S. G.; Matyjaszewski, K.; Sheiko, S. S.; Möller, M. *Macromolecules* **1998**, *31*, 9413.

44. Mecerreyes, D.; Atthoff, B.; Boduch, K. A.; Trollsås, M.; Hedrick, J. L. *Macromolecules* **1999**, *32*, 5175.

45. Cheng, G.; Böker, A.; Zhang, M.; Krausch, G.; Müller, A. H. E. *Macromolecules* **2001**, *34*, 6883.

46. Hawker, C. J. *J. Angew Chem., Int. Ed. Engl.* **1995**, *34*, 1456.

47. Gravert, D. J.; Datta, A.; Wentworth, P., Jr.; Janda, K. D. *J. Am. Chem. Soc.* **1998**, *120*, 9481.

48. Stehling, U. M.; Malmström, E. E.; Waymouth, R. M.; Hawker, C. J. *Macromolecules* **1998**, *31*, 4396.

49. Zhang, H. M.; Ruckenstein, E. *Macromolecules* **1998**, *31*, 746.

50. Ruckenstein, E.; Zhang, H. M. *Macromolecules* **1998**, *31*, 2977.

51. Schlaad, H.; Erentova, K.; Faust, R.; Charleux, B.; Moreau, M.; Vairon, J.-P.; Mayr, H. *Macromolecules* **1998**, *31*, 8058.

52. Schlaad, H.; Kwon, Y.; Faust, R.; Mayr, H. *Macromolecules* **2000**, *33*, 743.

53. Bates, F. S. *Science* **1991**, *251*, 898.

54. Lodge, T. P.; Muthukumar, M. *J. Phys. Chem.* **1996**, *100*, 13275.

55. Héroguez, V.; Gnanou, Y.; Fontanille, M. *Macromolecules* **1997**, *30*, 4791.

56. Héroguez, V.; Amédro, E.; Grande, D.; Fontanille, M.; Gnanou, Y. *Macromolecules* **2000**, *33*, 7241.

57. Tsubaki, K.; Ishizu, K. *Polymer* **2001**, *42*, 8387 and references therein.

58. Hong, K.; Wan, Y.; Mays, J. W. *Macromolecules* **2001**, *34*, 2482 and references therein.

59. Tsitsilianis, C.; Voulgaris, D. *Macromol. Chem. Phys.* **1997**, *198*, 997 and references therein.

60. Matyjaszewski, K.; Miller, P. J.; Pyun, J.; Kickelbick, G.; Diamanti, S. *Macromolecules* **1999**, *32*, 6526.

61. Boerner, H. G.; Beers, K.; Matyjaszewski, K.; Sheiko, S. S.; Moeller, M. *Macromolecules* **2001**, *34*, 4375.

62. Djalali, R.; Li, S-Y.; Schmidt, M. *Macromolecules* **2002**, *35*, 4282.

63. Ishizu, K.; Tsubaki, K.; Uchida, S. *Macromolecules* **2002**, *35*, 10193.

64. Ma, Q.; Remsen, E. E.; Kowalewski, T.; Wooley, K. L. *J. Am. Chem. Soc.* **2001**, *123*, 4627 and references therein.

65. Huang, H.; Remsen, E. E.; Kowalewski, T.; Wooley, K. L. *J. Am. Chem. Soc.* **1999**, *121*, 3805.

66. Liu, G. *Adv. Mater.* **1997**, *9*, 437.

67. Stewart, S.; Liu, G. *Angew Chem., Int. Ed. Engl.* **2000**, *39*, 340.

Chapter 2

1. Quirk, R. Q.; Yoo, T.; Lee, Y.; Kim, J.; Lee, B. *Adv. Polym. Sci.* **2000**, 153, 67.

2. Wieland, P. C.; Raether, B.; Nuyken, O. *Macromol. Rapid Commun.* **2001**, *22*, 700.

3. Raether, B.; Nuyken, O.; Wieland, P.; Bremser, W. *Macromol. Symp.* **2002**, *177*, 25.

4. Nuyken, O.; Wieland, P. C.; Heischkel, Y.; Raether, B. *Polym. Prepr.* **2002**, *43* (2), 84.

5. Hadjikyriacou, S.; Faust, R. *Macromolecules* **1996**, *29*, 5261.

6. Cao, X.; Faust, R. *Macromolecules* **1999**, *32*, 5487.

7. Bae, Y. C.; Faust, R. *Macromolecules* **1998**, *31*, 2480.

8. Bae, Y. C.; Faust, R. *Macromolecules* **1998**, *31*, 9379.

9. Schulz, G.; Hocker, H. *Angew. Chem., Int. Ed. Engl.* **1980**, *19*, 219.

10. Tung, L. H.; Lo, G. Y.-S. *Macromolecules* **1994**, *27*, 2219.

11. Quirk, R. P.; Tsai, Y. *Macromolecules* **1998**, *31*, 8016.

12. Paraskeva, S.; Hadjichristidis, N. *J. Polym. Sci. Part A: Polym. Chem.* **2000**, *38*, 931.

13. Fujimoto, T.; Zhang, H.; Kazama, T.; Isono, Y.; Hasegawa, H.; Hashimoto, T. *Polymer* **1992**, *33*, 2208.

14. Huckstadt, H.; Abetz, V.; Stadler, R. *Macromol. Rapid Commun.* **1996**, *17*, 599.

15. Lambert, O.; Dumas, P.; Hurtrez, G.; Riess, G. *Macromol. Rapid Commun.* **1997**, *18*, 343.

16. Lambert, O.; Reutenauer, S.; Hurtrez, G.; Riess, G.; Dumas, P. *Polym. Bull.* **1998**, *40*, 143.

17. Huckstadt, H.; Gopfert, A.; Abetz, V. *Macromol. Chem. Phys.* **2000**, *201*, 296.

18. Quirk, R. P.; Yoo, T.; Lee, B. *J. M. Sci.-Pure Appl. Chem.* **1994**, *A31*, 911 and references therein.

19. Fernyhough, C. M.; Young, R. N.; Tack, R. D. *Macromolecules* **1999**, *32*, 5760.

20. Hirao, A.; Hayashi, M.; Haraguchi, N. *Macromol. Chem. Phys.* **2000**, *21*, 1171.

21. Hayashi, M.; Hirao, A. *Kobunshi Ronbunshu* **2000**, *57(12)*, 781.

22. Hirao, A.; Hayashi, M. *Macromolecules* **1999**, *32*, 6450.

23. Hirao, A.; Hayashi, M. *Acta Polym.* **1999**, *50*, 219.

24. Hayashi, M.; Kojima, K.; Nakahama, S.; Hirao, A. *Polym. Prepr.* **1998**, *39(2)*, 478.

25. Hayashi, M.; Negishi, Y.; Hirao, A. *Proc. Jpn. Acad., Ser. B* **1999**, *75B*, 93.

26. Hayashi, M.; Kojima, K.; Hirao, A. *Macromolecules* **1999**, *32*, 2425.

27. Quirk, R. P.; Mathers, R. T.; Cregger, T.; Foster, M. D. *Macromolecules* **2002**, *35*, 9964.

28. Itsuno, S.; Tanaka, S.; Hirao, A. *Bioorg. Med. Chem. Lett.* **2002**, *12*, 1853.

29. Liaw, D.-J.; Tsai, J.-S.; Wu, P.-L. *Macromolecules* **2000**, *33*, 6925.

30. Szwarc, M. *Nature* **1956**, *178*, 1168.

31. Hsieh, H. L.; Quirk, R. P. *Anionic Polymerization: Principles and Practical Applications*; Marcel Dekker: New York, 1996.

32. See Chapter 1 for the general introduction for densely grafted copolymer synthesis.

33. Djalali, R.; Li, S-Y.; Schmidt, M. *Macromolecules* **2002**, *35*, 4282.

34. Ishizu, K.; Tsubaki, K.; Uchida, S. *Macromolecules* **2002**, 10193.

35. Ishizu, K.; Shen, X.-X.; Tsubaki, K. *Polymer* **1999**, *40*, 3251 and references therein.

36. Zhang, H.; Ruckenstein, E. *Macromolecules* **1998**, *31*, 4753.

37. Ma, Q.; Remsen, E. E.; Kowalewski, T.; Wooley, K. L. *J. Am. Chem. Soc.* **2001**, *123*, 4627 and references therein.

38. Trnka, T. M.; Grubbs, R. H. *Acc. Chem. Res.* **2001**, *34*, 18.

39. Schrock, R. R.; Murdzek, J. S.; Bazan, G. C.; Robbins, J.; DiMare, M.; O'Regan, M. *J. Am. Chem. Soc.* **1990**, *112*, 3875.

40. See Chapter 5, section 5-5b.

41. Klein, J. W.; Lamps, J.-P.; Gnanou, Y.; Rempp, P. *Polymer***1991**, *32*, 2278.

42. Wang, J.-S.; Varshney, S. K.; Jérôme, R.; Teyssie, Ph. *Polym. Sci. Part A: Polym. Chem.* **1992**, *30*, 2251.

43. Quirk, R. P.; Ma, J. J. *Polym. Sci. Part A: Polym. Chem.* **1988**, 26, 2031.

44. Anderson, B. C.; Andrews, G. D.; Arthur, P., Jr.; Jacobson, H. W.; Melby, L. R.; Playtis, A. J.; Sharkey, W. H. *Macromolecules* **1981**, *14*, 1599.

45. Compared with linear polymers, double-brush copolymers have very small hydrodynamic volumes relative to their molecular weights and have weak interactions with immobile phase due to their densely grafted architectures.

46. Locomte, P.; Meccereyes, D.; Dubois, P.; Demonceau, A.; Noels, A. F.; Jérôme, R. *Polymer Bull.* **1998**, *40*, 631.

47. Beyer, F. L.; Gido, S. P.; Poulos, Y.; Avgeropoulos, A.; Hadjichristidis, N. *Macromolecules* **1997**, *30*, 2373.

48. Sheiko, S. S.; Prokhorova, S. A.; Beers, K. L.; Matyjaszewski, K.; Potemkin, I. I.; Khokhlov, A. R.; Moller, M. *Macromolecules* **2001**, *34*, 8354 and references therein.

Chapter 3

1. *Chemistry and Industry of Macromonomers*; Yamashita, Y., Ed.; Hüthig & Wepf: Basel, Switzerland, 1993.

2. Ito, K. *Prog. Polym. Sci.* **1998**, *23*, 581.

3. Ito, K.; Kawaguchi, S. *Adv. Polym. Sci.* **1999**, *142*, 129.

4. Heroguez, V.; Gnanou, Y.; Fontanille, M. *Macromol. Rapid Commun.* **1996**, *17*, 137.

5. Shen, Y.; Zhu, S.; Zeng, F.; Pelton, R. *Macromolecules* **2000**, *33*, 5399.

6. Mecerreyes, D.; Pomposo, J. A.; Bengoetxea, M.; Grande, H. *Macromolecules* **2000**, *33*, 5846.

7. Shen, Y.; Zeng, F.; Zhu, S.; Pelton, R. *Macromolecules* **2001**, *34*, 144.

8. Sanda, F.; Hitomi, M.; Endo, T. *Macromolecules* **2001**, *34*, 5364.

9. Norman, J.; Moratti, S. C.; Slark, A. T.; Irvine, D. J.; Jackson, A. T. *Macromolecules* **2002**, *35*, 8954.

10. Hirao, A.; Hayashi, M.; Nakahama, S. *Macromolecules* **1996**, *29*, 3353.

11. Quirk, R. P.; Zhou, Q. *Macromolecules* **1997**, *30*, 1531.

12. Hayashi, M.; Nakahama, S.; Hirao, A. *Macromolecules* **1999**, *32*, 1325.

13. Shen, Y.; Zhu, S.; Pelton, R. *Macromolecules* **2001**, *34*, 376.

14. Miyauchi, N.; Kirikihira, I.; Li, X.; Akashi, M. *J. Polym. Sci. Polym. Chem. Ed.* **1988**, *26*, 1561.

15. Chiefari, J.; Jeffery, J.; Mayadunne, R. T. A.; Moad, G.; Rizzardo, E.; Thang, S. H. *Macromolecules* **1999**, *32*, 7700.

16. Bon, S. A. F.; Morsley, S. R.; Waterson, C.; Haddleton, D. M. *Macromolecules* **2000**, *33*, 5819.

17. Gibson, V. C.; Okada, T. *Macromolecules* **2000**, *33*, 655.

18. Morita, T.; Maughon, B. R.; Bielawski, C. W.; Grubbs, R. H. *Macromolecules* **2000**, *33*, 6621.

19. Jo, S.; Shin, H.; Shung, A. K.; Fisher, J. P.; Mikos, A. G. *Macromolecules* **2001**, *34*, 2839.

20. Nomura, E.; Ito, K.; Kajiwara, A.; Kamachi, M. *Macromolecules* **1997**, *30*, 2811.

21. Oike, H.; Mouri, T.; Tezuka, Y. *Macromolecules* **2001**, *34*, 6229.

22. Kubo, M.; Hibino, T.; Tamura, M.; Uno, T.; Itoh, T. *Macromolecules* **2002**, *35*, 5816.

23. Hawker, C. J.; Mecerreyes, D.; Elce, E.; Dao, J.; Hedrick, J. L.; Barakat, I.; Dubois, P.; Jerome, R.; Volksen, W. *Macromol. Chem. Phys.* **1997**, *198*, 155.

24. Wang, Y.; Huang, J. *Macromolecules* **1998**, *31*, 4057.

25. Roos, S. G.; Müller, A. H. E.; Matyjaszewski, K. *Macromolecules* **1999**, *32*, 8331.

26. Shinoda, H.; Miller, P.J.; Matyjaszewski, K. *Macromolecules* **2001**, *34*, 3186.

27. Yamada, K.; Miyazaki, M.; Ohno, K.; Fukuda, T.; Minoda, M. *Macromolecules* **1999**, *32*, 290.

28. Ishizu, K.; Tsubaki, K.; Ono, T. *Polymer* **1998**, *39*, 2935.

29. Djalali, R.; Hugenberg, N.; Fischer, K.; Schmidt, M. *Macromol. Rapid Commun.* **1999**, *20*, 444.

30. Tsubaki, K.; Ishizu, K. *Polymer* **2001**, *42*, 8387.

31. Henschke, O.; Neubauer, A.; Arnold, M. *Macromolecules* **1997**, *30*, 8097.

32. Shiono, T.; Azad, S. M.; Ikeda, T. *Macromolecules* **1999**, *32*, 5723.

33. Batis, C.; Karanikolopoulos, G.; Pitsikalis, M.; Hadjichristidis, N. *Macromolecules* **2000**, *33*, 8925.

34. Rempp, P.; Lutz, P.; Masson, P.; Chaumont, P.; Franta, E. *Makromol. Chem., Suppl.* **1985**, *13*, 47.

35. Ishizu, K.; Shimomura, K.; Saito, R.; Fukutomi, T. *J. Polym. Sci., Polym. Chem. Ed.* **1991**, *29*, 607.

36. Mecerreyes, D.; Atthoff, B.; Boduch, K. A.; Trollsås, Hedrick, J. L. *Macromolecules* **1999**, *32*, 5175.

37. Puts, R. D.; Sogah, D. Y. *Macromolecules* **1997**, *30*, 7050.

38. Feast, W. J.; Gibson, V. C.; Johnson, A. F.; Khosravi, E.; Mohsin, M. A. *Polymer* **1994**, *35*, 3542.

39. Breunig, S.; Héroguez, V.; Gnanou, Y.; Fontanille, M. *Macromol. Symp.* **1995**, *95*, 151.

40. Héroguez, V.; Breunig, S.; Gnanou, Y.; Fontanille, M. *Macromolecules* **1996**, *29*, 4459.

41. Héroguez, V.; Gnanou, Y.; Fontanille, M. *Macromolecules* **1997**, *30*, 4791.

42. Rizmi, A. C. M.; Khosravi, E.; Feast, W. J.; Mohsin, M. A.; Johnson, A. F. *Polymer* **1998**, *39*, 6605.

43. Mecerreyes, D.; Dahan, D.; Lecomte, P.; Dubois, P.; Demonceau, A.; Noels, A. F.; Jérôme, R. *J. Polym. Sci., Part A: Polym. Chem.* **1999**, *37*, 2447.

44. Héroguez, V.; Amédro, E.; Grande, D.; Fontanille, M.; Gnanou, Y. *Macromolecules* **2000**, *33*, 7241.

45. Allcock, H. R.; deDenus, C. R.; Prange, R.; Laredo, W. R. *Macromolecules* **2001**, *34*, 2757.

46. Nomura, K.; Takahashi, S.; Imanishi, Y. *Macromolecules* **2001**, *34*, 4712.

47. Wintermantel, M.; Schmidt, M.; Tsukahara, Y.; Kajiwara, K.; Kohjiya, S. *Macromol. Rapid Commun.* **1994**, *15*, 279.

48. Wintermantel, M.; Gerle, M.; Fisher, K.; Schmidt, M.; Wataoka, I.; Urakawa, H.; Kajiwara, K.; Tsukahara, Y. *Macromolecules* **1996**, *29*, 978.

49. Sheiko, S. S.; Gerle, M.; Fischer, K.; Schmidt, M.; Moller, M. *Langmuir* **1997**, *13*, 5368.

50. Dziezok, P.; Sheiko, S. S.; Fischer, K.; Schmidt, M.; Moller, M. *Angew. Chem., Int. Ed. Engl.* **1997**, *36*, 2812.

51. Wintermantel, M.; Fischer, K.; Gerle, M.; Ries, R.; Schmidt, M.; Kajiwara, K.; Urakawa, H.; Wataoka, I. *Angew. Chem., Int. Ed. Engl.* **1995**, *34*, 1472.

52. Tsukahara, Y.; Ohta, Y.; Senoo, K. *Polymer* **1995**, *36*, 3413.

53. Tsukahara, Y.; Kohjiya, S.; Tsutsumi, K.; Okamoto, Y. *Macromolecules* **1994**, *27*, 1662.

54. Nemoto, N.; Nagai, M.; Koike, A.; Okada, S. *Macromolecules* **1995**, *28*, 3854.

55. Wataoka, I.; Urakawa, H.; Kajiwara, K.; Schmidt, M.; Wintermantel, M. *Polym. Int.* **1997**, *44*, 365.

56. Gerle, M.; Fischer, K.; Roos, S.; Müller, A. H. E.; Schmidt, M.; Sheiko, S. S.; Prokhorova, S.; Möller, M. *Macromolecules* **1999**, *32*, 2629.

57. Tsukahara, Y.; Namba, S.; Iwasa, J.; Nakano, Y.; Kaeriyama, K.; Takahashi, M. *Macromolecules* **2001**, *34*, 2624.

58. Djalali, R.; Li, S-Y.; Schmidt, M. *Macromolecules* **2002**, *35*, 4282.

59. Ishizu, K.; Tsubaki, K.; Uchida, S. *Macromolecules* **2002**, *35*, 10193.

60. Trnka, T. M.; Grubbs, R. H. *Acc. Chem. Res.* **2001**, *34*, 18.

61. For the GPC analysis, poly(styrene-d_8) was assumed to have the same hydrodynamic volume as non-deutrated polystyrene when both of have the same *DP*, other than *MW*.

62. Refractive index detector cannot perform well in the *MW* range of **III-2**, because *dn/dc* can only be considered as constant for polymer species with *MW* no less than about 2000. At the same time, among the five columns installed in GPC instrument, only one of them, i.e. HR1, has separation effects for the *MW* range of **III-2**.

63. Two columns (HR1 and HR3) are effective in *MW* range of **III-2**.

64. Quirk, R. Q.; Yoo, T.; Lee, Y.; Kim, J.; Lee, B. *Adv. Polym. Sci.* **2000**, *153*, 67.

65. Klein, J. W.; Lamps, J.-P.; Gnanou, Y.; Rempp, P. *Polymer* **1991**, *32*, 2278.

66. Fayt, R.; Forte, R.; Jacobs, C.; Jerome, R.; Ouhadi, T.; Teyssie, Ph.; Varshney, S. K. *Macromolecules* **1987**, *20*, 1442.

67. Hsieh, H. L.; Quirk, R. P. *Anionic Polymerization: Principles and Practical Applications*; Marcel Dekker: New York, 1996.

68. Wright, P. V., in *Ring-Opening Polymerization*, Ivin, K. J., Saegura, T., Eds.; Elsevier: London, 1984; Vol. 2.

69. Lee, J.; Hogen-Esch, T. E.; *Macromolecules* **2001**, *34*, 2095.

70. *Polymer Handbook*, 3rd ed.; Brandrup, J., Immergut, E. H., Eds.; Wiley: New York, 1989.

71. Henry, C. M. *Chem. Eng. News* **2001**, *79(48)*, 35.

Chpater 4

1. Schrock, R. R.; Murdzek, J. S.; Bazan, G. C.; Robbins, J.; DiMare, M.; O'Regan, M. *J. Am. Chem. Soc.* **1990**, *112*, 3875.

2. Schrock, R. R. *Acc. Chem. Res.* **1990**, *23*, 158.

3. Norton, R. L.; McCarthy, T. J. *Macromolecules* **1989**, *22*, 1022.

4. Feast, W. J.; Gibson, V. C.; Johnson, A. F.; Khosravi, E.; Mohsin, M. A. *Polymer* **1994**, *35*, 3542.

5. Breunig, S.; Heroguez, V.; Gnanou, Y.; Fontanille, M. *Polym. Prepr.* **1994**, *35(2)*, 526.

6. Breunig, S.; Héroguez, V.; Gnanou, Y.; Fontanille, M. *Macromol. Symp.* **1995**, *95*, 151.

7. Heroguez, V.; Gnanou, Y.; Fontanille, M. *Macromol. Rapid Commun.* **1996**, *17*, 137.

8. Rizmi, A. C. M.; Khosravi, E.; Feast, W. J.; Mohsin, M. A.; Johnson, A. F. *Polymer* **1998**, *39*, 6605.

9. Héroguez, V.; Breunig, S.; Gnanou, Y.; Fontanille, M. *Macromolecules* **1996**, *29*, 4459.

10. Héroguez, V.; Six, J.-L.; Gnanou, Y.; Fontanille, M. *Macromol. Chem. Phys* **1998**, *199*, 1405.

11. Mecerreyes, D.; Dahan, D.; Lecomte, P.; Dubois, P.; Demonceau, A.; Noels, A. F.; Jérôme, R. *J. Polym. Sci., Part A: Polym. Chem.* **1999**, *37*, 2447.

12. Héroguez, V.; Gnanou, Y.; Fontanille, M. *Macromolecules* **1997**, *30*, 4791.

13. Héroguez, V.; Amédro, E.; Grande, D.; Fontanille, M.; Gnanou, Y. *Macromolecules* **2000**, *33*, 7241.

14. Allcock, H. R.; deDenus, C. R.; Prange, R.; Laredo, W. R. *Macromolecules* **2001**, *34*, 2757.

15. Lou, X.; Detrembleur, C.; Jérôme, R. *Macromolecules* **2002**, *35*, 1190.

16. Nomura, K.; Takahashi, S.; Imanishi, Y. *Macromolecules* **2001**, *34*, 4712.

17. Tian, G.; Boone, H. W.; Novak, B. M. *Macromolecules* **2001**, *34*, 7656.

18. Pasquale, A. J.; Allen, R. D.; Long, T. E. *Macromolecules* **2001**, *34*, 8064.

19. Elyashiv-Barad, S.; Greinert, N.; Sen, A. *Macromolecules* **2002**, *35*, 7521.

20. As an exception, ROMP with macromonomer with polybutadiene block cannot be considered as living polymerization, because of significant occurrence of side reactions resulted from considerable metathesis reactivity of carbon-carbon double bonds on the polybutadiene chain of macomonomer.

21. Schwab, P.; Grubbs, R. H.; Ziller, J. W. *J. Am. Chem. Soc.* **1996**, *118*, 100.

22. Trnka, T. M.; Grubbs, R. H. *Acc. Chem. Res.* **2001**, *34*, 18.

23. We purchased both Schrock and Grubbs catalysts from Strem. The typical Schrock catalyst $Mo(C_{10}H_{12})(C_{12}H_{12}N)[OC(CH_3)(CF_3)_2]_2$ became the most expensive chemical we used and the price is $654 per 2 g. But the typical Grubbs catalyst, $55 per gram, is much cheaper.

24. We did not prepare either type of catalyst. However, we did observe different requirements for storing and employing the two types of catalysts. The Grubbs catalyst has a good stability. No considerable chemical changes can be observed by keeping it in air for days, and therefore it can be weighed and handled in air. No significant changes in its concentration can be observed in solution of dichloromethane, chloroform, or THF for hours. As a contrast, the Schrock catalyst is very sensitive to air, moisture, and many others. It changed color slowly even in the period that we stored it under nitrogen in capped tube, therefore it is absolutely necessary to handle it under strictly inert atmosphere. Moreover, it has a poor stability in solution, and its solution in strictly purified THF changed color from yellow to brown in few hours.

25. Hsieh, H. L.; Quirk, R. P. *Anionic Polymerization: Principles and Practical Applications*; Marcel Dekker: New York, 1996.

26. Quirk, R. Q.; Yoo, T.; Lee, Y.; Kim, J.; Lee, B. *Adv. Polym. Sci.* **2000**, *153*, 67.

27. Klein, J. W.; Lamps, J.-P.; Gnanou, Y.; Rempp, P. *Polymer* **1991**, *32*, 2278.

28. Fayt, R.; Forte, R.; Jacobs, C.; Jerome, R.; Ouhadi, T.; Teyssie, Ph.; Varshney, S. K. *Macromolecules* **1987**, *20*, 1442.

29. As an explanation of MALDI peak positions: 2839 = 2800 (**IV-2** with *DP* of 23) + 39 (suggesting potassium cation).

30. Kurcok, P.; Dubois, P.; Sikorska, W.; Jedliński, Z.; Jérôme, R. *Macromolecules* **1997**, *30*, 5591.

31. As an explanation of MALDI peak positions: 1809 = 1634 (**IV-4** with *DP* of 19) + 23 (suggesting sodium cation).

Chapter 5

1. *Controlled Radical Polymerization*; Matyjaszewski, K., Ed.; American Chemical Society: Washington, DC, 1998; Vol. 685.

2. *Controlled/Living Radical Polymerization: Progress in ATRP, NMP, and RAFT*; Matyjaszewski, K., Ed.; American Chemical Society: Washington, DC, 2000; Vol. 768.

3. Davis, K. A.; Matyjaszewski, K. *Adv. Polym. Sci.* **2002**, *159*, 1.

4. Hawker, C. J.; Bosman, A. W.; Harth, E. *Chem. Rev.* 2001, *101*, 3661.

5. Matyjaszewski, K.; Xia, J. *Chem. Rev.* **2001**, *101*, 2921.

6. Kamigaito, M.; Ando, T.; Sawamoto, M. *Chem. Rev.* **2001**, *101*, 3689.

7. Chiefari, J.; Chong, Y. K.; Ercole, F.; Krstina, J.; Jeffery, J.; Le, T. P. T.; Mayadunne, R. T. A.; Meijs, G. F.; Moad, C. L.; Moad, G.; Rizzardo, E.; Thang, S. H. *Macromolecules* **1998**, *31*, 5559.

8. Kobatake, S.; Harwood, H. J.; Quirk, R. P.; Priddy, D. B. *Macromolecules* **1997**, *30*, 4238.

9. Kobatake, S.; Harwood, H. J.; Quirk, R. P.; Priddy, D. B. *Macromolecules.* **1999**, *32*, 10.

10. For instance, Chapter 6 describes our investigation of mediation effects on radical polymerization by carbon-centered stable radical.

11. Solomon, D. H.; Rizzardo, E.; Cacioli, P. U.S. Patent, 4,581,429, 1986.

12. Georges, M. K.; Veregin, R. P. N.; Kazmaier, P. M.; Hamer, G. K. *Macromolecules* **1993**, 26, 2987.

13. Veregin, R. P. N.; Georges, M. K.; Kazmaier, P. M.; Hamer, G. K. *Macromolecules* **1993**, *26*, 5316.

14. Hawker, C. J. *J. Am. Chem. Soc.* **1994**, *116*, 11185.

15. Benoit, D.; Grimaldi, S.; Robin, S.; Finet, J. P.; Tordo, P.; Gnanou, Y. *J. Am. Chem. Soc.* **2000**, *122*, 5929.

16. Benoit, D.; Chaplinski, V.; Braslau, R.; Hawker, C. J. *J. Am. Chem. Soc.* **1999**, *121*, 3904.

17. Chong, Y. K.; Ercole, F.; Moad, G.; Rizzardo, E.; Thang, S. H. *Macromolecules* **1999**, *32*, 6895.

18. Benoit, D.; Harth, E.; Fox.; Waymouth, R. M.; Hawker, C. J. *Macromolecules* **2000**, *33*, 363.

19. Grubbs, R. B.; Hawker, C. J.; Dao, J.; Fréchet, J. M. J. *Angew Chem., Int. Ed. Engl.* **1997**, *36*, 270.

20. Hawker, C. J. *Angew Chem., Int. Ed. Engl.* **1995**, *34*, 1456.

21. Gravert, D. J.; Datta, A.; Wentworth, P., Jr.; Janda, K. D. *J. Am. Chem. Soc.* **1998**, *120*, 9481.

22. Stehling, U. M.; Malmström, E. E.; Waymouth, R. M.; Hawker, C. J. *Macromolecules* **1998**, *31*, 4396.

23. Quirk, R. P.; Yoo, T.; Lee, Y.; Kim, J.; Lee, B. *Adv. Polym. Sci.* **2000**, *153*, 67.

24. Fayt, R.; Forte, R.; Jacobs, C.; Jerome, R.; Ouhadi, T.; Teyssie, Ph.; Varshney, S. K. *Macromolecules* **1987**, *20*, 1442.

25. The ^{1}H NMR signals were identified by 600 MHz ^{1}H-^{13}C GHMBC and ^{1}H-^{13}C GHMQC experiments. The experimental DP_n values were reported with two significant figures because the ^{1}H NMR signal of chain-end methyl proton (from DPHLi) slightly overlapped with adjacent ^{1}H NMR signals.

26. Dourges, M.-A.; Charleux, B.; Vairon, J.-P.; Blais, J.-C.; Bolbach, G.; Tabet, J.-C. *Macromolecules* **1999**, *32*, 2495.

27. Overlapped by the ^{1}H NMR resonance of *tert*-butyl protons of *t*-BMA, the ^{1}H NMR signals of eleven aliphatic protons of **V-1** were also in the region of 1.24-1.63 ppm, and their contribution was estimated (using the ^{1}H NMR resonance intensities of three protons of **V-1** at 4.01, 4.41, and 4.83 ppm as references), and then was subtracted from the total peak area of 1.24-1.63 ppm to give the ^{1}H NMR resonance intensity of *tert*-butyl protons.

28. Georges, M. K.; Hamer, G. K.; Listigovers, N. A. *Macromolecules* **1998**, *31*, 9087.

29. The molecular weights for main peak maxima of the last two trials were 422K, and 498K based on calibration curve *a* of **Figure 5-7**, and were very close to calculated M_n values of 421 000 and 506 000. Since intermolecular biradical coupling has little influence on the main peak maximum positions on GPC curves, such excellent agreement, in turn, supports the efficiency of the calibration used.

30. Lokaj, J.; Vlček, P.; Kříž, J. *Macromolecules* **1997**, *30*, 7644.

31. Burguiere, C.; Dourges, M.-A.; Charleux, B.; Vairon, J. P. *Macromolecules* **1999**, 32, 3883.

32. Hoover, M. F.; Butler, G. B. *J. Polym. Sci., Part C* **1974**, *45*, 1.

33. Steckler, R. U.S. Patent **1975**, 4,058,491.

34. Monroy Soto, V. M.; Galin, J. C. *Polymer* **1984**, *25*, 121.

35. Oh, J.-M.; Lee, H.-J.; Shim, H.-K.; Choi, S.-K. *Polym. Bull.* **1994**, *32*, 149.

36. Selective hydrolysis of *tert*-butyl ester group of linear polymers was investigated in my Master's thesis research (*Selective Anionic Polymerization of Allyl Methacrylate (AMA)*; Beijing Univ. of Chem. Tech., P.R.C., 1996): selective hydrolysis of *tert*-butyl ester group in the presence of allyl ester group occurred in THF with *p*-toluenesulfonic acid as catalyst for poly(AMA)-*b*-poly(*t*-BMA), poly(AMA)-*b*-poly(*t*-BMA)-*b*-poly(AMA), and poly(*t*-BMA)-*b*-poly(AMA)-*b*-poly(*t*-BMA), resulting amphiphilic block copolymers with different solubility.

37. Olah, G. A.; Narang, S. C. *Tetrahedron* **1982**, *38*, 2225.

38. Wang, J. S.; Varshney, S. K.; Jerome, R.; Teyssie, Ph. *J. Polym. Sci. Part A: Polym. Chem.* **1992**, *30*, 2251.

39. Shin, H. S.; Jung, Y. M.; Lee, J.; Chang, T.; Ozaki, Y.; Kim, S. B. *Langmuir* **2002**, *18*, 5523 and references therein.

40. Hawker, C. J.; Hedrick, J. L. *Macromolecules* **1995**, *28*, 2993.

Chapter 6

1. *Controlled Radical Polymerization*; Matyjaszewski, K., Ed.; American Chemical Society: Washington, DC, 1998; Vol. 685.

2. *Controlled/Living Radical Polymerization: Progress in ATRP, NMP, and RAFT*; Matyjaszewski, K., Ed.; American Chemical Society: Washington, DC, 2000; Vol. 768.

3. Davis, K. A.; Matyjaszewski, K. *Adv. Polym. Sci.* **2002**, *159*, 1.

4. Hawker, C. J.; Bosman, A. W.; Harth, E. *Chem. Rev.* 2001, *101*, 3661.

5. Matyjaszewski, K.; Xia, J. *Chem. Rev.* **2001**, *101*, 2921.

6. Kamigaito, M.; Ando, T.; Sawamoto, M. *Chem. Rev.* **2001**, *101*, 3689.

7. Chiefari, J.; Chong, Y. K.; Ercole, F.; Krstina, J.; Jeffery, J.; Le, T. P. T.; Mayadunne, R. T. A.; Meijs, G. F.; Moad, C. L.; Moad, G.; Rizzardo, E.; Thang, S. H. *Macromolecules* **1998**, *31*, 5559.

8. Ostu, T.; Yoshida, M.; Tazaki, T. *Makromol. Chem., Rapid Commun.* **1982**, *3*, 133.

9. Ostu, T.; Tazaki, T. *Polym. Bull.* **1986**, *16*, 277.

10. Tazaki, T.; Ostu, T. *Polym. Bull.* **1987**, *17*, 127.

11. Ostu, T.; Matsumoto, A.; Tazaki, T. *Polym. Bull.* **1986**, *16*, 323 and references therein.

12. Bledzki, A.; Braun, D. *Polym. Bull.* **1986**, *16*, 19.

13. Wieland, P. C.; Raether, B.; Nuyken, O. *Macromol. Rapid Commun.* **2001**, *22*, 700.

14. Raether, B.; Nuyken, O.; Wieland, P.; Bremser, W. *Macromol. Symp.* **2002**, *177*, 25.

15. Nuyken, O.; Wieland, P. C.; Heischkel, Y.; Raether, B. *Polym. Prepr.* **2002**, *43* (2), 84.

16. Maldonado-Textle, H.; De Leon-Saenz, M. E.; Putaux, J. L.; Ramos-De Valle, L. F.; Guerrero-Santos, R. *Macromolecules* **1998**, *31*, 2697.

17. Hageman, H. J. *Euro. Polym. J.* **1999**, *35*, 991 and references therein.

18. Sato, T.; Morita, N.; Seno, M. *Euro. Polym. J.* **2002**, *37*, 2055.

19. Viala, S.; Tauer, K.; Antonietti, M.; Krüger, R.-P.; Bremser, W. *Polymer* **2002**, *43*, 7231.

20. Selwood, P. W.; Dobres, R. M. *J. Am. Chem. Soc.* **1950**, *72*, 3860.

21. For chemistry of triarylmethyl radicals, see: Forrester, A. R.; Hay, J. M.; Thomson, R. H. *Oragnic Chemistry of Stable Free Radicals*; Academic Press: London, 1968; Chapter 2.

22. Lankamp, H.; Nauta, W. Th.; MacLean, C. *Tetrahedron Lett.* **1968**, 249.

23. Sizzmann, H.; Boese, R. *Angew. Chem., Int. Ed. Engl.* **1987**, *26*, 971.

24. DiMagno, S.; Waterman, K.; Sperr, D.; Streitwieser, A. *Angew. Chem., Int. Ed. Engl.* **1991**, *30*, 4679.

25. Scaiano, J. C.; Martin, A.; Yap, G. P. A.; Ingold, K. U. *Org. Lett.* **2000**, *2*, 899.

26. Fischer, H.; Radom, L. *Angew. Chem., Int. Ed.* **2001**, *40*, 1340.

27. Fieser, L. F.; Williamson, K. L. *Organic Experiments, 8th ed.*; Houghton Mifflin: Boston, 1998; Chapter 31.

28. Anderson, B. C.; Andrews, G. D.; Arthur, P., Jr.; Jacobson, H. W.; Melby, L. R.; Playtis, A. J.; Sharkey, W. H. *Macromolecules* **1981**, *14*, 1599.

29. Chiefari, J.; Jeffery, J.; Mayadunne, R. T. A.; Moad, G.; Rizzardo, E.; Thang, S. H. *Macromolecules* **1999**, *32*, 7700.

30. Bon, S. A. F.; Morsley, S. R.; Waterson, C.; Haddleton, D. M. *Macromolecules* **2000**, *33*, 5819.

31. Norman, J.; Moratti, S. C.; Slark, A. T.; Irvine, D. J.; Jackson, A. T. *Macromolecules* **2002**, *35*, 8954.

Chapter 7

1. Hawker, C. J.; Bosman, A. W.; Harth, E. *Chem. Rev.* **2001**, *101*, 3661.

2. Hawker, C. J.; Elce, E.; Dao, J.; Volksen, W.; Russell, T. P.; Barclay, G. G. *Macromolecules* **1996**, *29*, 2686.

3. Devenport, W.; Michalak, L.; Malmström, E.; Mate, M.; Kurdi, B.; Hawker, C. J.; Barclay, G. G.; Sinta, R. *Macromolecules* **1997**, *30*, 1929.

4. Cuervo-Rodriguez, R.; Fernández-Moneral, C.; Madruga, E. L. *J. Polym. Sci., Polym. Chem. Ed.* **2002**, *40*, 2750.

5. Butz, S.; Baethge, H.; Schmidt-Naake, G. *Macromol. Rapid. Commun.* **1997**, *18*, 1049.

6. Steenbock, M.; Klapper, M.; Mullen, K.; Pinhal, N.; Hubrich, M. *Acta Polym.* **1996**, *47*, 276.

7. Moad, G.; Ercole, F.; Krstina, J.; Moad, C. L.; Rizzardo, E.; Thang, S. H. *Polym. Prepr.* **1997**, *38* (1), 744.

8. Lokaj, J.; Vlcek, P.; Kriz, J. *Macromolecules* **1997**, *30*, 7644.

9. Burguiere, C.; Dourges, M.-A.; Charleux, B.; Vairon, J.-P. *Macromolecules* **1999**, *32*, 3883.

10. Odian, G. *Principles of Polymerization*, 4th ed.; Wiley: New York, 2003, in press.

11. White, D.; Makowski, M. P. *Polym. Prepr.* **2002**, *43* (2), 92.

12. Yousi, Z.; Jian, L.; Rongchuan, Z.; Jianliang Y.; Lizong, D.; Lansun, Z. *Macromolecules* **2000**, *33*, 4745.

13. Georges, M. K.; Hamer, G. K.; Listigovers, N. A. *Macromolecule* **1998**; *31*, 9087.